Fabrication, Characterization and Application of Low-cost Tubular Ceramic Membranes Derived from Fly Ash: A Waste to Resource Conversion Strategy

Thesis submitted in partial fulfillment of the requirements for the degree of

DOCTOR OF PHILOSOPHY

by

KAKALI PRIYAM GOSWAMI

Department of Chemical Engineering

Indian Institute of Technology Guwahati

Guwahati – 781039, India

September 2021

Fabrication, Characterization and Application of Low-cost Tubular Ceramic Membranes Derived from Fly Ash: A Waste to Resource Conversion Strategy

-Kakali Priyam Goswami

Fabrication, Characterization and Application of Low-cost Tubular Ceramic Membranes Derived from Fly Ash: A Waste to Resource Conversion Strategy

Thesis submitted in partial fulfillment of the requirements for the degree of

DOCTOR OF PHILOSOPHY

by

KAKALI PRIYAM GOSWAMI

Roll No.: 186107007

Department of Chemical Engineering

Indian Institute of Technology Guwahati

Guwahati – 781039, India

September 2021

Department of Chemical Engineering
Indian Institute of Technology Guwahati
Guwahati-781039, India

CERTIFICATE

This is to certify that the thesis entitled "**Fabrication, Characterization and Application of Low-cost Tubular Ceramic Membranes Derived from Fly Ash: A Waste to Resource Conversion Strategy"** being submitted by Ms. Kakali Priyam Goswami for the award of PhD degree has been carried out under my guidance and supervision. The work documented in this thesis has not been submitted to any other University or Institute for the award of any degree or diploma.

Date: 08-01-2022

(Signature of Thesis Supervisor)

Dr. G. Pugazhenthi

Professor

Department of Chemical Engineering

Indian Institute of Technology Guwahati

Guwahati-781039, Assam, India

DEDICATION

This Thesis is Dedicated to the Backbone of My Every Success, My Parents - Dr. Dharani Dhar Goswami and Mrs. Gitanjali Devi

Acknowledgements

It is a matter of genuine pleasure to express my profound gratitude and sincere thanks to my mentor, philosopher and guide Prof. G. Pugazhenthi for providing me the continuous support and guidance during my tenure in IIT Guwahati as a PhD scholar. His overwhelming attitude to help his students in every possible way has definitely made my journey quite a bit easier in the Institute. From rigorous discussions on different topics to making me a way to utilize the facilities available in the Institute in the best possible manner, he was there with me at every single step throughout the course. His critical analysis on different topics, scholarly advice, meticulous scrutiny as well as scientific approach is what every student strives for in their mentor. I shall always be obliged to him for his guidance, love and care for me as without his cooperation, assistance and advice, it would not have been possible from my end to complete this degree.

I am also indebted to my Doctoral Committee members Prof. K. Pakshirajan, Prof. N.R. Peela and Prof. P.R. Venkatesh for reviewing my work and providing their valuable suggestions, which definitely had helped me in improvising my work.

I would like to convey my sincere thanks and gratitude to all the faculty members and staffs of Department of Chemical Engineering, IIT Guwahati for providing me all the required facilities to complete my degree in time. I am also thankful to the faculties and staffs associated with Central Instruments Facility, IIT Guwahati for providing me necessary help and support in carrying out my experimental works.

I would also like to acknowledge my seniors Ms. Barnali Bhui, Mr. Pradeep Sahu, Mr. Shekhar Jyoti Pathak, Mr. Pradip Das, Mrs. Rajashree Borgohain, Ms. Thangsei Nengneilhing Baite, Mr. Arun Sakthivel and Ms. Tanushree Paul for their help and support in smooth completion of my degree.

I wish to convey my heartfelt thanks to my friends Mrs. Doli Hazarika, Mr. Roni Mallick, Mr. Partha Pratim Baruah, Ms. Poorva Mishra and Mr. Joy Patar for constantly motivating me to complete this task in the best possible manner. I thank each one of you for being the shoulder I can depend on!

I would also like to thank my lab mates Mr. N. Arul Manikandan, Ms. Purnima Madu, Ms. Satti Venu Gopala Kumari, Mr. Sashi Bhushan Singh and Mr. Arif Ahmed for their friendly support and timely assistance.

Someone has rightly said, "Family gives you the roots to stand tall and strong". I will always remain indebted to my family members: My beloved parents, Dr. Dharani Dhar Goswami and Mrs. Gitanjali Devi, my little brother Mr. Ankur Jyoti Goswami and my husband Mr. Dipankar Kashyap for sticking by my side throughout this journey. A thank you will definitely not be sufficient for the love, care and encouragement you showed for me.

Last but not the least, I would like to bow down in front of the Almighty for bestowing his blessings on me. It is his blessings, that kept me motivated to stay stronger and work harder. I will always remain humble to the Goddess Maa Kamakhya for lifting me up every time when I was low, for every miracle that had happened to me and for continuously showering her blessings on me.

Sincerely,

Kakali Priyam Goswami

Abstract

Implementation of ceramic membrane technology in various separation processes is one of the most discussed topics among the researchers in recent times due to its outstanding properties, including thermal, chemical and mechanical stabilities. Even though the ceramic membranes demonstrated their successful application in lab-scale and in some commercial systems, their implementation in industrial scale is still limited owing to the high capital cost. In view of this, several researchers have been working on the development of low-cost ceramic membranes by utilizing cheap precursors such as kaolin, fly ash, Tunisian clay, Moroccan clay, and so on. However, it is worth mentioning that improper dumping of vast quantities of fly ash generated from thermal power plants across the globe is a potential source of air and water pollution. Keeping this point in mind, this work focuses on fabrication of fly ash-based tubular ceramic membranes via extrusion process and their applications in three different liquid phase separations. It can be commented that recycling of fly ash not only produces low-cost membranes, but it is also a waste-to-resource conversion strategy that addresses the aforementioned environmental concerns associated with improper disposal of fly ash.

In this work, membranes using four different compositions of fly ash (65 – 80 wt.%) and calcium carbonate (0 – 15 wt.%) along with 20 wt.% of quartz were fabricated and characterized to find out the optimum raw material composition. Furthermore, in order to evaluate the effect of binder concentration (Sodium salt of carboxy methyl cellulose; Na-CMC) on membrane properties, the optimized raw materials composition (75 wt.% fly ash, 20 wt.% quartz, 5 wt.% calcium carbonate) was utilized to fabricate tubular membranes with varied binder concentrations (2 – 3.5 wt.% Na-CMC solution). In the aforementioned cases, different characterization techniques such as X-Ray Diffraction analysis, X-Ray Fluorescence analysis, Energy Dispersive X-Ray analysis, Field Emission Scanning Electron Microscope, Laser

Abstract

Particle Size analysis were carried out in order to arrive at optimum raw material composition as well as binder concentration to be used for fabrication of fly ash based ceramic membrane. Experiments revealed that increased binder concentration led to agglomeration in membrane matrix, causing formation of large and uneven pores along with decreasing membrane's chemical and mechanical stability. Therefore, on the basis of rigorous experiments conducted, 2 wt.% solution of Na-CMC was found to be sufficient in imparting good physical and mechanical properties to the membrane. The membrane prepared with optimized raw materials composition (75% fly ash, 20% quartz, 5% calcium carbonate) and binder concentration (2 wt.% Na-CMC solution) possessed an average pore size of 0.133 µm, hydraulic permeability of 4.93×10^{-8} m^3/m^2skPa *and porosity of 40.17%, along with outstanding chemical and mechanical strength.*

This optimized membrane was further used for three different separation processes, namely poultry slaughterhouse wastewater treatment, starch processing wastewater treatment and separation of glycerol from biodiesel. In case of poultry slaughterhouse wastewater treatment, the membrane was able to achieve complete reduction of Chemical Oxygen Demand (COD), Total Suspended Solids (TSS) and turbidity content at all applied pressures in the range of 207-483 kPa, thus satisfying the necessary environment protection norms regarding discharge and reuse as prescribed by Central Pollution Control Board (CPCB), India. The versatility of membrane's performance in treating starch processing wastewater was evaluated by conducting microfiltration experiments with 1% (w/v) synthetic starch suspension at various applied pressures (207-483 kPa), cross flow velocities (5.55-11.11$\times10^{-6}$ m^3/s*) and also for three different starch sources, namely corn, wheat and rice. A significant fact noticed during the experiments is that with increasing applied pressure, the permeate flux passes through a maximum, with the highest quantity of permeate being obtained at 345 kPa. In terms of rejection efficiency, the permeate obtained through the membrane was absolutely free of*

turbidity and TSS. However, a slight COD content was observed, which is also below the permissible limit for discharge into surface water, as prescribed by Central Pollution Control Board (CPCB), India. The membrane's efficiency regarding removal of glycerol from biodiesel was tested by conducting microfiltration of biodiesel emulsion with a glycerol content of 8.33 wt.%, at different applied pressures lying between 207 and 483 kPa. Experiments revealed that microfiltration was successful in bringing down the glycerol content of biodiesel and the permeate obtained in the pressure range of 207-345 kPa contained even less than 0.02 wt.% free glycerol, thus satisfying the norms prescribed by ASTM D6751 and EN14214.

Lastly, the economic feasibility assessment was also carried out for all three separation processes taken into consideration. The process of cost estimation started with estimating membrane fabrication cost, which came out to be 250.00 USD/m^2. The reported cost of the membrane is lower than that of commercially available ceramic membranes (500-1000 USD/m^2 for α - alumina membranes and 3000 USD/m^2 for stainless steel membranes). Thus, the membrane can be regarded as low cost without compromising its various characteristics. The cost estimation of all three treatment processes was carried out in the next step, considering both lab-scale and pilot-scale setups. The lab-scale set up consisted of one membrane tube (Filtration area: 0.00172788 m^2; Length: 100 mm; I.D.: 5.5 mm; O.D.: 11.5 mm) while the pilot-scale setup comprised of three parallel membrane housing, with seven membrane tubes in each housing (Filtration area: 0.07257 m^2, Length: 200 mm; I.D.: 5.5 mm; O.D.: 11.5 mm). The total cost involved in the aforementioned separation processes varied from 1.10-5.15 USD/L of permeate produced for lab-scale setup, which further reduced to 0.06-0.47 USD/L when estimated for pilot-scale setup. Therefore, it can be inferred that the developed membrane could be a perfect candidate for three different separation processes due to its high flux, outstanding separation efficiency and low cost.

Contents

List of Tables

List of Figures

Abbreviations

APHA	American Public Health Association
ASTM	American Society for Testing and Materials
BOD	Biochemical Oxygen Demand
CFU	Colony Forming Unit
COD	Chemical Oxygen Demand
CPCB	Central Pollution Control Board
DBP	Disinfection By-Products
DTG	Differential Thermogravimetry
EDX	Energy Dispersive Spectroscopy
FESEM	Field Emission Scanning Electron Microscope
FOG	Fats, Oil and Grease
HP	Horse Power
IUPAC	International Union of Pure and Applied Chemistry
JCPDS	Joint Committee on Powder Diffraction Standards
kW	Kilo-Watt
LPSA	Laser Particle Size Analyser
LRV	Log Reduction Value
MF	Microfiltration
MWCO	Molecular Weight Cut-Off
Na-CMC	Sodium Salt of Carboxymethyl Cellulose
NF	Nanofiltration
NTU	Nephelometric Turbidity Unit

PES	Polyether Sulfone
PFU	Plaque Forming Unit
PVA	Polyvinyl Alcohol
PVDF	Polyvinylidene Fluoride
PVP	Polyvinylpyrrolidone
RO	Reverse Osmosis
SBGR	Static Bed Granular Reactor
TGA	Thermogravimetric Analysis
TKN	Total Kjeldahl Nitrogen
TS	Total Solids
TSS	Total Suspended Solids
UF	Ultrafiltration
USA	United States of America
USD	Us Dollar
UV	Ultraviolet
VMD	Vacuum Membrane Distillation
WHO	World Health Organization
XRD	X-Ray Diffraction

Notations

a	Years of use of the equipment
A	Area of the membrane used for filtration
B	Weight of the biodiesel sample
C	Concentration factor

C_f	Concentration of feed
CFV	Cross flow velocity
C_p	Concentration of permeate
D	Depreciation cost of the equipment
d_i	Pore diameter of *i-th* fraction
d_p	Average pore diameter
J_w	Water flux
k	Flow consistency index
l	Pore length
L_h	Pure water permeability
n	Flow behavior index
n_i	*i-th* pore
n_s	Remaining service life of the equipment
P	Pressure
r	Pore length
T	Temperature
t	Time
V	Total volume of the membrane
W	Amount of HCl
W_{dry}	Weight of the dry membrane
W_{final}	Dry weight of the sample after chemical treatment
$W_{initial}$	Dry weight of the sample before chemical treatment
W_{wet}	Weight of the wet membrane
V_a	Book value of the equipment
V_F	Volume of feed

V_o	Original delivered cost of the equipment
V_R	Volume of retentate
V_w	Volume of water collected

Greek symbols

ρ	Density of water
μ	Viscosity of pure water
ε	Membrane porosity
β	Gamma
γ	Beta
α	Alpha
τ	Shear stress
φ	Phi
τ_m	Tortuosity of the membrane

Chapter 1

Introduction, Literature Review and Objectives

Introduction, Literature Review and Objectives

The initial section of this chapter presents a brief discussion about the various aspects of membrane technology. This is followed by a detailed discussion about fabrication and applications of low-cost ceramic membranes using fly ash as one of the precursors. This chapter also gives an insight about the fields where membrane technology has been successfully implemented. The scrupulous literature analysis carried out in this chapter reveals the possible scopes for further research in the aforementioned topics, based on which the objectives of this thesis are formulated. Lastly, this chapter also gives an idea about the organization of this thesis according to the formulated objectives.

1.1 Introduction to membrane technology

The need for separation processes can be observed very often in our everyday life. Separation can be regarded as the process of differentiating a mixture into its various constituents. Starting from extraction of valuable components to wastewater purification, the concept of separation science is playing a key role in every sphere of human activities. From the very ancient times, the different separation techniques that are being practiced for recovery and purification of valuable resources are solvent extraction, selective adsorption, distillation, membrane separation, just to name a few (Richardson, 1990). However, besides the aforementioned objective of carrying out any separation process, the capability of the membranes to protect the environment and public health through a sustainable development process has helped the membrane-based separation processes to grow with no bounds. Membrane-based separation technologies, which came to the notice of researchers through a significant breakthrough in the year 1960, have now established themselves as one of the most promising separation technologies with 60 years of rapid development (Fane et al., 2010). Following are the

numerous advantages associated with membrane-based separation technology, which have made this technology stand out from its conventional counterparts.

- Membrane separation processes are relatively simple and easy to operate, making them completely user-friendly (Scott et al., 1996).
- Membrane separation processes are based on physical separation mechanisms and involve no thermal, chemical or biological changes of component (Cui et al., 2010).
- Membranes are known to have higher selectivity in separating components, which helps in recovering most of the valuable products (Scott et al., 1996).
- Energy requirements and cost associated with the membrane processes are comparatively lower than the other conventional processes, which make them affordable to all standards of people in the society (Kumar et al., 2020).

The above-mentioned advantages offered by membranes have made membrane science a potential area of research for many scientists. However, membrane science, in itself, is such a vast area that further classifications are needed while carrying out a research project. IUPAC (International Union of Pure and Applied Chemistry) has defined membranes as ***the structure, having lateral dimensions much greater than its thickness, through which mass transfer may occur under a variety of driving forces*** (Koros et al., 1996). The driving forces aiding in successful membrane separation operations can be categorized into pressure, temperature, concentration and electrical potential (Mulder, 1996). However, amongst them, pressure-driven membrane separation processes are gaining much more interest as compared to other counterparts owing to various benefits offered by the pressure-driven membrane separation techniques.

1.2 Pressure driven membrane technology

Pressure-driven membrane separation processes are those where pressure is applied across the membrane to allow fluid along with the desired solutes to pass through the membrane, undesired ones being retained on the membrane surface to different extents, completely dependent on the structure of the membrane (Mulder, 1996).

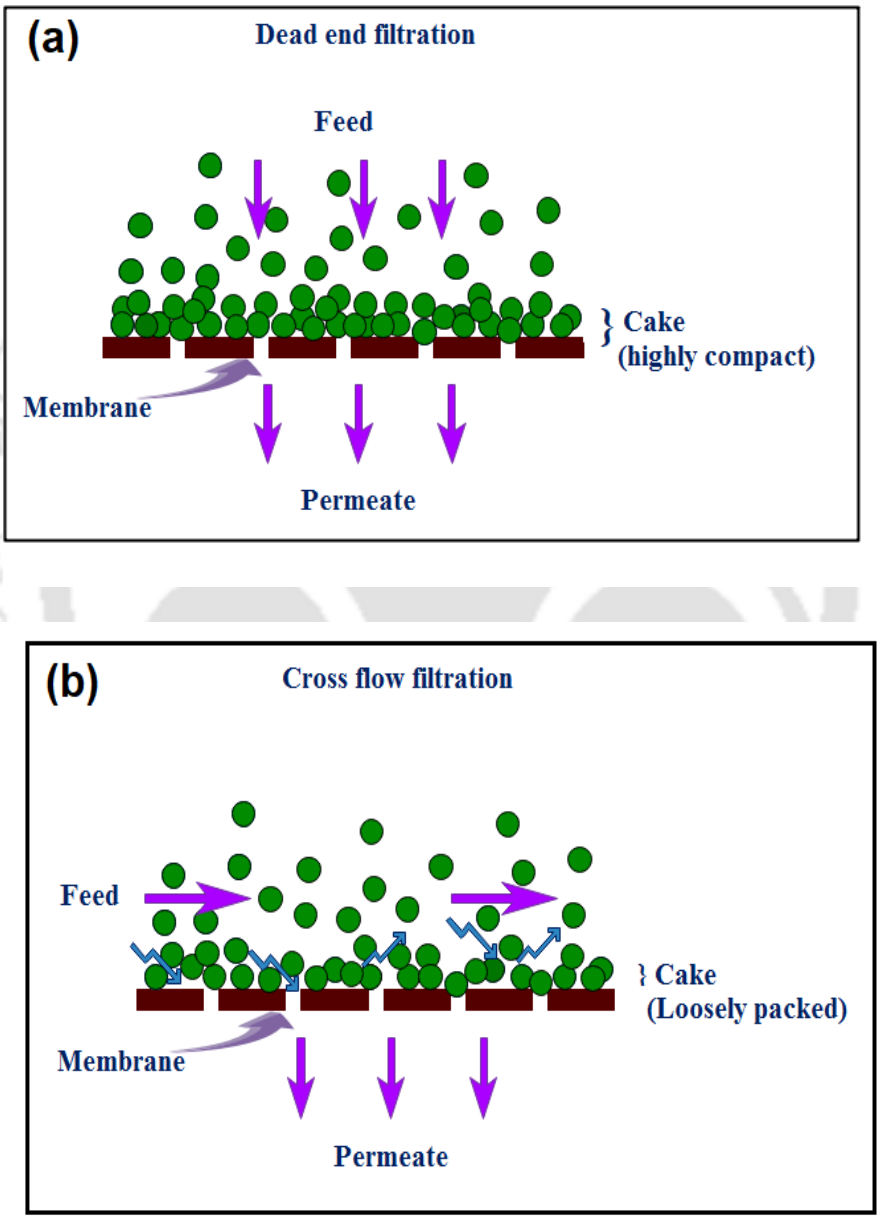

Fig. 1.1 Cross flow and dead-end filtration mode

The application of external pressure creates a steady permeate flow across the membrane. Pressure-driven membrane separation processes can be operated in two different modes,

namely dead-end filtration and cross flow filtration (Cui et al., 2010). In the dead-end filtration mode, the feed is allowed to enter perpendicular to the membrane surface, while in cross flow filtration mode, the feed entry is done tangentially (Fig. 1.1). Application of feed perpendicular to the membrane surface is, however, detrimental to the membrane's long-term performance as it leads to pronounced effect of concentration polarization, thus reducing the permeate flux across the membrane. In case of cross flow filtration, the application of shear force due to tangential movement of feed reduces the concentration polarization to a significant level (Van der Bruggen, 2018). Besides the mode of application, pressure-driven membrane processes can also be categorized differently into the following categories based on their ability to retain solute particles (Fig. 1.2).

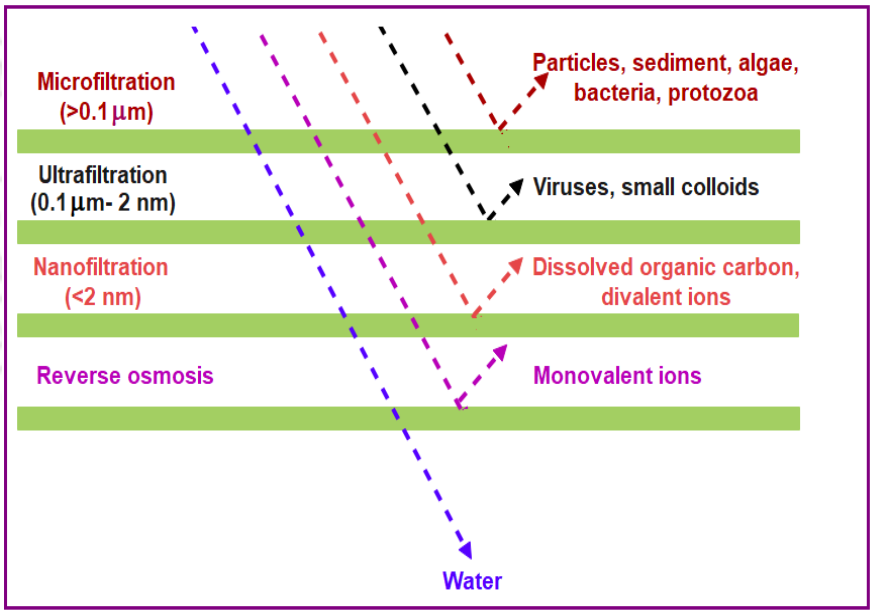

Fig. 1.2 Pressure driven membrane separation processes

- **Microfiltration:** In this process, external pressure is applied for separating macromolecules of sizes greater than 0.1 µm (Koros et al., 1996).
- **Ultrafiltration**: This process is applied for the separation of particles as well as dissolved macromolecules within the size range of 0.1 µm to 2 nm (Koros et al., 1996).

- **Nanofiltration**: Nanofiltration is performed the same way as the above two categories; however, the size range of particles to be separated here is lesser than 2 nm (Koros et al., 1996).
- **Reverse osmosis**: Reverse osmosis corresponds to those membrane separation processes, where an applied transmembrane pressure causes selective movement of solvent across the membrane against the osmotic pressure difference (Koros et al., 1996). This is the most sophisticated pressure-driven membrane filtration technology as it can block the passage of all suspended solids, colloid, dissolved solids and organic matter, having a molecular weight greater than 100 (Youcai, 2018).

It should be kept in mind that the growing importance for the pressure-driven membrane processes is because of the inherent advantages associated with these processes. The benefits of pressure-driven membrane processes can be summarized in the following points:

- **Longer lifetime:** Pressure-driven membrane separation processes offer great durability with a service life of up to several years, if maintained properly. Durability of such processes makes it suitable for industrial use (Díez and Rosal, 2020).
- **Easy handling:** These processes provide a simpler and easier way of installation as well as handling of the filtration apparatus, with minimal manual intervention. Moreover, these processes can easily and efficiently be scaled up as and when needed. Operational ease makes the pressure-driven membrane separation technologies one of the most sought-after technologies among people (Díez and Rosal, 2020).
- **Higher recovery:** Aforementioned processes are known to possess high productivity and selectivity towards both organic as well as inorganic contaminants (Suwaileh, 2020). Based on the inherent size characteristics of the contaminant to be removed, the selection of membrane with optimum pore size can be made for a particular separation

process, which not only helps in achieving higher yield, but also results in a reduction in energy consumption during the process (Gwak and Hong, 2018).

Owing to the number of benefits offered by the pressure-driven membrane technology, it has been widely implemented in various separation applications in different industries. Some of the potential users of this membrane technology are being mentioned in the following text.

- **Food and dairy industry:** The widescale application of membrane technology in food industries can be seen in clarification of fruit and vegetable juice using microfiltration and ultrafiltration membranes. Similarly, in beer industry, membranes are used for recovering the maturation and fermentation tank bottoms. Starch industry also uses membranes for treating the large quantities of wastewater generated during starch processes along with subsequent recovery of starch (Ikonić et al., 2010). In dairy industries, membrane technology has found immense application in the removal of bacteria and vegetative spores from milk. Moreover, membranes are also being extensively used in processes such as whey protein concentration and milk protein standardization in the dairy industry (Daufin et al., 2001).
- **Textile industry:** The wastewater generated from different operations carried out in textile industries contains huge quantities of harmful constituents such as dyes, different salts, heavy metals, surfactants, just to name a few. For instance, the wastewater generated during the scouring process contains oil and grease in emulsified form, the removal of which can be challenging using conventional techniques. In such a situation, membrane filtration can serve the purpose very efficiently. Similarly, the utilization of membrane technology can also be seen in other textile industry processes such as latex recovery, dye recovery, recovery of salt from dyestuffs and dye baths, and so on (Giwa and Ogunribido, 2012).

- **Pharmaceutical industry:** The increased concentration of pharmaceutically active compounds as well as endocrine disrupting agents in wastewater generated in different stages of the pharmaceutical industry has become a matter of concern now-a-days and membrane technology is seen to have successfully addressed this issue. Besides, membranes are also being used in recovering antibiotics and isolation as well as purification of different biologically active compounds such as enzymes and viruses from pharmaceutical industry wastewater (Samaei et al., 2018).
- **Petroleum industry:** Petroleum industries can also be considered as one of the significant implementors of membrane technology. The wastewater generated in petroleum industries contains very high oil concentrations and microfiltration operations play a great role in treating such wastewater. Besides, membranes have also found their application in the treatment of produced water obtained during the process of drilling (Padaki et al., 2015; Alzahrani and Mohammad, 2014).

Implementation of pressure driven membrane technology in above-mentioned processes is primarily dependent on the size of the solute to be separated from its solvent. Membranes with pore size lower than the size of the solute are quite effective in achieving satisfactory separation efficiency. However, it should be kept in mind that among the aforementioned four pressure-driven membrane separation processes, microfiltration is being practiced to a much greater extent than the rest three processes. It is worth to mention that microfiltration has the largest industrial market within the field of membrane technology itself and is responsible for almost 40% of total sales in Europe and USA (Huisman, 2000). Low pressure requirement, lesser energy consumption, cost-effectiveness, simpler operation and the ability to separate contaminants possessing a wide range of molecular diameter have definitely fuelled in the tremendous development of microfiltration membranes since 1960 (Huisman, 2000; Díez and Rosal, 2020).

1.3 Materials used for membrane fabrication

Though the history of membrane processes started with the development of polymeric membranes, the enhancement of technology has resulted in the use of different ceramic materials for the fabrication of membranes. In recent times, ceramic membranes are being preferred over polymeric ones, all thanks to the inherent advantages associated with the former, which is quite evident from Table 1.1. Ceramic membranes, besides possessing good chemical, mechanical as well as thermal stability, are quite resistant to fouling and hence, are preferred in various industrial applications (Hofs et al., 2011; Samaei et al., 2017).

Table 1.1 Comparison of properties of polymeric and ceramic membranes

Title	Polymeric membranes	Ceramic membranes	References
Thermal stability	Poor	Excellent	Hofs et al., 2011
Mechanical stability	Poor	Excellent	Hofs et al., 2011
Chemical stability	Poor	Excellent	Hofs et al., 2011
Pathogen tolerance	Poor	Excellent	Samaei et al., 2017
Cost	Inexpensive	Expensive	Park et al., 2014
Fouling behaviour	Poor	Good	Samaei et al., 2017
Weight	Light	Heavy	Muntha et al., 2016
Flux	Less	High	Park et al., 2014

Moreover, the flux obtained through ceramic membranes is comparatively higher than their polymeric counterparts (Park et al., 2014). The only drawback that may limit the use of ceramic membranes is their high cost (Park et al., 2014). However, this issue has also been addressed by several researchers across the globe through fabrication of ceramic membranes using various low-cost precursors. The use of naturally available low-cost materials such as kaolin, Moroccan clay, Tunisian clay, fly ash, zeolite has successfully reduced the cost of ceramic membranes. The various low-cost precursors used till date for the production of low-cost ceramic membranes are represented in Fig 1.3 (Abdullayev et al., 2019). It is evident from the figure that among different clays, kaolin and fly ash are being used most extensively for

fabricating low-cost membranes. Emani et al. fabricated a disc-shaped ceramic membrane using kaolin as a key precursor for treating oil-in-water emulsion and successfully achieved 98.52% reduction in oil content (Emani et al., 2014). Research work of Fatimah et al. also mentions about the fabrication of tubular ceramic membrane using kaolin and its subsequent application in water filtration (Fatimah et al., 2015). Another cheap precursor that is being considered for fabricating low-cost ceramic membranes is Moroccan clays. Membrane prepared using Moroccan red clay and natural phosphate had an average pore size of 2.5 μm and hydraulic permeability of 928 L/(hm^{2}bar). It displayed good turbidity removal efficiency for seawater, FeS tannery beamhouse effluent as well as synthetic salt water (Mouiya et al., 2018). Several other literatures also cite the use of materials such as Moroccan Perlite, bentonite, etc., for the fabrication of ceramic membranes to be implemented in the treatment of industrial wastewater (Majouli et al., 2012; Bouazizi et al., 2016). Another such clay material that is also being used for low-cost membrane fabrication is Tunisian clay. Khemakhem et al. extruded a paste of Tunisian silty marls to obtain tubular ceramic membranes, which were further used for cuttlefish effluents treatment. The membrane successfully reduced the turbidity of the permeate to below 1 NTU, along with a significant decrease (around 65%) in the COD value (Khemakhem et al., 2009). Another microfiltration membrane, fabricated using similar clay material, was implemented in the water treatment plant of Sfax, Tunisia. The membrane showed outstanding rejection performance by completely removing Biochemical Oxygen Demand (BOD) and 99% turbidity in treated effluent (Kamoun et al., 2020). Besides these clay materials, another cheaper precursor that is being widely used for low-cost membrane fabrication is fly ash. Flat ceramic membranes with a pore size range of 1.30-1.44 μm were fabricated for the treatment of oil-water emulsion. The fabricated membranes well served their purpose by achieving rejection up to 97% (Suresh et al., 2016). A similar study carried out by another group of scientists reported the preparation of disk-type membrane using fly ash for

oil-water separation, where a rejection of 99.2% was observed with a membrane pore diameter of 1.2 µm (Singh and Bulasara, 2015). A mixture of fly ash and kaolin was also used for the preparation of circular ceramic membranes. The fabricated membranes were found to be very effective in separating humic acid from water, with an average rejection of 98.46% (Rawat and Bulasara, 2018).

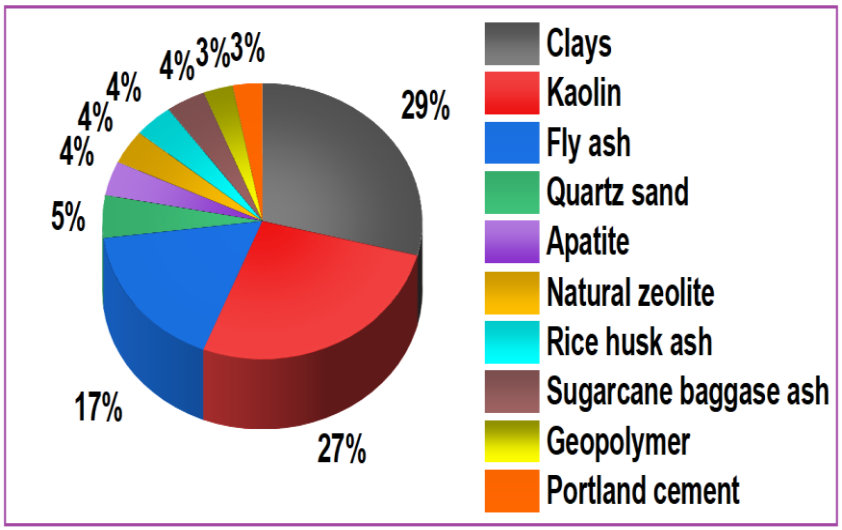

Fig. 1.3 Precursors used for fabrication of low-cost ceramic membranes

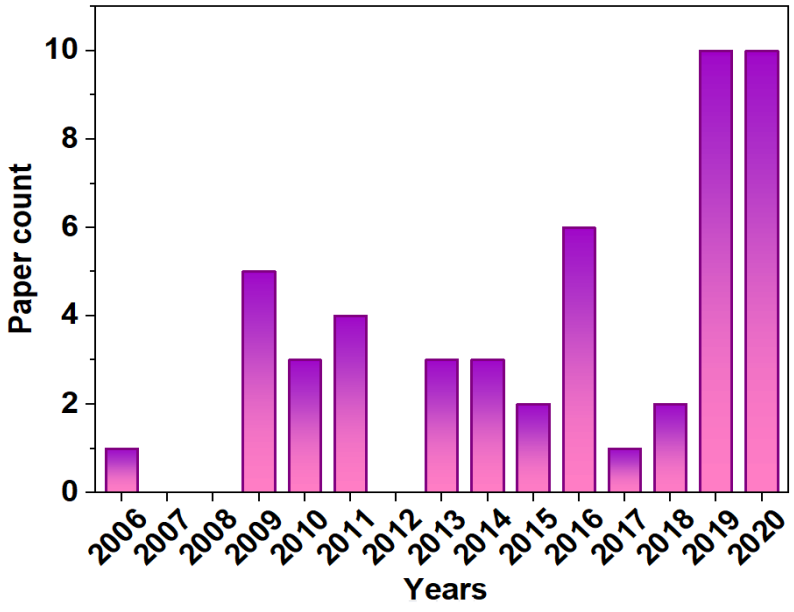

Fig. 1.4 Number of journal publications on fabrication of fly ash-based membranes (Courtesy: Google Scholar) (Accessed on 7th March, 2021)

The research on fly ash for membrane fabrication was initiated in 2006 and only very recently, publications on this topic have started to increase steadily, as depicted in Fig. 1.4. The growing importance over utilization of fly ash in membrane fabrication can be attributed to the generation of huge quantities of fly ash by different thermal power plants across the world.

Fly ash is considered as a great threat to the ecosystem as it can pollute water and air equally. Fly ash generated from thermal power plants is one of the leading causes of respiratory health problems owing to its silica content that causes irritation to mucus membrane of the lungs, diseases like asthma, allergy, pulmonary fibrosis and even cancer (Cho et al., 1994; Dhadse et al., 2008). The fly ash is also a potential source of ground water contamination due to its heavy metal content (Gamage et al., 2011). India ranks second in the countries of world in fly ash generation and China is the largest producer with approximately 600 MT of fly ash generated every year (Yao et al., 2015). In India, the coal used for generating power in thermal power plants is of very poor quality with an ash content of almost 30-45%. Fly ash generation in India has increased significantly from 86 MT in 2000-01 to 217.04 MT in the year 2018-19. The exact scenario regarding the generation and utilization of fly ash in India is pictorially depicted in Fig. 1.5.

This huge quantity of fly ash generated is partially used in cement, bricks and tiles industries, filling of mines and low-lying areas, construction of flyovers and bridges, etc. However, as of 2018-19, 22.41% of fly ash generated remains unutilized and is dumped inappropriately in open places leading to air as well as water pollution (Yousuf et al., 2020). Therefore, it can be inferred that the use of fly ash in membrane fabrication is beneficial as it not only reduces the membrane cost but also overcomes the problem with improper dumping of the waste material (Goswami and Pugazhenthi, 2020b). Moreover, the use of fly ash in membrane fabrication is attractive as a process of converting waste into a valuable material that can further be utilized for various purification purposes. Observing the two-fold benefits associated with using fly ash

as key precursor in membrane fabrication, it can be said that preparation of fly ash-based ceramic microfiltration membrane can be a great area for researchers to focus on in the coming years.

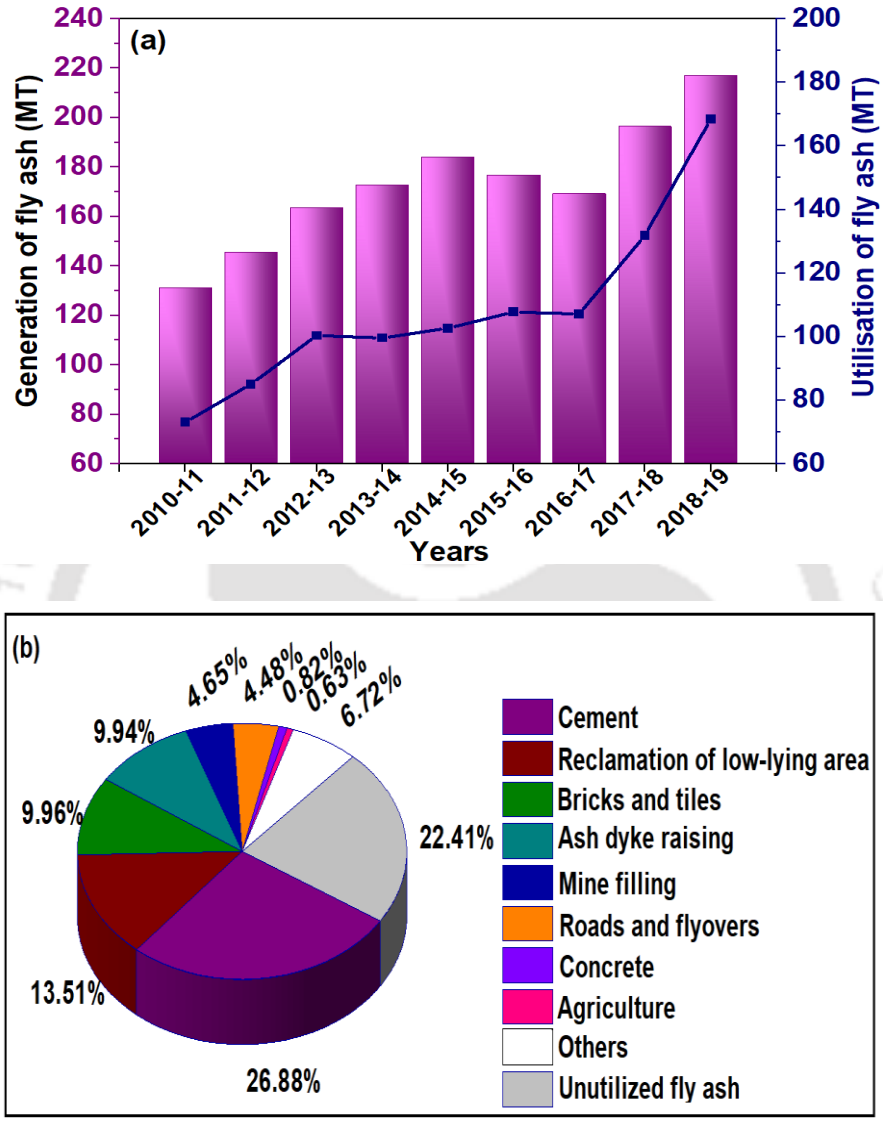

Fig. 1.5 Fly ash generation (a) and utilization (b) in India (Yousuf et al., 2020)

1.4 Different membrane configurations

The important fact to mention here is that after determining the precursor to be used for membrane fabrication, membranes can be fabricated into different shapes. Among the different shapes, membranes with flat, hollow fibre, spiral wound as well as tubular configuration, as

shown in Fig. 1.6, are known to be used widely in various industrial applications (Martín Martín, 2016).

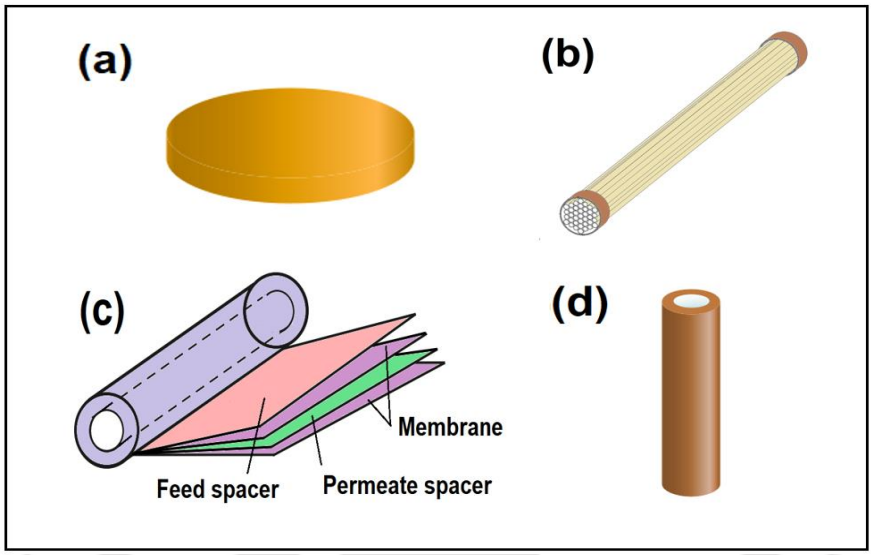

Fig. 1.6 Different membrane configurations

Flat-shaped membranes are especially useful for laboratory purposes and require support owing to very low packing density (Zari and Kargari, 2018). In case of hollow fibre membrane modules, numerous capillary sized tubes are packed into one membrane matrix, giving the module a compact structure with very high packing density. However, these membranes are very much prone to membrane fouling, thereby restricting their use in treating solutions with higher viscosity (Berk, 2009). Spiral wound modules are fabricated by keeping a permeable tube surrounded by several membranes, the latter being further separated by porous materials (Martín Martín, 2016). However, in case of spiral wound modules, the flow path of permeate to the collecting pipe sometimes becomes so long that it causes significant pressure losses (Harlacher and Wessling, 2015). On the contrary, tubular membranes resemble shell and tube heat exchangers, where the flow can be done in both ways: inside-out as well as outside-in. These membranes allow the application of high cross flow velocity, which helps in treating even solutions with very high concentrations of suspended solids. Moreover, a comparatively larger inner diameter of these membranes makes their cleaning as well as inspection a very

easy process. Moreover, the clogged membrane can also be cleaned easily by reversing the flow during the cleaning process (Berk, 2009). Owing to the aforementioned benefits associated with the use of tubular membranes, even though having comparatively lower packing density, these membranes are being extensively used in different industrial separation operations.

1.5 Membrane fabrication methods

1.5.1 Fabrication of membrane support

Different configurations of membranes can be fabricated using a variety of membrane fabrication techniques. The detailed discussion about various methods used for the fabrication of ceramic membranes along with their pictorial representation is presented in the following section.

1.5.1.1 Extrusion method

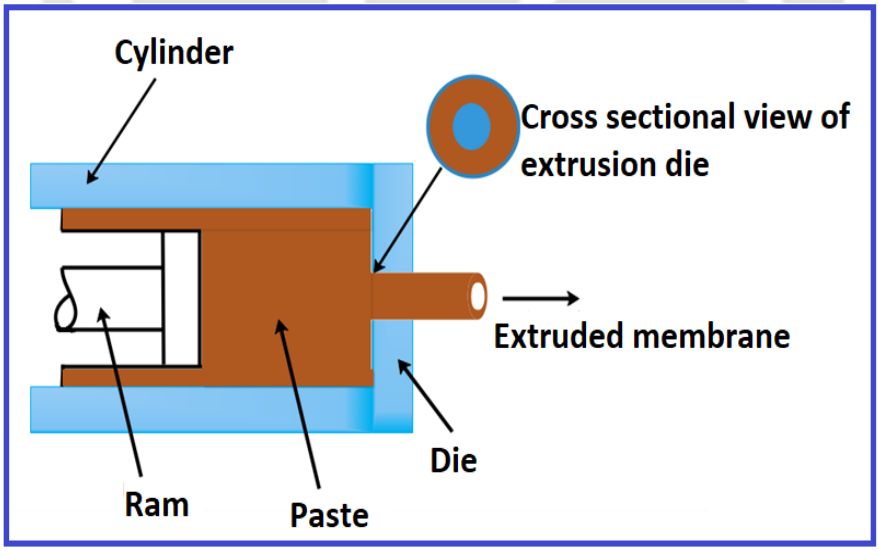

Fig. 1.7 Schematic of extrusion process

Extrusion is the process of fabricating inorganic membranes, which involve feeding of raw materials in paste form and it is used to fabricate membranes of tubular configuration. The

ceramic paste is forced through the opening of a die with the help of an endless screw or piston. The membranes can be produced with various diameters as well as different numbers of channels depending upon the structure of the die used in fabrication (Fig. 1.7). The high surface to volume ratio of the fabricated tubular membranes helps in handling large feed rates, which is the prime cause of its enhanced application in various industries (Monash et al., 2013). In certain cases, the use of binders helps in improving the plasticity and binding ability of the ceramic paste (Boussemghoune et al., 2020).

1.5.1.2 Slip casting method

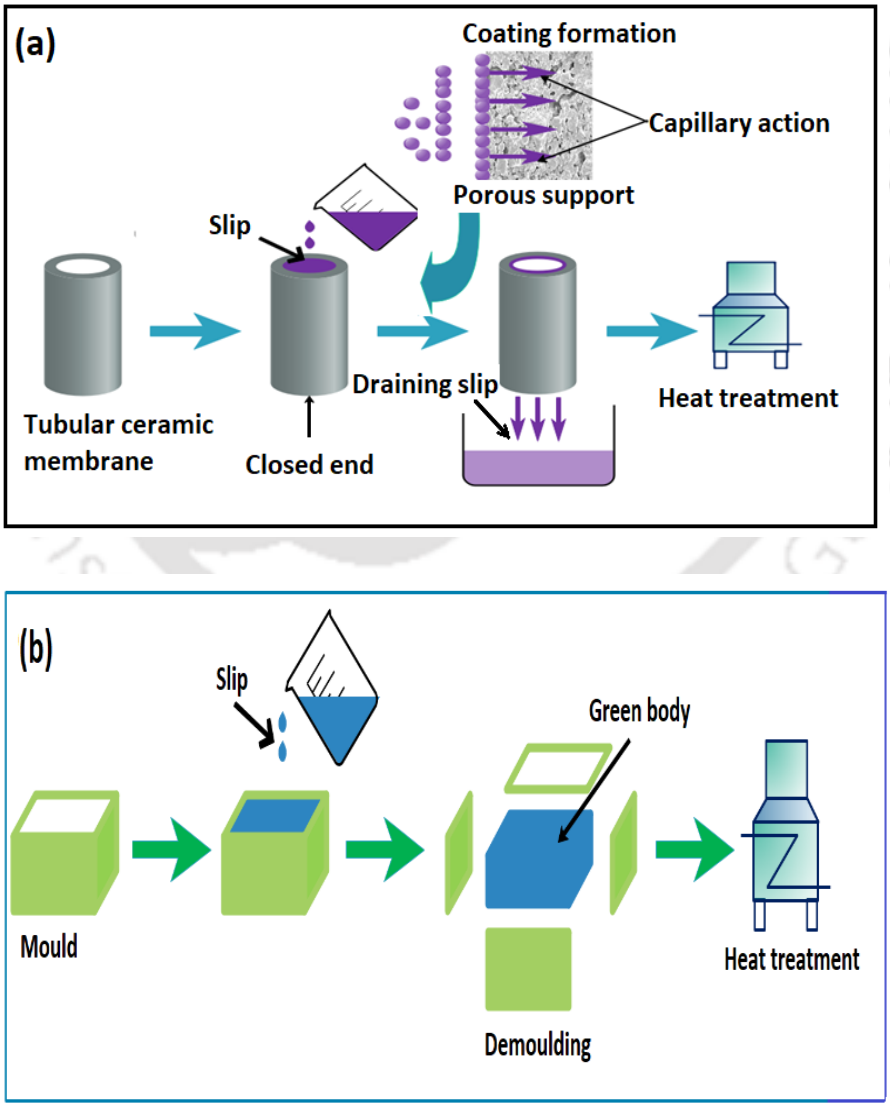

Fig. 1.8 Schematic of two different variations of slip casting

Slip casting is one of the most essential techniques implemented for the production of ceramic products. A slip is prepared by dispersing the raw material for membrane fabrication in a medium such as water or any other organic solvent. Use of deflocculating agents and binders in preparing the slip is known to enhance stability of the slip and enable easy handling of the green body (Adams, 1971). The slip is then poured in a predesigned mold and allowed to set for a certain duration. The wall of the mold absorbs the liquid medium, thus making the slip solidify very quickly. Once the slip is dried, the mold is removed and the dried slip subsequently takes the shape of the mold (Trunec and Maca, 2014) (Fig. 1.8).

This method is greatly being used for the fabrication of ceramic composite membranes, wherein one or more number of active layers are deposited over the already prepared ceramic support. This method is quite inexpensive as it does not involve the use of any sophisticated equipment. The fabricated green body is known to possess higher green density than the ones fabricated using pressing technique (Adams, 1971).

1.5.1.3 Pressing method

For the past few decades, pressing method is widely used for fabricating ceramics and tiles in ceramic manufacturing industries. This method of pressing can be broadly classified into axial and isostatic pressing. In both these methods, the raw materials are pressed in a mold to get the desired flat shape. The axial pressing method involves applying pressure axially in one or two directions, depending upon whether uniaxial or biaxial pressing is preferred (Monash et al., 2013). On the contrary, isostatic pressing is hydrostatic in nature, which involves the application of uniform pressure in all directions (Francis, 2015). However, so far as the literature is concerned, the membranes fabricated using fly ash as one of the key precursors are mainly manufactured using uniaxial pressing (or uniaxial compaction) method. The process of uniaxial pressing can be summarized into three main steps as shown in Fig. 1.9: filling the die

or mold, compaction at high pressure and ejection of the green compact body (Lemoisson et al., 2005). However, uniaxial pressing can be again categorized into dry as well as wet pressing. In dry pressing, the raw materials are used in dry form, whereas in wet pressing, binder solution is added to raw materials to form a paste (Monash et al., 2013). The paste is then pressed in a similar way as dry pressing under high pressure in a mold of desired shape. The green compact body, thus obtained after compaction, needs to be dried and sintered to get membranes with desired grain density as well as mechanical strength (Francis, 2015). This is a very simple method for fabricating symmetric flat ceramic membranes with a very low fabrication cost. The method is preferred for bulk production of flat ceramic membranes **(**Lemmoison et al., 2005).

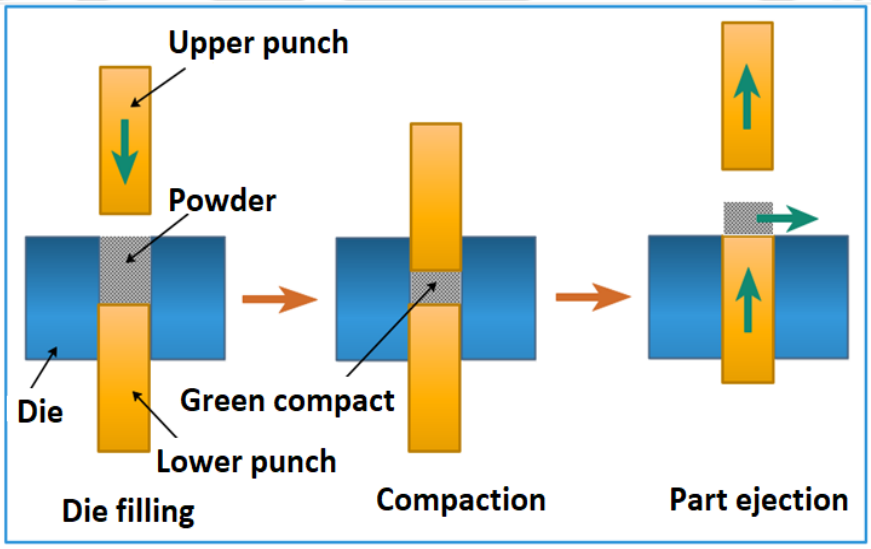

Fig. 1.9 Schematic for uniaxial pressing method

1.5.1.4 Centrifugal casting method

Centrifugal casting is a process specifically used for fabricating tubular ceramic membranes. In this method, ceramic paste is poured into a launder projecting into the end of a horizontal or vertical cylinder and centrifugal force is used to hold the ceramic paste in the cylinder wall, thus forming tubular ceramic membrane (Richardson et al., 1994). Rotational speed of the mold

is the source of centrifugal force in this process. During this process, the larger particles will move to the mold wall first, followed by the smaller particles. The quality of inner surface of the fabricated membrane primarily depends on the quantity of smaller particles present in the raw material suspension, while the quality of the outer surface is mostly dependent on the quality of the mold (Monash et al., 2013). The fabricated ceramic tubes are then dried and sintered for further use in separation processes. Fig. 1.10 is the schematic representation of centrifugal casting process used for fabrication of tubular membrane.

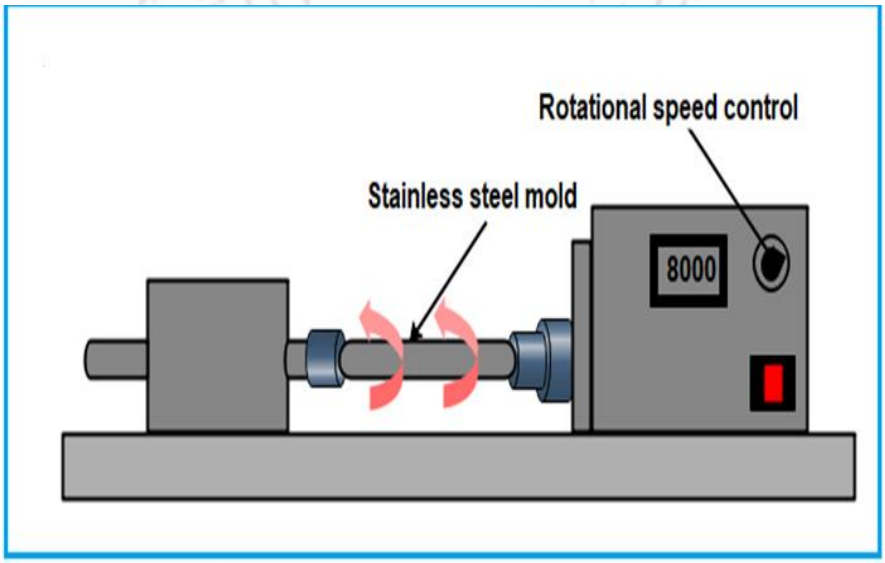

Fig. 1.10 Centrifugal casting process

1.5.1.5 Tape casting method

In this process, as observed in Fig. 1.11, the ceramic suspension is spread over a moving plastic conveyor belt using a doctor's blade. The ceramic slurry used in tape casting is mainly a non-aqueous slurry, consisting of binders, plasticizers and other additives along with the raw materials used for membrane fabrication. The obtained green flat sheet membrane is then heat treated, during which the solvent vaporizes and the membrane with desired properties is formed (Trunec and Maca, 2014; Gadow and Kern, 2014). Prior to sintering, the obtained green membranes can be cut into desired shape and dimensions.

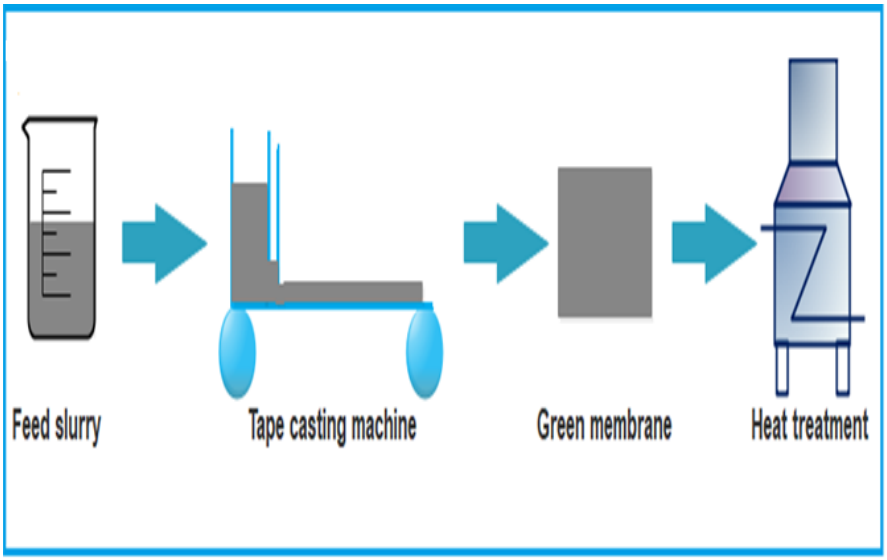

Fig. 1.11 Tape casting process

1.5.1.6 Phase inversion method

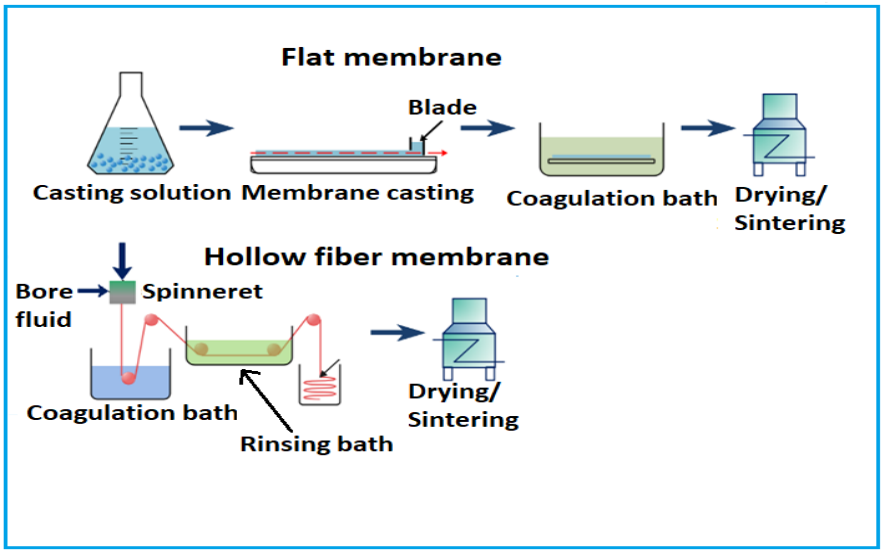

Fig. 1.12 Phase inversion process

In this process, suspension used for membrane fabrication is transformed from liquid to solid state in a controlled manner to obtain a desired membrane structure. The suspension is first cast on a suitable support surface using a Doctor's blade and then immersed into a coagulation bath. In case of hollow fiber membrane, the suspension needs to be extruded through a spinneret to get the desired membrane shape. The coagulation bath contains non-solvent, which gets

exchanged with the solvent in the casted membrane during immersion and, as a result, precipitation of polymer film takes place (Brown, 2001; Abdulhameed et al., 2017). The membrane body, thus obtained, is further subjected to sintering. The schematic representation of the whole process is represented in Fig. 1.12.

1.5.2 Fabrication of composite membrane

Several researchers have focused on membrane coating on pre-synthesized support to reduce the membrane pore size for an efficient filtration. The fabricated composite membranes thus have an asymmetric structure with a thin layer of permselective material deposited over highly porous support. The coating can be carried out in many ways, including dip coating, spray coating, chemical vapor deposition, hydrothermal synthesis, etc. (Fig 1.13 (a)-(d)). Dip coating is one of the cheapest coating techniques practiced by many researchers. In this process, the support membrane is dipped in a slurry solution containing the ceramic powders, binder and solvent. When the support is withdrawn from the slurry solution, a film of slurry is deposited over its surface, which is then dried and sintered for use in filtration applications (Mohammadzadeh et al., 2020). The thickness of the film deposited can be maintained by controlling the various parameters associated with the dip coating process such as withdrawal speed, immersion time, cycles of coating, loading of ceramics in the slurry, etc. (Lončarević and Čupić, 2019).

Similar to dip coating, membrane supports are also being used for fabricating composite ceramic membranes through the process of spray coating. Suspension with desired composition is sprayed over the membrane surface from a certain distance using a spray gun. The coated surface is then dried and sintered to obtain membranes with desired physical and mechanical properties (Zou et al., 2019a).

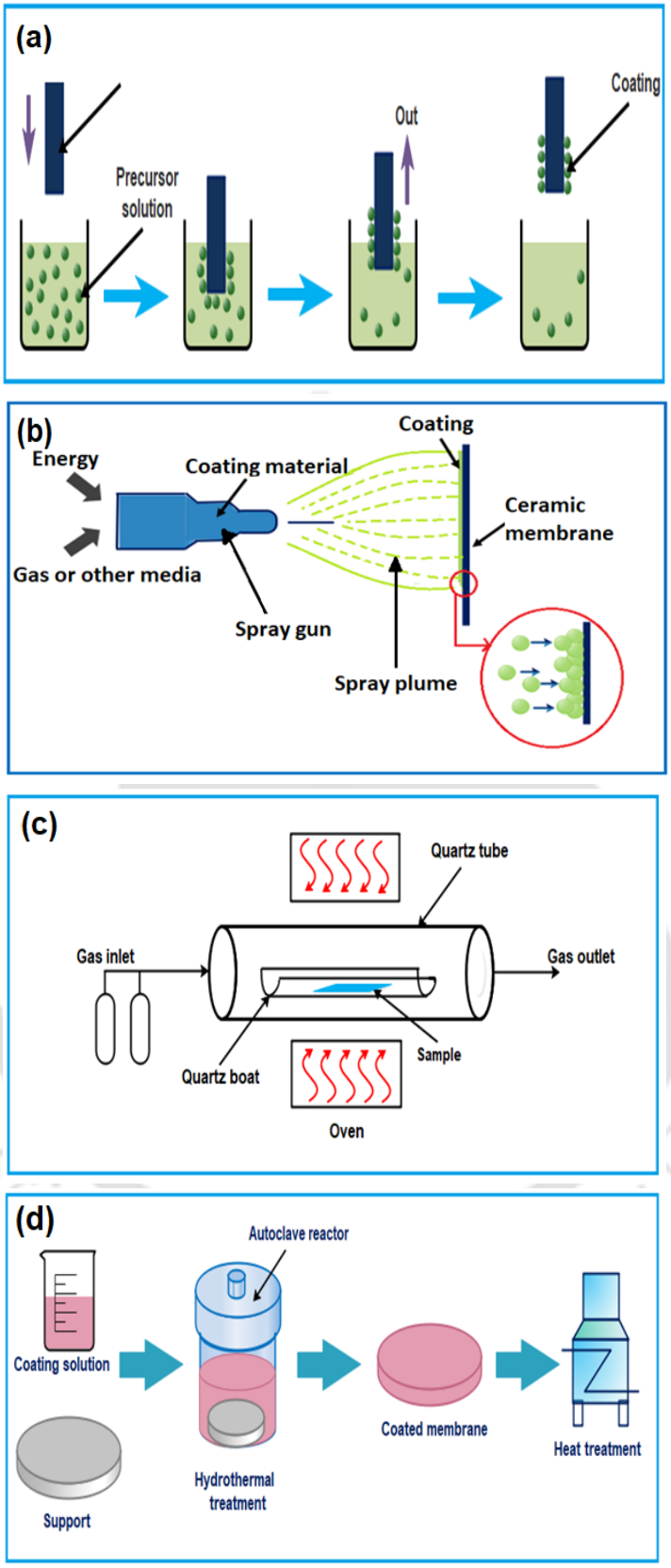

Fig. 1.13 Various methods used for fabrication of composite ceramic membranes [(a) Dip coating (b) Spray coating (c) Chemical vapor deposition (d) Hydrothermal synthesis]

Chemical vapor deposition is also gaining importance in recent times for coating purposes. In this process, the support is exposed to one or more volatile precursors, usually under vacuum. When a precursor is in contact with the support matrix, it reacts and/or decomposes to form a coating over it **(**Bunshah, 1994; Behera et al., 2020). Chemical vapor deposition is known for its exceptionally high deposition rates and, hence, it is preferred over other conventional deposition processes (Creighton and Ho, 2001). In addition to these methods, hydrothermal synthesis can be used for coating fly ash supports. In this method, heating of gels or flocculates is done in the presence of water in a high-pressure autoclave within a temperature range of 373-573 K (Avci and Önsan, 2018). Crystal formation and deposition on the support matrix as well as the surface take place during the process, thus reducing the pore size of the support membrane.

1.6 State-of-the-art

This section of the thesis primarily discusses about the scrupulous literature review carried out on fabrication and application of fly ash-based ceramic membranes. Besides, it also throws light on different liquid phase separation processes that can be targeted for the implementation of fly ash-based membrane filtration.

1.6.1 Fabrication and application of fly ash-based ceramic membranes

As previously mentioned, in search of low-cost precursors that can reduce the fabrication cost of ceramic membranes, researchers have started using fly ash for membrane fabrication from the very beginning of 21st century. Fly ash-based membranes are being prepared through a variety of methods, pressing, extrusion and slip casting, centrifugal casting, phase inversion, just to name a few. However, most of the literature available till date regarding fabrication of fly ash-based membranes talks about flat ceramic membranes prepared by uniaxial pressing

method. It has been found in literature that membranes fabricated using recycled fly ash and slight quantity of calcium carbonate resulted in membranes with outstanding mechanical properties, all thanks to the compound anorthite that formed from the reaction between fly ash and calcium carbonate (Wei et al., 2016). Works of Suresh et al. regarding fabrication of fly ash membranes also mentioned about improvement of membrane properties by addition of calcium carbonate (Suresh et al., 2016).

Besides $CaCO_3$, there are ample examples in literature that talks about the addition of kaolin to fly ash for membrane fabrication (Gupta and Anandkumar, 2018; Gupta and Anandkumar, 2019; Gupta et al., 2020). Addition of few percentages of kaolin is known to increase the mechanical strength of the membrane through formation of compounds such as metakaolin and nepheline due to high temperature phase transformation of kaolin (Rawat et al., 2018; Agarwal et al., 2020). It has also been found that addition of dolomite to fly ash and kaolin mixture resulted in the formation of high hardness compound cordierite, giving membranes with improved mechanical strength (Malik et al., 2020).

Few researchers integrated the effect of co-sintering on fabricating fly ash-based microfiltration membrane. Compared to the conventional sintering process, co-sintering makes the sintering process faster and reduces the membrane fabrication cost by eliminating drying and sintering steps. Moreover, the support as well as active layers present over the support are sintered together, thus improving the linkage between the two in a better way (Cui, 2016). Detailed investigation on the process of co-sintering for fabricating fly ash-based ceramic membrane revealed that minimum shrinkage between the support and intermediate layer is a prerequisite for obtaining a stable composite membrane. The inclusion of mullite whiskers to support membrane, in this case, served the purpose as these high temperature resilient mullite fibers prevent smaller particle migration during the sintering process, thus restricting contraction of the support membrane (Zou et al., 2019a).

It is worth mentioning that mullite formation is utmost essential for obtaining fly ash membranes with outstanding properties and hence, different researchers have mentioned in their work about using additives for this purpose. Usually, for raw material mixtures of fly ash and bauxite, the growth of mullite crystals starts at around 1200 °C and with increasing temperature, the growth of these crystals increases. During high temperature sintering, the secondary mullitization phenomenon takes place as a result of reaction between corundum and crystoballite present in the bauxite-fly ash mixture. This secondary mullitization results in unique self-expansion of membrane matrix at a temperature in the range of 1250-1450 °C. This expansion results in increased membrane porosity and pore size within the mentioned temperature range. However, at such high sintering temperatures, the formation of glassy phase may drastically alter the porosity values, which needs to be addressed by using sintering additives such as tungsten oxide, aluminium fluoride, titania molybdenum oxide, just to name a few. These compounds prevent the formation of glassy phase by lowering the secondary mullitization temperature along with providing fly ash-based ceramic membranes with interlocked mullite whiskers in its matrix (Zhu et al., 2015a; Dong et al., 2010; Chen et al., 2016).

Along with the pressing method, extrusion is also gaining popularity for the fabrication of fly ash-based tubular ceramic membranes. Jedidi et al. (2009) laid the foundation for fabricating tubular ceramic membranes using fly ash. Extensive investigations carried out on the prepared membranes revealed that though the increase in sintering temperature increased the mechanical strength of the membrane samples, it adversely affected the porosity as well as pore size of the membrane. Membrane porosity was observed to decrease with an increase in sintering temperature, whereas the membrane pore diameter increased from 4.0 μm to 4.9 μm within a temperature rise of 30 ˚C (Jedidi et al., 2009). Research works of Qin et al. (2015) and Fang et al. (2011) also mentioned the fabrication of fly ash membranes through extrusion process. Their

research work revealed that with a decrease in the size of fly ash particles, the pore size of membranes also followed a decreasing trend, which may be due to the close packing of small sized particles (Qin et al., 2015; Fang et al., 2011). These membranes, except for the case of Qin et al. (2015), were further used for fabricating composite membranes using fly ash slips via slip casting. It has been observed that films are coated on the membrane surface by slip casting through the combined action of film coating and capillary phenomenon. Moreover, slip concentration, casting time and withdrawal speed were found to be the crucial factors determining the properties of the fabricated membranes (Jedidi et al., 2011; Fang et al., 2013). Besides the aforementioned technologies, membranes were also fabricated using several other processes such as centrifugal casting, phase inversion and tape casting. During fabrication of tubular membranes using fly ash and alumina via centrifugal casting, it was found that the centrifugal force allows the large sized fly ash particles to get deposited in the mold wall whereas the small sized alumina particles were deposited over the fly ash layer. Hence, an increase in fly ash content leads to the formation of membranes with increased surface roughness owing to the larger sized fly ash grains (Rocha et al., 2021). Again, fabrication of membranes through phase inversion process resulted in asymmetric membrane with finger-like voids originating from the inner and outer surface of the membrane along with a spongy intermediate layer (Zhu et al., 2016).

As previously mentioned, several research groups used different coating methods such as dip coating, spray coating, chemical vapor deposition, hydrothermal synthesis coating, etc. on pre-synthesized support to reduce the pore size of the membrane (Qin et al., 2016; Suresh et al., 2017; Zhu et al., 2019; Zou et al., 2019a; Zou et al., 2019b). While all the other coating methods are conventional ones, one new addition to the field of spray coating is thermal spray coating, where the support is heated to volatilize the dispersant as it falls on the membrane surface, thus

forming a coating on the surface. Thus, it helps in avoiding the penetration of coating material into the membrane matrix (Zou et al., 2019b).

The wide range of properties of fly ash-based membranes obtained via fabrication through various processes is highly attractive for different separation operations. As per the literature, most of the fly ash membranes developed till date have been utilized to treat oily wastewater and all of them were quite successful in turning turbid and milky white wastewater into pellucid permeate, with very high rejection efficiencies (Zhu et al., 2015b; Singh and Bulasara, 2013; Malik et al., 2020; Zou et al., 2019b; Agarwal et al., 2020). Fly ash-based membranes were also found to be quite successful in treating textile industry wastewater as they achieved chemical oxygen demand removal efficiency (COD) up to 75%, which is very much appreciable. Along with this result, turbidity of the produced permeate was 0.5 NTU and color reduction efficiency in the feed was 90% (Jedidi et al, 2011).

In addition to the above, the implementation of fly ash-based membranes has been demonstrated for areas like fruit juice clarification, treatment of humic acid contaminated water, separation of protein, starch and bacteria from water, and so on (Qin et al., 2015; Rawat and Bulasara, 2018; Gupta and Anandkumar, 2018; Diana et al., 2019). During kiwi fruit juice clarification, it was found that the membrane significantly improved the quality of juice in terms of color, clarity and suspended solids, keeping other necessary properties intact (Qin et al., 2015). The works of Rawat and Bulasara (2018) demonstrate the successful implementation of fly ash-based membrane in removing humic acid from water with a rejection efficiency of 98.46% (Rawat and Bulasara, 2018). While in case of separating bovine serum albumin from water, maximum rejection of 92% was observed at a feed concentration of 200 ppm, rejection above 99% was reported in case of corn starch separation from water (Gupta and Anandkumar, 2018; Rocha et al., 2020). Similarly, fly ash membranes fabricated by Diana et al. successfully removed 99.048% of bacterial colonies from contaminated water (Diana et al., 2019).

Table 1.2 Available literature on fabrication and application of fly ash membrane

Raw materials	Method	Configuration	Sintering temperature (ºC)	Porosity (%)	Pore size (µm)	Mechanical strength (MPa)	Applications	Rejection (%)	References
Fly ash, $CaCO_3$, PVA	Pressing	Flat	1300	~45	1.2	~40	-	-	Wei et al., 2016
Fly ash, $CaCO_3$, Na_2CO_3, Boric acid, Sodium metasilicate	Pressing	Flat	900	34.76	1.202	~15	Oil-in-water suspension	99.2	Singh and Bulasara, 2013
Fly ash, $CaCO_3$, Na_2CO_3, Boric acid, Sodium metasilicate	Pressing	Flat	900	42.7	0.885	43.6	Humic acid separation	98.46	Rawat and Bulasara, 2018
Fly ash, Dolomite, Kaolin, Boric acid, Sodium	Pressing	Flat	900	46.3	0.62	~50	Oil-in-water suspension	97.4-98.8	Malik et al., 2020
Fly ash, PVA, Bauxite, TiO_2	Pressing	Flat	1450	46.64-42.92	7.28-6.52	28.27-36.05	-	-	Dong et al., 2010
Fly ash, PVA, Clay, Water	Pressing	Tubular	700	-	1.6-2.0	-	*E.Coli* separation	99.948	Diana et al., 2019
Fly ash, Bauxite, PVA, MoO_3, AlF_3	Pressing	Flat	1200	48.6±0.5		81.2±3.2	-	-	Zhu et al., 2015a
Fly ash, Bauxite, PVA, WO_3, AlF_3	Pressing	Flat	1400	51.9 ± 0.3	0.48	68.7 ± 6.1	Oil-in-water emulsion	99	Chen et al., 2016
Fly ash, PVA	Slip casting	Tubular	800	51	0.25	-	Textile water	**COD:** 75 **Color:** 90	Jedidi et al., 2011

Raw materials	Method	Configuration	Sintering temperature (ºC)	Porosity (%)	Pore size (µm)	Mechanical strength (MPa)	Applications	Rejection (%)	References
Fly ash, Kaolin, $CaCO_3$, H_3BO_3, Na_2CO_3, $Na_2SiO_3.9H_2O$	Pressing	Flat	750-900	~34.36 –39.0	~0.65 – 1.81	-	Oil-in-water emulsion	96.7–99.5	Agarwal et al., 2020
Fly ash, Kaolin, Sodium metasilicate, Na_2CO_3, Boric acid, Fullers' clay	Pressing	Flat	800	29.9	0.428	24.4	Protein (Bovine serum albumin) rich water	92	Gupta and Anandkumar, 2018
Fly ash, Quartz, $CaCO_3$, PVA	Pressing	Flat	1100	39	1.3	6.99	Oil-in-water emulsion	96.972	Suresh et al., 2016
Fly ash, Methocel, Amijel, Starch	Extrusion	Tubular	1125	51	4.5	19.5	-	-	Jedidi et al., 2009
Fly ash, Methylcellulose	Extrusion	Tubular	1190	-	2.13	-	-	-	Fang et al., 2011
Fly ash, methylcellulose	Extrusion	Tubular	950-1190	41±1	1.25	-	Kiwi juice clarification	SS: 100 Color: 100	Qin et al., 2015
Fly ash, Water, Methylcellulose, DSX 3290, Lomar D	Slip casting	Tubular	1000	-	0.77	-	Oil-in-water emulsion	95	Fang et al., 2013
Alumina, Coal fly ash	Centrifugal casting	Tubular	1200	~25-40	-	7.4-12	Corn starch water	> 99	Rocha et al., 2021
Fly ash, Bauxite, PES, PVP, N-methyl-2-pyrollidone	Phase inversion	Hollow fibre	1400	51	1.02	85.8±3.1	Oil-in-water emulsion	92-97	Zhu et al., 2016

Therefore, the aforementioned reports on the implementation of fly ash ceramic membranes in various wastewater treatment processes clearly reveal its versatile application in the environment sector. Due to their excellent rejection and appreciable permeate flux, these membranes are of interesting topic for future research in the field. The summary of various literatures available on fly ash-based ceramic membrane is presented in Table 1.2.

1.6.2 Applications of pressure driven membrane technology

As previously mentioned, the numerous advantages associated with the use of membrane technology in separation and purification operations have made the applications of this technology manifolded. Observing the success stories of implementation of membrane technology in different purification operations, an attempt has been made to evaluate the efficiency of the fabricated fly ash-based tubular ceramic membrane while implementing in various separation processes. The following literature review, therefore, corresponds to the various options that can be explored in regard to implementation of the fabricated membrane in different liquid phase separation processes.

1.6.2.1 Treatment of poultry slaughterhouse wastewater

Poultry slaughterhouse industry needs a huge quantity of water for its processing, which generates a large amount of wastewater. Starting from slaughtering and scalding to evisceration of birds, a huge amount of water is needed. A survey conducted on the generation of wastewater by poultry industries reported that almost 26.5 litres of water is required for processing one broiler. Thus, one can have an idea about the amount of wastewater generated by those industries across the world. The wastewater generated is highly rich in protein, fat, BOD, COD as well as total solids content. The total solids content in such water ranges from 600-800 mg/L, along with BOD and COD as high as 2000 and 9000 mg/L, respectively, which makes them

inappropriate for disposing directly to the environment (Malmali et al., 2018). The conventional treatment methods found in literature used for treating poultry processing water are gradually diminishing with the upliftment of membrane filtration technology. Conventional processes such as dissolved air flotation, activated sludge process and electrocoagulation nullify the chances of potential recovery of nutrient proteins that are available in such water as these processes turn all the valuable nutrients into sludge, thus reducing their reusability. Moreover, processes like electrocoagulation, flocculation may allow the residual iron or other toxic components to combine with precipitated protein, thus reducing their usability in biological applications (Avula et al., 2019). Membrane filtration, being a zero-chemical technology, helps to overcome these disadvantages. Keeping in mind the numerous advantages offered by membrane filtration, various research groups have reported the use of this technology for the treatment of poultry slaughterhouse wastewater (Shih and Kozink, 1980; Sardari et al., 2018; Bialas et al., 2015; Basitere et al., 2017). However, the literature study regarding the treatment of poultry processing wastewater using membrane filtration revealed that research works already done were primarily carried out using polymeric membranes. The use of ceramic membranes for this purpose is still in an infant stage. The history of using membranes for treating poultry wastewater started back in late-80s, when Jason and co-workers made an attempt to treat poultry processing wastewater with the purpose of recovering nutritional by-products. Commercial non-cellulosic tubular membrane with MWCO of 50 kDa was used for this purpose and the membrane significantly reduced the total solids, nitrogen, protein as well as COD content of the feed water along with recovering 24-45% of fat and 30-35% of protein as the by-product (Shih and Kozink, 1980). Commercial membranes made up of polyether sulfone and regenerated cellulose, having molecular weights in the range of 10-300 kDa, were also used to purify bird washer and chiller water generated in poultry industry. Those membranes were capable of achieving BOD and COD reductions above 90% along with

complete removal of total suspended solids and fats, oil and grease present in the feed water. It was also noticed that the membranes performed well in case of bird washer water as compared to chiller water as the size of particles present in chiller water is way smaller than the former one (Avula et al., 2019). A similar kind of rejection performance was also observed with UF-25-PAN membrane (Yordanov, 2010). The high molecular weight compounds present in poultry processing water cause severe membrane fouling, which demands the use of a pre-treatment step before proceeding towards membrane filtration. Keeping this fact in mind, another group of researchers adopted a hybrid process consisting of electrocoagulation followed by membrane separation using a regenerated cellulose embedded polypropylene membrane. Implementation of electrocoagulation before membrane separation not only reduced fouling, but also improved retention performance of the membrane. The combined process effectively reduced almost 85% of total suspended solids and fats, oil and grease from the raw water sample (Sardari et al., 2018). Another article mentioned about the use of a thin film nanofiltration membrane with pore sizes in the range of 150-300 Da, which reduced the COD level of poultry wastewater by 90%. Combination of this membrane and a polysulfone ultrafiltration membrane was able to achieve even higher COD removal than this. It needs mention that the authors also investigated the efficiency of RO membranes in COD removal and found that those membranes offer the highest removal of organic matter. But, owing to higher cost associated with RO membranes, the use of RO in treating poultry wastewater is limited (Coskun et al., 2016). Another group of researchers also investigated the efficacy of polysulfone membrane in achieving higher rejection of proteins from poultry processing water. Use of 30 kDa polysulfone membrane, thus helped them achieve almost 100% retention of all crude proteins present in the wastewater. The COD level of the permeate also went down by 58.86%, albeit the achieved COD is not under the safe discharge limit. It has been concluded that besides the poultry processing waste products, the different kinds of chemicals used during

the whole processing also contribute to the COD of the sample. Higher content of organic matter is the prime cause of severe membrane fouling observed during the experimental run. It is advised that running the experiments far above the isoelectric point of protein can offer little help towards reducing the membrane fouling through reduction of protein agglomeration and coagulation (Lo et al., 2005). Microfiltration and ultrafiltration was also carried out separately to purify poultry processing wastewater, where the microfiltration process resulted in more than 75% and 90% reduction in COD and TSS, respectively. On the contrary, the ultrafiltration process removed greater than 85% COD and above 99% TSS, respectively (Białas et al., 2015). Basitere et al. made an appreciable effort to couple static bed granular reactor (SBGR) with a 40 nm ceramic α-alumina membrane to separate out the suspended solids, fats, oils, etc. present in poultry slaughterhouse wastewater and reported about very high removal efficiency of the membrane (Basitere et al., 2017). Table 1.3 corresponds to the summary of available literature regarding the use of membrane technology in the treatment of poultry slaughterhouse wastewater.

1.6.2.2 Treatment of starch processing industry wastewater

Starch processing industries are one of the major food processing industries and are responsible for the generation of a huge quantity of wastewater during various operations. From steeping to recovery of different by-products such as starch and fibers, water is being used as a carrier in most of the starch industries. Use of such a large quantity of water during processing is the prime cause behind the generation of large volumes of wastewater in these industries. It has been reported that any standard corn starch industry generates 5-11 m^3 of wastewater for grinding one metric ton of starch (Subhaneel et al., 2018). The wastewater generated in the starch processing industry contains starch as its main constituent. Starch rich wastewater comprises of a vast amount of total suspended solids (TSS) and is known to have high turbidity

as well as chemical oxygen demand (COD) (Cancino et al., 2006). Such water, when discharged to water bodies without proper pre-treatment, can cause hazards for aquatic flora and fauna by depleting the dissolved oxygen level of water bodies. Moreover, the suspended solids in water can act as the site of adsorption for various metals and pathogens, thus polluting water in a very destructive way (Gray et al., 2000). In this context, the need of the hour is to find a solution to reduce the increased rate of water pollution across the globe.

The increased popularity of membrane separation processes drives researchers' attention for its implementation in separation and purification of starch processing industry wastewater. Starch granules, being micron-sized, can be retained using microfiltration membranes, whose pore diameters range from 0.1-10 µm (Baker, 2012). Few studies have mentioned the efficacy of microfiltration membranes in the treatment of starch processing industry wastewater. Rocha et al. fabricated asymmetric ceramic membranes using coal fly ash to treat synthetic corn starch wastewater and was able to achieve above 99% retention of starch (Rocha et al., 2020). Another group of scientists used similar model solutions and complete retention of starch molecules was observed by a tubular stainless steel-titania composite membrane, all thanks to the bigger size range of starch molecules, ranging from 1-10 µm (Shukla et al., 2000). Real corn starch industry wastewater was treated by a combination process of sedimentation, microfiltration and reverse osmosis. While sedimentation as well as microfiltration are mainly used for removing suspended particles in corn starch wastewater, reverse osmosis does the job of removing biochemical oxygen demand perfectly (Cancino-Madariaga and Aguirre, 2011). Synthetic suspensions of sago as well as wheat starch were also taken under consideration for microfiltration purposes, and satisfactory performance of membrane regarding removal of turbidity, total suspended solids and chemical oxygen demand was observed (Ikonić et al., 2011; Ling-Chee et al., 2019). During the treatment of wheat starch suspension, it was observed that the optimum condition for running the filtration experiment is maximum cross flow rate

and minimum concentration as it corresponds to minimum membrane fouling and subsequent flux decline (Ikonić et al., 2011). Ling-Chee et al. observed severe flux decline with increased transmembrane pressure, thus concluding that membrane separation operations should be conducted at lower pressures to avoid a drastic decline in flux. They also reported that use of membranes with higher surface area is beneficial for obtaining higher permeate flux (Ling-Chee et al., 2019).

Besides being used to reduce the above-mentioned parameters of starch industry effluent, membranes can also be applied to recover the starch present in wastewater. As already mentioned, starch industry wastewater mainly consists of starch with traces of impurities. Hence, after microfiltration of starch wastewater, the starch present in concentrated feed can be recovered for reuse in different food processing applications. Reuse of recovered starch, with minimal further processing, thus will aid in preventing its wastage (Ikonić et al., 2011). Concentration factor of 5.6 (56 per m^2 membrane area) was observed during the tangential flow filtration of sago starch suspension. It was recommended that the recovered starch has the potential to be used as cattle feed (Ling-Chee et al., 2019). Similar experiments were also conducted to recover starch from suspensions of wheat and amaranth starch. However, the recovery efficiency of these starch is not as good as the sago starch, concentration factor lying at around 25 per m^2 membrane area (Hinková et al., 2005). Table 1.4 represents the summary of the literature regarding treatment of starch suspensions using membrane filtration technology.

Table 1.3 Summary of literature regarding treatment of poultry processing water using membrane filtration

Membrane	**Pore size**	**Conditions**	**Permeate flux ($10^6 \times m^3/m^2 s$)**	**Rejection/recovery**	**References**
Non-cellulosic tubular membrane (Abcor HFM)	50000 Da	**P:** 275 kPa **CFV:** 57 L/min	4.71	**TSS**: 85% **COD:** 95% **Ash:** 63% **TKN**: 86% **Protein**: 94%	Shih and Kozink, 1980
PES and regenerated cellulose commercial membrane	10-300 kDa	**T**: Ambient temperature **CFV:** 1.21 L/min **P:** 67.5 kPa	-	**BOD**: upto 93% **COD**: upto 94% **TSS**: 100% **FOG:** 100%	Malmali et al., 2018
Commercial UF-25-PAN polymeric membrane	-	**P:** 400 kPa	-	**Fat**: 99% **TSS:** 98% **COD, BOD:** >94%	Yordanov et al., 2010
Regenerated cellulose embedded polypropylene support	30 kDa	**pH**: 6.7 **CFV:** 1.2 L/min **P:** 70 kPa **Coagulant in electrode**: Fe or Al	~25	**FOG, TSS**: 100% **BOD, COD**: >90%	Sardari et al., 2018
UF: Polysulfone **NF:** Thin film	**UF:** 30000 **NF:** 150-300	**pH:** 6.6 ± 0.1 **P**: 500-2500 kPa	~0.833	**COD:** 90% (NF)	Coskun et al., 2015
Polysulfone	30 kDa	**pH:** 7.0 **T:** 25 ˚C **P:** 96 kPa	27.78	**COD:** 58.86% **TS:** 35.79% **Crude proteins**: ~100%	Lo et al., 2005

Membrane	Pore size	Conditions	Permeate flux ($10^6 \times m^3/m^2s$)	Rejection/recovery	References
MF: Commercial membrane **UF**: Regenerated cellulose Commercial membrane	**MF**: 0.22 µm **UF:** 3 and 30 kDa	**MF:** **T:** 20 ˚C; **CFV:** 2 m/s; **P:** (30±5) kPa **UF:** **T:** 20 ˚C; **CFV:** (2.5±0.2) m/s; **P:** (200±15) kPa	-	**MF:** **COD:** >75% **TSS**: >90% **UF:** **COD:** >85% **TSS**: >99%	Bialas et al., 2014
α-alumina	40 nm	**pH**: 6.78 **T:** 21.2 ˚C	-	**COD:** 98% **TSS:** 99.8% **FOG:** 92.4%	Basitere et al., 2017

[#]P: Pressure, T: Temperature, CFV: Cross flow velocity, MF: Microfiltration, UF: Ultrafiltration, TKN: Total Kjeldahl Nitrogen, FOG: Fats, Oil and Grease

Table 1.4 Summary of prior arts regarding treatment of starch suspension/wastewater

Membrane material	Starch source	Configuration	Pore size (µm)	Conditions	Permeate flux ($\times 10^6$ m^3/m^2s)	Rejection	C.F	C.F/m^2	References
α-Alumina	Wheat	Tubular	0.2	**A:** 0.125 m^2 **P:** 300 kPa **C_f:** 5 g/L **CFV:** 1.39×10^{-4} m^3/s **T:** 22-25 °C	-	99%	3	24	Ikonić et al., 2011
Polysulfone	Sago	Flat sheet	0.45	**A:** 0.1 m^2 **C_f:** 10 g/L **CFV:** 7.5×10^{-5} m^3/s **T:** 20 °C	93.9	**TSS:** 100% **Turbidity:**> 99.5% **COD:** > 80%	5.6	56	Ling-Chee et al., 2019

Membrane material	Starch source	Configuration	Pore size (µm)	Conditions	Permeate flux ($\times 10^6$ m^3/m^2s)	Rejection	C.F	C.F/m^2	References
Titania on stainless steel support	Corn	Tubular	0.1	**A:** 0.35 m^2 **C_f:** 10 g/L **P:** 140 kPa **CFV:** 5 m/s **T:** 49 °C	~ 41.7	100%	-	-	Shukla et al., 2000
Alumina, Coal fly ash	Corn	Tubular	-	**C_f:** 0.25 g/L **P:** 200 kPa **CFV:** 4.17×10^{-5} m^3/s **T:** 24 °C	-	99%	-	-	Rocha et al., 2020
Commercial membrane (Composition not known)	Amaranth	Tubular	0.1	**A:** 0.2 m^2 **C_f:** 3% **P:** 100 kPa **CFV:** 5 m/s **T:** 40 °C	5.56	-	5	25	Hinková et al., 2005
Polyethersulfone		Plate and frame	0.65	**A:** 0.04 m^2 **C_f:** 4.09 g/L **P:** 250 kPa **CFV:** 1.83×10^{-4} m^3/s **T:** 20.11 °C	68.67	98.7%	-	-	Sargolzaei et al., 2011

[#]P: Pressure, T: Temperature, CFV: Cross flow velocity, A: Area of the membrane used for filtration, C_f: Concentration of feed

1.6.2.3 Treatment of silk floss processing wastewater

The process of raw silk production involves the extraction of silk fibres from the cocoon by killing off the cocoons and degumming those silk yarns. The whole process of cooking the cocoons and degumming the silk threads requires a huge quantity of water. The generated wastewater is very high in organic matters with CODs ranging from 7-20 g/L. Usually, silk industries produce two types of wastewater: one comes from the cocoon cooking operation, where the silk worm cocoons are heated to get the silk threads out of it. Second source of wastewater is the silk degumming process, where the raw silk sheets are treated with alkaline agents to remove the gums sticking to them. These glue-like substances are highly rich in sericin protein, which needs to be separated for further use. It has been observed that the sericin content in cocoon cooking water is way lesser than the water obtained from degumming process. The conventional ways for recovering sericin from silk processing wastewater include drying as well as acidulation precipitation. But, drying at higher temperatures can cause denaturation of sericin protein, restricting its further use. Similarly, the acidulation precipitation process requires the use of rugged equipment which are capable of withstanding a high acidic environment. Moreover, both processes are highly expensive. Owing to these disadvantages, membrane filtration is being implemented in recent times for treating silk floss processing wastewater and subsequent separation of sericin from silk processing wastewater. Membrane filtration, besides being affordable, also retains the physical properties of sericin protein without any damage. Moreover, the water obtained as filtrate can further be reused, which may not be possible for the other conventional processes. These advantages of membrane filtration over the conventional processes made the researchers to consider this process as one of the alternatives for sericin recovery from silk processing wastewater.

It is to be mentioned that the use of membrane in treating silk floss processing wastewater is still in its infant stage. In the mid 90-s, the use of membrane for sericin recovery from silk

industry wastewater started. Commercial spiral wound polymeric membranes (polyvinylidene fluoride and polyamide) with different molecular weights were used for this purpose. The membranes were able to recover more than 90% of the sericin present in the wastewater along with high reduction in COD values. It has been found that the sericin recovery from water decreases with the ageing of the wastewater. Hence, it is always advisable to filter the wastewater immediately after production to achieve highest sericin recovery (Fabiani et al., 1996). Another study reported the use of thin film and polyether sulfone ultrafiltration and nanofiltration membranes to treat the cocoon cooking wastewater. It was observed that the membrane roughness also plays a crucial role in the recovery of sericin protein as they get adhere to the membrane surface, causing membrane fouling and severe flux decline. The experimental results revealed that the ultrafiltration membrane could retain only 37-60% of the sericin, while the nanofiltration membrane retained almost 97-99% of the sericin present in the cocoon cooking water (Capar et al., 2008). However, treatment of sericin laden water sometimes causes severe membrane fouling, which affects the membrane performance. Taking this matter into consideration, another group of scientists made an effort to integrate three hybrid processes: acidulation, ultrafiltration as well as nanofiltration for the treatment of such water. It was reported that the combination of acidulation as well as polymeric membrane filtration efficiently recovered almost 86% of the sericin from raw water. The researchers repeatedly diluted and subsequently filtered the sericin permeate obtained from membrane filtration to achieve more and more sericin recovery (Li et al., 2015). Another study reported the reduction of 96-97% BOD and COD from silk reeling water using membrane filtration. Moreover, the quality of sericin recovered through membrane ultrafiltration was found to be compatible with the quality of commercially available sericin (Vaithanomsat et al., 2008). Table 1.5 represents the summary of literatures available regarding treatment of silk reeling wastewater and subsequent recovery of sericin from concentrated feed.

Table 1.5 Summary of literature regarding treatment of silk floss processing water using membrane filtration

Membrane	Pore size	Conditions	Recovery/rejection	References
Spiral wound (MOCU): Composite polyamide **Spiral wound (OSMO 411TA):** PVDF (All are commercial membranes)	**Spiral wound (MOCU):** 15000 Da **Spiral wound (OSMO 411TA):** 15000-20000 Da	**Spiral wound (MOCU): P:** 300-350 kPa; **T:** 20-40 ˚C; **CFV:** 9.72×10^{-4} m^3/s **Spiral wound (OSMO 411TA): P:** 330 kPa; **T:** 35-40 ˚C; **CFV:** 8.89×10^{-4} m^3/s	**Spiral wound (MOCU):** 92% sericin, 87% COD **Spiral wound (OSMO 411TA):** 95% sericin, 97% COD	Fabiani et al., 1996
Thin film, PES	**UF:** 1-20 kDa **NF:** 190-100 Da	**P:** **UF:** 200 kPa; **NF:** 500 kPa **T:** **UF:** 18-22 ˚C; **NF:** 21-25 ˚C	**NF:** 97-99% sericin **UF:** 37-60% sericin	Capar et al., 2008
UF: Polysulfone **NF**: Polypiperizine-amide	**UF:** 6 nm **NF:** 1-5 nm	**P:** 100-1000 kPa **T**: 20 ˚C	**Sericin:** 86% (Combined UF and NF)	Li et al., 2015
UF: PVC alloy; **NF:** Aromatic polyamide	**UF**: 10 nm; **NF:** 0.1 nm	**UF:** **P:** 300 kPa; **Flux:** 1.2 L/min **NF:** **P:** 350 kPa; **Flux:** 0.8 L/min	**Sericin:** 26% (Combined UF and NF)	Wu et al., 2014
Millipore UF membrane (Amicon model)	20-80 kDa	**pH:** 7.5, 8.5, 9.5 **T**: 50, 55, 60 ˚C	**BOD, COD:** around 96-97%; **TS:** 99%	Vaithanomsat et al., 2008

[#]P: Pressure, T: Temperature, CFV: Cross flow velocity, UF: Ultrafiltration, NF: Nanofiltration

1.6.2.4 Separation of glycerol from biodiesel

Biodiesel, in recent times, is one of the most sought-after fuel alternatives owing to its biodegradability, renewability, non-toxicity as well as excellent emission characteristics (Mishra and Goswami, 2018; Kiss et al, 2006). However, biodiesel used in engines should satisfy the required norms provided in ASTM D6751 and EN14214 in order to maintain the engines in good condition (ASTM D6751-20; EN 14214). Glycerol, the major by-product obtained in biodiesel production via methanol transesterification, can be the cause of severe engine corrosion. Besides, the excess glycerol content in biodiesel deposits in the tank bottom, thus creating issues in storage and handling (Gomes et al., 2010). In view of this, the glycerol phase of the biodiesel emulsion needs to be removed and the residual free glycerol content of biodiesel should be reduced to below 0.02 wt%. The glycerol produced during the transesterification process is generally separated using conventional processes such as centrifugation, decantation (Raman et al., 2019; Saleh et al., 2010). These processes result in the formation of two-layered phases; the one with higher density corresponds to the glycerol rich phase while the lean phase represents the methyl ester phase. Even though the decantation of glycerol is an affordable technique, it is quite a time-consuming process. Centrifugation is an efficient process and also reduces operational time. However, it is highly expensive (Raman et al., 2019; Saleh et al., 2010). It has also been found in the literature that many industries perform water washing of the crude biodiesel to remove the glycerol from the biodiesel (Atadashi et al., 2011). However, water washing process cannot be considered an efficient method as the separation is highly dependent on temperature as well as water to biodiesel ratio. The separation efficiency was found to increase with increasing the value of both the factors. The need for higher water to biodiesel ratio not only generates the demand of multistage water washing, but also releases a huge quantity of wastewater laden with high COD and pH, and the treatment of this wastewater becomes another matter of concern (Atadashi et al., 2011; Rahayu

and Mindaryani, 2007). The aforementioned restrictions associated with the conventional processes for separating glycerol from biodiesel made the scientists to think of membrane filtration as a possible alternative. Moreover, the conventional methods, in many cases, cannot produce biodiesel with required standards and hence, the need for another treatment process, such as membrane filtration, is required (Atadashi et al., 2011).

A few studies have reported about the use of membrane filtration for the separation of glycerol from biodiesel (Gomes et al., 2010; Alves et al., 2013; Bansod and Rathod, 2018; Wang et al., 2009; Gomes et al., 2013). Alves et al. reported the use of commercial cellulose ester microfiltration membranes (0.22 µm and 0.3 µm) as well as poly (ether sulfone) ultrafiltration membranes (10 kDa and 30 kDa) for the separation of excess free glycerol from crude biodiesel, which was remained even after four stages of decantation process (Alves et al., 2013). It was found that the membrane process resulted in biodiesel permeate having only 0.02-0.03 wt% free glycerol (Alves et al., 2013). Another group of researchers used polyacrylonitrile membranes with pore sizes of 6 kDa and 15 kDa for the same purpose and was capable of producing permeates, satisfying the required norms (Bansod and Rathod, 2018). Wang et al. reported the use of ceramic membranes for the separation of free glycerol from biodiesel produced from refined palm oil, where commercial multichannel tubular membranes with pore sizes 0.1 µm, 0.2 µm and 0.6 µm were used for the treatment purpose (Wang et al., 2009). A couple of experiments conducted using these membranes made the researchers to conclude that the membrane having 0.1 µm pore size was capable of giving high flux along with higher rejection (Wang et al., 2009). Reports were also found regarding the use of commercial α-alumina/TiO_2 membranes with pore diameters in the range of 0.05-0.2 µm to separate glycerol directly from biodiesel emulsion, without any pre-treatment process. Experiments were conducted for a wide range of pressures, and it was found that the permeate produced satisfied the norms provided in ASTM D6751 and EN14214 (ASTM D6751-20; EN 14214; Gomes et

al., 2010; Gomes et al., 2013). The summary of the available literatures regarding separation of glycerol from biodiesel is mentioned in Table 1.6.

1.6.2.5 Removal of bacteria from milk

Milk can be considered as one of the most important fluids after water, upon which human lives are completely dependent. Drinking milk not only helps in the growth and development of the bones, but it can also be useful in preventing various undesired health consequences such as breast cancer, colon cancer, rickets, obesity in children, and so on (Swami, 2011). The numerous advantages associated with drinking milk have resulted in an exponential increase in milk production worldwide and subsequent growth of the dairy industry. It has been reported that the world has seen a significant increase in milk production from 530 million tonnes in 1988 to 843 million tonnes in 2018, which is more than 59%. India being the largest producer, contributes to almost 22% of world's production, followed by the Europian Union and USA (Food and Agriculture Organization of the United Nations, 2020). However, this huge quantity of milk produced needs to be purified before consumption as it may also be the shelter for various pathogens; some of them may cause serious health consequences to human being. The conventional way of milk sterilization makes use of high temperature pasteurization. However, thermotolerant bacteria can withstand very high temperatures, making the pasteurization process ineffective. In some cases, the inactivated bacteria continue to release some enzymes, causing spoilage of milk (Madaeni and Yasemi, 2009; Saboya and Maubois, 2000). Besides, the temperature rise may also cause change in phase, denaturation of protein as well as loss in sensory attributes of milk (Kumar et al., 2013).

Table 1.6 Encapsulation of literature corresponding to treatment of glycerol enriched biodiesel using membrane filtration

Membrane composition	Pore size	Experimental conditions	Free glycerol in permeate (wt%)	Permeate flux[#]	References
ommercial ceramic membrane (Pall Membrane CO., USA)	0.1 µm	**T:** 60 ˚C **P:** 150 kPa	0.0108±0.0034	300.00 L/m^2h	(Wang et al., 2009)
Commercial α-AlO_3/TiO_2 membrane (Shumacher GmbH-Ti 01070	0.2 µm	**T:** 60 ˚C **P:** 200 kPa **C_f:** 10 wt%	0.06±0.009	~50.00 kg/m^2	(Gomes et al., 2010)
Commercial α-AlO_3/TiO_2 membrane (Jiangsu Jiuwu Hi-Tech Co., China)	0.02 µm	**T:** 40 ˚C **P:** 200 kPa **C_f:** 0.42 wt% **CFV:** 150 L/min	0.007	9.08 kg/m^2h	(Atadashi et al., 2012)
Commercial polyether sulfone membranes (GE Osmonics, USA)	10 kDa	**T:** 25 ˚C **P:** 400 kPa **C_f:** 0.049 wt%	0.020	55.00 kg/m^2h	(Alves et al., 2013)
Commercial α-AlO_3/TiO_2 membrane (Shumacher GmbH-Ti 01070)	20 kDa	**T:** 50 ˚C **P:** 300 kPa **C_f:** 6.80 wt%	0.014±0.002	70.00 kg/m^2h	(Gomes et al., 2013)
Polyacrylonitrile membrane	6 kDa	-	0.017	-	(Bansod and Rathod, 2018)
Commercial α-AlO3/TiO2 membrane (Shumacher GmbH-Ti 01070)	0.05 µm	**T:** 50 ˚C **P:** 100 kPa **C_f:** ~ 7 wt%	0.013±0.003	101.1 kg/m^2h	(Gomes et al., 2015)
Commercial α-AlO3/TiO2 membrane (Shumacher GmbH-Ti 01070)	0.2 µm	**T:** 50 ˚C **P:** 200 kPa **C_f:** 6.2 wt%	0.006±0.002	6.9 kg/m^2h	(Gomes et al., 2011)

[#]P: Pressure, T: Temperature, C_f: Concentration of feed

These disadvantages raised the need for an efficient alternative for bacteria removal from milk, thus convincing Olesen and Jensen to bring membrane filtration into the picture in the late-80s. Being an initiative in this area, this process was able to remove almost 99.99% of the total bacteria that was present in the feed milk (Olesen and Jensen, 1989). Following the footsteps of Olesen, another group of scientists carried out microfiltration to separate *Salmonella* and *Listeria* cells from milk. These cells are representative of the pathogenic cells bearing the same nomenclature. *Salmonella* infection can induce symptoms like diarrhea, fever, etc., in human beings, while the infection from *Listeria* can be more fatal to human causing meningitis, abnormal birth consequences, miscarriages, etc. (Gray and Killinger, 1996; Kurtz et al., 2017). A commercial membrane with 1.4 µm pore size was able to achieve log normal reductions (LRVs) up to 1.9 and 2.5 at 35 ˚C for *Listeria* and *Salmonella*, respectively. It was observed that with increasing temperature, retention of *Salmonella* increased while no significant variation was observed in the rejection of *Listeria*, the latter being more heat resistant. Though the effect of milk temperature during microfiltration is known to have minimal influence on membrane's rejection performance in most of the cases, but it has been reported that an increase in feed temperature can significantly increase the quantity of permeate flux obtained (Wang et al., 2019). This might be because of the reduction in the apparent viscosity of feed as well as permeate at higher temperatures (France et al., 2010). Other commercial ceramic membranes with a similar pore diameter were also used for this purpose and all of them reported similar patterns of bacterial retention (Pafylias et al., 1996; Trouvé et al., 1991). Another study carried out by Holm et al. also showed promising results in bacteria retention by microfiltration membrane. In this study, milk was first separated into cream and skim milk portions, the latter being used for microfiltration. The microfiltered milk permeate could reduce the bacterial content by 99.7% and hence, it could be used for commercial purposes without further sterilization (Holm et al., 1989). A similar approach was made by another group of researchers,

where after separation of the cream from raw milk, the use of a 1.4 µm pore-sized ceramic microfiltration membrane could reduce the total bacterial count of skim milk by 2-3 LRV (Hoffman et al., 2006).

However, the process of milk microfiltration can cause severe membrane fouling, which can be taken care of by the use of either high cross flow velocity or by periodic reversal of transmembrane pressure through backshock (Fritsch et al., 2005; Jonsson et al., 1997). Use of third generation membranes, where modifications are made on its configuration, can also serve this purpose, thereby giving almost uniform permeate flux throughout the experimental duration. Experiments conducted using various third generation membranes reveal that membranes with geometries resulting in higher shear stress are more effective in minimizing the effect of concentration polarization, thus improving the flux produced through it (Fernández García and Rodríguez, 2015). Another membrane property that influences the rejection performance of the third generation membranes is their pore size distribution. Among various third generation membranes with the same mean pore diameter, the ones with narrower pore size distribution is found to show better microbial retention efficiency as compared to the ones with broader pore size distribution (GeÂsan-Guiziou, 2010).

Literature has also reported about the use of membranes having pore sizes lesser than 1.4 µm for the removal of bacteria from milk. A polyvinylidene fluoride membrane with 0.22 µm pore size retained almost 99% of the total bacteria present in the milk, thus enhancing the shelf life of the milk (Madaeni and Yasemi, 2009). Tomasula et al. reported that microfiltration carried out with 0.8 µm membrane also portrayed promising results in attaining log normal reductions above five. However, lesser pore sized membranes have the disadvantage of retaining casein protein of milk as the molecular weight of casein protein is very high (Tomasula et al., 2011). Moreover, the flux obtained through such membranes is very low in quantity. Observing these disadvantages, most of the research groups recommended the use of membranes with 1.4 µm

pore size for microfiltration of milk, which can facilitate satisfactory removal of bacterial contaminants from milk without compromising on flux or retention of healthy milk components (Fernández García et al., 2013). The detailed information about the literatures available regarding milk microfiltration is mentioned in Table 1.7.

1.6.2.6 Removal of viruses and bacteria from contaminated water

Different unlawful human induced activities such as improper disposal of sewage, failure of the septic system, disposal of animal wastes can be considered as the main culprits for water contamination across the globe (Owa, 2014). It has been observed that discharge of such materials to surface water not only increases the turbidity, BOD and COD of the water but also leads to the growth of various harmful pathogens (e.g., viruses, bacteria, oocysts) present in them. A study revealed that as of 2012, almost 25% of the world's population is drinking such faecally contaminated water, which is laden with a huge number of harmful pathogens (Gall et al., 2015). Consumption of such contaminated water can be the cause of some severe health consequences, diarrhoea, hepatitis, meningitis, encephalitis, polio, just to name a few. The alarming increase in water pollution and subsequent scarcity in drinking water has led people to go for various conventional technologies of wastewater treatment such as chlorination, boiling, ultraviolet and infrared disinfection and so on. However, use of chlorine in water treatment plants cannot be recommended as it reacts with the humic acid as well as fulvic acid present in surface water producing a wide range of disinfectant by-products (DBPs), which may have adverse effects on human health, causing bladder cancer and abnormal birth outcomes (Villanueva et al. 2007; Waller et al., 1998). Moreover, boiling is an extremely energy consuming process and use of ultraviolet and infrared disinfection cannot be afforded by all sections of society owing to high expenses associated with them (McCutcheon et al., 2005).

Table 1.7 Summary of literature regarding microfiltration of milk for bacteria rejection

Membrane	Pore size	Bacteria	Conditions	Permeate flux ($10^5\times$ m^3/m^2s)	Rejection	Reference
Membralox filter	1.4 µm	-	**C_f**: 10^8-10^9 CFU/mL; **pH**: 6.7±0.1; **P:** 100 kPa	9.72	4-5 LRV	(Pafylias et al., 1996)
Membralox cartridge filter	1.4 µm	*Salmonella* and *Listeria* cells	**T:** 35 ˚C; **P:** 320-350 kPa **C_f:** 10^2-10^6 CFU/mL	19.4	*Salmonella*: 2.5 LRV *Listeria*: 1.9 LRV	(Madec et al., 1992)
Membralox multi channel ceramic filter	1.4 µm; 0.8 µm	*Bacillus anthracis*	**CFV:** 6.2 m/s; **P:** 127.6 kPa	7.58; 6.11	4.5±0.35 LRV; 5.91±0.05 LRV	(Tomasula et al., 2011)
Commercial Inside ceram (ZrO_2- TiO_2/TiO_2), Isoflux (TiO_2/TiO_2, Sterilox-GP (multi-layer α-alumina) membrane	1.4 µm	-	**CFV:** 6m/s **T:** (21±2) ˚C **C_f:** (5-10)×10^4 CFU/mL **P:** 50 kPa	~12.5	3.5-5 LRV	(Fernández García and Rodríguez, 2015)
Commercial Millipore polyvinyledenefluoride	0.22 µm	Vegetative cells and spores	-	-	99.1-99.5%	(Madaeni and Yasemi, 2009)
Commercial membrane (TAMI)	1.4 µm	-	**T:** 6 ± 1˚C; **CFV:** 7 m/s; **P:** 69 kPa	1.13	>3 LRV	(Fritsch et al., 2008)
Membralox ceramic membrane	1.4 µm	-	**T:** 50 ˚C	-	2-3 LRV	(Hoffmann et al., 2006)
Societe des Ceramiques Techniques α-Alumina membrane	1.4 µm	*E.Coli, B. Cereus*	**T:** 40 ˚C (Beginning); 60 ˚C (End)	-	99.7%	(Holm et al., 1989)

Membrane	**Pore size**	**Bacteria**	**Conditions**	**Permeate flux ($10^5\times$ m^3/m^2s)**	**Rejection**	**Reference**
Commercial membrane (TAMI)	1.4 µm	Vegetative cells	**T:** 6±1 ˚C; **CFV:** 7 m/s; **P:** 75 kPa; **C_f:** 4.11± 0.48 CFU/mL	0.58	3.4 LRV	(Wang et al., 2019)
Isoflux tubular membrane	1.2 µm	*Bacillus licheniformis; Geobacillus sp.*	**T:** 6 ˚C; **CFV:** (4.14 ± 0.01) m/s; **P:** 69.87 kPa; **C_f:** 10^6 CFU/mL	*Bacillus licheniformis*:1 .25; *Geobacillus sp:* 1.07	*Bacillus licheniformis*:4.57 LRV; *Geobacillus sp:* > 6 LRV	(Griep et al., 2018)
-	1.4 µm	*Bacillus cereus*	-	-	> 3.5 LRV	(Olesen and Jensen, 1989)
Alumina Membralox membrane	1.4 µm	*Clostridium tyrobutyricum*	**T:** 50±1 ˚C	18.83	> 4.5 LRV	(Trouvé et al., 1991)
Membralox XLAB3 membrane	1.4 µm	-	**T**: 40 ˚C; **CFV:** 7 m/s	6.92	> 3LRV	(Beolchini et al., 2004)

[#]P: Pressure, T: Temperature, CFV: Cross flow velocity, C_f: Concentration of feed, LRV: Log Reduction Value

Looking at the restrictions associated with the use of conventional methods, membrane filtration has become one of the most sought alternatives among all classes of people of society. The literature available regarding the separation of viruses from the water mostly denotes the use of polymeric membranes, along with few ceramic membranes (Table 1.8). Experiments conducted using bacteriophage Qβ and T4 as model viruses with different ceramic and polymeric membranes resulted in complete rejection of bacteriophage T4 and 99-99.9999% rejection of bacteriophage Qβ through all the membranes (Urase et al., 1996). In 1995, series of experiments conducted using polysulfone microfiltration membrane (0.20 µm) and polyvinyledene fluoride ultrafiltration membrane (30 kDa MWCO) for separation of polio virus alone as well as from mixtures containing polio virus along with either turbidity or *E.coli* revealed that the ultrafiltration membrane showed about 99% rejection at the cost of very low permeate flux. It was further observed that the presence of turbidity or *E.coli* improves the retention performance of the membrane by either blocking the larger pores or forming a cake layer on the membrane surface (Madaeni et al., 1995). Similar observation regarding retention of the virus through the addition of dirt or particulates into contaminated water was also reported by several other research groups (Huang et al., 2012; Urase et al., 1993; Urase et al.,1994). Moreover, it has been observed in many instances that size exclusion usually acts as the basic principle of virus separation from water. While zirconia ceramic nanofiltration membranes achieved virus retention up to 6 LRV, a commercial polyvinylidene fluoride hollow fibre membrane achieved a log normal rejection value of greater than three for bacteriophage MS2 and φX174, through size exclusion (Kroll et al., 2012a; Elhadidy et al., 2013). However, the role of electrostatic interaction in rejection of bacteriophage MS2 in the latter case cannot be denied, which may be attributed to the lower iso-electric point of the virus (Elhadidy et al., 2013). The research works of Van Voorthuizen et al. and Wallis et al. also mentioned about similar electrostatic virus retention mechanism through membranes made up of cellulose

acetate and cellulose nitrate membranes, respectively (Van Voorthuizen et al., 2001; Wallis et al., 1972). Ceramic membranes are also being fabricated using compounds such as yttria and magnesium oxide, which give positive charge to the membrane surface and aid in the retention of virus via electrostatic interaction (Werner et al., 2014; Wegmann et al., 2008; Michen et al., 2013). Besides these two mechanisms, successful virus retention can also be achieved through functionalization of larger pore sized membrane surface as well as through hydrophilic-hydrophobic interactions at the membrane surface. The results of all the above-mentioned literatures regarding virus removal using membrane technology are portrayed in Table 1.8.

Literature study on the use of membrane filtration technology for purifying bacteria contaminated water revealed the use of both polymeric as well as ceramic membranes. Polymeric membranes made up with materials such as polycarbonate, polypropylene, cellullose diacetate could achieve bacterial retention even greater than 9 LRV from contaminated water (Gander et al., 2000; Suchecka et al., 2003). Similarly, ceramic membrane modules with different configurations fabricated using various low-cost membrane precursors were also used for the purification of bacteria contaminated water, where the fabricated membranes retained 85-99.9999% of the bacteria present in the feed using the basic principle of size exclusion (Vasanth et al., 2011; Kaniganti et al., 2014; Diana et al., 2019). Another literature reported the use of titanium suboxide membranes, which could inactivate bacteria by synergistic interaction of electrochemical effects and depth filtration (Liang et al., 2018). Moving a step ahead, some researchers also tried to functionalize the membrane surface like the ones opted for virus separation to achieve better bacteria retention characteristics. It is well documented in literature that the use of substances with antimicrobial properties such as lysozyme, Degussa P-25 and poly(N-vinyl carbazole) for membrane surface functionalization can significantly improve membrane's bacteria rejection performance (Kroll et al., 2012b, Kroll et al., Kroll et al., 2012c; Ciston et al., 2008; Musico et al., 2014).

Table 1.8 Encapsulation of literature regarding separation of viruses from water using membrane technology

Membrane material	Pore size	Viruses	Conditions	Permeate flux ($10^5\times$ m^3/m^2s)	Rejection	Reference
Millipore polysulfone (MF) and Amicon polyvinylidene fluoride membrane (UF) (Commercial)	MF: 0.22 µM UF: 30 kDa	Poliovirus	**P:** 25, 50, 100, 200 kPa **C_f:** 10^4 PFU/mL	-	MF: 99% UF: 100%	(Madaeni et al., 1995)
Polysulfone, polycarbonate, polyvinylidene fluoride, etc.	-	Coliphage Qβ and T4	**CFV:** 0.8-1.2 m/s **P:** 20-50 kPa **C_f:** 10^7–10^8 PFU/mL	-	2-6 LRV	(Urase et al., 1996)
Polyvinyledene fluoride (hollow fibre)	0.1 µm	Bacteriophage MS2	**pH:** 6.7-7.7	1.50	Up to 3 LRV	(Huang et al., 2012)
Polyvinylidene fluoride	Median: 9 nm Distribution: 2-56 nm	Bacteriophage MS2, φX174	**pH:** 6.5; 7.6; 9.4 **T:** 22.0; 22.8; 23.5 ˚C **C_f:** **Bacteriophage MS2:** 3×10^9 PFU/mL ***φ*X174:** 10^{10} PFU/mL	1.58	Up to 4.7 LRV	(Elhadidy et al., 2013)
Polyvinylidene fluoride	0.22 µm	Bacteriophage MS2	**T:** 10–15 ˚C **C_f:** 10^2 PFU/mL	104.50-106.17	4.3-5 LRV	(Van Voorthuizen et al., 2001)
Commercial Millipore membrane filter	0.45 µm	Bacteriophage MS2	**C_f:** 10^4 PFU/mL	-	>80%	(Farrah, 1982)
Yttria stabilised Zirconia, 3-aminopropyltriethoxysilane, PVA	56.1 nm (closed packed); 58.6	Bacteriophage MS2, φX174	**C_f:** 10^9 PFU/mL	0.14	≥ 4 LRV	(Werner et al., 2014)

Membrane material	Pore size	Viruses	Conditions	Permeate flux ($10^5\times$ m^3/m^2s)	Rejection	Reference
	nm (loosely packed)					
Diatomaceous earth-based Katadyn filters coated with colloidal yttria	0.2 – 2 µm	MS2 Coliphage	**C_f:** 10^7 PFU/L **pH:** 5-9 **P:** 300 kPa	-	> 4 LRV	(Wegmann et al., 2008)
diatomaceous earth, layered silicates and MgO	1.6-2.0 µm	Bacteriophage MS2, φX174	**C_f:** 2×10^4 PFU/L **pH:** 7	-	about 4 LRV	(Michen et al., 2013)
Zirconia powder, 3-aminopropyltriethoxysilane, PVA	24 nm	Bacteriophage MS2, φX174	**C_f:** 10^7 PFU/mL **pH:** 5.8	-	6 LRV	(Kroll et al., 2012a)
Commercial ceramic water filter	-	Bacteriophage MS2	**C_f:** (5.7-9.5) $\times10^4$ PFU/mL	-	0.21-0.45 LRV	(Salsali et al., 2011)

[#]P: Pressure, T: Temperature, CFV: Cross flow velocity, C_f: Concentration of feed, LRV: Log Reduction Value

Table 1.9 Encapsulation of literature regarding separation of bacteria from water using membrane technology

Membrane	Pore size	Bacteria	Conditions	Permeate flux ($10^5\times$ m^3/m^2s)	Rejection	Reference
Clay, saw dust, water	40 µm	*E.coli*	**C_f:** 10^5-10^7 CFU/100 mL	-	>4 LRV	(Halem et al., 2016)
Mixed clay, fly ash	1.6-2.0 µm	*E.Coli*	**P:** 25 kPa	~0.69	99.048%	(Diana et al., 2019)
Polypropylene; polysulfone	5 µm; 0.4 µm	Coliforms	**P:** 6 kPa	-	5 LRV; 9 LRV	(Gander et al., 2000)

Membrane	Pore size	Bacteria	Conditions	Permeate flux (10^5× m^3/m^2s)	Rejection	Reference
Polypropylene, cellulose diacetate and polycarbonate hollow fibre membranes	0.2 µm, 0.4 µm	*Pseudomonas Diminuta*	-	-	9.15-13.9 LRV, almost all membranes showed 100% rejection	(Suchecka et al., 2003)
Commercial cellulose acetate membrane	0.8 µm	*E.coli, Bacillus subtilis*	**Surface modifier:** Poly(N-vinylcarbazole)-graphene oxide	-	*E. Coli:* 3 LRV *B.Subtilis*: 4 LRV	(Musico et al., 2014)
Kaolin, β-Quartz, $CaCO_3$	1.30 µm	*E. coli*	**T:**25˚C; **P:** 69-275 kPa; **C_f:** 6×10^4-6×10^5 CFU/mL	12.60-63.00	85%	(Vasanth et al., 2011)
Kaolin, Quartz, Boric acid, $CaCO_3$, PVA, Na_2CO3, Sodium metasilicate	(4.5±0.2) µm	*E. coli*	**P:** 206.7 kPa **C_f:** (14.9±0.5) $\times10^5$ CFU/mL	351.00	99.9999%	(Kaniganti et al., 2014)
Yttria stabilised zirconia membrane stabilized with 3-aminopropyltriethoxysilane, Piranha solution, N-(3-dimethylaminopropyl)-N-ethylcarbodiimide hydrochloride	≤0.2 µm	*Micrococcus luteus*	-	-	99.9%	(Kroll et al.,2012c)

Membrane	Pore size	Bacteria	Conditions	Permeate flux (10^5× m^3/m^2s)	Rejection	Reference
Zirconia UF membrane coated with Degussa P25, Anatase and mixed (anatase and rutile) phase sol gel	300 kDa	*Pseudomonas putida*	**C_f :** 10^6 CFU/mL	-	-	(Ciston et al., 2008)
Rice husk, naturally sourced raw clay-based membrane coated with silver nitrate solution	-	*E.coli*	**pH:** 7.0 and 7.8 **T:** 29 – 30˚C **C_f:** <1 and 145 CFU/100mL **Turbidity:** 1.1 and 8.4 NTU	-	~ 99%	(Brown and Sobsey, 2010)
Commercial Katadyn ceramic filter	0.2 µm	Thermo tolerant coliform	-	-	100%	(Clasen et al., 2004)
Commercially available Katadyn candle filter coated with colloidal silver	1 µm	Thermo tolerant coliform		-	4 LRV	(Clasen et al., 2005)
Soil, flour, grog	2.03 µm	*E.coli*	**C_f:** (7±2) × 10^9 MPN/100 mL	-	100%	(Oyanedel-Craver and Smith, 2008)

[#]P: Pressure, T: Temperature, CFV: Cross flow velocity, C_f: Concentration of feed, LRV: Log Reduction Value

Besides these examples, in countries such as Bolivia, Cambodia, Ghana, and Colombia, locally produced ceramic pot filters are being extensively used for purification of pathogen contaminated water. Such filters, after being impregnated with silver could achieve very high bacteria removal efficiency through the combined action of membrane filtration and bacteriostasis caused by silver impregnation (Brown and Sobsey, 2010; Clasen et al., 2004; Clasen et al., 2005; Oyanedel-Craver and Smith, 2008). Encapsulation of literatures regarding the removal of bacteria from water is presented in Table 1.9.

1.7 Scope for further research

The comprehensive literature review carried out in the previous sections helped in finding out the scopes for further research work regarding the fabrication and application of fly ash-based ceramic membranes. The above extensive literature review on fly ash-based membrane primarily discusses about the preparation of flat membranes, examples of tubular membrane fabrication being very few. Besides, the pore sizes of the membranes reported in the literature are slightly on the higher side (0.25-7.28 μm), which reduces their multi-folded use in different separation applications. Besides, few literature reported the use of high sintering temperature (~1400 ºC) in the membrane fabrication process that leads to increase the production cost. Therefore, this work focuses on the development of fly ash-based tubular membranes with lower average pore size than those reported in the literature. The work also aims to reduce the sintering temperature of membrane fabrication so as to bring down the cost associated with the fabrication process.

The analysis of literature regarding possible applications of the prepared fly ash-based membranes revealed that extensive work had been carried out regarding the removal of bacteria from contaminated water. Moreover, in case of treating silk floss processing wastewater and virus contaminated water, use of ultrafiltration and nanofiltration membranes is recommended

owing to the small particles' size. Though few research works reported the use of microfiltration membranes for the treatment of virus contaminated water, these membranes were functionalized through some prior treatment before being implemented in virus separation process. Regarding removal of bacteria from milk, membranes with pore size lesser than 1.4 µm cannot be recommended as they affect the quality of milk by retaining larger casein molecules. On the contrary, treatment of poultry slaughterhouse wastewater, starch industry wastewater and separation of glycerol from biodiesel can be easily carried out using a microfiltration membrane. Therefore, the aforementioned three liquid phase separation operations will be targeted as a part of this research work.

The available literature on the application of membrane filtration in purifying poultry slaughterhouse wastewater reveals mainly the use of polymeric membranes. In certain cases, the membrane filtration is combined with processes like electrocoagulation, flocculation, reverse osmosis, etc., in order to reduce fouling and obtain high quality permeate. However, the use of these hybrid processes cannot be the best alternative ever. In processes like coagulation, the residual mineral from coagulants, if present in the filtrate, can be proved detrimental to human health as mentioned earlier. Processes like reverse osmosis, though produce high quality permeate, are highly expensive and cannot be afforded by all class of people in the society. Article mentioning the use of ceramic membrane for the treatment of poultry slaughterhouse wastewater is mostly made up of α-alumina, which is way too costly. Similar is the case for treatment of starch industry wastewater and separation of glycerol from biodiesel, which primarily discussed about the use of polymeric and commercial ceramic membranes. Few cases regarding the separation of glycerol from biodiesel also reported the use of membrane separation in reduction of free glycerol content retained after decantation or water washing. Use of prior pre-treatment steps unnecessarily increases the operational cost associated with the process. Therefore, the purpose of this work is to develop a low-cost

versatile membrane from fly ash that can address all the issues mentioned above and satisfactorily carry out all the three aforementioned separation operations.

1.8 Objectives

Keeping in mind the studied state-of-the-art, the following objectives are framed for a planned and successful completion of the research activity.

- Fabrication, characterization and optimization of composition for fly ash-based tubular ceramic microfiltration membrane.
- Study the effect of binder concentration on properties of the fabricated membrane using the optimized composition of objective 1 and subsequent finalization of an optimum binder concentration for carrying out further research work.
- The use of the developed tubular ceramic membrane in various liquid phase separation processes, namely treatment of poultry slaughterhouse wastewater, treatment of starch processing wastewater and separation of glycerol from biodiesel.
- Economic feasibility assessment of fly ash-based tubular ceramic membrane fabrication process and its subsequent application in various liquid phase separation processes.

1.9 Organization of the thesis

Based on the research works carried out for completing the above-mentioned objectives, the doctoral thesis is organized in the following six chapters:

Chapter 1 represents the introduction, literature review and objectives of the thesis.

Chapter 2 presents a detailed discussion about fabrication and optimization of composition for tubular ceramic membranes fabricated using fly ash as a key precursor. The raw materials and the fabricated membranes were characterized using different standard techniques such as Laser Particle Size Analyzer (LPSA), X-Ray Fluoroscence analysis (XRF), X-Ray Diffraction

analysis (XRD), Field Emission Scanning Electron Microscope (FESEM), Energy Dispersive X-Ray Spectroscopy (EDX), Thermogravimetric Analysis (TGA). The fabricated membranes after sintering were characterized for evaluating porosity, permeability, pore size, mechanical and chemical stability. Based on the obtained properties, an optimized composition is fixed for membrane fabrication and subsequent application in microfiltration operations.

Chapter 3 portrays a detailed analysis of the effect of binder concentration on membrane properties. The rheological properties of binder solution at various concentrations are evaluated. Moreover, membranes with different concentrations of the binder (Na-CMC) are fabricated and characterized to evaluate the optimum concentration of binder to be used for membrane fabrication.

Chapter 4 discusses about the versatility of the membrane when implemented in three different liquid phase separation operations, namely treatment of poultry slaughterhouse wastewater, treatment of starch rich wastewater and separation of glycerol from biodiesel. The permeate obtained in all the above-mentioned cases is tested using standard protocols to check whether they meet the necessary norms as prescribed by the authorities.

Chapter 5 corresponds to the economic feasibility assessment of all three separation processes taken into consideration, namely poultry slaughterhouse wastewater treatment, treatment of starch rich wastewater and separation of glycerol from biodiesel. Cost estimation starts with estimating the membrane fabrication cost, which is followed by analysis of cost necessary for all three separation operations. The estimation of process cost is carried out for both lab-scale and pilot-scale setups.

Chapter 6 summarizes the inferences drawn from the aforementioned chapters and provides some suggestions for future works to be carried out based on the work mentioned in this thesis.

Chapter 2

Fabrication, Characterization and Optimization of Composition for Fly Ash-based Tubular Ceramic Microfiltration Membrane

Fabrication, Characterization and Optimization of Composition for Fly Ash-based Tubular Ceramic Microfiltration Membrane

This chapter presents a detailed discussion about the fabrication of tubular ceramic membranes derived from fly ash as a key precursor, along with few percentages of quartz and calcium carbonate. Four different sets of composition were used for membrane fabrication and all of the fabricated membranes were characterized using standard methods and techniques. Based on the properties of membranes evaluated through various characterization techniques, the optimized membrane composition was selected for further microfiltration operations.

2.1 Experimental

2.1.1 Raw materials

The selection of raw materials is one of the most crucial factors of the membrane fabrication process. Proper choice of raw material composition is the key to obtain membranes with outstanding physical as well as chemical properties. The purpose behind the use of three different raw materials in this study is mentioned in Table 2.1.

Table 2.1 Significance behind the addition of different raw materials

Raw material	Significance	References
Fly ash	Offers refractory property and increases mechanical strength	Kamara et al., 2020; Zulkifli et al., 2019; Abdullayev et al., 2019
Quartz	Increases mechanical and thermal stability	Abdullayev et al., 2019
Calcium carbonate	Acts as pore former as well as sintering aid	Abdullayev et al., 2019; Falamaki et al., 2004
Sodium salt of carboxy methyl cellulose (Na-CMC)	Acts as binder	Falamaki et al., 2006

Fly ash, the key precursor used in the fabrication of tubular ceramic membrane, was collected from Guwahati, Assam, while the other ingredients such as calcium carbonate ($CaCO_3$) and sodium salt of carboxymethylcellulose (Na-CMC) were supplied by Merck (I) Ltd. Quartz was collected from Kanpur, Uttar Pradesh. Besides, the chemicals used for evaluating membranes' chemical stability, namely hydrochloric acid (HCl), and sodium hydroxide (NaOH), were also procured from Merck (I) Ltd.

2.1.2 Fabrication of fly ash-based tubular ceramic membranes

The process of membrane fabrication starts with kneading the different raw material compositions mentioned in Table 2.2 with two mass percent aqueous solution of sodium salt of carboxymethyl cellulose (Na-CMC) to get a uniform paste. The paste thus obtained will be forced to pass through a horizontal extruder (M/s VB Ceramic Consultants, Chennai, India), as shown in Fig 2.1(a), having moulds of inner diameter 5.5 mm and outer diameter 11.5 mm to get the desired shape of the membranes (Fig 2.1(b)). The green membranes thus obtained from the extruder are kept at room temperature for a day and then allowed to dry at 100 ˚C for 24 hours in a hot air oven. This was followed by drying the membranes at 200 ˚C for 24 hours and finally, sintering of the dried membranes was done in a box furnace (M/s VB Ceramic Consultants, Chennai, India) at 1100 ˚C for a duration of 6 hours. Drying at 200 ˚C and further sintering of the membranes was done at a heating rate of 2 ˚C/min to avoid any bending or deformation in membrane structure. Both the ends of the sintered membranes were then smoothened by abrasive paper (No. C-220) to get membranes of 100 mm length. Finally, the membranes were dipped in water and put in an ultra-sonication bath to remove any loose particles attached to its surface. Cleaned membranes were further dried at 110 ˚C to get the membranes to be used for filtration experiments. The pictorial representation of the different

steps involved in membrane fabrication and the temperature-time schedule involved in membrane drying and sintering is presented in Fig 2.2.

Table 2.2 Different compositions of raw materials used for membrane preparation

Raw material	**Composition (%)**			
	K1	**K2**	**K3**	**K4**
Fly ash	65	70	75	80
Quartz	20	20	20	20
Calcium carbonate	15	10	5	0

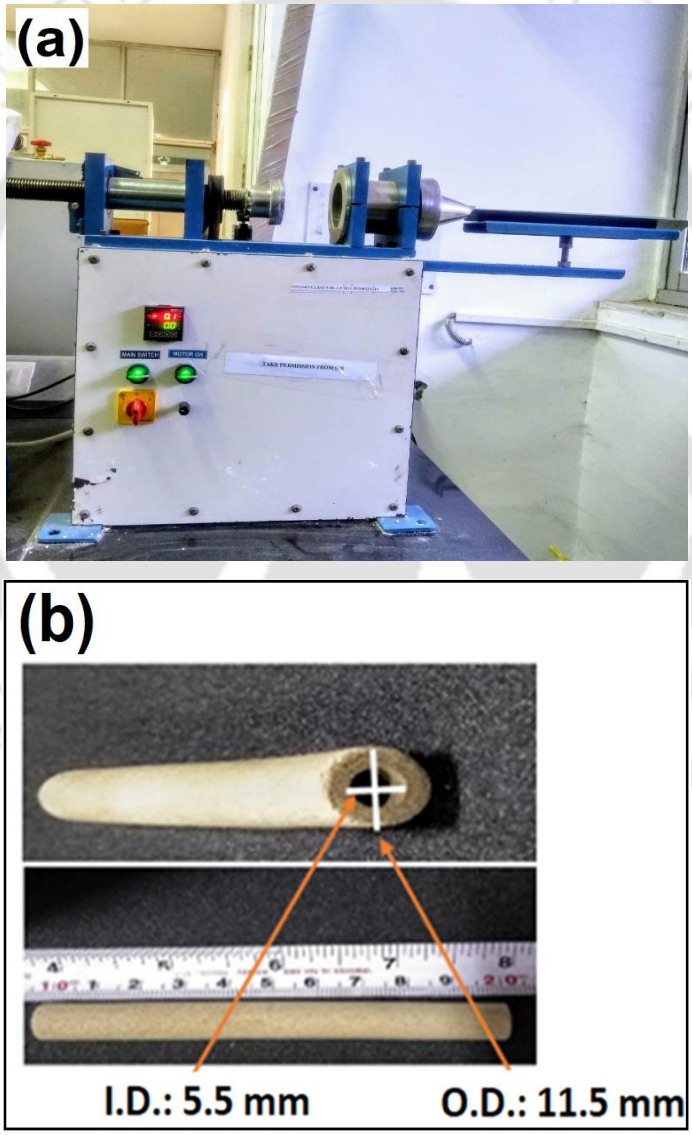

Fig 2.1 (a) Horizontal extruder used for membrane fabrication and (b) image of the fabricated membrane

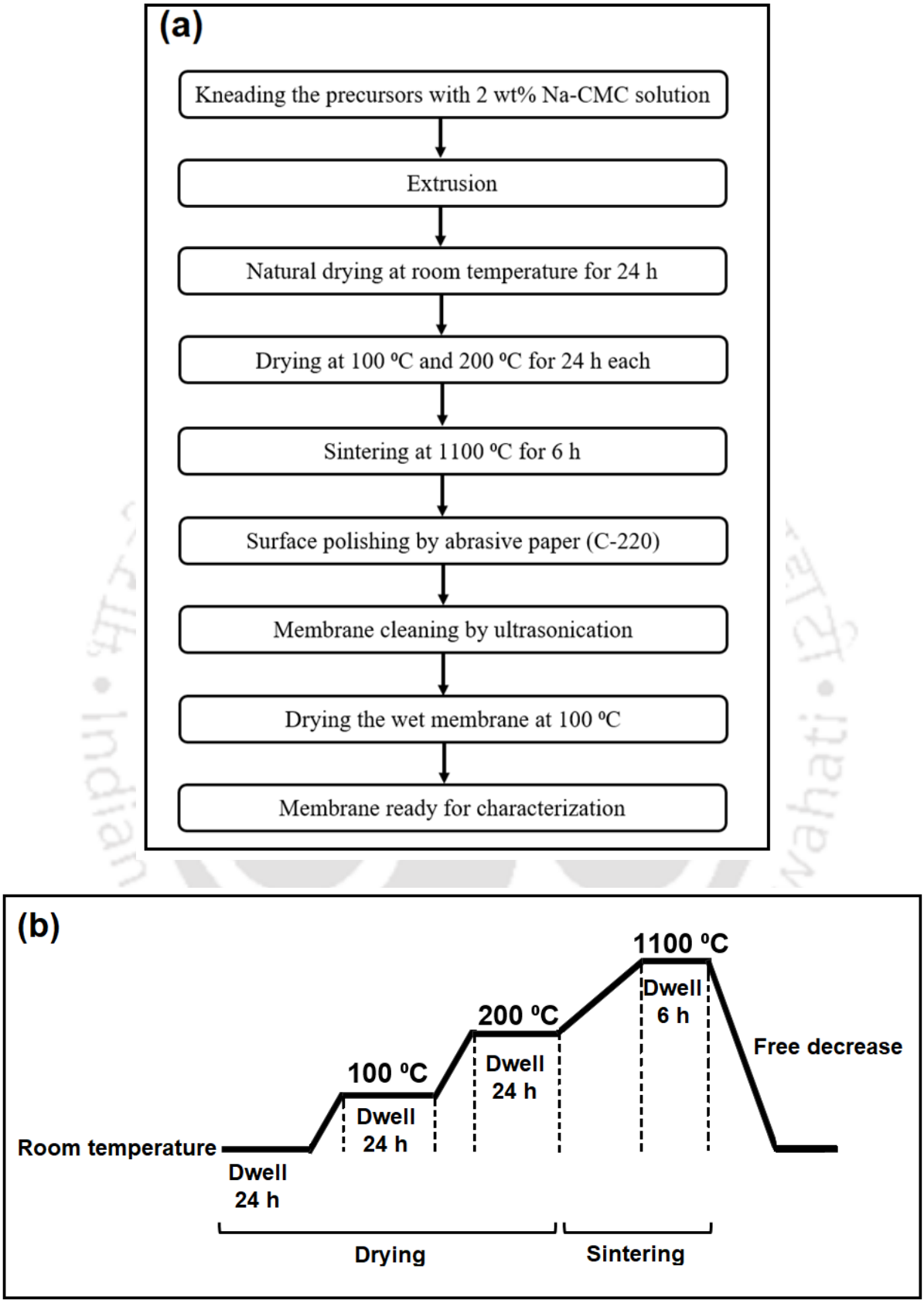

Fig. 2.2 (a) Steps of membrane fabrication process and (b) Temperature-time schedule of membrane drying and sintering

2.1.3 Characterization of raw materials and fabricated membranes

The raw materials used in the membrane fabrication process and the fabricated membranes were characterized through various tests in order to investigate membrane properties and presence of defects or faults in it. Thermal stability of the raw materials was evaluated using a Thermogravimetric analyzer (Make: Netzsch, Model: STA449F3A00) up to 1100 ˚C at a heating rate of 10 ˚C/min in argon (Ar) environment. X-ray Diffraction analysis of the individual raw materials and various membrane samples before and after sintering were carried out using advanced X-ray Diffractometer (model: AXS D8 ADVANCE manufacturer: Bruker, Germany), at a scanning rate of 0.05˚/s within a 2θ range of 5-90˚, using Cu-Kα radiation of wavelength 1.5406 Å. The particle size analysis of individual raw materials was carried out in wet dispersion mode using Laser Particle Size Analyzer **(**Model No.: Master sizer 2000; Make: M/s Malvern, UK). The pump speed was maintained at 1800 rpm and ultrasonication of feed was done in constant manner to avoid the formation of lumps of clay powders in water. The chemical composition of fly ash and quartz was evaluated using X-Ray Fluorescence Spectrometer (XRF) (Make: Malvern, Model: PANalytical Zetium). The elemental composition of the individual raw materials was studied using Energy Dispersive X-Ray Analysis.

The morphological analysis of the membranes was carried out using Field Emission Scanning Electron Microscope (FESEM) (Make: Zeiss, Model: Gemini). The inner and outer surfaces of the membranes were coated with a layer of gold and then analysed at 2000 magnification of FESEM. The FESEM images were also utilized to evaluate the pore sizes of the membranes using ImageJ software, where a total number of hundred pores from three different images were taken for each membrane composition to calculate the average pore size of the membranes. The equation used for evaluating the average pore size of the membranes from the individual pore diameters can be written as shown in equation (2.1) (Bouazizi et al., 2016).

$$d_p = \sqrt{\frac{\sum_{i=1}^{n} n_i d_i^2}{\sum_{i=1}^{n} n_i}} \quad (2.1)$$

where d_p is the average pore diameter, n_i is the i^{th} pore and d_i is the corresponding pore diameter. Moreover, EDX analysis using the same machine mentioned earlier was also carried out to study the elemental mapping of the fabricated membranes.

The porosity of membranes is usually evaluated by Archimedes' principle. This method requires dipping the membrane for 48 hours in Millipore water. The difference in weight of the membrane before and after dipping is the volume of water absorbed by the membranes, which corresponds to the pore volume of the membrane and when it is divided by the total membrane volume, porosity can be obtained by equation (2.2):

$$\text{Porosity (\%)} = \frac{W_{wet} - W_{dry}}{V \times \rho} \times 100 \quad (2.2)$$

Where, W_{wet} is the weight of the wet membrane and W_{dry} is the weight of the dry membrane, V is the total volume of the membrane and ρ is the density of water (Kumar et al., 2015a). Four membranes from two different batches (two membranes from each batch) were used to evaluate the average porosity of membranes of that particular composition.

The mechanical strength of the prepared membrane samples was evaluated using ASTM C1424-99 standard in an Electromechanical Universal Testing Machine (Make: Zwick Roell: Z005TN) with a load cell of 5 kN and a cross head speed of 2 mm/min. The aspect ratio of the sample to be tested was kept as 2.0.

To evaluate chemical stability, the membranes, after taking their dry weights, were dipped into strong acid (Hydrochloric acid, pH=1) and alkali (Sodium hydroxide, pH=13) solutions separately. After a week, the membranes were taken out, washed and ultra-sonicated for 15 minutes to remove any precipitate deposited on their surfaces as a result of the chemical treatment. This is followed by drying the samples at 100 ˚C and measuring their weight again

(Suresh et al., 2016; Nandi et al., 2008). The resultant weight loss is considered to be the consequence of the chemical stability test and is calculated using equation (2.3).

$$\text{Weight loss (\%)} = \frac{W_{initial} - W_{final}}{W_{final}} \times 100 \quad (2.3)$$

Where, $W_{initial}$ is the dry weight of the sample before chemical treatment and W_{final} is the dry weight of the sample after chemical treatment. Four membranes from two different batches (two membranes from each batch) were tested for chemical stability and mechanical strength measurements and the average value is being reported.

2.1.4 Water permeability and pore size evaluation

The experimental setup shown in Fig. 2.3 was used to measure pure water permeability and treatment of poultry wastewater. Before evaluating the water permeability, the membrane was compacted using Millipore water (Millipore, ELIX-3 Instrument) at a high pressure to remove any loose particles present in the membrane. The water from the feed tank (1) was pumped to the membrane module (5) and the resulting permeate was collected in the permeate tank (6). The retentate stream was sent back to the feed tank. There are two valves in the whole setup: one valve (3), known as the bypass valve, is used to maintain the pressure at the inlet of the membrane module, while the other valve (8), known as retentate valve, controls the cross-flow velocity. The rotameter (9) fixed in the experimental setup is used to monitor the cross-flow velocity. The pressure gauge (4) was used to measure the pressure at the inlet of the membrane module.

After compaction, the pure water flux was measured at five applied pressures (69, 138, 207, 276 and 345 kPa). Equation (2.4) is used to calculate the water flux for each pressure from the volume of water collected (Kumar et al., 2015b).

$$J_w = \frac{V_w}{A \times t} \quad (2.4)$$

where, J_w stands for water flux, V_w is the volume of water collected, t is the time and A is the area of the membrane used for filtration.

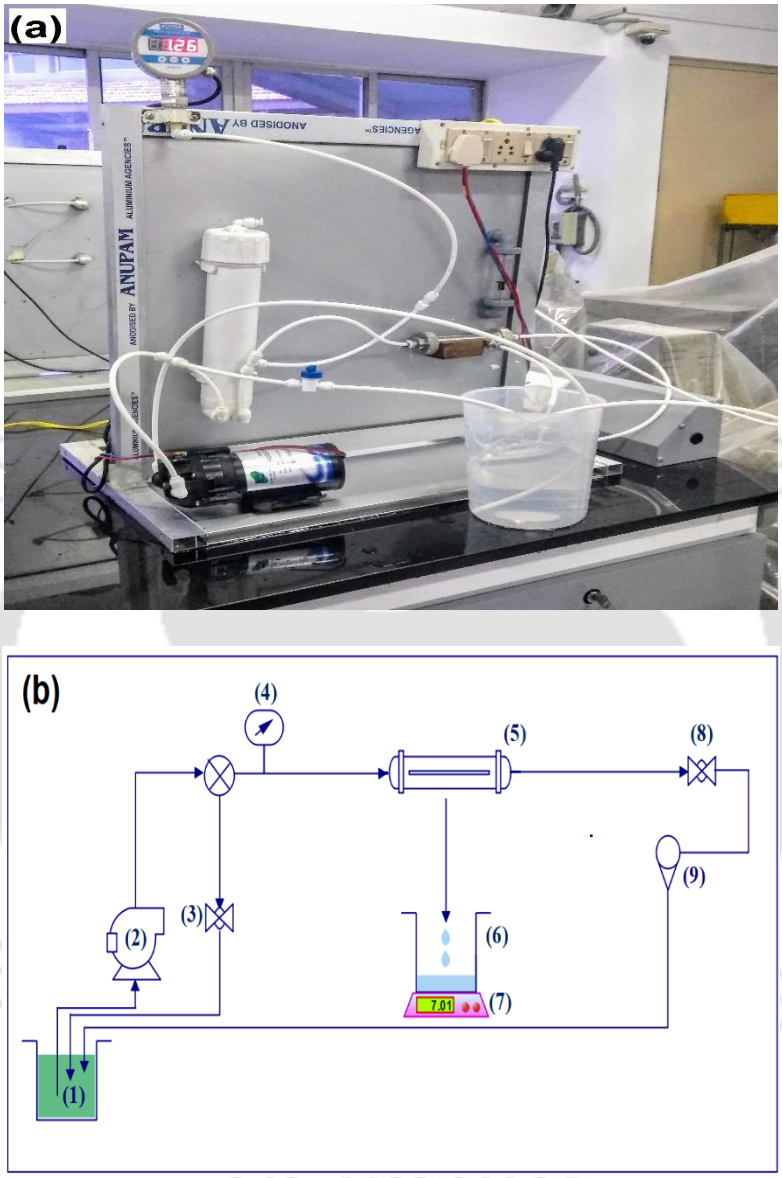

Fig. 2.3 Experimental setup [a: Original setup; b: Schematic (1: Feed water tank, 2: Pump; 3,8: Ball valve, 4: Pressure gauge, 5: Membrane module, 6: Permeate tank, 7: Weighing balance; 9: Rotameter)]

From the water flux data obtained after running the experiments for all five pressures, the graph is plotted between pure water flux and applied pressure and the corresponding slope of the

graph will yield the water permeability value (L_h), which is in accordance with the Darcy's law of convection as depicted in equation (2.5) (Kumar et al., 2015c).

$$J_w = L_h \Delta P \tag{2.5}$$

The L_h value obtained is further used to calculate the pore size of the membrane using Hagen-Poiseuille equation (equation (2.6)) (Kumar et al., 2016):

$$r^2 = \frac{8\mu\tau_m l L_h}{\varepsilon} \tag{2.6}$$

Where, r is the pore radius, μ is the viscosity of pure water at 25 ˚C, l is the pore length (assuming the pores are present throughout the membrane thickness, l = 0.003 m), ε is membrane porosity, L_h is the pure water permeability and τ_m is the tortuosity of the membrane. The tortuosity of the membranes can be evaluated using equation (2.7) (Boudreau, 1996).

$$\tau_m{}^2 = 1 - 2 \ln \varepsilon \tag{2.7}$$

2.2 Results and discussion

2.2.1 Characterization of raw materials

2.2.1.1 Thermogravimetric analysis

In the thermogravimetric analysis of raw material mixture with Na-CMC (Fig. 2.4), the first minimal weight loss occurred around 110-130 ˚C owing to the evaporation of physisorbed moisture present in the sample (Kumar et al., 2015b). The second peak in the DTG curve occurs at a temperature of 284.84 ˚C, which may be attributed to the thermal decomposition of sodium salt of carboxymethyl cellulose (Na-CMC), the binder used in the membrane fabrication process. At this temperature, the thermal oxidative degradation of Na-CMC causes different reactions to take place, thus changing the composition of the sample. During thermal degradation process, the fragments obtained from Na-CMC molecular chain undergo rearrangement that leads to the formation of some polyunsaturated chain products. These

materials may get oxidized at a higher temperature, leading to the generation of CO_2 and minor weight loss (Tan et al., 2017). In the TGA (inset) and DTG graphs of the raw material mixture without additive, the absence of second peak at around 280 ˚C temperature also confirms that that particular peak corresponds to decomposition of Na-CMC. The similarity of both the graphs, except that particular peak, reveals the decomposition of Na-CMC at that particular temperature.

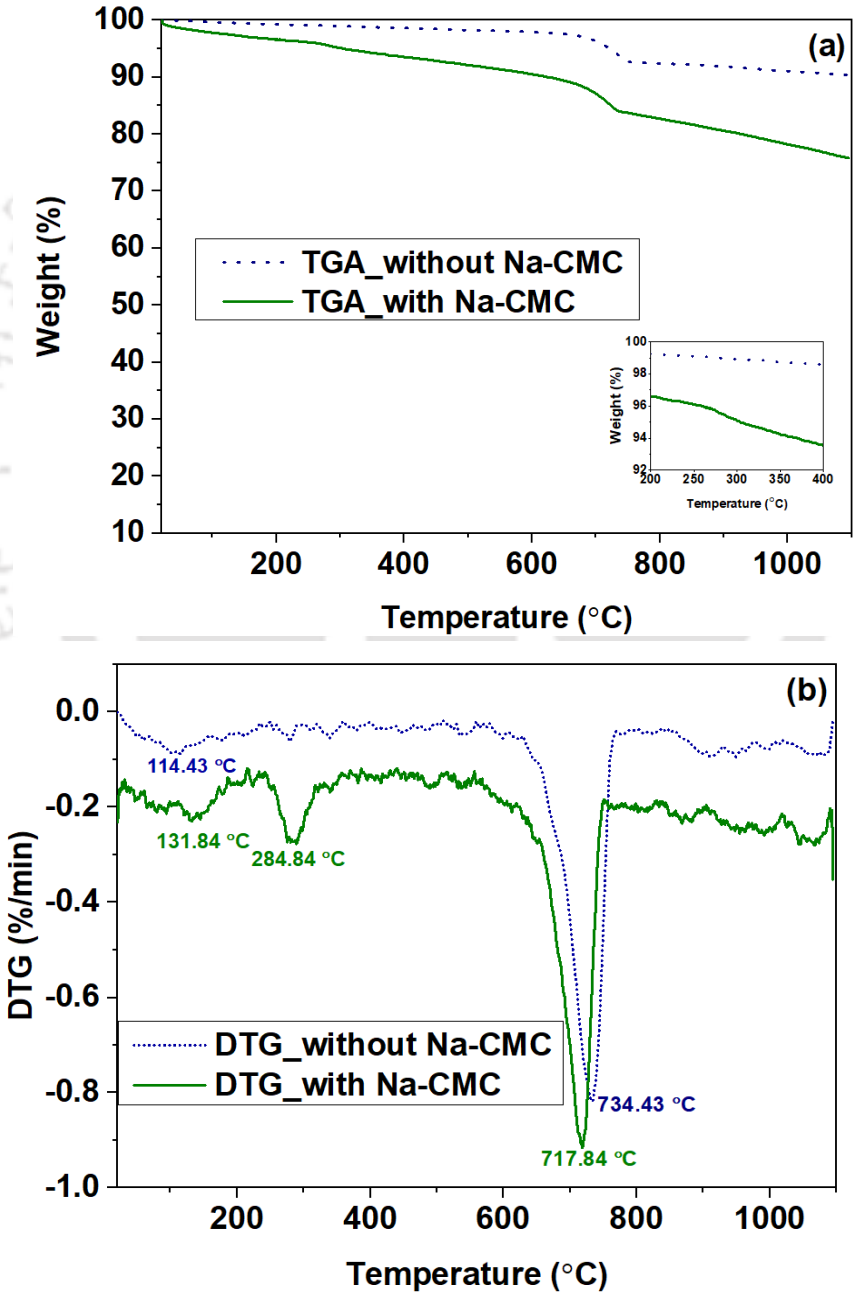

Fig. 2.4 (a) TGA and (b) DTG of raw material mixture with and without Na-CMC (K3 membrane)

The significant weight loss observed around 710-730 ˚C is owing to the thermal decomposition of calcium carbonate ($CaCO_3$), yielding calcium oxide (CaO) and carbon dioxide (CO_2) as products, according to the reaction mentioned in equation (2.8).

$$CaCO_3 \rightarrow CaO + CO_2 \quad (2.8)$$

The carbon dioxide formed as a result of this process leaves the sample and is considered responsible for the formation of pores in the membrane (Cheryan, 1998). The process of pore formation by $CaCO_3$ decomposition and diffusion of CO_2 through membrane matrix is depicted pictorially in Fig. 2.5.

It is worth mentioning that the mass loss for the mixture without Na-CMC is around 10% at 1100 ˚C, while it increased to around 24% for the mixture containing Na-CMC. It has been observed that weight loss after 1000 ˚C is minimal. Moreover, for fly ash-based membranes, the mechanical strength of membranes increases with increasing sintering temperature. Reports have mentioned that only 50 ˚C increase in temperature leads to an enormous increase in membrane strength (Černý and Tůmová; 2016).

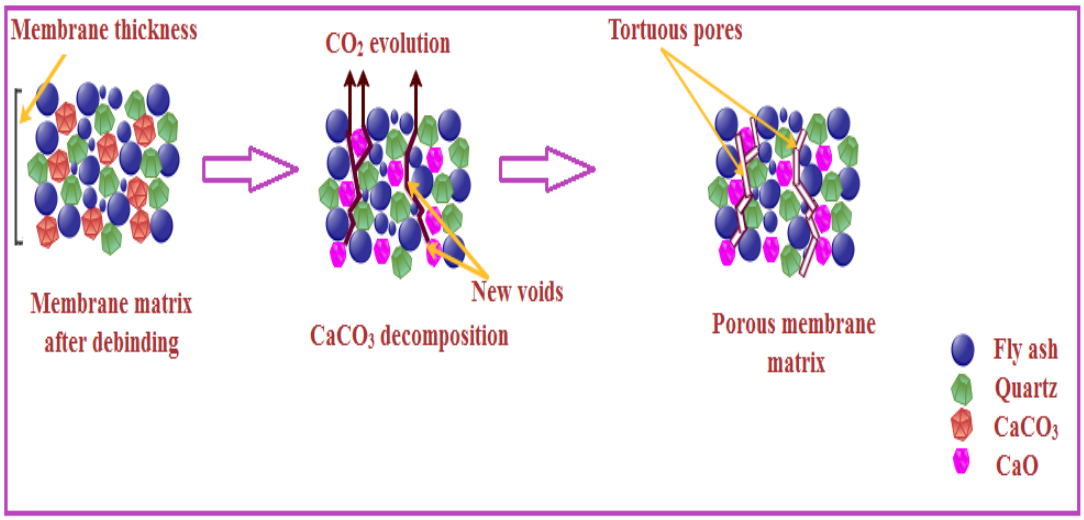

Fig. 2.5 Formation of pores in the membrane matrix

2.2.1.2 X-ray Diffraction analysis

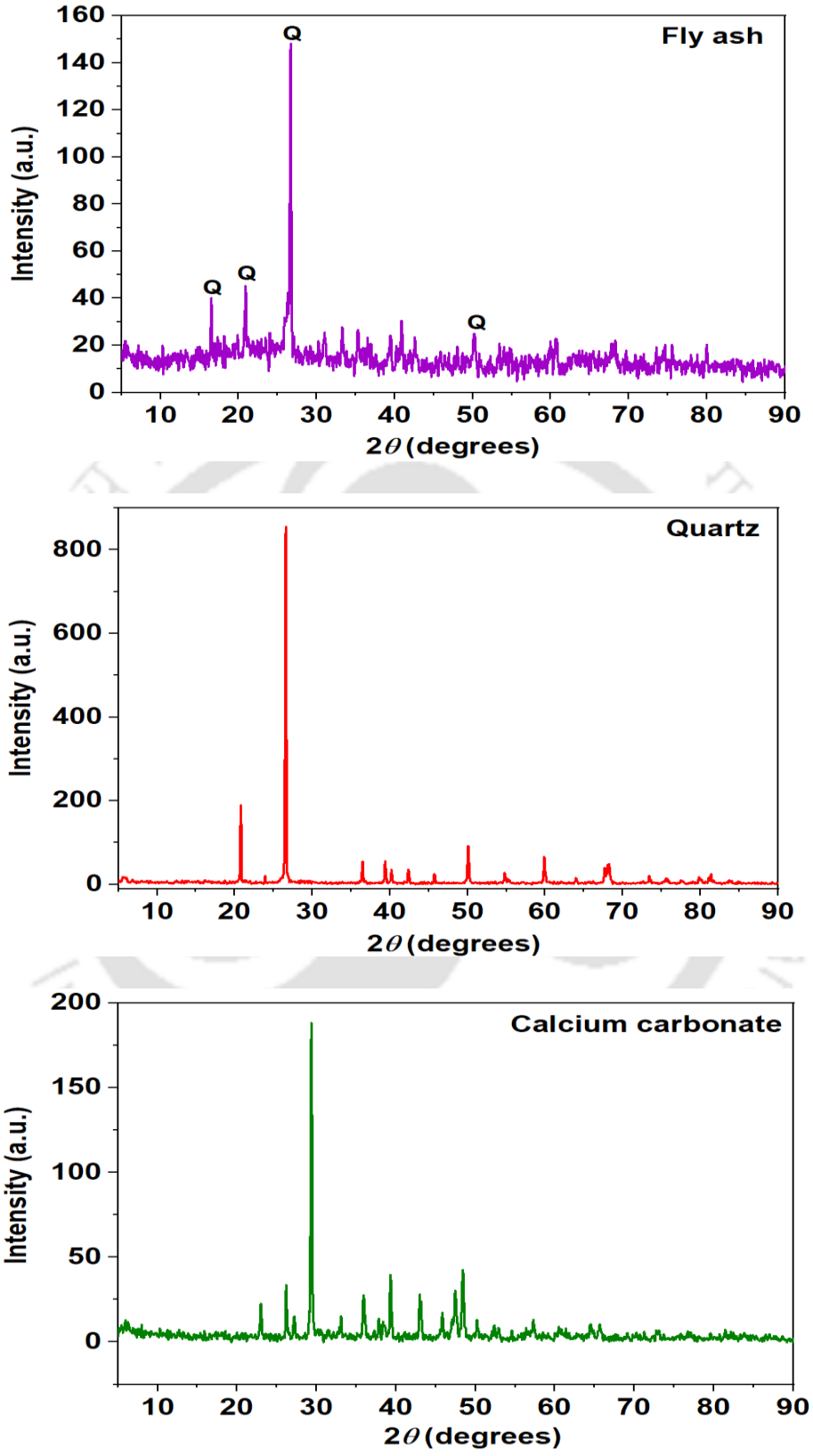

Fig. 2.6 XRD patterns of individual raw materials (Q: Quartz)

X-ray Diffraction analyses of individual raw materials used in the fabrication of membranes, i.e., fly ash, quartz and calcium carbonate, were successfully carried out and the results of the same are depicted in Fig. 2.6. Diffractograms show that peaks of calcium carbonate occurred at 2θ values of 23.05, 26.2, 29.35, 35.95, 39.35, 43, 47.5 and 48.45˚; while the peaks of quartz appeared at 2θ values of 20.8, 23.6, 26.6, 36.5, 39.4, 42.75, 50.1, 59.9 and 68.3˚ respectively. Prior art regarding the X-ray analysis of calcium carbonate reveals the occurrence of peaks at similar positions and the peaks obtained for quartz too matched with standard JCPDS pattern number 46-1045 (JCPDS. 2000), thus verifying the authenticity of the instrument as well as raw materials (Rahman et al., 2013; Thriveni et al., 2014). Peaks corresponding to fly ash appeared at 2θ values of 16.5, 20.95, 26.7 and 50.15˚, thus signifying that fly ash has quartz as its main component.

2.2.1.3 Laser particle size analysis

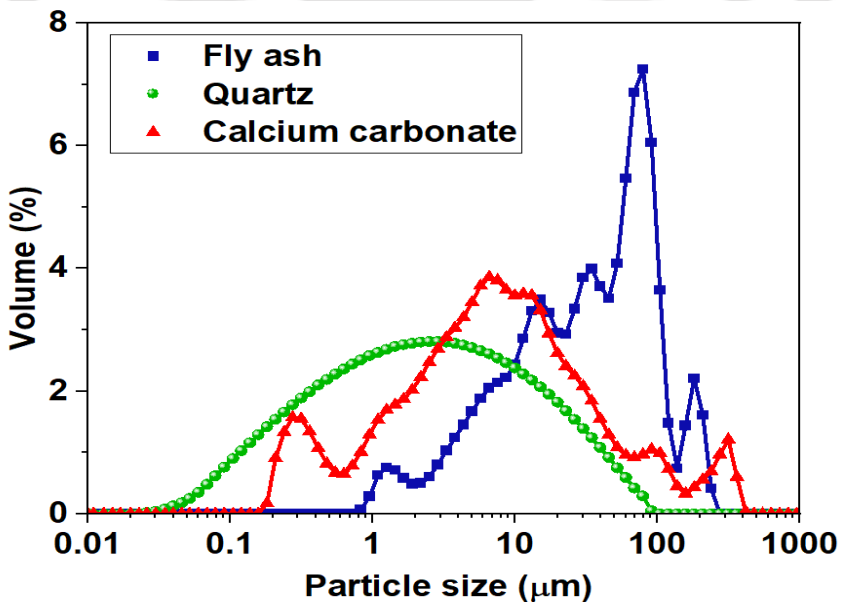

Fig. 2.7 Laser particle size analysis of raw materials used for membrane fabrication

Particle size distribution is utmost important for getting a membrane with good physical and mechanical properties. Finer particles lead to the formation of a compact membrane with very smaller pore size and higher mechanical strength. On the contrary, the pores formed by using

coarser particles are comparatively larger, which results in a membrane with lesser mechanical strength (Wang et al., 2007). Porosity is also less for membranes fabricated using smaller particle sizes (Norliza et al., 2001). In this work, laser particle size analysis revealed that the raw materials used for fabrication of ceramic membranes, namely fly ash, quartz and calcium carbonate, have $d_{0.5}$ values of 37.733, 2.459 and 7.356 µm, respectively (Fig. 2.7). As evident from literature, membranes fabricated with raw materials having similar particle size have proven to offer excellent properties (Almandoz et al., 2004; Norliza et al., 2001). Therefore, the raw materials with aforementioned particle sizes were used further for membrane fabrication, looking at these prior arts.

2.2.1.4 X-Ray Fluorescence Spectrometer Analysis

The X-Ray Fluorescence Spectrometer analysis (XRF) of fly ash presented in Table 2.3 reveals that it contains silica as its main constituent along with some quantities of alumina and iron oxide and traces of oxides of manganese, magnesium, calcium, potassium, titanium and phosphorus. Similarly, the XRF analysis of quartz proves that the quartz used mostly comprises of silica, thus signifying the purity of raw materials used. It has been found that the procured data by carrying out XRF analysis of fly ash and quartz appreciably matches with those available in earlier literatures (Ibrahim et al., 2015; Singh and Subramaniam, 2018). Moreover, presence of any harmful heavy metals was not detected in the XRF analysis of fly ash samples. It is worth mentioning that as the calcium carbonate used for membrane fabrication is having greater than 99% purity, XRF analysis of the same has not been carried out.

Table 2.3 XRF analysis of fly ash and quartz (All values are in wt.%)

Sample	**SiO_2**	**Al_2O_3**	**Fe_2O_3**	**MnO**	**MgO**	**CaO**	**K_2O**	**TiO_2**	**P_2O_5**
Fly ash	65.39	17.64	5.38	0.068	0.54	1.80	1.50	2.11	0.41
Quartz	86.97	7.59	0.49	0.022	0.03	0.18	0.20	0.02	0.005

2.2.1.5 Energy Dispersive X-ray Analysis

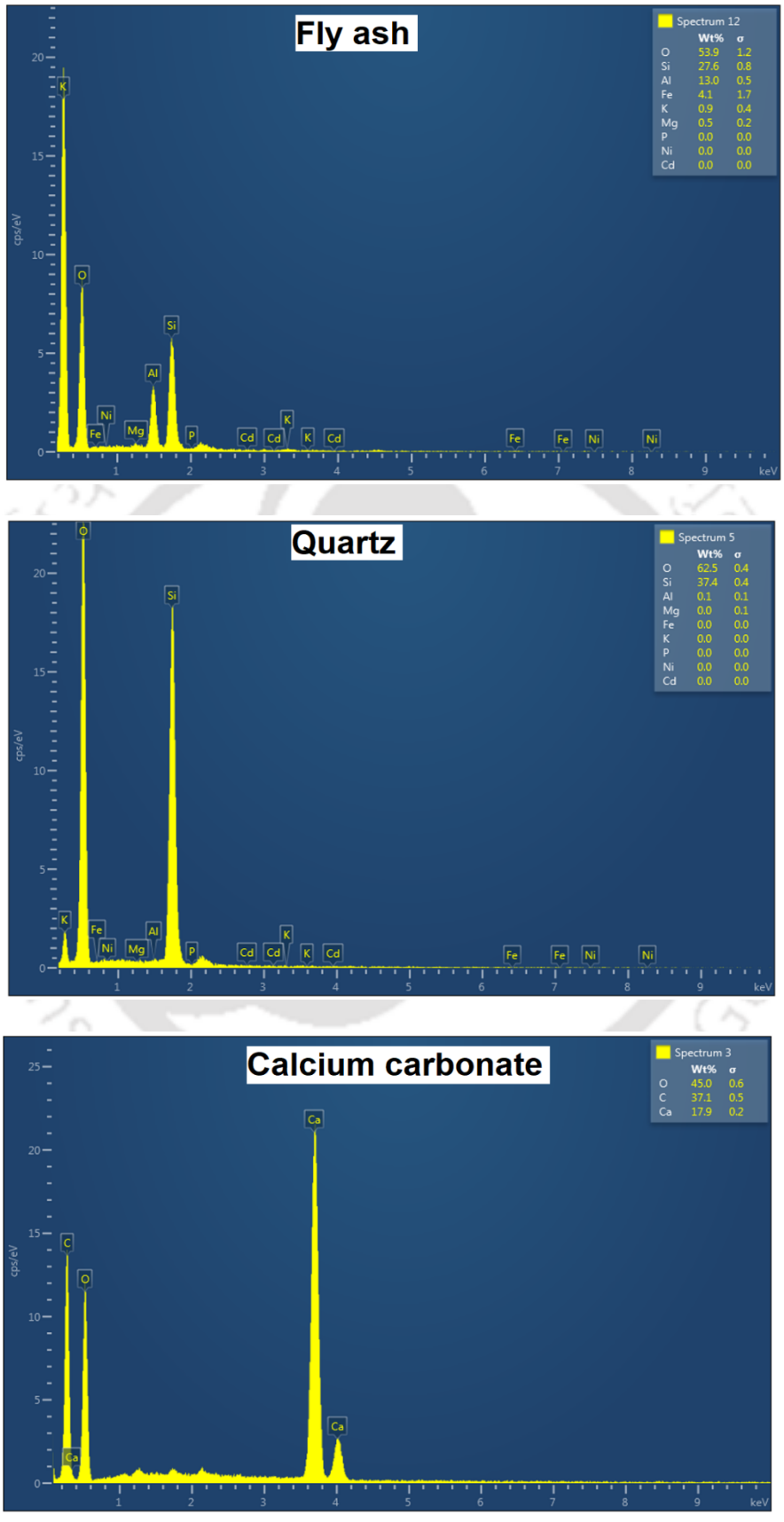

Fig. 2.8 EDX analysis of raw materials

Energy Dispersive X-ray analysis of individual raw materials (Fig. 2.8) helped to get an idea about the various elements present in them. EDX analysis of fly ash revealed the presence of aluminium (Al), silicon (Si), oxygen (O_2) as the main elements with little amounts of iron (Fe), magnesium (Mg) and potassium (K). Presence of similar elements in the aforementioned raw materials have already been reported in the previous literature (Längauer et al., 2021). The higher quantity of Si and O_2 signifies that quartz is the major component of fly ash, which was also confirmed through XRF and XRD analysis (Ahmaruzzaman, 2010). Moreover, the EDX analysis also reveals that the fly ash used in this study does not contain any heavy metals such as nickel (Ni), cadmium (Cd), which are harmful to human beings. Quartz showed the presence of silicon (Si) and oxygen (O_2) with 0.1 wt% Aluminium (Al), thus signifying its high purity with silica as the main constituent. EDX analysis of calcium carbonate ($CaCO_3$) demonstrates the presence of calcium (Ca), carbon (C) and oxygen (O_2), thus showing the purity of the raw material used.

2.2.2 Characterization of fabricated membranes

2.2.2.1 Morphology study using Field Emission Scanning Electron Microscope

The structural uniformity of the fabricated membranes is confirmed by Field Emission Scanning Electron Microscope. FESEM images of inner and outer surfaces of the membranes (K1-K4) are portrayed in Fig. 2.9 and Fig. 2.10. The darker portion in the images represents pores present in the membrane (indicated by red arrow marks), while the lighter portion depicts clay particles. All the images show homogeneity in the membrane surface with numerous pores in it. One can clearly see from the images that the membranes are completely crack free. The images of inner as well as the outer sections of the membranes are almost similar. It has already been mentioned that the FESEM images were used for determining the pore sizes of all the membranes and it was found that the average pore sizes of K1, K2, K3 and K4 membranes are

0.915, 0.714, 0.818 and 0.983 µm, respectively. The pore size distribution, as evaluated using the FESEM images, is presented in Fig. 2.11.

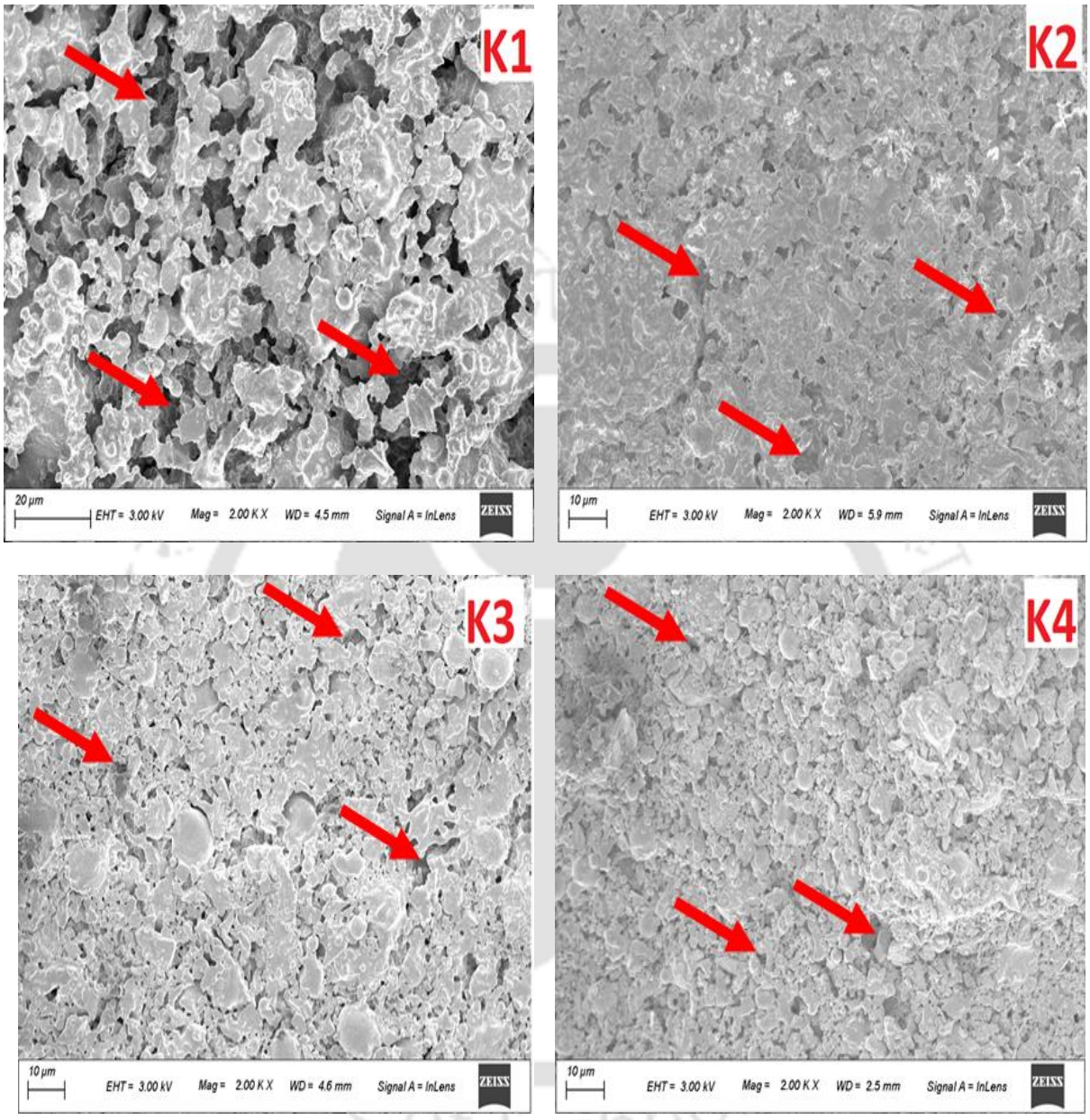

Fig. 2.9 FESEM images of inner surfaces of membranes K1, K2, K3 and K4

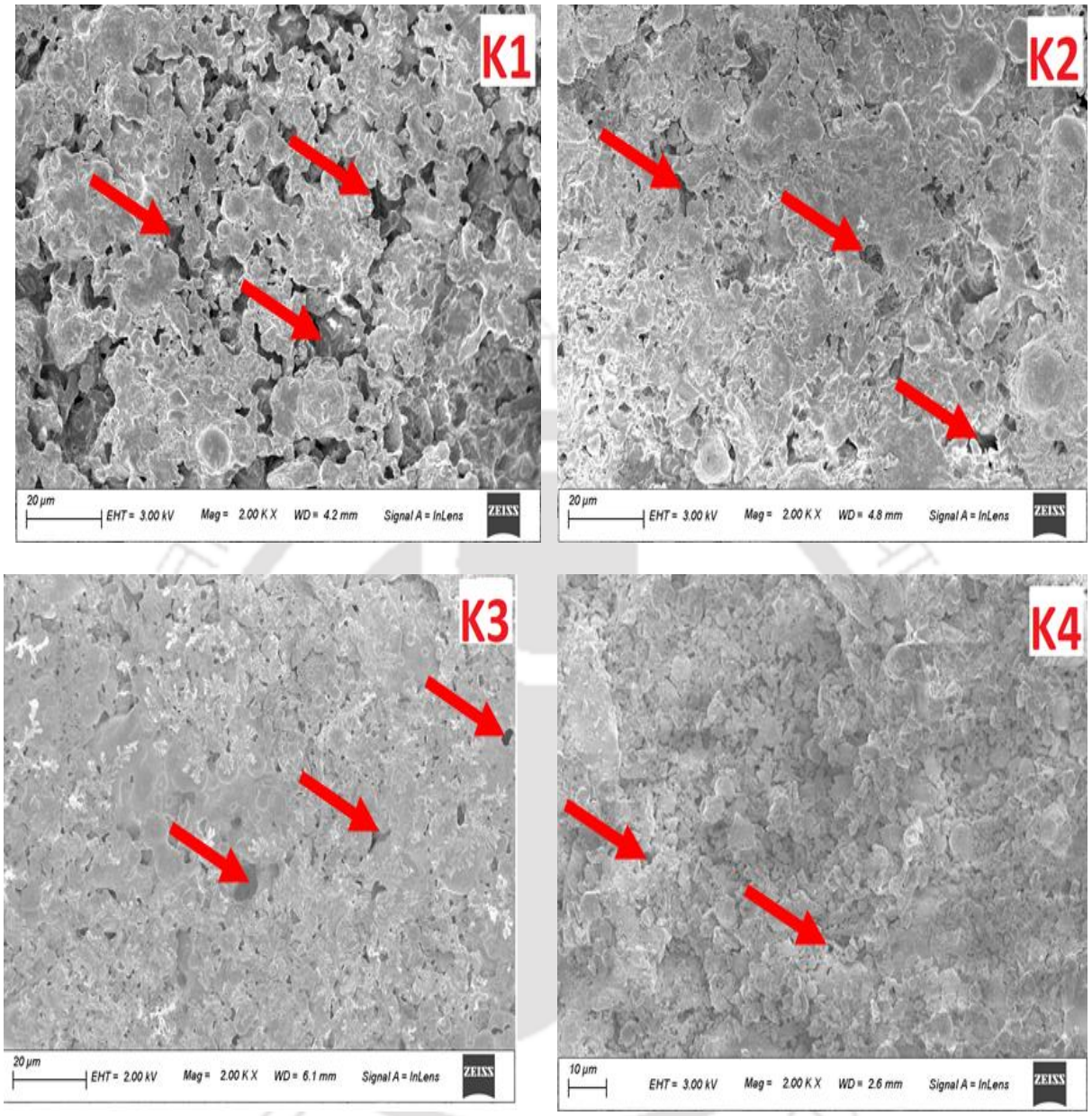

Fig. 2.10 FESEM images of outer surfaces of membranes K1, K2, K3 and K4

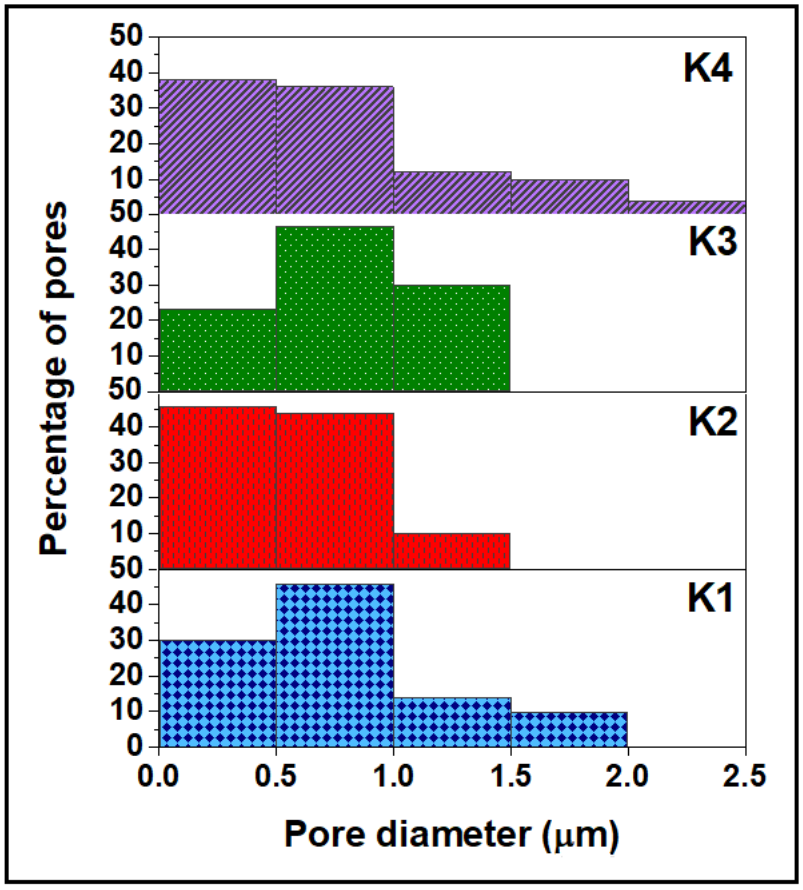

Fig. 2.11 Pore size distribution of membranes (K1-K4) evaluated using FESEM images

2.2.2.2 X-ray Diffraction analysis

Fig. 2.12 portrays the X-ray Diffraction analysis of raw material mixtures used for membranes fabrication and the sintered membranes (K1-K4). It has been observed that the raw material mixtures showed the presence of peaks at 2θ angles of 20.85, 26.7, 29.35, 50.2, 60 and 68.4˚. The peak appearing at a 2θ value of 29.35˚ corresponds to calcium carbonate, while all other peaks present in the diffractogram correspond to quartz, thus also confirming that quartz is the main constituent of fly ash (JCPDS, 2000; Rahman et al., 2013; Thriveni et al., 2014). In the case of sintered membranes, the appearance of new peaks at 2θ values of 21.95˚ and 28˚ was observed owing to the phase change of quartz and decomposition of calcium carbonate at higher temperatures. The peak at 2θ value of 21.95˚ signifies the phase transformation of quartz

to β-crystoballite (RRUFF, 2019). It needs to mention that quartz is a quite stable compound. Hence, only a smaller fraction of it gets transformed into β-crystoballite at temperatures above 850 ˚C, leaving most of it as it is, even after high temperature sintering. Conversely, calcium carbonate in the raw material decomposes around 720 ˚C (evident in the results of TGA) and forms CaO (Balaganesh et al., 2018). The peak corresponding to CaO is noticed at a 2θ value of 28˚ (Balaganesh et al., 2018). Since the membrane K4 is fabricated using quartz and fly ash only, no peaks corresponding to calcium carbonate as well as calcium oxide are observed in the XRD profile of raw material mixture (K4) and calcined sample (K4).

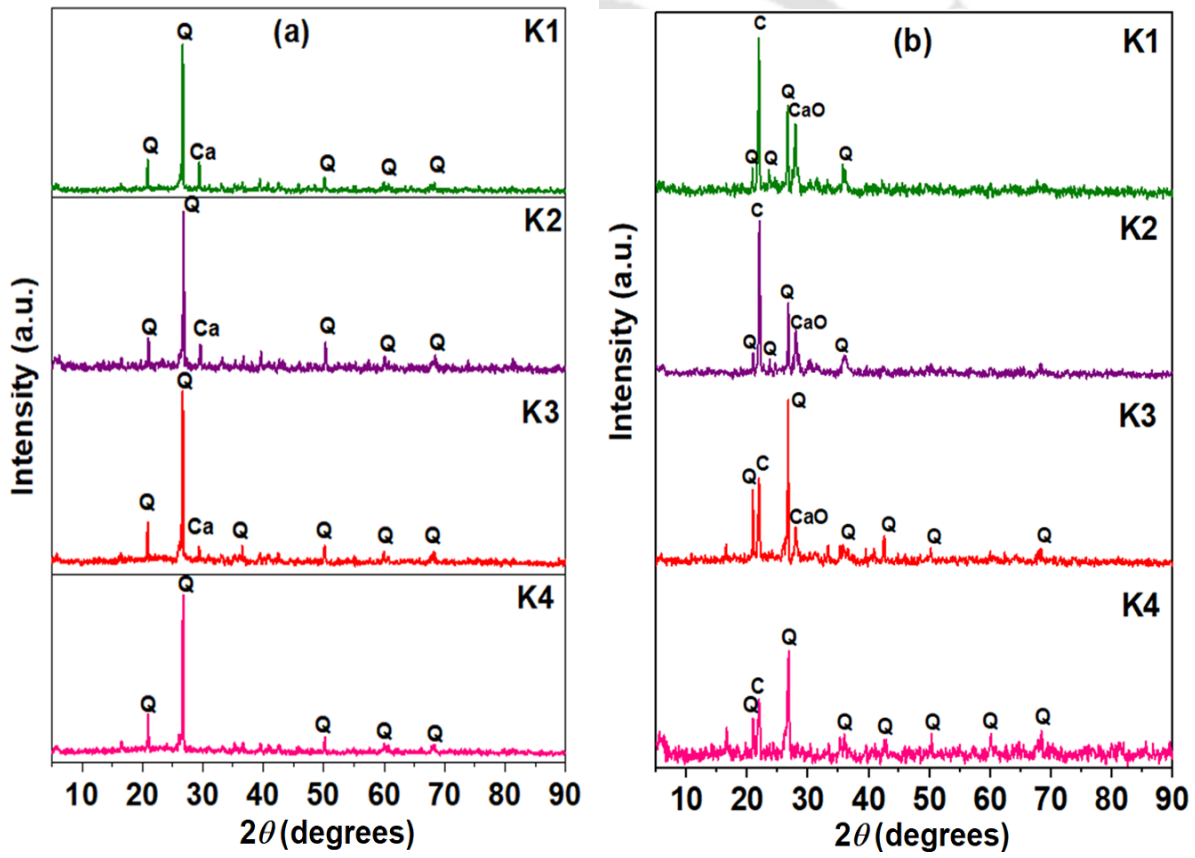

Fig. 2.12 XRD patterns of raw material mixture (left) and sintered membranes (right)

(Q: Quartz; Ca: Calcium carbonate; CaO: Calcium oxide; C: Crystoballite)

2.2.2.3 Energy Dispersive X-ray Analysis

The EDX mapping of all four membranes was also carried out and all of them reported similar uniform distribution of elements in their matrix. Therefore, EDX mapping of only one membrane (K3) is presented in Fig. 2.13. As observed in the figure, the major constituents of the membrane matrix, namely Si, Al, O, and Ca are homogenously distributed without any agglomeration or lumps. The elements, Si and Al, come from the fly ash itself, while the source for Ca is primarily from calcium oxide that is retained after $CaCO_3$ decomposition. Traces of iron is also observed, which comes from the Fe_2O_3 present in the fly ash. It is worthy to mention that Fe_2O_3 is responsible for the light-yellow tint of the sintered membrane (Zhu et al., 2016).

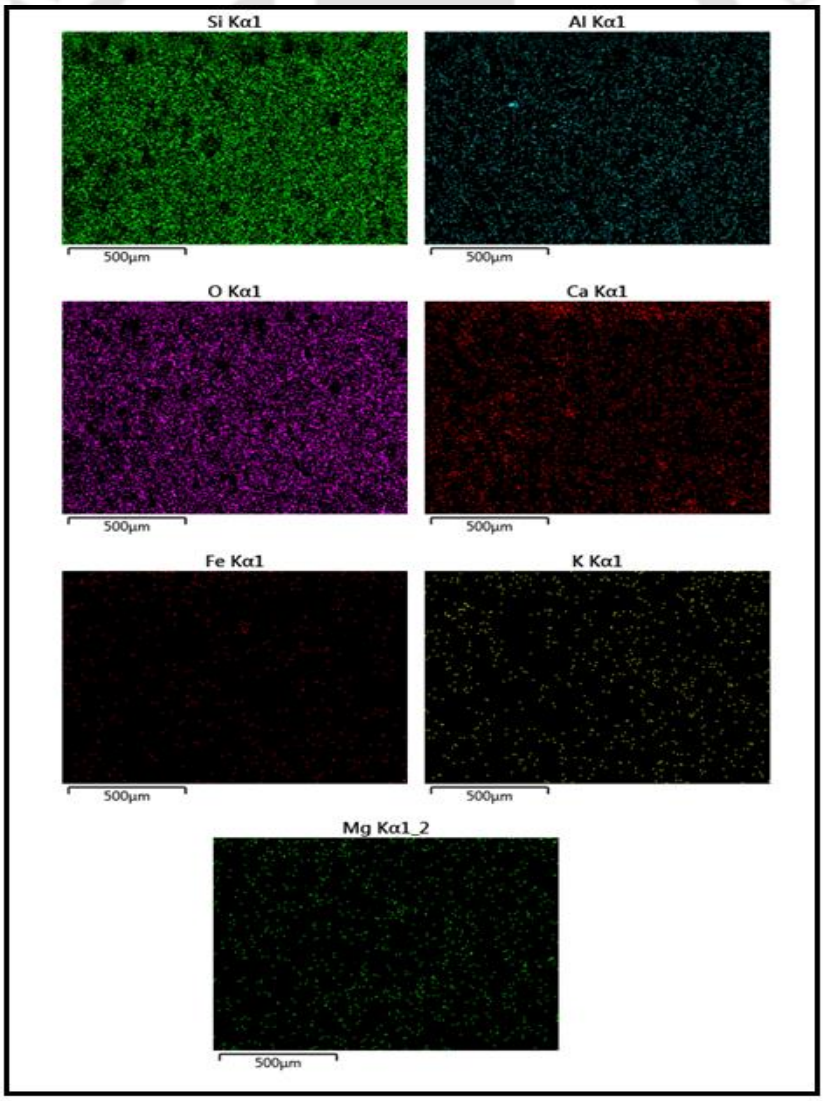

Fig. 2.13 EDX mapping of K3 membrane

Besides iron, mapping of membrane matrix also detects the presence of minute quantities of magnesium (Mg) and potassium (K) in it, which comes from fly ash, as evident from Fig 2.6. All these trace compounds were also found to be distributed uniformly across the membrane matrix. The presence of oxygen in a larger quantity can be attributed to the oxide forms of all the elements mentioned above (Zou et al., 2019; Wei et al., 2016; Zhu et al., 2016).

2.2.2.4 Porosity

Experiments conducted to evaluate the porosity of the fabricated membranes reveal that with increasing concentration of calcium carbonate, the porosity of the membrane increases (Table 2.4). An increase in the concentration of pore former ($CaCO_3$) leads to increased production of carbon dioxide owing to its thermal decomposition at a higher temperature, resulting in enhancement of the porosity of the membranes (Simão et al., 2015). A similar kind of trend regarding the change in membrane porosity with changing concentrations of $CaCO_3$ has also been reported by Kaur et al., where membranes fabricated with kaolin as the main precursor showed increased porosity values at higher $CaCO_3$ concentrations (Kaur et al., 2016).

2.2.2.5 Mechanical strength

It has been observed from the experiments that there is a sharp increase in the mechanical strength of the membranes with decreasing the quantity of calcium carbonate from 15% to 5 wt.%. This is attributed to the decrease in porosity of the membranes as a consequence of decreasing $CaCO_3$ concentration. The obtained results are in good agreement with the results reported by Liu (1997). The researcher has also observed that increasing concentration of pore former (Polyvinyl butyral) in the hydroxyapatite ceramics resulted in decreased compressive strength owing to the increased pore volume (Liu, 1997). The decrease in porosity values implies that voids in the membrane are less, thus making the membrane more rigid. However,

a reverse scenario is observed for the membrane having no $CaCO_3$, where the compressive strength of the membrane drastically reduces to 8.75 MPa. Macroporous ceramic supports fabricated using mixtures of quartz and silica also displayed a similar trend, where supports with zero pore former had the lowest strength (Kouras et al., 2017). With increasing the concentration of pore former material, mechanical strength starts increasing up to a certain extent, after which it starts following a decreasing pattern. This sharp decrease in compressive strength of the membrane is because of the absence of effective sintering aid, i.e., $CaCO_3$, which enhances membrane densification and its subsequent mechanical strength by bringing the clay particles together during the time of sintering (Kouras et al., 2017; Falamaki et al., 2004).

2.2.2.6 Chemical stability

The results of chemical stability test of the membranes (Table 2.4) elucidate that the weight loss of the membrane in the alkaline environment is very minimal (<5%), indicating the membranes can be applicable in harsh alkaline conditions. However, the weight loss in the acidic environment is somewhat higher and also increases with increasing concentration of $CaCO_3$. The probable reason is that the precipitation reaction takes place between the hydrochloric acid (HCl) and calcium oxide (CaO) present in the sample, resulting in the formation of calcium chloride ($CaCl_2$), as shown in equation (2.9) (Suresh et al., 2016). A precisely similar trend of chemical stability of the membrane in acid with changing the concentration of $CaCO_3$ was observed in the research work carried out by Vasanth et al., where the reduction in $CaCO_3$ quantity in the raw material mixture from 25% to 15% resulted in a decrease in weight loss from 6% to 1% (Vasanth et al., 2013). As membrane K4 is fabricated without using calcium carbonate, the weight loss in hydrochloric acid is very less for that membrane.

$$CaO + HCl \rightarrow CaCl_2 + H_2O \quad (2.9)$$

Hence, it is advisable not to use the membranes in strong acidic environments.

2.2.3 Water permeability and pore size calculation

The pure water flux experiments were conducted with four membrane compositions for the duration of 40 minutes at pressures 69, 138, 207, 276 and 345 kPa. Fig. 2.14 represents the pure water flux data collected for all four membranes at different pressures, while Fig. 2.15 represents the graph for the evaluation of water permeability of all the membranes. Compaction at high pressure makes the membrane saturated by filling the pores with water. Hence, after saturation, the flux was constant during the whole experiment. It is observed that pure water flux increases with an increase in the applied pressure owing to the increased driving force (Suresh and Pugazhenthi, 2017). The pure water permeability values obtained from Fig. 2.15, tortuosity values calculated using equation (2.7) and the corresponding pore size evaluated using equation (2.6) are listed in Table 2.4. It needs to mention that the pore sizes determined using FESEM images of the membranes follow a similar trend as that of the ones evaluated using pure water permeability. However, the average pore diameter calculated using FESEM images is somewhat higher than the ones calculated using hydraulic flux. For instance, the mean pore size of K1, K2, K3, K4 membranes is 0.144, 0.103, 0.133, 0.151 µm, respectively, when measured using the hydraulic flux values. On the contrary, the average pore diameter estimated from FESEM images is found to be 0.915, 0.714, 0.818 and 0.983 µm, respectively, for K1, K2, K3 and K4 membranes. The reason for this variation is that the FESEM technique captures only the surface pores of the membrane, which may become narrower throughout the membrane thickness. Moreover, pores considered in FESEM images may contain dead-end pores and also the membrane tortuosity cannot be taken into consideration in this technique. It is to be noted that the mean pore size determined using water permeation data takes into account the entire permeation pathway through which water molecule travels. Hence, the pore sizes

obtained through water permeability values are considered for further separation work, as they seem to be more realistic. This result is in agreement with the results obtained by Sinha and Purkait (2013) and Suresh and Pugazhenthi (2016).

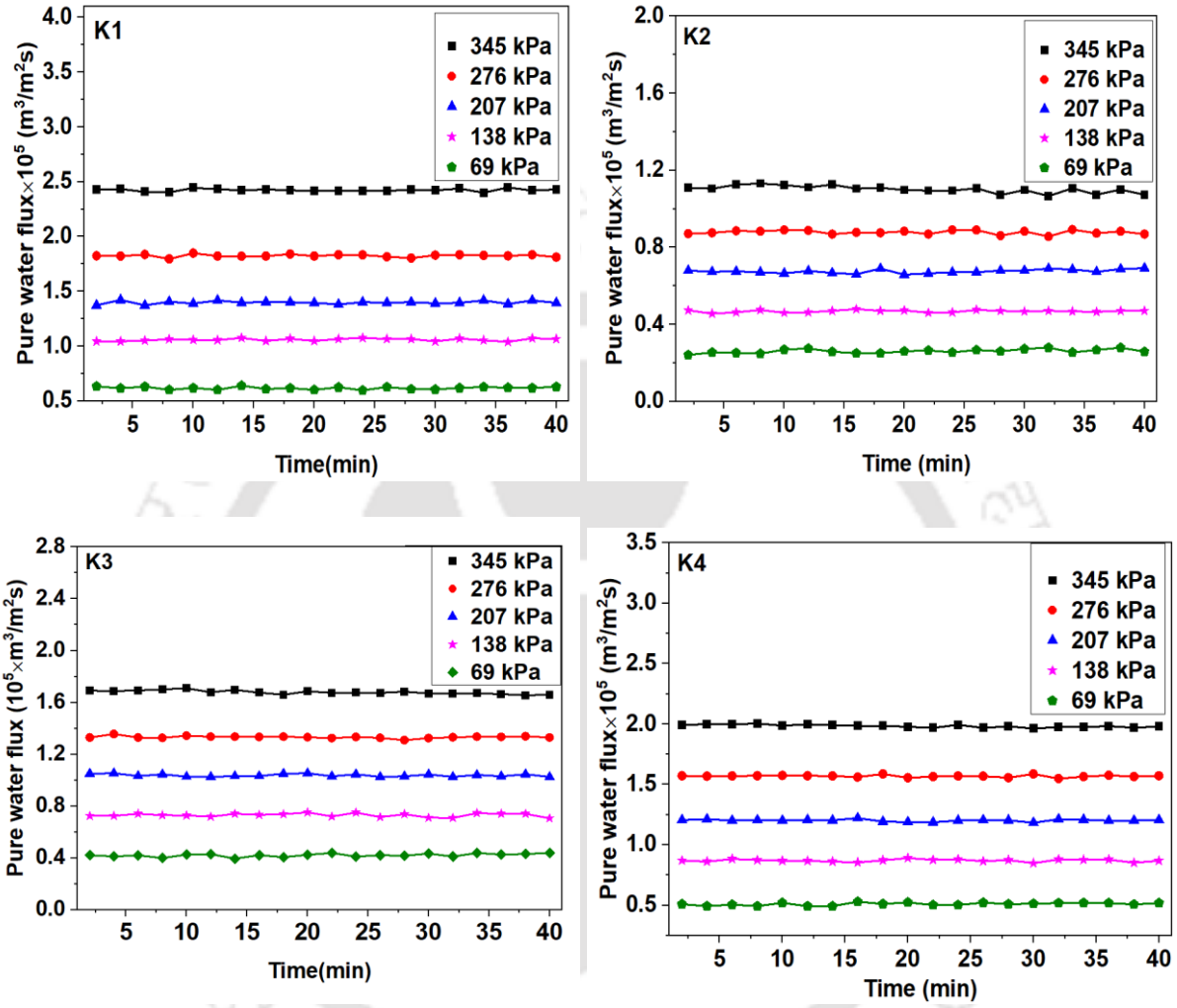

Fig. 2.14 Pure water flux with time at different pressures for membranes K1, K2, K3 and K4

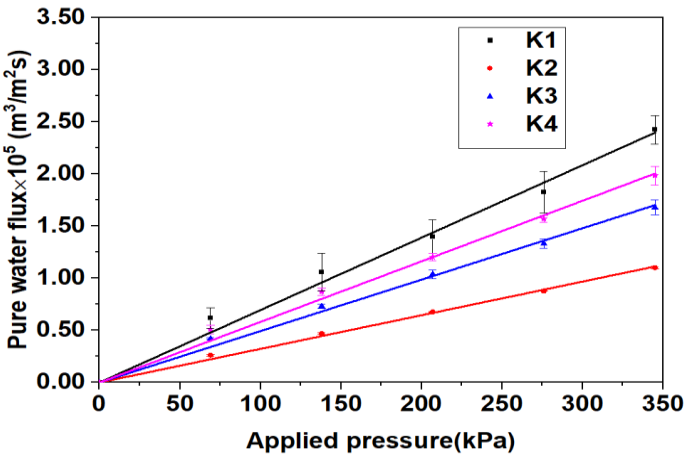

Fig. 2.15 Plot of pure water flux versus pressure for membranes K1, K2, K3, K4

Table 2.4 Summary of properties of prepared membranes (K1-K4)

Membrane	Porosity (%)	Tortuosity	Pure water permeability ($10^8 \times m^3/m^2skPa$)	Pore size (µm)	Chemical stability (Weight loss %)		Mechanical strength (MPa)
					Base	Acid	
K1	46.13±2.67	1.60	6.95±0.64	0.144	1.31±0.88	14.46±1.23	12.61±2.30
K2	42.8±2.41	1.64	3.23±0.025	0.103	2.04±0.58	12.67±0.89	18.42±2.54
K3	40.17±1.04	1.68	4.93±0.19	0.133	2.77±0.67	6.56±1.67	20.28±2.09
K4	37.36±1.16	1.72	5.81±0.21	0.151	3.93±1.11	3.28±0.35	8.75±1.47

It is observed from Table 2.4 that except membrane K1, the mean pore size of the membrane increases with decreasing content of $CaCO_3$. This may be due to the weak binding between clay particles because of the availability of a lesser amount of sintering aid ($CaCO_3$) (Falamaki et al., 2004). Even though K1 membrane has a smaller pore size than the K4 membrane, the exceptionally high value of water permeability is attributed to the very high porosity of K1 membrane (almost 46%), which ultimately surpassed the effect of sintering aid.

2.3 Optimization of membrane composition

The results obtained from various characterizations are summarized in Table 2.4. It is evident that the pore sizes of the membranes are almost in the similar range. However, in terms of mechanical strength, membrane K3 performs the best and chemical stability of this membrane is also comparatively good over K1 and K2 membranes. Though membrane K4 has the best chemical stability among all four membranes, its mechanical strength is the lowest. The porosity of K1 and K2 is higher as compared to K3. However, the lower mechanical strength of these membranes (K1 and K2) puts restrictions on their use. Moreover, a membrane porosity value within 30-40% is quite acceptable and K3 satisfies this criterion. Hence, looking at all the above-mentioned features, membrane K3 is finalized for further separation operations.

2.4 Comparison with prior arts

As evident from Table 2.5, this work represents the successful fabrication of a ceramic membrane with tubular configuration. Besides, as discussed in Chapter 1 of this thesis, the fabrication was carried out at comparatively lower sintering temperature and pore size of the membrane fabricated with optimized raw material composition is 0.133 µm. This, to the best of author's knowledge, is the least pore size to be reported in literature, and therefore can be considered having good potential for implementation in multiple separation operations.

Therefore, it can be concluded that this work successfully addresses all the major research gaps mentioned in Chapter 1 regarding the fabrication of fly ash-based ceramic membrane.

Table 2.5 Comparison of the fabricated membrane with prior arts

Material	Configuration	Sintering temperature (ºC)	Pore size (µm)	References
Fly ash, TiO_2, $CaCO_3$, PVA	Flat	800	1.47	Suresh, 2020
Fly ash, $CaCO_3$, PVA	Flat	1300	1.2	Wei et al., 2016
Fly ash, Bauxite, PVA, WO_3, AlF_3	Flat	1400	0.48	Chen et al., 2016
Fly ash, Alumina	Flat	1250	-	Yang et al., 2019
Fly ash, Bauxite, PES, PVP, N-methyl-2-pyrollidone	Hollow fiber	1400	1.02	Zhu et al., 2016
Fly ash, Methocel, Amijel, Starch	Tubular	1125	4.5	Jedidi et al., 2011
Fly ash, Quartz, Calcium carbonate	**Tubular**	**1100**	**0.133**	**This work**

2.5 Summary

Ceramic membranes using four varied compositions of fly ash, quartz and calcium carbonate were successfully prepared. The raw materials used for membrane fabrication were characterized using different techniques such as XRD, XRF, EDX, TGA and LPSA before fabricating the membranes. XRD and EDX analysis revealed silica to be the main constituent of fly ash. TGA and DTG analysis revealed that the weight loss of raw material mixture (including the binder Na-CMC) is very minimal above 1000 ºC, which justifies the use of 1100 ºC as the membrane sintering temperature. The prepared membranes using these raw materials were further characterized for evaluating different properties such as porosity, pore size, mechanical stability and chemical stability. The fabricated membranes portrayed a wide range of properties (mechanical strength 8.75-20.28 MPa, average pore diameter 0.103-0.190 µm,

porosity 37.36 - 41.65%) and hence, an optimized composition of 75% fly ash, 20% quartz and 5% calcium carbonate (Membrane K3) was chosen for fabricating membranes to be used for separation operations. Membrane with the optimized composition has a pore size of 0.133 µm and porosity of 40.17% and offers outstanding chemical and mechanical stability (compressive strength of 20.28 MPa), thus making itself suitable for implementing in various separation operations.

Chapter 3

Study of Effects of Binder Concentration on Properties of the Fly Ash-based Tubular Ceramic Membrane

Study of Effects of Binder Concentration on Properties of the Fly ash-based Tubular Ceramic Membrane

This chapter summarizes the results of the study carried out to evaluate the effect of binder (Sodium salt of carboxymethyl cellulose (Na-CMC)) concentrations on membrane properties. Membranes with optimized raw material composition, as mentioned in Chapter 2, were prepared with varied binder concentrations. Besides carrying out the extensive rheology study of the binder solutions of different concentrations, the fabricated membranes were also characterized using different standard techniques and based on the evaluated properties, the optimized binder concentration to be used for membrane fabrication was decided.

3.1 An overview of binders

Binders can be regarded as the materials that are added to the membrane fabrication process in order to impart good mobility and stability to the raw material paste. Binder becomes far more important in case of membranes manufactured via extrusion process as it helps in improving the water retention capacity of the raw materials, which is indeed a crucial parameter in the extrusion process. Lack of plasticity and mobility of the feed material can cause the formation of cracked membranes in the extrusion process, thus restricting their application in further separation processes (Fan et al., 2016).

As evident from the literature, both organic and inorganic binders have been used in the manufacturing of ceramic membranes via extrusion process (Bose and Das, 2014; Jedidi et al., 2009). However, organic binders such as carboxymethyl cellulose, polyvinyl alcohol, polyethylene glycol, etc. have taken over the inorganic binders, namely boric acid, sodium metasilicate, and so on. It needs to mention that the benefits associated with organic binders are quite large in comparison to the inorganic ones. Organic binders not only decompose at

comparatively lower temperatures than the inorganic binders, but also are quite earth-friendly, thus leaving no harmful residues after decomposition. Moreover, the organic binders come with a massive quantity of carbon, which is oxidized into carbon dioxide during the sintering process of the membrane (Zhi et al., 2016).

Among the various organic binders available, sodium salt of carboxymethyl cellulose (Na-CMC) attracted attention owing to the substantial number of benefits offered by this binder (Liu et al., 2019; Wüstenberg, 2014). Na-CMC is known to form a sticky colloidal solution in water, all thanks to its long chain structure that leads to the formation of a stronger three-dimensional network, which ultimately helps in holding the fly ash particles together (Liu et al., 2019). Moreover, the water retention capacity of Na-CMC is on the higher side, thus contributing to the formation of a good paste to produce tubular membranes through extrusion process (Wüstenberg, 2014). This water retention property of Na-CMC becomes far more useful while preparing fly ash-based membranes, as fly ash is quite hydrophobic in nature with very poor water retention capacity (American Coal Ash Association, 2003). On account of the aforementioned perks of using Na-CMC solution as a binder in the membrane fabrication process, along with the other benefits of organic binders mentioned earlier in this section, this work focuses on using Na-CMC solution to prepare tubular ceramic membranes and further investigate the effect of binder solution concentration on the variation of different membrane properties.

It has been reported in the literature that decomposition of binder takes place during the process of membrane sintering and drying. In case of Na-CMC, the thermal degradation takes place at around 280 ºC, leading to the generation of different low molecular weight hydrocarbons along with formation of some polyunsaturated products, which on further heating at higher temperature get converted to CO_2 (Tan et al., 2017). This process of binder removal is known as debinding. This process is very delicate and needs to be carried out carefully because rapid

evolution of gases during this step can cause formation of blisters and cracks in the membrane. Moreover, after removal of binder, the membrane becomes very brittle as the particles in the matrix are held together by only weak physical interactions and gain strength only after sintering (Pfaffinger, 2015; Trunec,1996). It needs to mention here that during the process of sintering, particles of the brittle membrane matrix fuse together by the process of necking and grain growth. Initially, the contact among the particles increases and bridging of particle occurs through neck formation and grain growth in the temperature range of 900-1000 ˚C (Diana et al., 2020). The contact between particles increases further on increasing temperature up to 1100 ˚C, which causes shrinkage and densification of membrane. This whole process of necking, shrinkage and densification during the process of membrane sintering leads to increased membrane strength (Zou et al., 2019c; Derlet, 2017). The mechanism of thermal debinding and sintering of membrane is shown in Fig. 3.1.

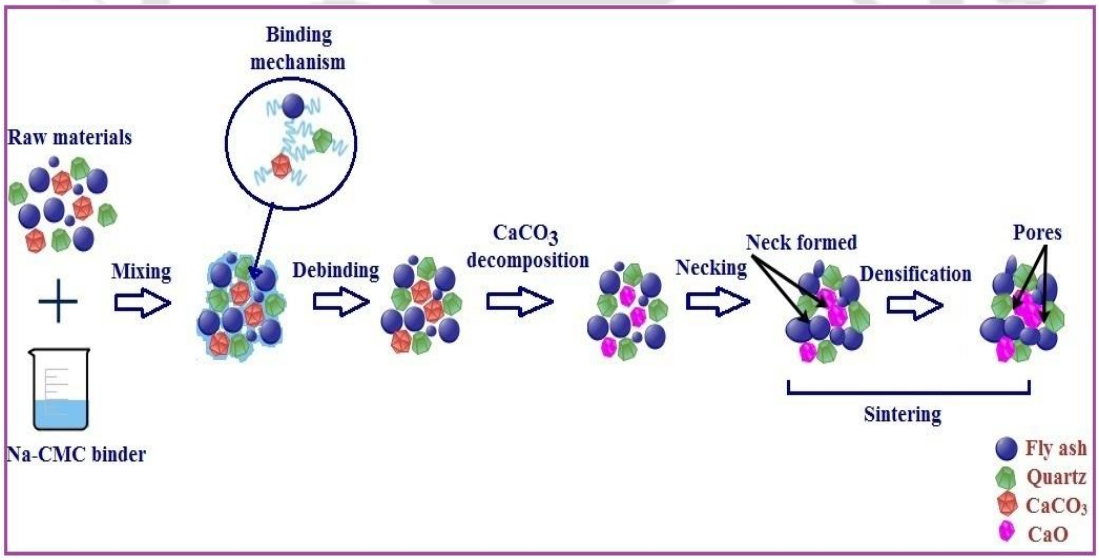

Fig. 3.1. Debinding and sintering phenomena

3.2 Experimental

3.2.1 Raw materials

The raw materials used for membrane fabrication in this Chapter are Fly ash, Quartz, Calcium carbonate and Sodium salt of carboxy methyl cellulose (binder). All of these materials were procured from the same source, as mentioned in Chapter 2 of this thesis.

3.2.2 Membrane fabrication

The optimized raw materials composition (75 wt.% fly ash, 20 wt.% quartz and 5 wt.% calcium carbonate) suggested in Chapter 2 was selected for making tubular membranes in order to examine the influence of binder concentration (Na-CMC) on properties of the membranes. The same procedure mentioned in Chapter 2 was employed for the fabrication of tubular membranes. Briefly, the raw materials were mixed with various concentrations of the binder solution (2, 3 and 3.5 wt.% Na-CMC solution) to obtain a semi-plastic ceramic paste, which was then extruded through an extruder to get tubular-shaped membranes. The obtained green membrane tubes were dried in open air for 24 hours, followed by oven drying at 100 ˚C and 200 ˚C respectively, for 24 hours in each case. After that, membranes were sintered at a temperature of 1100 ˚C with a holding time of 6 hours. The dimensions of the fabricated tubular membranes are 5.5 mm inner and 11.5 mm outer diameters with a length of 100 mm. The prepared membranes are named as M2, M3 and M3.5, where numbers 2, 3 and 3.5 refer to the concentration of the binder solution.

It needs to mention here that the hydrophobic characteristic of fly ash makes it impossible to fabricate the membranes without binder. Even the viscosity of 1 wt.% aqueous solution of Na-CMC is so low that it could not hold the feed paste together and hence, binder concentrations from 2 wt.% onwards were considered for membrane fabrication. The detailed rheological

investigations that led to considering these three binder concentrations for this study have been discussed in section 3.3.1 of this Chapter.

3.2.3 Characterization of raw materials and fabricated membranes

As the objective of this Chapter is to focus on the effect of binder concentrations on membrane properties, hence the rheological characteristics of aqueous solutions of Na-CMC at different concentrations were carried out using an interfacial rheometer (Anton Paar, Physica MCR 301). The parallel plate configuration was used to evaluate the rheological behaviour of the Na-CMC solutions at ambient temperature, and the experiments were carried out over a shear rate of 0.01-1000 s^{-1}. The obtained stress, strain as well as viscosity values were plotted using the power law model, as shown in equation (3.1), to calculate the zero-shear viscosity as well as the flow behaviour indices (Reddy, 2015).

$$\tau = k\gamma^n \tag{3.1}$$

Where, τ is the shear stress, γ is the applied strain, k is the flow consistency index and n is the flow behaviour index. For rheological study of Na-CMC solution, rheometer was preferred over viscometer as latter one works best for Newtonian fluids, which are independent of shear rate. On the contrary, Na-CMC solution follows highly non-Newtonian behaviour, and hence, the use of a rheometer is always preferred in studying the rheology of this type of solution (British Plastics and Rubber, 2020).

The fabricated membranes have undergone a variety of characterization techniques, based on which their properties are evaluated. The membranes were characterized for evaluation of structural homogeneity, porosity, pore size, chemical as well as mechanical stability. The detailed description of each of these techniques is already mentioned in the previous Chapter.

3.3 Results and discussions

3.3.1 Rheological behaviour of Na-CMC solutions

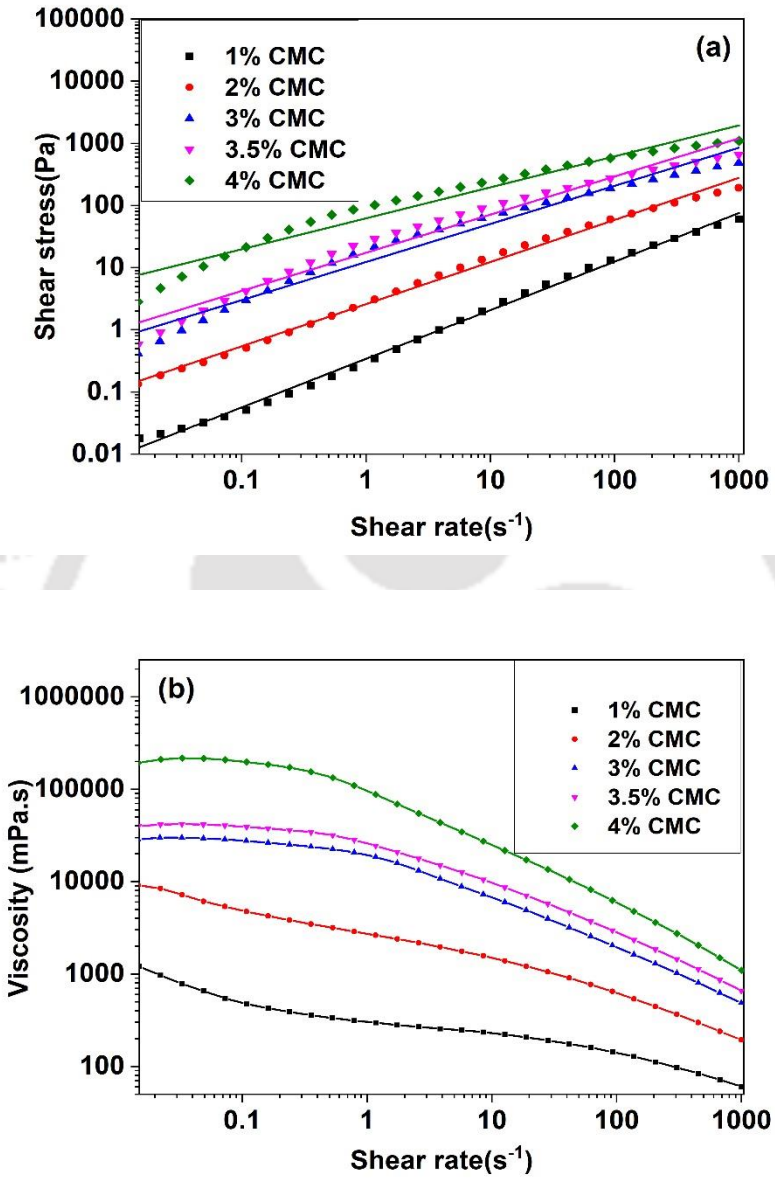

Fig. 3.2 (a) Stress-strain curve and (b) Viscosity-strain curve of Na-CMC solutions with different concentrations

The study of rheological behaviour of aqueous solutions of different concentrations of Na-CMC solution revealed that the solution viscosity increases drastically with an increase in the Na-CMC concentration. The detailed analysis reported in Fig. 3.2 and Table 3.1 has shown that increasing binder solution concentration from 1% to 4% resulted in a decrease in the values of

flow behaviour index (Reddy, 2015). This signifies that the increased concentration makes the solutions divert from Newtonian behaviour, thus making their mixing more difficult (Kao et al., 2015; Dickey, 2015). It has also been observed that the zero-shear viscosity showed a steep rise when the solution concentration changed from 3.5% to 4%. Hence, Na-CMC concentrations above 3.5% were not considered for membrane fabrication to avoid the formation of agglomerates owing to improper mixing. Though the zero-shear viscosity of 1 wt.% Na-CMC solution was quite low, it was not considered for membrane fabrication, as the solution was unable to hold the clay particles together properly, leading to the formation of deformed shaped membranes (Fig. 3.3).

Fig. 3.3 Deformed shaped membrane with 1 wt.% Na-CMC solution

Table 3.1 Rheological data of different concentrations of aqueous Na-CMC solution at 25 ˚C

Na-CMC concentration (wt.%)	Zero shear viscosity (Pa.s)	Flow behaviour index (n)
1	1.21	0.782
2	9.13	0.677
3	28.62	0.613
3.5	39.72	0.613
4	193.70	0.498

The rheological observations mentioned above are in good agreement with the previous works reported in earlier literature (Reddy, 2015).

3.3.2 Morphology study of membranes

Once the membranes with different concentrations of binder solution were fabricated, the morphology of the membranes needs to be checked in order to confirm their usability in separation processes further. Fig. 3.4 corresponds to the inner as well as outer surface images of membranes M2, M3 and M3.5, respectively. The darker portions in the images represent pores, which are marked by red arrows, while the lighter areas represent the ceramic particles. The membrane surfaces are smooth and are devoid of any defects such as pinholes or cracks. However, it has been observed that the membrane fabricated with higher binder concentration shows non-uniformity in its pore size. The results illustrated in Fig. 3.5 also reveal the same, showing a narrow pore size distribution of M2 membrane compared to the M3 and M3.5 membranes. The pore sizes of M2 membrane are within the range of 0 - 1.5 µm, while the pores are scattered over a wide range of 0 - 5.0 µm and 0 - 3.5 µm in case of M3 and M3.5 membranes, respectively. The possible reason behind this non-uniformity may be the increased viscosity of the solutions, which causes stronger particle agglomeration in the membrane matrix. During sintering at 1100 ^{o}C, these agglomerates compact and lead to a wider pore size distribution (Das, 1999).

However, this problem of agglomeration is not observed in the case of M2 membrane due to comparatively lower solution viscosity. It needs to mention that FESEM images, using the same procedure as described in Chapter 2, were also being used to evaluate the average pore size of the membranes. The calculated average pore diameters of M2, M3, M3.5 membranes are 0.81, 1.96 and 1.16 µm, respectively (Bouazizi et al., 2016; Jana et al., 2010). This

observation is sufficient to prove the fact that comparatively smaller sized pores are present in M2 membrane as compared to the other two membranes.

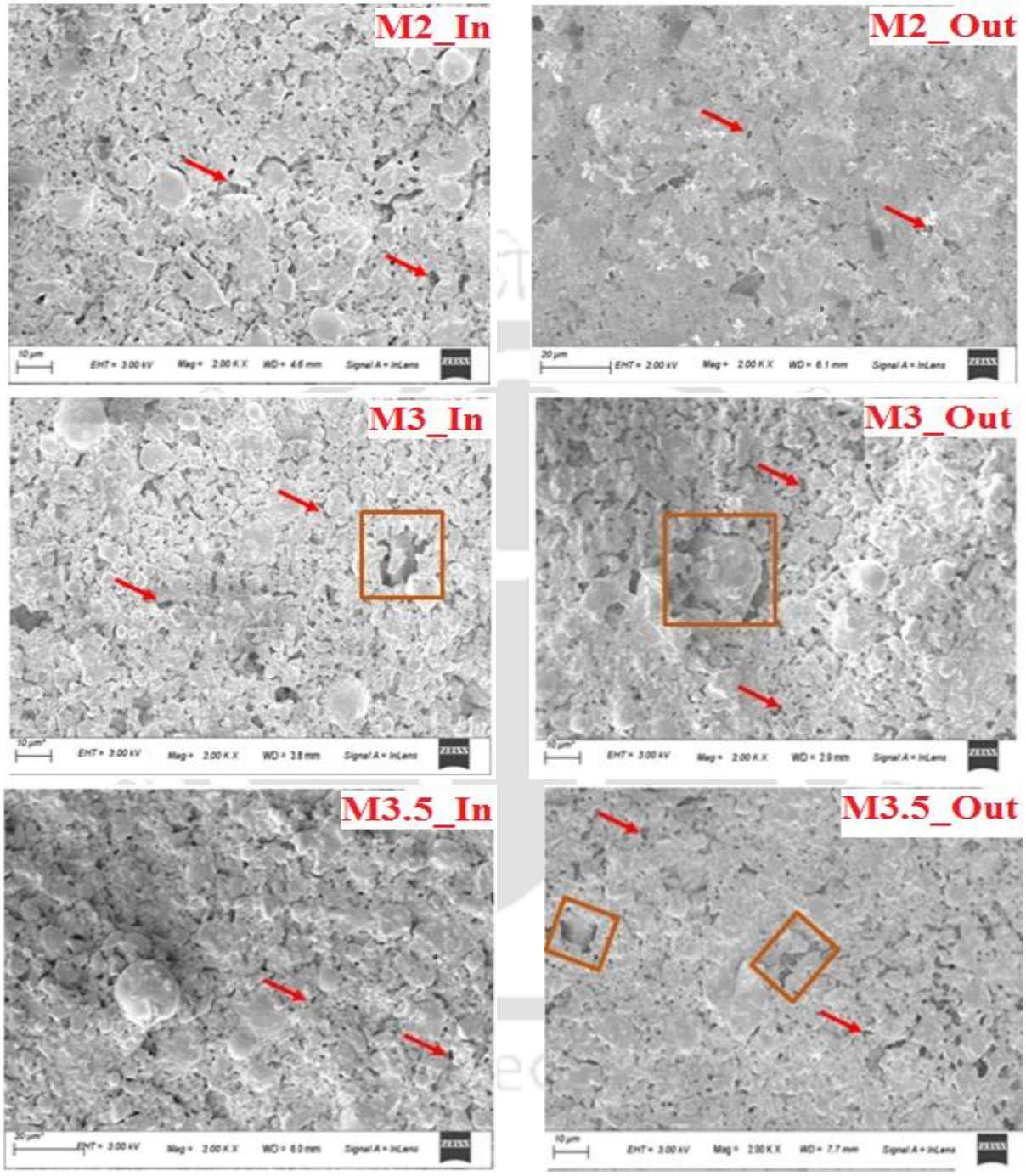

Fig. 3.4 FESEM images of inner and outer surfaces of the membranes (M2-M3.5) (Red arrows in the picture denote the pores in the membrane while the brown boxes correspond to the wider pores resulted due to agglomeration caused by increased binder content)

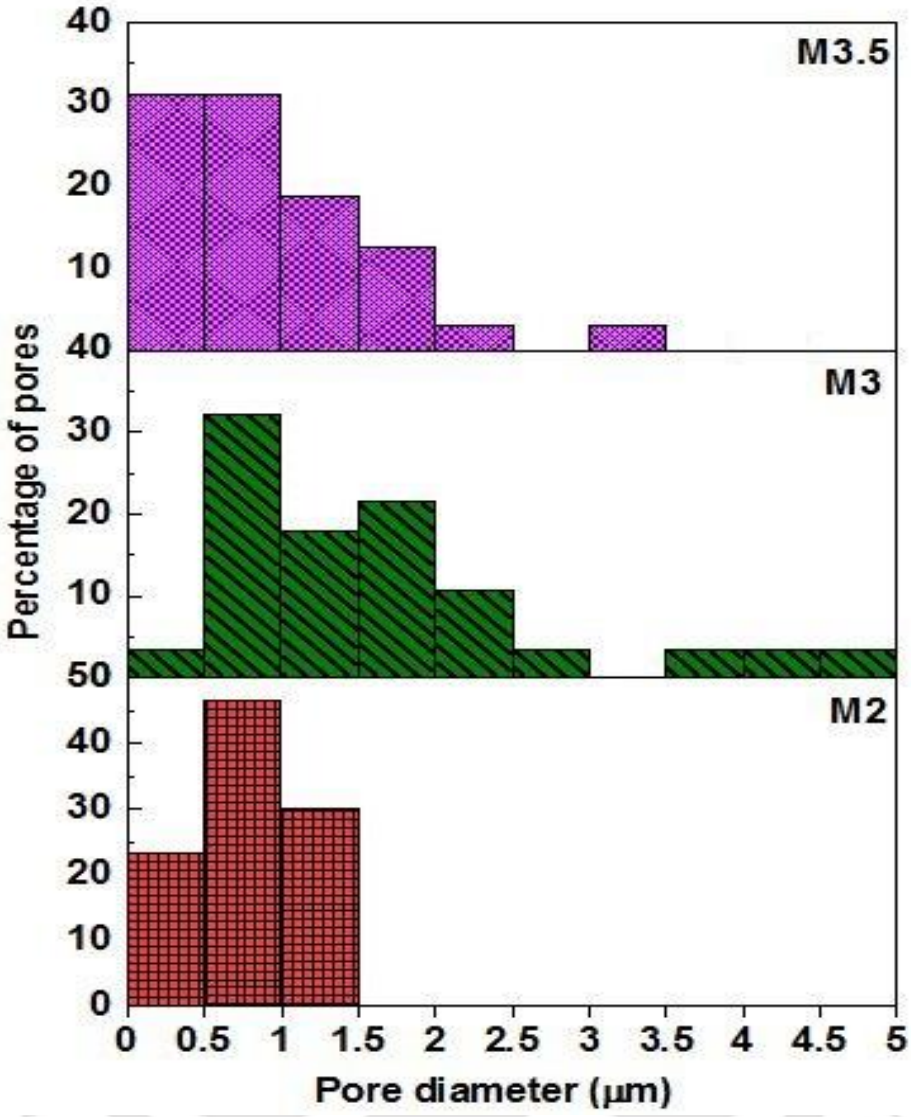

Fig. 3.5 Pore size distribution of M2, M3 and M3.5 membranes

3.3.3 Porosity

The average porosity values of M2, M3 and M3.5 membranes fabricated using various concentrations of binder solution are 40.17±1.04, 41.65±2.20 and 41.24±0.79%, respectively. It has been observed that there is no significant variation in the membrane porosities with increasing the concentration of binder. Compared to M2 membrane, the membranes (M3, M3.5) prepared with higher binder content (> 2 wt.% Na-CMC solution) demonstrate similar porosity values even after showing the presence of bigger pores, as evidenced from FESEM

analysis (Figs. 3.4 and 3.5). This may be attributed to the fact that the membrane M2 may possess larger numbers of smaller pores as compared to membranes M3 and M3.5, where lesser number of pores with bigger diameters may present, thus compensating for the overall membrane porosity. The pore density of M2, M3 and M3.5 membranes are found out to be 17.7×10^9, 12.2×10^9 and 14.5×10^9 pores/m^2, respectively, which is in accordance with the above-mentioned justification. Similar trend of variation in membrane porosity with binder content has been observed in the works of Das (Das, 1999). The obtained porosity values in this work are consistent with the other ceramic membranes prepared by various authors. As evident from the literature, ceramic membranes with 40% porosity are considered to be highly suitable for separation applications (Benito et al., 2015; Vasanth et al., 2011; Kumar et al., 2015a).

3.3.4 Mechanical strength

The mechanical strength of the membranes is observed to decrease with an increase in binder concentration. The mechanical strength of M2, M3 and M3.5 membranes, as obtained from compression strength evaluation test, are 20.28±2.09, 14.98±1.44 and 12.60±2.00 MPa, respectively. As evident from FESEM images (Figs. 3.4 and 3.5), at higher binder concentrations, the formation of bigger sized pores in the membrane is noticed due to the burn out of binder agglomerates, which suppresses the driving force of densification. This results in a comparatively hollow structure inside the membrane as compared to the membranes fabricated using lower binder content. Consequently, a significant decline in the mechanical strength is noticed at higher binder concentrations. It is well documented in the literature that membranes having dense structures possess higher membrane strength than those having bigger pores as bigger pores are very much prone to defect formation on application of compressive force (Adam et al., 2020). To sum up, the high porosity fly ash-based ceramic

membranes prepared in this work display moderate mechanical strength compared with those of clay-based porous ceramic membranes reported by other authors (Zou et al., 2019c; Jedidi et al., 2009).

3.3.5 Chemical stability

Results of chemical stability tests indicated that only minimal weight loss of the membranes is observed in basic medium (2.77±0.67, 3.60±0.65 and 3.02±1.26% for M2, M3 and M3.5 membrane, respectively), thus signifying the potential applicability of the membranes in harsh basic condition. However, the weight loss of the membranes is on the higher side in acidic environments, restricting their use in low pH environments. The corresponding weight loss for M2, M3 and M3.5 membrane in acidic medium is 6.56±1.67, 10.83±1.16 and 12.23±1.67%, respectively. As mentioned in Chapter 2, CaO present in the sintered membranes is mainly responsible for the decrease in membrane weight after acid treatment. CaO reacts with hydrochloric acid, forming precipitates of calcium chloride, thus leading to loss of weight (Suresh et al., 2016).

However, it is seen that membranes fabricated with increased binder content demonstrate higher weight loss in acidic condition. As evident from FESEM images (Fig. 3.4), at higher binder concentrations, the formation of abnormally large pores takes place in the membrane and such large pores can be considered as the main cause of poor chemical resistance of the membranes. The large sized pores allow the acidic solution to enter into the pores more easily by offering lesser diffusional resistance and thus, contribute to higher weight loss (Saxena et al., 1974). The findings obtained in this work are in good agreement with those reported by Bose and Das (Bose and Das, 2014).

3.3.6 Water permeability and pore size evaluation

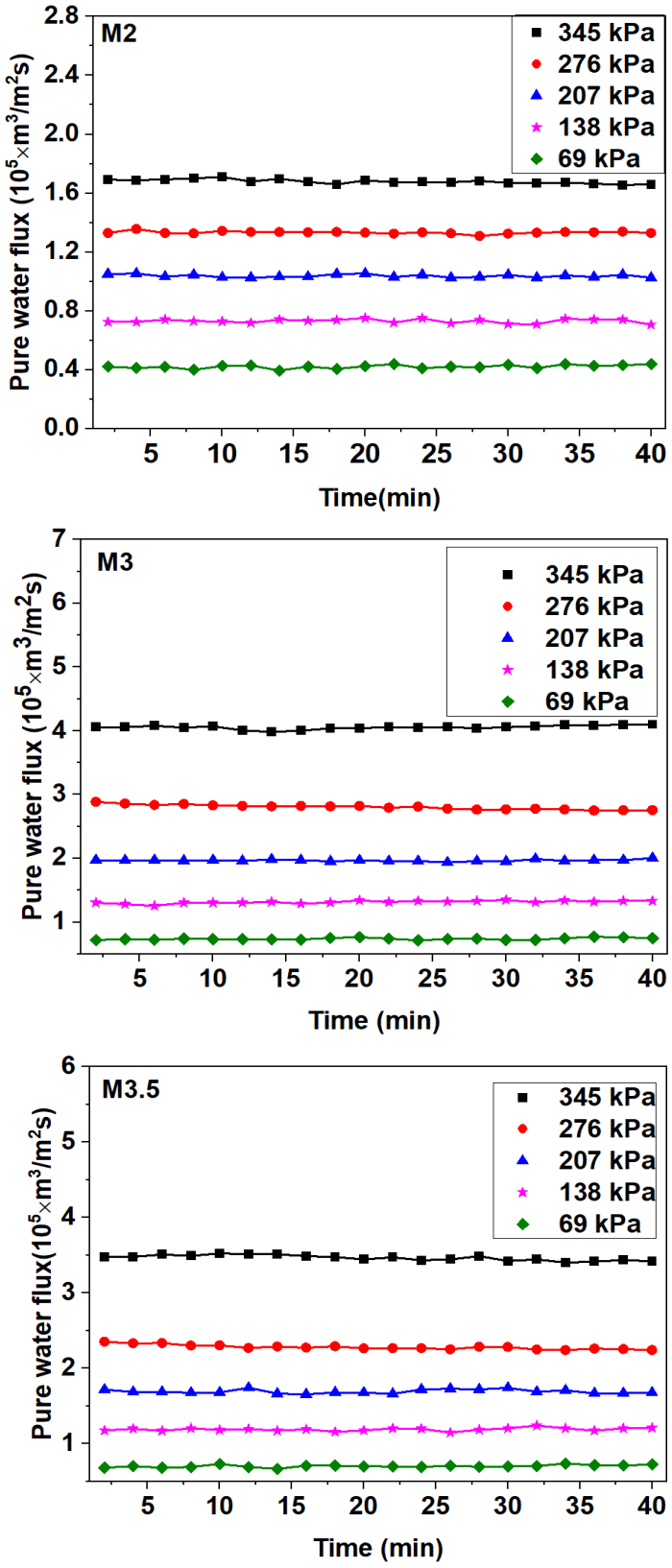

Fig. 3.6 Pure water flux as a function of operating time for membranes M2, M3 and M3.5

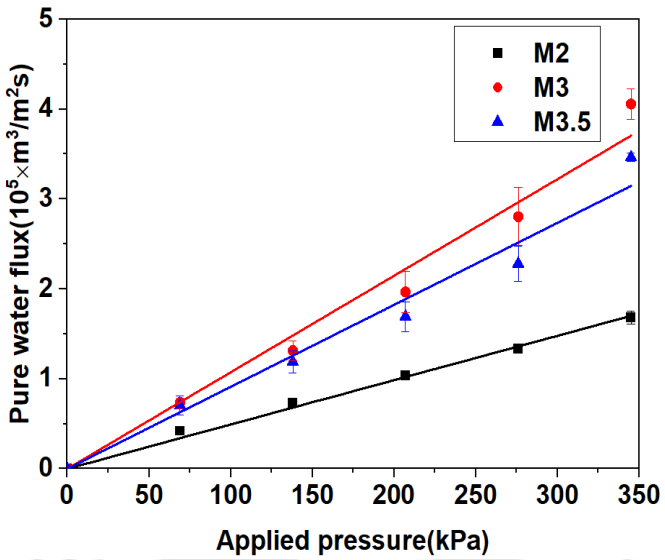

Fig. 3.7 Pure water flux at different applied pressures for membranes M2, M3 and M3.5

Results of pure water flux of the three membranes (M2, M3 and M3.5) performed using cross-flow filtration setup are depicted in Fig. 3.6. The constant water flux for the entire duration of experiment at a specific pressure signifies the saturation of the membrane pores with water molecules. For all the membranes, the water flux rises with an increase in the applied pressure (Fig. 3.7) and this effect is solely because of an enhancement in the driving force, which pushes more water through the membrane pores. As evident from Fig. 3.7, an increased pure water flux is observed at higher concentration of binder (Na-CMC). This can be ascribed to the presence of bigger pores in the membrane. Moreover, the pore size evaluated using water permeability data reveals that the membrane pores are in the similar size range for M3 and M3.5 membranes, average pore size being 0.190 µm for M3 membrane and 0.177 µm for M3.5 membrane. However, the pore sizes of these membranes are slightly higher than that of M2 membrane (0.133 µm), which may be contributed by the few bigger pores present in the former membranes as it has already been mentioned that the agglomeration effect is more pronounced in those two membranes (Das, 1999). This trend of pore size variation of membranes is quite similar to that calculated from FESEM images using ImageJ software. However, the size of

pores obtained from FESEM images is comparatively larger as this method considers all the surface pores, including the dead-end ones (Sinha and Purkait, 2013).

3.4 Optimization of binder composition

Different characterization experiments conducted on the membrane samples (M2-M3.5) revealed that binder content used in the clay paste for fabrication of membrane has immense effect on the membrane properties. It has been found that with an increase in binder content from 2 to 3.5 wt.%, the chemical as well as mechanical stabilities of the membranes decreased significantly. Issues were also faced in mixing the binder solutions having higher concentration (> 3 wt.%) with raw materials owing to the enhanced viscosity of the solution. Moreover, the formation of abnormally larger pores in the membranes was evident in the FESEM images. Hence, in view of the above, membrane M2, fabricated with 2% Na-CMC binder solution, was finalized for use in further separation processes. Membrane M2 offers an appreciable porosity value of 40.17±1.04%, an excellent mechanical strength of 20.28±2.09 MPa with a mean pore diameter of 0.133 µm. The chemical stability of the membrane was also quite satisfactory and hence, the use of this binder concentration for membrane fabrication is quite justifiable.

3.5 Comparison with prior arts

The rapid growth of membrane filtration processes has made the researchers put their efforts in analyzing the various crucial parameters affecting membrane properties. Membranes are fabricated with various binders in order to get the best of the membrane properties. A scrupulous analysis of different binders used in the fabrication of fly ash-based membranes has revealed the applications of binders such as polyvinyl alcohol, methocel, methyl cellulose, and so on (Table 3.2). The membranes fabricated using the above-mentioned binders resulted in larger pore diameters, thus restricting their multi-folded application. Larger pore sized

membranes not only have lesser rejection performance, but also are more prone to irreversible membrane fouling caused by pore blocking phenomenon (Hwang et al., 2008).

Table 3.2 Encapsulation of literature corresponding to use of various binders in the fabrication of fly ash-based membrane

Composition of membrane	**Binder**	**Sintering temperature (˚C)**	**Pore diameter (µm)**	**References**
Fly ash, Amijel, Starch	Methocel	1125	4.50	Jedidi et al., 2009
Fly ash	Methyl cellulose	1190	2.13	Fang et al., 2011
Fly ash, natural bauxite, Vanadium pentoxide, Aluminium fluoride	Polyvinyl alcohol	1300	0.39	Cao et al., 2014
Fly ash	Polyvinyl alcohol, Glycerol	1050	~1.00-2.00	Zou et al., 2019c
Fly ash, Quartz, Calcium carbonate	**Sodium salt of carboxymethyl cellulose**	**1100**	**0.133**	**This work**

However, the membrane fabricated in this work using Na-CMC binder represents the least pore size compared to fly ash membranes reported in literature (Table 3.3). The sintering temperature involved in the production of membrane is also relatively lower than most of the cases, thus signifying the low cost associated with the sintering process (Zhi et al., 2016; Benito et al., 2015). This work is focused on reducing the cost of membrane fabrication process and the use of a low sintering temperature justifies its purpose.

Therefore, it can be inferred that the number of benefits associated with the membrane fabricated using Na-CMC binder convinced the authors to consider this binder as a potential alternative for use in the preparation of fly ash-based ceramic membrane.

Table 3.3 Encapsulation of literature corresponding to use of carboxymethyl cellulose in the fabrication of ceramic membrane

Composition of membranes	Sintering temperature (˚C)	Pore size (µm)	References
α-Alumina, Glycerol, CuO/TiO_2, Carboxymethyl cellulose	1200	-	Zhi et al., 2016
Kaolin, Alumina, Carboxymethyl cellulose	1400	1.00	Huang et al., 1998
SiC particles, graphite, activated carbon, Carboxymethyl cellulose	1300	-	Xu et al., 2019
α-Alumina, SiO_2, Polyethylene glycol, Carboxymethyl cellulose	1600	1.20	Benito et al., 2005
Fly ash, Quartz, Calcium carbonate	**1100**	**0.133**	**This work**

3.6 Summary

Tubular ceramic membranes using fly ash as the base material (75%) along with requisite quantities of quartz (20%) and calcium carbonate (5%) have been prepared by varying the quantity of binder (Na-CMC). Experiments revealed that increased binder concentration leads to agglomeration in the membrane matrix, causing the formation of large and uneven pores in the membrane. The mechanical strength and chemical stability of the membranes reduced significantly with an increase in binder concentration. Hence, based on rigorous experiments conducted to evaluate the properties of fabricated membranes, 2 wt.% solution of Na-CMC is found to be sufficient in imparting good physical as well as mechanical properties to the membrane. Membrane M2, fabricated using the aforementioned binder concentration, possesses an average pore diameter of 0.133 µm and porosity of 40.17%, besides having the capability of withstanding mechanical strength of about 20.28 MPa. Moreover, the membrane possesses a quite appreciable hydraulic permeability value of 4.93×10^{-8} m^3/m^2skPa, signifying the capability of the membrane to produce high flux. The chemical stability of the membrane

is also quite satisfactory for application in industrial processes. Therefore, it can be concluded that the use of 2 wt.% aqueous solution of Na-CMC as a binder in fly ash-based tubular ceramic membrane fabrication is quite appreciable for producing membranes with good physical, mechanical as well as chemical properties.

Chapter 4

Performance Evaluation of Fly Ash-based Tubular Ceramic Membrane in Liquid Phase Separation Processes

Performance Evaluation of Fly Ash-based Tubular Ceramic Membrane in Liquid Phase Separation Processes

This chapter discusses about the versatility of fabricated fly ash-based tubular ceramic membrane for implementing in different liquid phase separation processes. Three different feeds, namely poultry slaughterhouse wastewater, starch processing wastewater and glycerol rich biodiesel emulsion, were used to evaluate the performance of the membrane. In all the aforementioned cases, the feed and the permeate were characterized using standard techniques to investigate the extent of rejection that can be achieved by the membrane and whether the produced permeate satisfies the required norms as prescribed by the respective authorities.

4.1 Treatment of poultry slaughterhouse wastewater

4.1.1 Chemicals

Poultry slaughterhouse wastewater used for experimental works was supplied by a local vendor from Ganeshguri, Assam. The reagents required for measuring Chemical Oxygen Demand (COD) of feed and permeate samples of poultry slaughterhouse wastewater treatment are mercury sulfate, silver sulfate, sulfuric acid and potassium dichromate. Amongst them, sulfuric acid and potassium dichromate were supplied by Merck (I) Ltd., Mumbai, India, while the rest two were delivered by Hi-Media (I) Ltd..

4.1.2 Experimental methodology and investigations

Poultry slaughterhouse wastewater contains a higher level of impurities, which leads to higher Chemical Oxygen Demand (COD), turbidity as well as total suspended solids (TSS). Hence, it is of utmost importance to evaluate the characteristics of feed water before sending it through the filtration apparatus. The pH of the feed sample was evaluated using a pH meter (Eutech

Instruments, Model: pH 700) and the turbidity was evaluated using a turbidity meter (Hintron Instruments, Model: HI-142). COD and TSS of feed and permeate samples were calculated using standard APHA protocols (APHA, 1998).

The performance of the optimized membrane in treating poultry wastewater was evaluated using the experimental setup shown in Fig. 4.1. With raw poultry wastewater, the filtration tests were conducted at pressures 207, 276, 345, 414 and 483 kPa with a constant cross flow rate of 11.11×10^{-6} m^3/s for three hours. The performance of the membrane was evaluated in terms of reduction in the Chemical Oxygen Demand (COD), turbidity as well as total suspended solids (TSS) in the permeate. Equation (4.1) is used for the calculation of the rejection performance of the membrane (Kumar et al., 2016).

$$Rejection\ efficiency\ (\%) = \left(1 - \frac{C_p}{C_f}\right) \times 100 \qquad (4.1)$$

Where, C_f and C_p are the concentration of parameters under consideration in the feed and permeate, respectively.

After performing the filtration experiment at a specific pressure, the membrane was first cleaned with Millipore water for 30 minutes, followed by cleaning with a detergent solution (1 g/L surf excel solution) for the duration of 1 hour. It was well documented in the literature that the detergent treatment is one of the most effective methods to solubilize the components present in poultry processing wastewater as the majority of these components are fats, oil and grease (Pirooz et al., 2018). After detergent cleaning, the membrane was ultra-sonicated for 15 minutes to remove any pore-blocking material present in it. The ultrasonic cleaning process uses the principle of cavitation to remove the contaminants present not only in the membrane surface, but also in the pores of the membrane (Welker, 2010).

The MF setup with the membrane was once again cleaned by passing Millipore water for 30 minutes to remove residual soap in it. Then the water permeability tests were conducted before running filtration experiments for the next pressure to ensure whether the membrane regains

its original water flux value. It needs to mention that the regenerated membrane shows water permeability values within ±5% of its initial water flux value. It clearly signifies that the membrane got cleaned. All the above-mentioned experiments were conducted at room temperature. The various parameters maintained for the filtration experiment and subsequent cleaning are presented in Table 4.1.

Table 4.1 Operational parameters of wastewater treatment process

Parameter	**Values**
Temperature	25 ˚C
Pressure	207- 483 kPa
Cross flow velocity	11.11×10^{-6} m^3/s
Filtration experiment duration	3 hours
Concentration of detergent solution used for cleaning	1 g/L

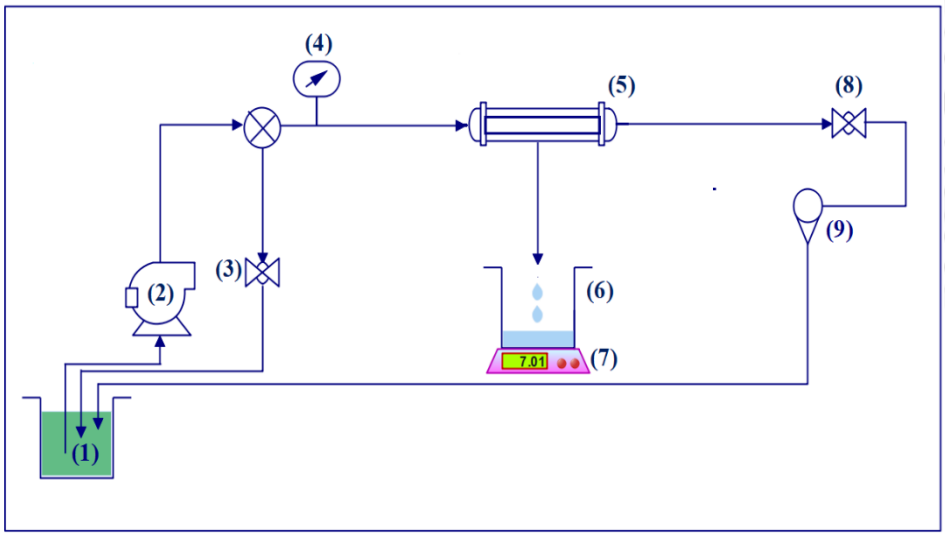

Fig. 4.1 Experimental setup [1: Feed water tank, 2: Pump; 3,8: Ball valve, 4: Pressure gauge, 5: Membrane module, 6: Permeate tank, 7: Weighing balance, 9: Rotameter]

4.1.3 Results and discussions

Poultry processing wastewater is highly laden with organic matters. Among the various contaminants present in poultry wastewater, almost 35% corresponds to the large floating debris resulting from the agglomeration of grease and fat, while the major fraction (around

55%) corresponds to suspended solids containing lipids, proteins, pathogenic microbes, etc. These suspended solids are the prime reason for the formation of opaque haze in poultry wastewater. The rest 5-10% of contaminants are contributed by particles sticking to the emulsified globules present in the wastewater (Avula et al., 2009). Hence, the characteristics of the poultry wastewater collected for testing the filtration performance of the membrane were also evaluated and the results are mentioned in Table 4.2. It needs to mention that the BOD_5 value of the raw wastewater mentioned in Table 4.2 was calculated using the ratio $BOD_5/COD = 0.6$. This ratio has been extensively used in many research works related to poultry slaughterhouse wastewater to calculate the BOD_5 values from the experimentally obtained COD values (Shih and Kozink, 1980; Whitehead, 1976).

Table 4.2 Characteristics of poultry slaughterhouse wastewater (feed)

Parameter	**Values**
pH	6.19 ± 0.07
Total suspended solids (mg/L)	414.50 ± 69.50
Turbidity (NTU)	20.70
COD (mg/L)	271.95
BOD_5 (mg/L)	163.17

The poultry wastewater was passed through the membrane module at five different pressures, keeping all the other parameters constant, as mentioned in Table 4.1. It is evident from Fig. 4.2 that the permeate flux increases with an increase in the applied pressure. The pressure being the driving force in this membrane separation process, its increasing value causes increased driving force, thus leading to a higher flow of permeate (Zhang et al., 1997). However, the flux declines with time, which may be due to the resistance offered by pore blocking and formation of the cake layer. In the initial period of filtration, a rapid decrease in the flux is noticed due to pore blocking of foulant particles. However, the fouling caused by the formation of cake layer on the membrane surface due to the deposition of foulants makes the decline of the permeate

flux gradual. The fouling occurred due to cake layer formation over the membrane surface is regarded as the reversible form of membrane fouling (Rodrigues and Fernandes, 2012).

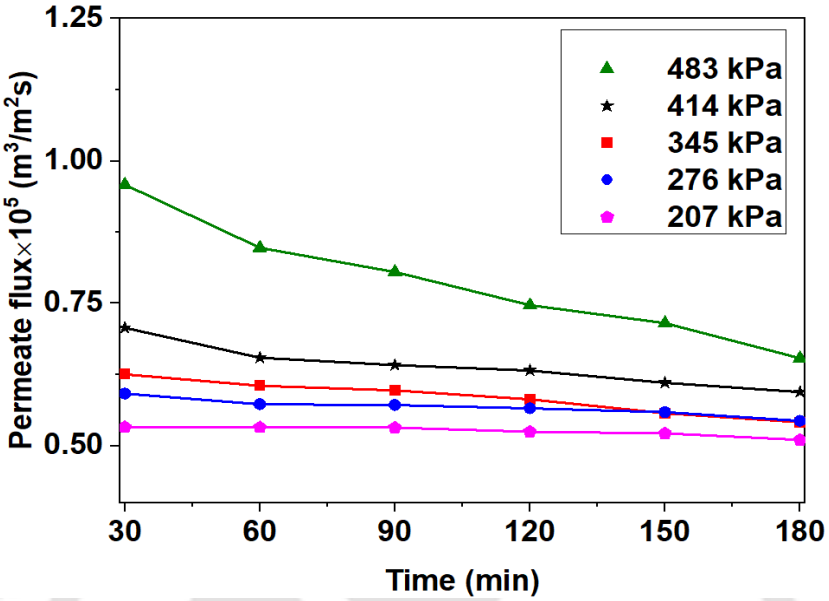

Fig. 4.2 Permeate flux collected for the duration of three hours at pressures 207, 276,345, 414 and 483 kPa (Cross flow rate: 11.11×10^{-6} m^3/s)

It was reported in the literature that the proteins present in poultry wastewater do not possess a fixed conformation and hence, they get destabilized on the application of high shear, leading to membrane fouling and subsequent flux decline (Lo et al., 2015). As evidenced, the flux decline is faster and more pronounced at higher pressures as a higher shear rate breaks the organic matters and leads to enhanced pore blocking (Kumar et al., 2016). At lower pressures, insufficient shear rate makes the breaking of foulant particles quite difficult, thus resisting pore blocking. Hence, the decline in flux at 207 kPa is quite insignificant as compared to other pressures (Ren et al., 2019). It can be said that the fouling at higher pressures is attributed to the combined effect of cake formation as well as pore blocking, while the impact of pore blocking gets diminished at lower pressures.

If the question comes for choosing an optimum pressure at which the system needs to be operated, 414 kPa can be considered as it not only gives 100% rejection, but also gives high

flux with lesser flux decline. Pressure 483 kPa cannot be taken as the optimum operating pressure, albeit providing a higher flux, owing to its higher flux decline during the operation time. The obtained permeate is clear in colour with zero turbidity value for all five pressures, as depicted in Fig. 4.3. As evident from Fig. 4.4, complete removal of COD and TSS is achieved through this membrane. The larger size of the particulate matters present in the poultry slaughterhouse wastewater is the prime reason for achieving 100% reduction in COD, TSS and turbidity of the processed water. The major contaminants of poultry slaughterhouse wastewater are the suspended solids having the size in the range of 20-50 µm. As we mentioned earlier that the fats and globules present in the wastewater are in the form of large agglomerates and debris that float on the water surface and hence, these can be easily removable. The rest of the contaminants, which are found to be bound with emulsified globules, have sizes of around 5 mm (Avula et al., 2009). It is noteworthy to mention that the pore size of the membrane (0.133 µm) is lower than the sizes of the above-mentioned organic matters present in poultry wastewater, which generally contribute to COD and TSS content. Hence, the membrane could achieve the complete removal of them via size exclusion principle.

As previously mentioned, as filtration proceeds, the formation of a cake layer takes place on the membrane surface by the foulants present in poultry slaughterhouse wastewater. In order to investigate the formation of cake layer on the membrane surface, after end of microfiltration, the inner surface of the membrane, where feed was passed through it, was screened under Field Emission Scanning Electron Microscope (FESEM), as reported in Fig. 4.5. As evident from Fig. 4.5, particles present in the wastewater were deposited on the membrane, which reduces the porous structure of the membrane during filtration. It is worth mentioning that the permeate water collected through the process satisfies the COD and TSS norms provided by Central Pollution Control Board, India, for its reuse as well as discharge into the environment. It also justifies the regulation given by the World Health Organisation in terms of turbidity value that

can even be accepted for drinking purposes (Tatwawadi, 2017; WHO, 2017). Looking at the high quality of permeate produced, it can be inferred that the water is safe to discharge into the environment and can also be reused in the poultry industry itself to tackle the stringent water demand.

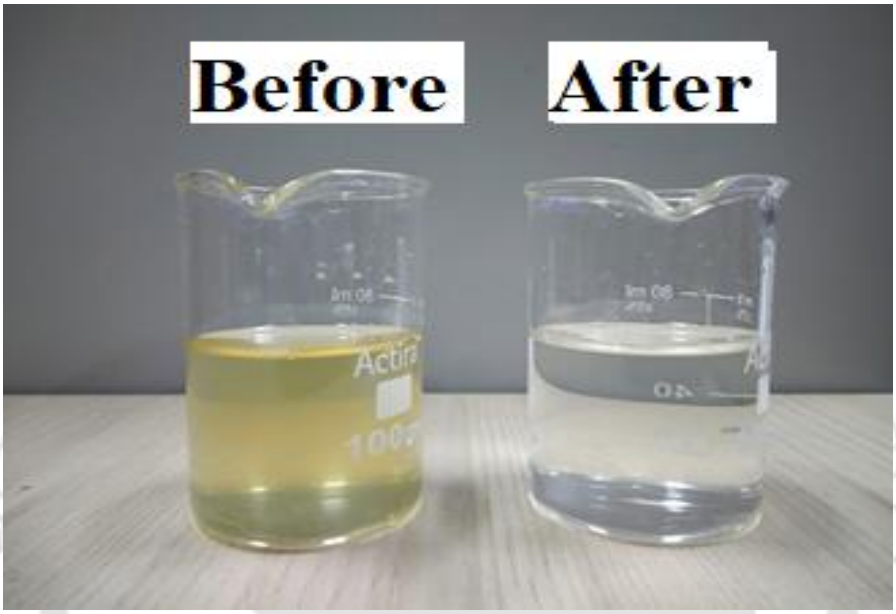

Fig. 4.3 Poultry slaughterhouse wastewater before and after membrane filtration

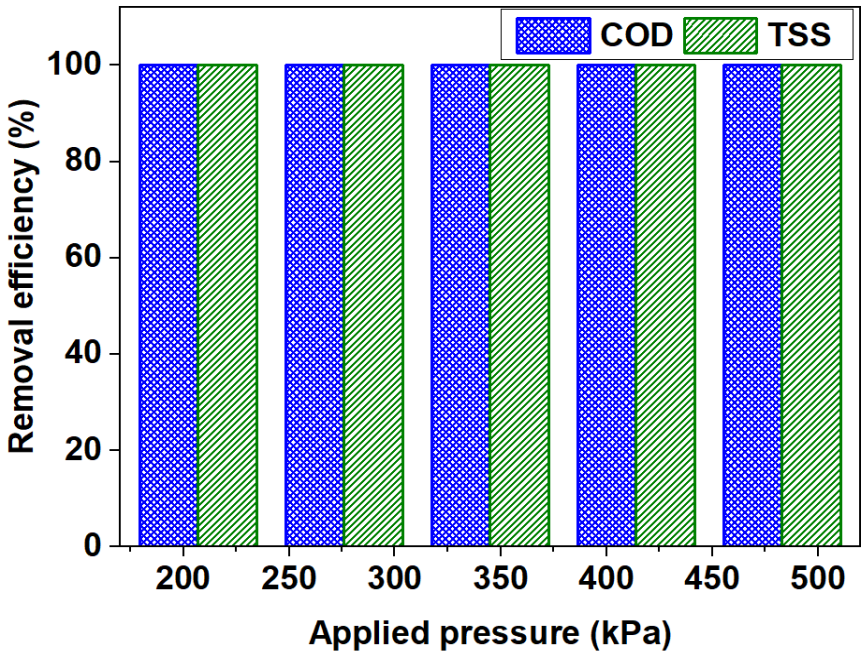

Fig. 4.4 COD and TSS reduction after membrane filtration at all five different pressures

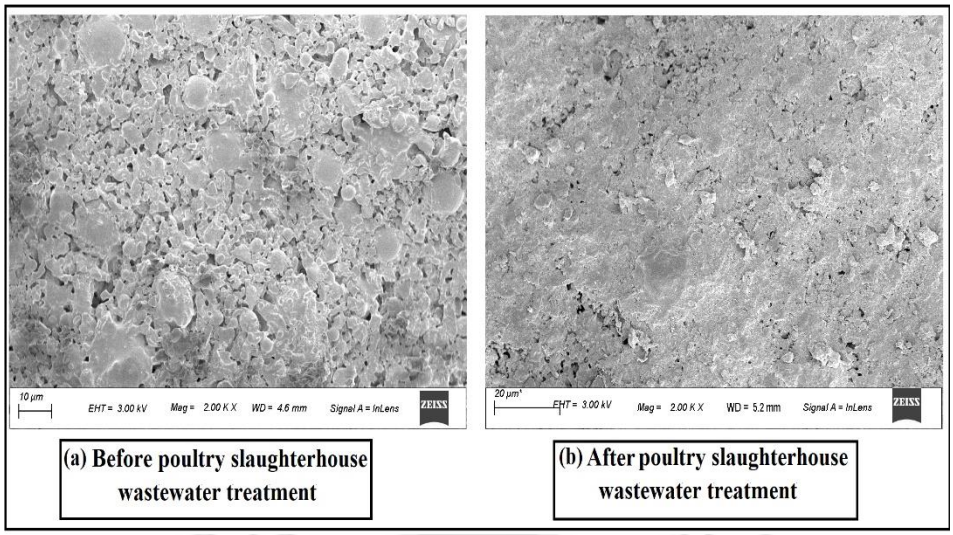

Fig. 4.5 Inner surface of the membrane as observed under FESEM (a) before and (b) after poultry slaughterhouse wastewater treatment

4.1.4 Distinction over prior arts

Literature available regarding the use of membrane filtration in the treatment of poultry processing wastewater mostly talks about commercial polymeric membranes (Table 4.3), which are not only expensive, but are also very brittle. Even though the flux obtained by using polymeric membranes is higher than that of the membrane used in this work, the use of polymeric membranes cannot be considered as a potential solution for long term separation processes owing to their very poor chemical as well as mechanical strength (Malmali et al., 2018; Gupta and Anandkumar, 2018; Kaur et al., 2016; Rodrigues and Fernandes, 2012). Basitere et al., though reported the use of ceramic membranes, the raw materials used in its fabrication make it very expensive. Certain cases also mentioned about the use of hybrid processes such as static granular bed reactor (Basitere et al., 2017), which again makes the whole process a big-budgeted one. The fabricated membrane overcomes all the above-mentioned disadvantages and offers complete rejection without even compromising with the permeate flux, which contemplates its superiority over the other membranes used earlier for purification of poultry slaughterhouse wastewater.

Table 4.3 Performance evaluation of the fabricated membrane with the ones mentioned in prior arts regarding poultry slaughterhouse wastewater treatment

Membrane	**Pore size**	**Conditions**	**Permeate flux ($\times 10^6$ m^3/m^2s)**	**Rejection/recovery**	**References**
PES and regenerated cellulose commercial membrane	10-300 kDa	**T**: Ambient temperature **Flow rate**: 1.21 L/min **P:** 67.5 kPa	~13.9-97.2	**COD**: upto 94% **TSS**: 100%	(Malmali et al., 2018)
Commercial UF-25-PAN membrane	-	**P:** 400 kPa	91.7	**TSS:** 98% **COD**>94%	(Yordanov, 2010)
Thin film nanofiltration membrane	**UF:** 30000 **NF:** 150-300	**pH:** 6.6 ± 0.1 **TMP**: 500-2500 kPa	~3.9-9.2	**COD:** 90%	(Coskun et al., 2016)
Polysulfone	30 kDa	**pH:** 5.5-7.0 **Flow rate:** 0.6-0.8 L/min **P:**96.5 kPa	> 55.6	**COD:** 58.86% **TS:** 35.79%	(Lo et al., 2015)
α-alumina	40 nm	**pH**: 6.78 **T:** 21.2 ˚C	-	**COD:** 98% **TSS:** 99.8%	(Basitere et al., 2017)
Fly ash, Quartz, Calcium carbonate	0.133 µm	**Feed pH:** 6.19 ± 0.07 **T:** 25 ˚C **Cross flow rate:** 0.667 L/min **P:** 207-483 kPa	5.2-7.9	**COD:** 100% **TSS:** 100%	This work

4.2 Treatment of starch processing wastewater

4.2.1 Chemicals

Starch processing wastewater was simulated in the laboratory and for that purpose, rice, corn and wheat starch were collected from Urban Platter, Mumbai; Padmavathi Distributors, Vijayawada and Naturevibe Botanicals, Raigad respectively. The reagents required for measuring Chemical Oxygen Demand (COD) of feed and permeate samples of starch processing industry wastewater treatment were collected from the same source as in the case of poultry slaughterhouse wastewater treatment. The Lugol's reagent used for qualitative analysis of starch in feed and permeate was procured from Hi-Media (I) Ltd.

4.2.2 Experimental methodology and investigations

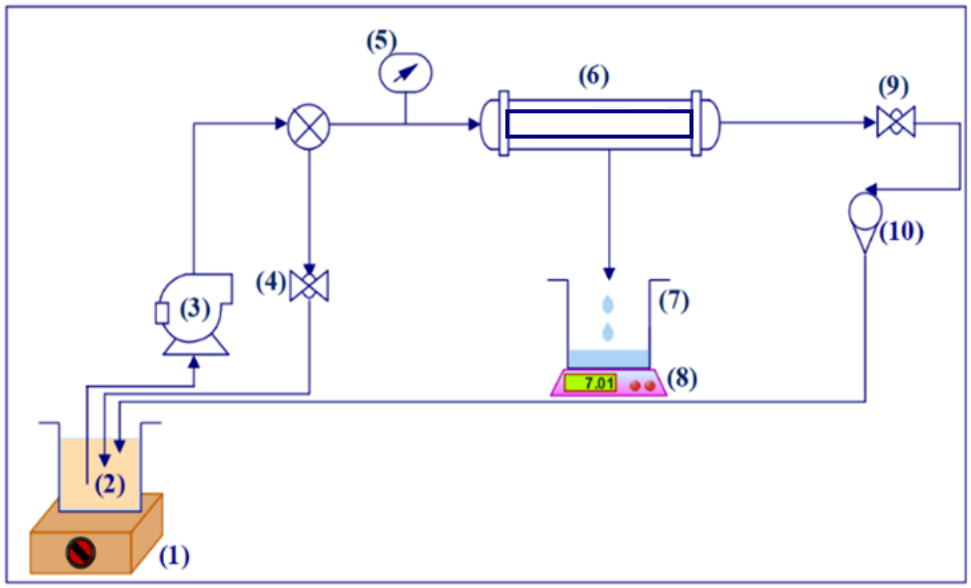

Fig. 4.6 Experimental setup for starch processing wastewater treatment [1: Magnetic stirrer; 2: Feed tank; 3: Pump; 4: By-pass valve; 5: Pressure gauge; 6: Membrane housing; 7: Permeate tank; 8: Weighing balance; 9: Retentate control valve; 10: Rotameter]

The primary constituent of wastewater generated in the starch processing industry is starch. However, the starch content in the effluent wastewater is usually so high that direct

microfiltration seems unhealthy for long run membrane performance due to severe fouling. Hence, it is always advisable to allow the effluent wastewater to settle for a duration of 2-4 h, so that a certain percentage of starch settles at the bottom, thus decreasing the load on the membrane. After precipitation, the concentration of wastewater in terms of starch content remains approximately 1% (w/v), which is equivalent to 10 g/L (Ikonić et al., 2011). Hence, to mimic starch processing industry wastewater, 1% (w/v) aqueous solution of three different starches, namely corn, wheat and rice, was made individually for experimental purposes. The separation experiments were carried out using the setup illustrated in Fig. 4.6.

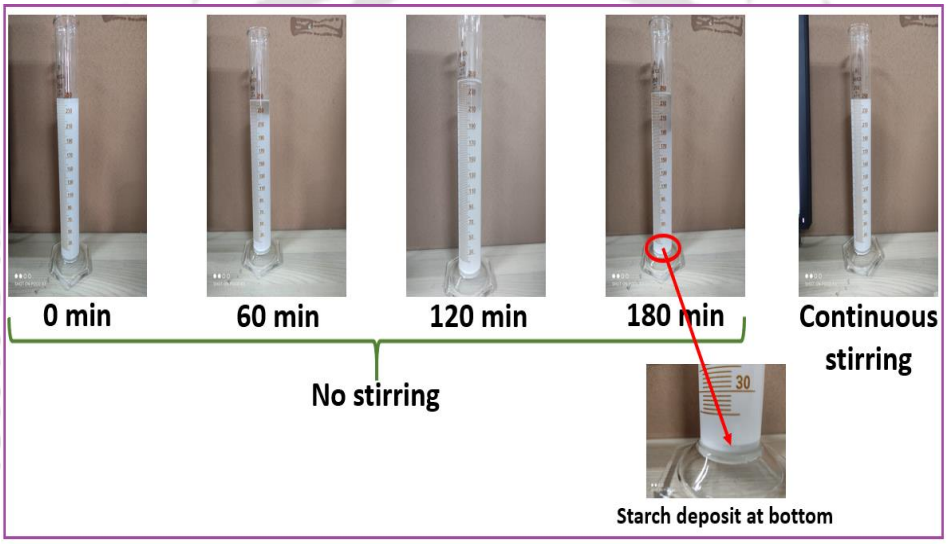

Fig. 4.7 Effect of stirring in preventing starch sedimentation during microfiltration

In the entire course of microfiltration studies, the simulated starch wastewater was stirred mechanically. Stirring was done in order to avoid settling of starch molecules. The effect of stirring in preventing sedimentation of starch granules during the experiment can be well observed from Fig. 4.7. The feed and permeate samples were also characterized for their Chemical Oxygen Demand (COD), total suspended solids (TSS) and turbidity content using the same protocols as mentioned in Sub-section 4.1.2. The COD values reported in this article corresponds to the total COD of the starch solution. Moreover, the size of all three starch molecules was analyzed using Laser Particle Scattering Analyzer (Model No.: Master sizer

2000; Make: M/s Malvern, UK). Morphology of the starch molecules was studied under Field Emission Scanning Electron microscope (Make: Zeiss, Model: Sigma 300) and the presence of starch molecules in feed and the permeate was evaluated qualitatively using Lugol's Iodine reagent.

To evaluate the rejection performance of the membrane with variations in applied pressure, experiments were conducted between the pressure ranges of 207 kPa and 483 kPa, the cross-flow velocity being maintained at 8.33×10^{-6} m^3/s. The study of effect of pressure on membrane performance helped us to identify the optimum pressure that can be recommended for efficient membrane separation. This was followed by studying how the membrane behaves to starch wastewater treatment with variations in cross flow velocity. The versatility of membrane retention performance while treating wastewater generated from different starch sources was also evaluated. To calculate the rejection performance of the membranes under different operating conditions, equation (4.1) is used. The recovery efficiency of the membrane is also studied to assess its efficacy in recovering starch from concentrated feed after microfiltration, which can be used for some other purposes. After completing one set of experiments, the whole setup was flushed with Millipore water for 30 minutes, which was further followed by cleaning with 1 g/L surf excel detergent solution for another 30 minutes. The setup was rinsed again with Millipore water for 20 minutes, and the hydraulic permeability of the membrane was checked. In all the cases, the pure water permeability of the membrane after regeneration falls within ±5% of its original hydraulic permeability.

4.2.3 Results and discussions

4.2.3.1 Characterization of different starch sources

The three different starch sources used for simulating starch industry wastewater are namely corn, wheat and rice. As in case of microfiltration, the size of solute particles present in the

feed solution plays a pivotal role in the separation performance of the membrane. Hence, it is utmost important to carry out particle size analysis of the solute. Keeping this point in mind, the particle size distribution of all three starch sources was carried out using two different techniques, namely Laser Particle Size Analyzer (LPSA) and Field Emission Scanning Electron Microscope (FESEM). FESEM micrographs of all the sources that were used to evaluate the particle size distribution are presented in Fig. 4.8. The particle size distribution of three starch suspensions performed using Laser Particle Size Analyzer (LPSA) is presented in Fig. 4.9 (a). It has been observed from the figure that all the three starch sources show unimodal size distribution, which is in accordance with the data available in the literature (Sinaki and Scanlon, 2016; Martens et al., 2018; Corgneau et al., 2019). It has been observed that granules of rice starch are the smallest among the three, which was followed by wheat and corn starch granules. The average sizes of corn, wheat and rice starch granules calculated from the data obtained through LPSA are found to be 14.01, 7.69 and 3.36 µm, respectively. Similar size ranges for the aforementioned starch sources are well documented in earlier literature (Wani et al., 2012; Sikora and Izak, 2006). The size analysis based on FESEM micrographs was carried out using ImageJ software (https://imagej.nih.gov/ij/). Particles captured in four different FESEM micrographs were considered for evaluating the average particle size of starch granules. As evident from Fig. 4.9 (b), it also displays a similar pattern with corn, wheat and rice starch granules showing average sizes of 10.33, 8.64 and 4.27 µm, respectively. However, slight variations in the results obtained through the aforementioned techniques are obvious, as both the instruments work on two different principles. It has been reported that LPSA processes a huge quantity of particles per assay, while in case of the image analysis carried out using FESEM micrographs, only a few hundred particles are taken into consideration resulting in a slight variation in the particle size analysis (Hegel et al., 2014).

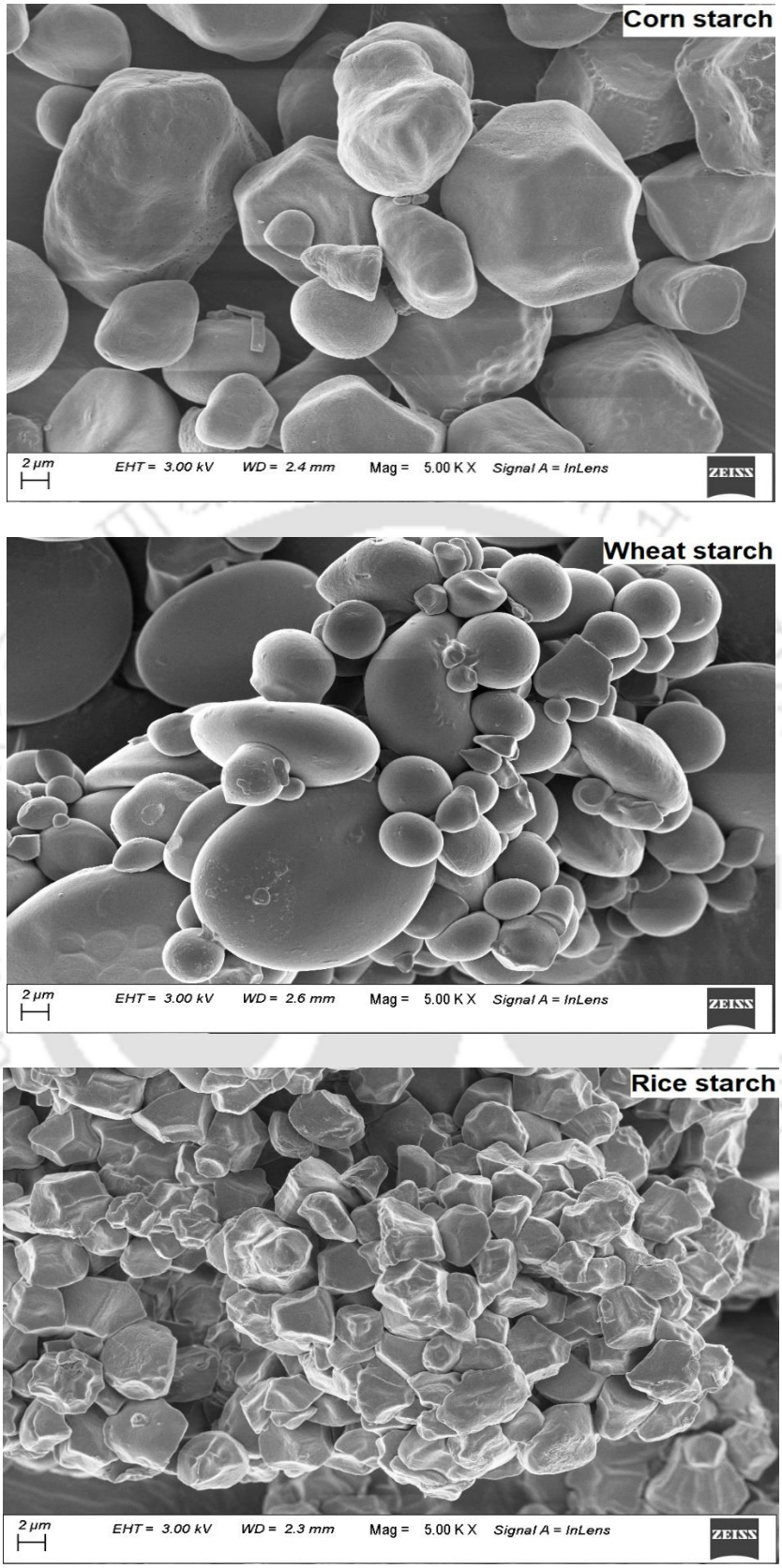

Fig. 4.8 FESEM images of corn, wheat and rice starch granules

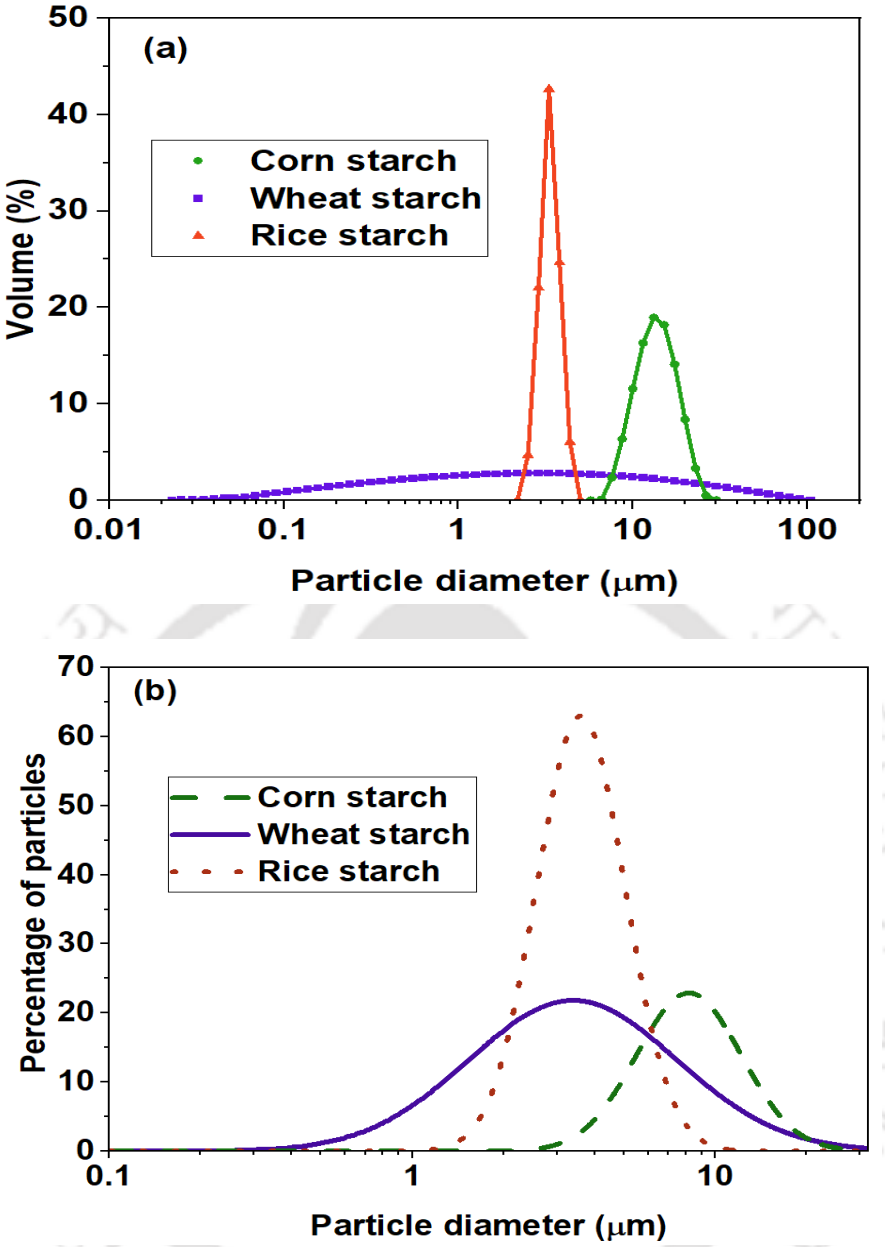

Fig. 4.9 Particle size distribution of starch granules using (a) LPSA and (b) FESEM micrographs

Besides particle size analysis, the other characterizations that need to be carried out before performing microfiltration experiments of simulated starch wastewater are those, based on which membrane's rejection performance will be evaluated. As the efficiency of fly ash based tubular ceramic membrane in rejecting starch from its suspension will be estimated on the basis of reduction in COD, TSS and turbidity values. Hence, all these parameters were evaluated for

all three starch sources before carrying out microfiltration operations. The summary of aforementioned parameters for all three sources of starch is represented in Table 4.4.

Table 4.4 Characteristics of wastewater generated from different starch sources

Starch source	Parameters		
	COD (g/L)	**TSS (g/L)**	**Turbidity (NTU)**
Corn	11.36±0.68	9.00±0.20	3935±11.67
Wheat	14.35±2.54	9.50±0.30	3245±240.00
Rice	13.27±1.56	7.95±0.05	4925.84±140.84

4.2.3.2 Effect of pressure on membrane performance

As mentioned earlier, the effect of applied pressure on membrane performance was evaluated by conducting a series of experiments using corn starch wastewater at various applied pressures ranging from 207 kPa to 483 kPa. The characteristics of feed (1 wt.% corn starch suspension) used for evaluating the membrane performance are mentioned in Table 4.4.

It has been observed that with an increase in the applied pressure, the quantity of permeate flux obtained also increases initially. This can be attributed to the fact that with increasing applied pressure, the augmented driving force aids in the increased production of permeate (Suresh et al., 2016; Khemakhem et al., 2009; Purnima et al., 2020). However, after a certain duration, it has been observed that permeate flux obtained at higher applied pressure is comparatively lower than the ones obtained at lower applied pressure. It has been well documented in the literature that after a specific duration, the increased accumulation of solute particles on the membrane surface results in the formation of cake layer with a very low porosity value (Hong et al., 1997). Such a thick cake layer provides extra resistance for permeate to flow across the membrane and at some point of time, when this resistance becomes dominant over the increased driving force for permeate flow, the permeate flux becomes independent of applied pressure (Hong et al., 1997). In such a situation, the difference between the final permeate flux value obtained at different applied pressure decreases and the final permeate flux obtained at

higher pressures becomes almost equal or sometimes even less than the ones obtained through applying lower pressure (Buetehorn et al., 2010; Gomes et al., 2013; Koltuniewicz et al., 1995). Because of this trend of permeate flux with variations in applied pressures, the cumulative permeate flux obtained during microfiltration goes through a maximum, as observed in Fig. 4.10 (a) (Inset).

The rejection performance of the membrane was found to be excellent at all applied pressures as it was successful in achieving complete removal of total suspended solids and turbidity content of starch wastewater. Moreover, the COD value of permeate also decreased significantly. It was found to be in the range of 165-190 mg/L, which is far below the permissible discharge limit as prescribed by the Central Pollution Control Board, India (Saxena and Choudhary, 2017). The satisfactory removal of starch granules through membrane separation can be attributed to the fact that the membrane has a pore size that is way lower than the average size of corn starch granules. The larger sized granules were restricted by the small sized pores of the membrane, thus achieving almost complete removal of starch from wastewater (Shukla et al., 2009). However, it is well documented in the literature that prolonged filtration leads to increased starch concentration in the feed, resulting in an enhanced fouling rate in the membrane. An over fouled membrane leads to the generation of high transmembrane pressure that may break bigger starch molecules into smaller ones and push them through the membrane pores to the permeate side (Ling-Chee et al., 2019). This may be the possible reason for a certain COD value even after the complete absence of TSS and turbidity in the permeate.

The experiments conducted to study the changes in membrane's performance with variations in applied pressure reveal two key points, the first being membrane's rejection efficiency remains almost unaffected by variation in applied pressure. Secondly, the membrane produces the highest quantity of permeate flux at an applied pressure of 345 kPa. Keeping note of these

two points, 345 kPa is determined to be the optimum pressure for carrying out microfiltration of starch wastewater.

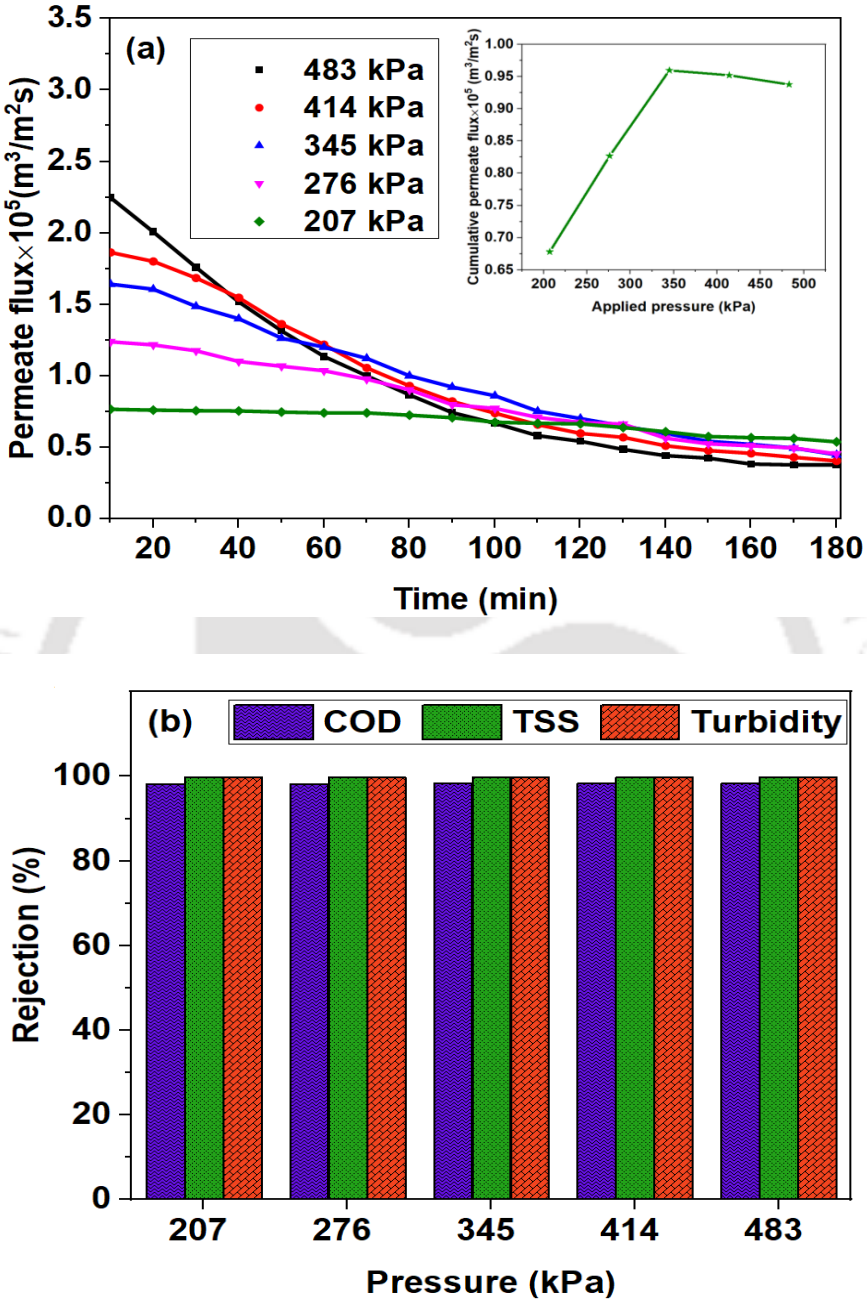

Fig. 4.10 Effect of applied pressure on (a) permeate flux and (b) rejection performance of the membrane

4.2.3.3 Effect of cross flow velocity on membrane performance

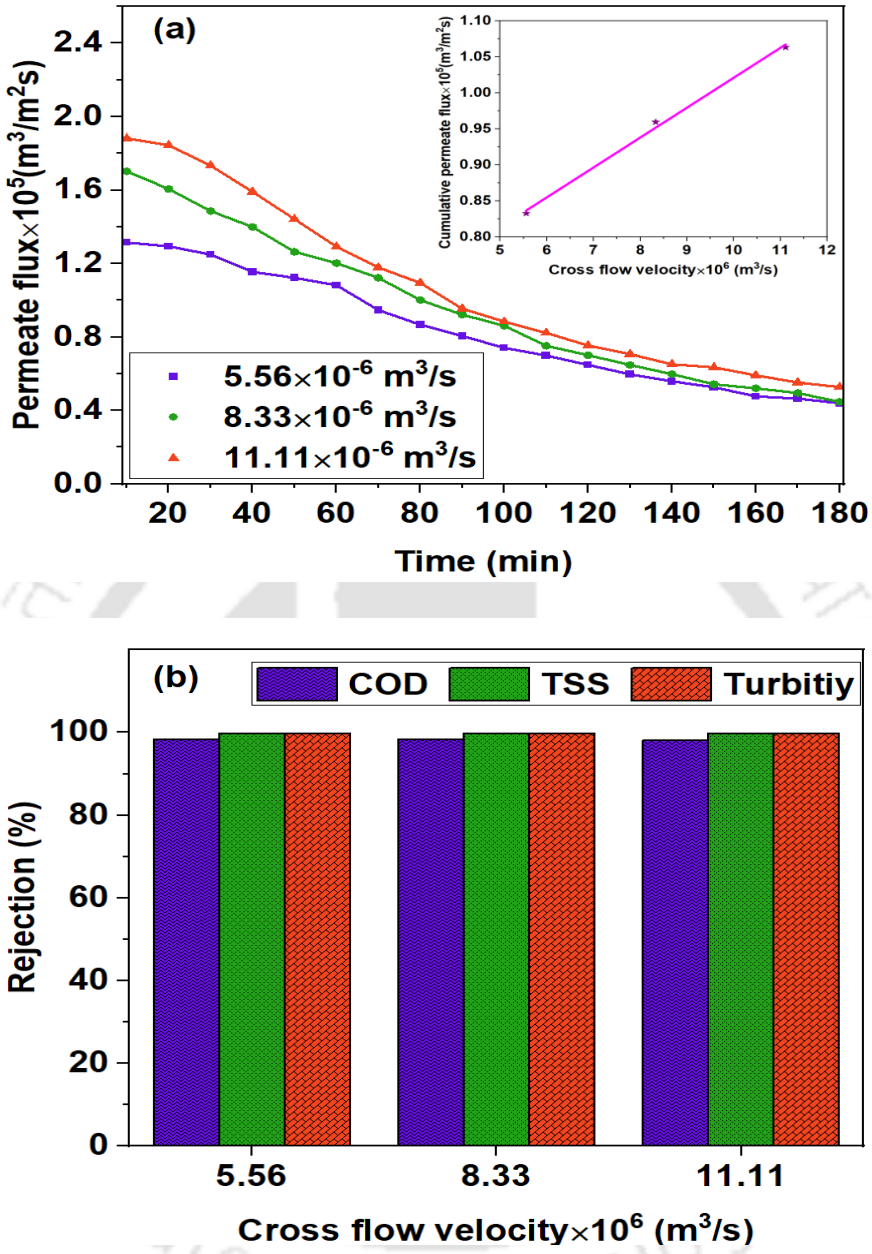

Fig. 4.11 Effect of cross flow velocity on (a) permeate flux and (b) rejection performance of the membrane

Fig. 4.11 describes the performance of membrane in terms of flux and rejection at different cross flow velocities for corn starch suspension. It has been observed from Fig. 4.11 (a) that an increasing value of cross flow velocity aids in enhancing the permeate flux through the membrane almost linearly (Choi et al., 2005). The phenomenon of membrane fouling is closely related to cross flow velocity across the membrane as higher cross flow velocity is known to

reduce the effect of concentration polarization in the membrane surface by increasing sweeping action over the membrane surface. This ultimately helps in increasing the surface area of membranes available for a given separation, thus producing higher quantities of permeate flux (Kumar et al., 2011). However, starch rejection performance of the membrane in terms of COD, TSS and turbidity is almost the same at all cross-flow velocities. It signifies that for solutes with an average size greater than membrane pore size, cross flow velocity does not significantly affect membrane rejection. In such cases, size exclusion plays a crucial role in separation and only the solute particles having lesser size than membrane pore diameter can pass into the permeate side (Chang et al., 2017).

Though an increasing cross flow velocity aids in enhancing the quantity of permeate obtained, it comes with a disadvantage of increased operational cost due to pumping (Siedel and Elimelech, 2002). Therefore, keeping these two points in mind, 8.33×10^{-6} m^3/s is considered to be the optimum cross flow rate to carry out starch wastewater treatment using the aforementioned fly ash based tubular membrane.

4.2.3.4 Effect of starch source on membrane performance

The versatility of membrane's performance in treating three different varieties of starch wastewater, having feed characteristics mentioned in Table 4.4 is depicted pictorially in Fig. 4.12. It has been observed that the membrane produced the largest quantity of permeate while treating the corn starch wastewater. It is clear from Fig. 4.12 (a) (inset) that with increasing size of starch granules, the quantity of permeate obtained through membrane also increases. It has been mentioned in literature that as microfiltration starts, permeate flux starts to decline due to membrane fouling through combined effect of pore plugging and cake formation. However, as the granule size increases, the deposition rate of granules to the membrane surface also decreases, which helps in reducing the flux decline (Jung and Ahn, 2019). This can be

regarded as the possible cause for obtaining higher permeate flux from the very beginning, in case of microfiltration of starch wastewater containing bigger starch granules.

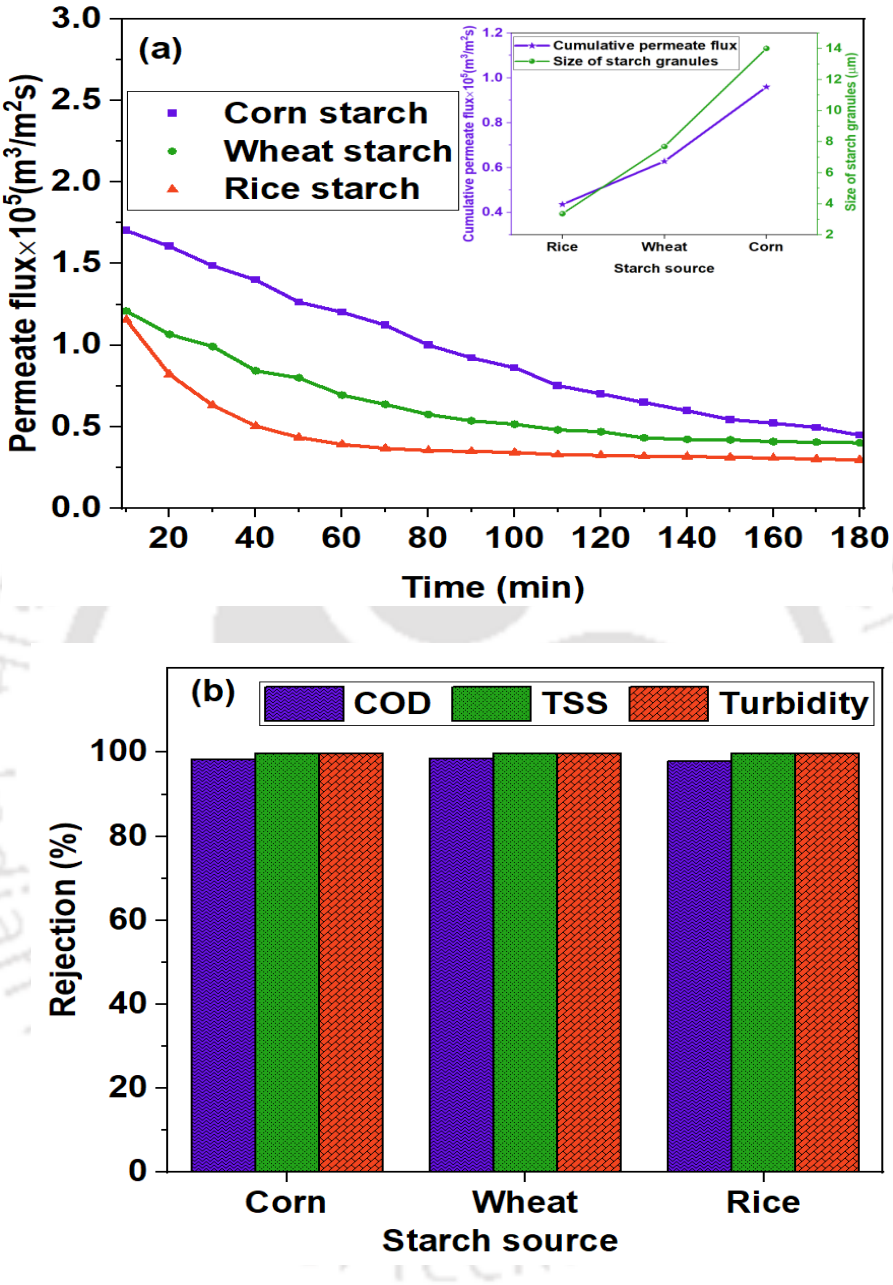

Fig. 4.12 Effect of source of starch on (a) permeate flux and (b) rejection performance of the membrane

Moreover, in case of cake formation during later stages of filtration, solute particles with larger particle diameters lead to the formation of cake with high voidage, unlike the ones having smaller particle diameters where the cake formed is very compact in nature. This high porosity cake formed on the membrane surface provides comparatively lesser resistance to permeate

flow than the compact cakes, thus producing a larger quantity of permeate even at the end of microfiltration (Hwang et al., 1996). Therefore, in the microfiltration of starch wastewater, starch granules with larger particle diameters helped in generating larger volumes of permeate. However, the membrane's performance in terms of starch rejection could not be differentiated, all thanks to the larger average size of starch molecules that could not penetrate through membrane pores.

Almost complete removal of starch granules from wastewater in all the aforementioned cases using a membrane having pore diameter far less than the average size of starch granules compels to consider size exclusion to be the dominant mechanism of separation. A schematic representation of this size exclusion mechanism is illustrated in Fig. 4.13. Besides, it needs to mention that the permeate produced in all the cases is clear and transparent, unlike the milky white turbid feed solution (Fig. 4.14a). Moreover, the qualitative analysis of the feed and permeate using Lugol's Iodine solution also reveals the successful separation of starch granules from its solution (Fig. 4.14b). The starch present in the feed reacts quickly with Lugol's Iodine solution, turning the color of the solution into dark blue. On the contrary, yellow color of permeate sample on addition of Lugol's Iodine solution signifies almost complete removal of starch granules from its solution (Rocha et al., 2020). The photo comparison of feed and permeate in both cases is shown in Fig. 4.14.

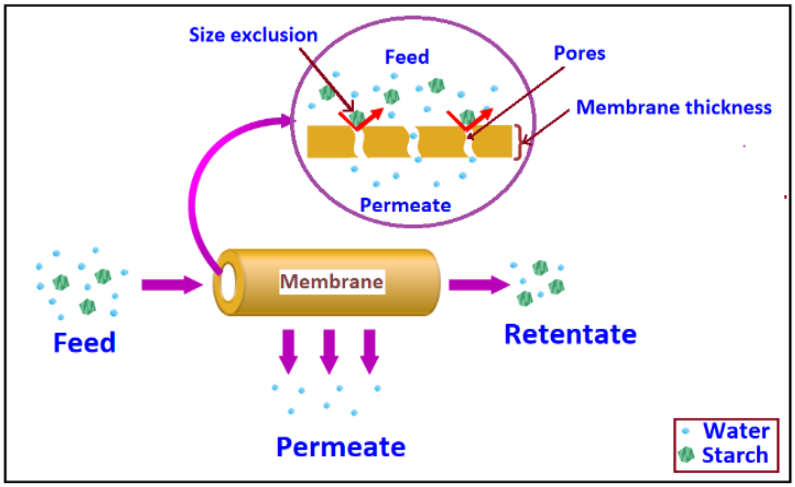

Fig. 4.13 Schematic of the size exclusion mechanism

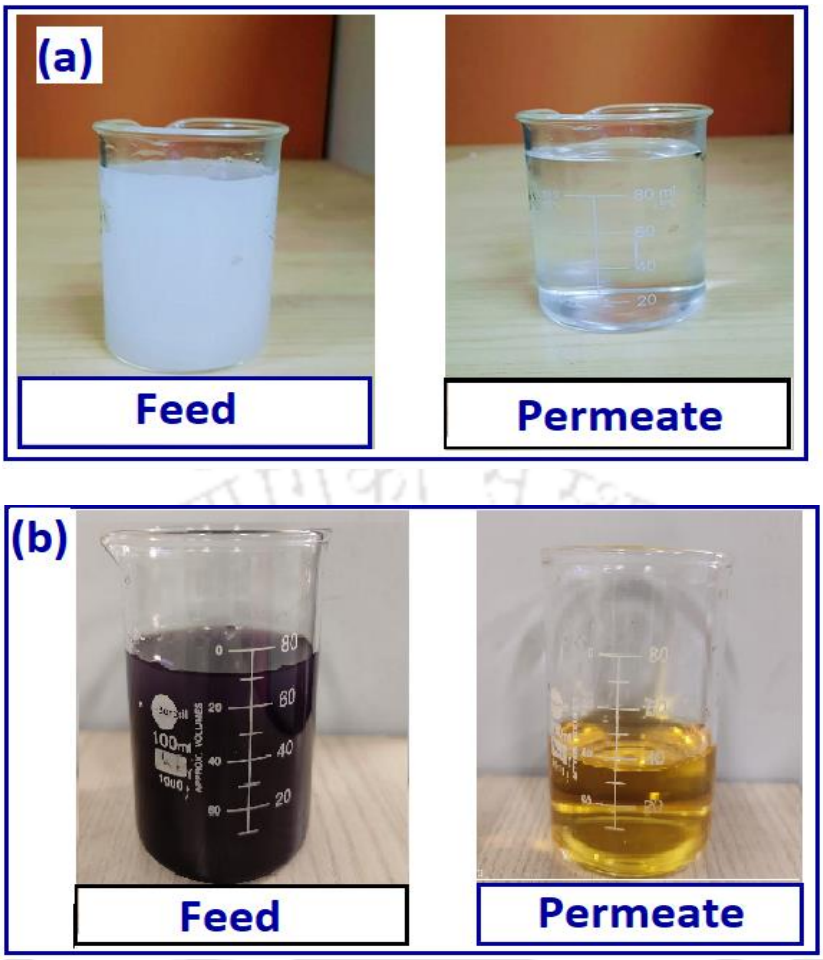

Fig. 4.14 Photo comparison of feed and permeate: (a) without addition of Lugol's Iodine solution, (b) with addition of Lugol's Iodine solution

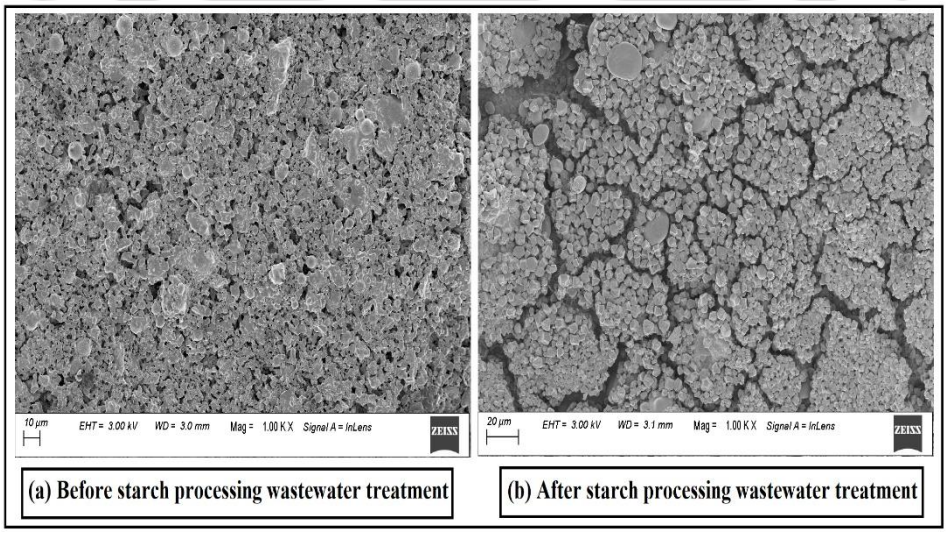

Fig. 4.15 Inner surface of the membrane as observed under FESEM (a) before and (b) after starch processing wastewater treatment

Besides, the membrane surface was also investigated under Field Emission Scanning Electron Microscope (Fig. 4.15) after microfiltration of corn starch wastewater to check whether cake formation is the dominant mechanism of membrane fouling, as previously mentioned in this chapter. It is quite clear from Fig. 4.15 (b) that after microfiltration, the clean membrane surface as observed in Fig. 4.15 (a) is completely covered by clusters of starch granules, which led to membrane fouling and subsequent blockage of paths for permeate flow.

4.2.3.5 Recovery performance of membrane

It has already been mentioned that as filtration proceeds, the concentration in the feed tank increases due to separation of water and starch granules. Therefore, membrane filtration can also be used simultaneously for recovering starch from the concentrated feed. With this intention, the concentration factor for the membrane at different operating conditions is evaluated using equation (4.2) (Ikonić et al., 2011). A high concentration factor is always preferable for getting greater recovery of starch.

$$\text{Concentration factor (C.F)} = \frac{V_F}{V_R} \tag{4.2}$$

where, V_F and V_R correspond to the volumes of feed and retentate, respectively.

It has been observed from Fig. 4.16 that the concentration factor per m^2 of membrane area did not vary significantly with altering operating conditions as permeate flux obtained at different processing conditions are not having drastic differences in their values. Among the various applied pressures, 345 kPa corresponds to the maximum concentration factor ($645.8/m^2$) owing to the highest quantity of permeate and lowest quantity of retentate produced. Due to a similar reason, the concentration factor corresponding to a cross flow velocity of 11.11×10^{-6} m^3/s and corn starch wastewater treatment remains the highest amongst the different cross flow velocities and sources of starch wastewater, respectively.

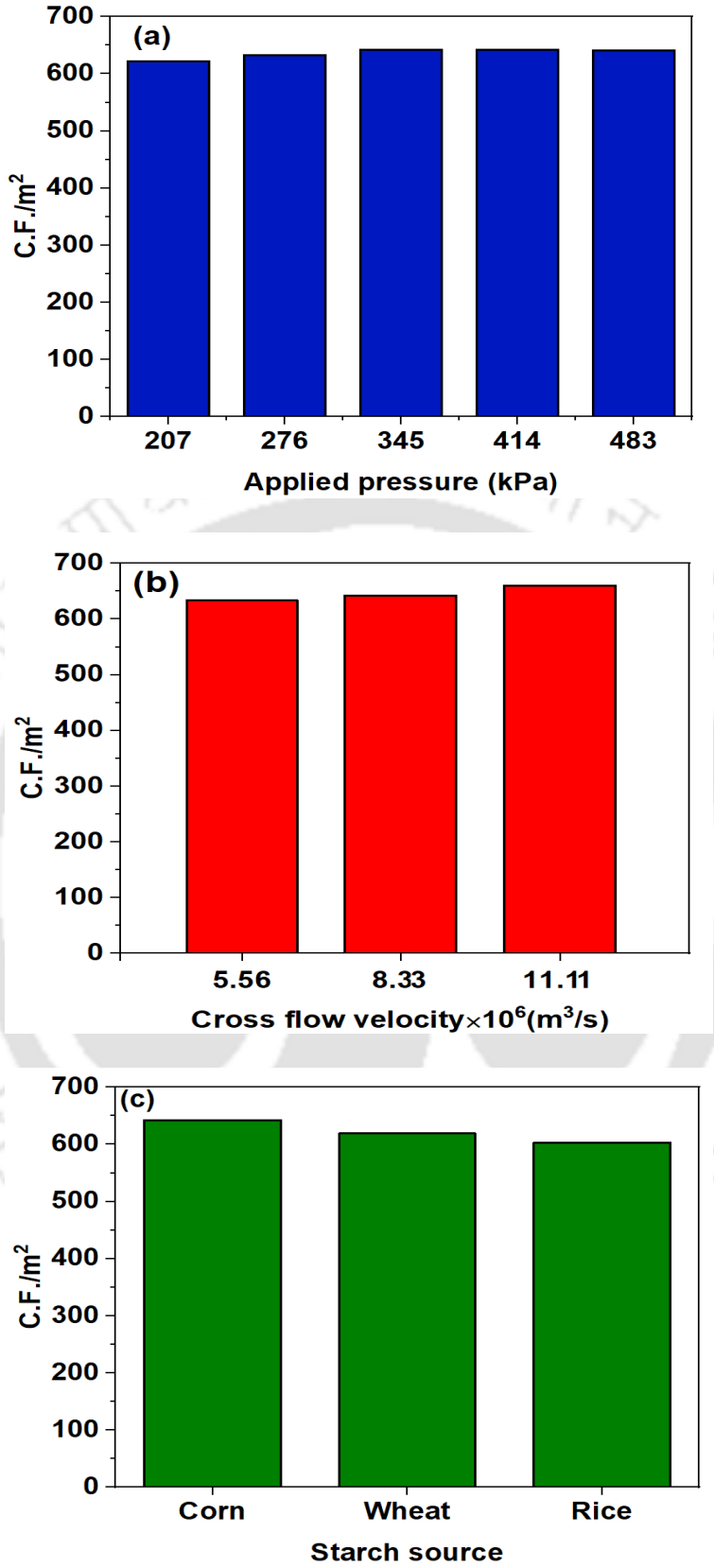

Fig. 4.16 Variation of concentration factor (C.F) per m^2 of membrane area with (a) applied pressures and (b) cross flow velocities for corn starch suspension, and (c) three starch sources

4.2.4 Distinction over prior arts

As evident from Table 4.5, the literature available regarding starch wastewater treatment using membrane technology is very few. It has been observed from the table that existing prior arts use commercial membranes of ceramic as well as polymer origin. However, commercial ceramic membranes are relatively expensive and cannot be considered a cost-effective approach towards starch wastewater treatment. The disadvantages associated with polymeric membranes have already been mentioned in earlier sections of this thesis. On the contrary, the membrane used in this work is not only better in terms of its properties, but is also quite affordable for treating starch wastewater. It needs to mention that this is the first instance, to the best of authors' knowledge, where a low-cost membrane with 95% of its composition comprising of naturally available raw materials is being implemented for treating starch wastewater. With respect to the performance of the membranes, the developed membrane performs quite well compared to its counterparts mentioned in previous literature. With the complete rejection of turbidity and total suspended solids along with 98-99% reduction in COD value, the membrane serves its purpose quite satisfactorily. As mentioned by Ling-Chee et al., the COD rejection was only 80%, which is way lesser than the ones obtained in this work (Ling-Chee et al., 2019).

Moreover, many of the articles reported about treating starch wastewater with concentrations ranging between 0.25-5 g/L. But, in actual practice, even after carrying out a sedimentation step prior to membrane filtration, 10 g/L of starch remains in suspended form (Rocha et al., 2020; Ikonić et al., 2011; Hinková et al., 2005; Sargolzaei et al., 2011). Therefore, experiments should be conducted at concentrations around 10 g/L, so as to have a proper idea about membrane's performance when implemented in industrial applications. Another important fact about this work is the very high concentration factor per m^2 filtration area of the membrane as compared to other membranes mentioned in previous literature. Ikonić et al. and Hinková et

al., in their research articles cited about achieving concentration factors of 24 and 25 per m^2 area of the membrane, while Ling-Chee et al. achieved a slightly higher concentration factor of 56 per m^2 of membrane area (Ikonić et al., 2011; Ling-Chee et al., 2019; Hinková et al., 2005). However, this work mentions obtaining concentration factors in the range of 605-645 per m^2 of membrane area for three different starch wastewater after completion of the filtration experiment.

As evident from the above discussion, this process is not only cost effective, but is also efficient in terms of rejecting starch from its suspension and further recovery of the same from the concentrated feed solution. Such a good combination of membrane efficiency and cost affordability is not observed in the open literature portrayed in Table 4.5, making this piece of work distinct from its previous counterparts.

4.3 Separation of glycerol from biodiesel

4.3.1 Chemicals

Synthetic biodiesel emulsion was prepared in the laboratory by mixing required proportions of biodiesel, methanol and glycerol procured from SVM Agroprocessor, Nagpur, Merck (I) Ltd. and Hi-Media (I) Ltd., respectively.

Besides, the chemicals required to determine the free glycerol content in biodiesel and permeate samples through UV-vis spectrophotometer such as n-hexane, acetylacetone, sodium periodate, ethanol were supplied by Hi-Media (I) Ltd. Isopropyl alcohol used in determining soap content of the samples was procured from Loba Chemie Pvt Ltd., while the bromophenol blue indicator was supplied by Hi-Media (I) Ltd.

Table 4.5 Performance evaluation of the fabricated membrane with the ones mentioned in prior arts

Membrane material	**Starch source**	**Pore size (µm)**	**Conditions**	**Permeate flux ($\times 10^6$ m^3/m^2s)**	**Rejection**	**C.F/m^2**	**References**
α-Alumina	Wheat	0.2	**TMP:** 300 kPa **C_f:** 5 g/L **CFV:** 1.39×10^{-4} m^3/s **T:** 22-25 °C	-	99%	24	(Ikonić et al., 2011)
Polysulfone	Sago	0.45	**C_f:** 10 g/L **CFV:** 7.5×10^{-5} m^3/s **T:** 20 °C	93.9	**TSS:** 100% **Turbidity:** > 99.5% **COD:** > 80%	56	(Ling-Chee et al., 2019)
Alumina, Coal fly ash	Corn	-	**C_f:** 0.25 g/L **P:** 200 kPa **CFV:** 4.17×10^{-5} m^3/s **T:** 24 °C	-	99%	-	(Rocha et al., 2020)
Commercial membrane (Composition not known)	Amaranth	0.1	**C_f:** 3% **P:** 100 kPa **CFV:** 5 m/s **T:** 40 °C	5.56*	-	25	(Hinková et al., 2005)
Polyethersulfone		0.65	**C_f:** 4.09 g/L **P:** 250 kPa **CFV:** 1.83×10^{-4} m^3/s **T:** 20.11 °C	68.67	98.7%	-	(Sargolzaei et al., 2011)
Fly ash, Quartz, Calcium carbonate	Corn, Wheat, Rice	0.133	**C_f:** 10 g/L **P:** 345 kPa **CFV:** 8.33×10^{-6} m^3/s **T:** 25 °C	**Corn:** 9.60 **Wheat:** 6.28 **Rice:** 4.36	**TSS:** 100% **Turbidity:** 100% **COD:Corn:** 98.43% **Wheat:** 98.70% **Rice:** 97.95%	**Corn:** 645.58 **Wheat:** 621.80 **Rice:** 605.93	This work

4.3.2 Experimental methodology and investigations

The microfiltration experiment regarding the separation of glycerol from biodiesel was carried out by preparing a synthetic solution of biodiesel mixture using biodiesel, glycerol and methanol. Prior to the preparation of synthetic solution, the procured biodiesel was characterized for its free glycerol as well as the soap content, and all the properties of the biodiesel along with these two have been mentioned in Table 4.6.

Table 4.6 Properties of procured biodiesel

Parameter	**Value**
Free glycerol[#]	0.015 wt.%
Soap[#]	(612.15±7.95) ppm
Water content	0.13 wt.%
Methanol	0.01 wt.%
Calorific value	40,794 J/kg
Kinematic viscosity (40 ˚C)	6 cSt

[#] Properties evaluated in our laboratory, while rest are reported as obtained from the supplier

It has been observed that the residual glycerol present in the biodiesel is very less, amounting to only 0.015 wt.%. However, the soap content in the biodiesel was found to be very high (612.15±7.95 ppm), which needs to be reduced before filtration so as to reduce the membrane fouling. This issue has been addressed later in this section.

It has been revealed in the literature that for the production of biodiesel using vegetable oil and methanol via transesterification in the presence of an alkaline catalyst, 1:6 molar ratio of oil and alcohol produced the highest yield (Freedman et al., 1985). Keeping this in mind, a stoichiometric calculation was carried out using the below-mentioned reaction scheme (equation 4.3) to evaluate the final composition of biodiesel emulsion produced via methanol transesterification process for the above-mentioned feed ratio. It was found that the final product was a mixture of 80% biodiesel, 10% glycerol and 10% methanol; all percentages are being weight percentage. Hence, an emulsion with the above-mentioned composition was

prepared using a probe ultrasonicator (IKA T10 basic, ULTRA-TURRAX) for the experiment purpose.

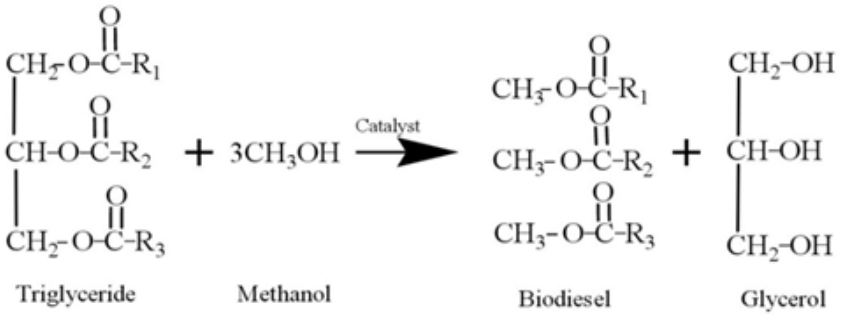

(4.3)

Once the solution was prepared, acidified water (0.5% HCl) was added to the emulsion in such an amount that the water weight corresponds to 20% of the total weight of the emulsion (Gomes et al., 2013). Addition of acidified water significantly reduced the excessive soap content of the emulsion to 168.54±4.45 ppm by converting the soap present in biodiesel into soluble salts.

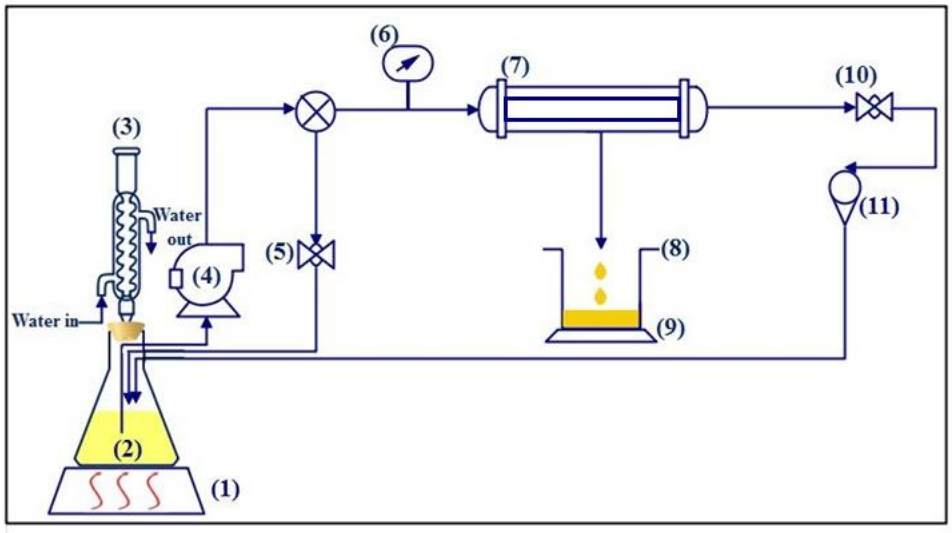

Fig. 4.17 Cross flow filtration setup for separation of glycerol from biodiesel (1: Magnetic stirrer with heater, 2: Feed tank, 3: Reflux condenser (Used only during microfiltration of biodiesel), 4: Pump; 5, 10: ball valve, 6: pressure gauge, 7: membrane module, 8: permeate tank, 9: Weighing balance, 11: Rotameter)

For the microfiltration of biodiesel emulsion, the experiments were conducted at 60 ˚C using cross-flow filtration setup (Fig. 4.17), as the solution viscosity at this temperature is

comparatively lower, which helps in reducing the load on the pump (Gomes et al., 2010). The possible evaporation losses of solvent from the emulsion at higher temperature were prevented by the use of reflux condenser during the experiment (Bell, 1925; Gerpen et al., 2004). The permeation experiments were conducted at a cross flow rate of 8.33×10^{-6} m^3/s, using five different pressures within the range of 207 to 483 kPa. The permeate collected after each run was tested for free glycerol and soap content after evaporating the residual water and methanol in a rotary evaporator (Rotavapor R-300, Buchi, Switzerland) for a duration of 30 minutes at 90 ˚C bath temperature.

The soap content of feed as well as permeate samples was determined by dissolving 10 g of biodiesel in isopropyl alcohol, which was followed by the addition of 12-15 drops of bromophenyl blue indicator until the solution acquires a blue tint. The resultant mixture was then titrated against 0.01N HCl until the solution turns yellow. The amount of HCl required to achieve this colour change was used to calculate the soap content in biodiesel using equation (4.4):

$$Soap\ content\ (ppm) = \frac{W\times0.01\times C}{1000\times B}\times 10^6 \qquad (4.4)$$

where, *W*, *C* and *B* represent the amount of HCl (in mL), concentration factor (318 for biodiesel produced using sodium methoxide as a catalyst) and weight of the biodiesel sample (in grams), respectively (Atadashi et al., 2015).

The free glycerol content in biodiesel as well as permeate sample was analyzed using UV-vis spectrophotometer (UV-2600, Shimadzu, Singapore). For the analysis, formaldehyde structure was first formed by the reaction between biodiesel and sodium periodate, which on further reaction with acetylacetone produced a yellow-coloured complex, 3,5-diacetyl-1,4-dihydrolutidine having a very high specific absorption band at 410 nm wavelength (Bondioli and Bella, 2005; Nogueira, 2019). This method of determining free glycerol content in

biodiesel is quite simple, fast and cost effective than the conventional method like Gas Chromatography technique (Nogueira et al., 2019).

A microscope with 20X magnification (Model No.: Zeiss Axio Scope.A1, Make: Carl Zeiss Microscopy GmbH Germany) was used to capture the images of droplets of biodiesel emulsion prepared at 60 ^{o}C. The droplet size distribution and average size of the biodiesel emulsion were evaluated by analysing three different microscope images using ImageJ software (Open-source software, https://imagej.nih.gov/ij/).

On completion of each experiment, the setup was initially flushed with methanol for 30 minutes as the emulsion easily solubilises in methanol, which makes the cleaning easy. This was followed by cleaning the setup with 1 g/L surf excel solution for 30 minutes. An aqueous NaOH solution (1 wt.%) was allowed to pass through the setup for another 30 minutes to remove the traces of emulsion that may be present in the setup (Atadashi et al., 2015). Finally, flushing with Millipore water was carried out and the water permeability of the cleaned membrane was measured again. It was found that the hydraulic permeability of the cleaned membrane was within ±4% of its original value, which signifies the reusability of the membrane for further experiments.

4.3.3 Results and discussions

The synthetic biodiesel emulsion feed, after addition of acidified water, was used for the filtration purpose. The separation experiments conducted at different pressures of 207, 276, 345, 414 and 483 kPa revealed satisfactory rejection of glycerol through the membrane, as evident from the minimal free glycerol content in the permeate. It has been observed from Fig. 4.18 that an increase in the applied pressure helped in augmenting permeate flux through the membrane, all thanks to the increased driving force across the membrane. The inset in Fig. 4.18 shows that the cumulative flux increases as the applied pressure increases. Several authors have

also reported an enhanced permeate flux with increasing transmembrane pressure for ceramic membranes (Khemakhem et al., 2009; Jana et al., 2010; Suresh et al., 2016; Kumar et al., 2016).

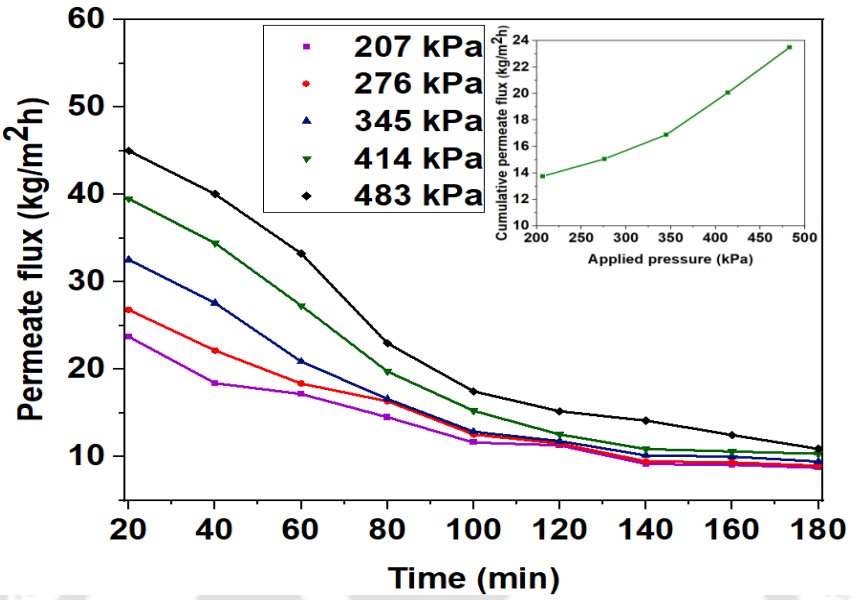

Fig. 4.18 Effect of applied pressure on the permeate flux (Cross flow velocity: 8.33×10^{-6} m^3/s)

As evident from the flux versus time curves (Fig. 4.18), a relatively rapid flux decline is noticed at the beginning of the filtration, followed by a more gradual decrease, until a pseudo-steady state flux is reached (Rodrigues and Fernandes, 2012). However, it is worth to mention that only at the start of the filtration process, the effect of increasing the applied pressure on permeate flux is significant and as filtration proceeds, the difference between steady state permeate flux for all the investigated pressures decreases (Buetehorn et al., 2010; Gomes et al., 2013). The resistance of the cake layer formed by retained agglomerates on the membrane surface controls the flux at this phase of separation process. A previous study also indicated that thicker cake layer is formed at higher applied pressures due to which the influence of flux at latter phase of cross flow filtration is not significant (Buetehorn et al., 2010; Hong et al., 1997).

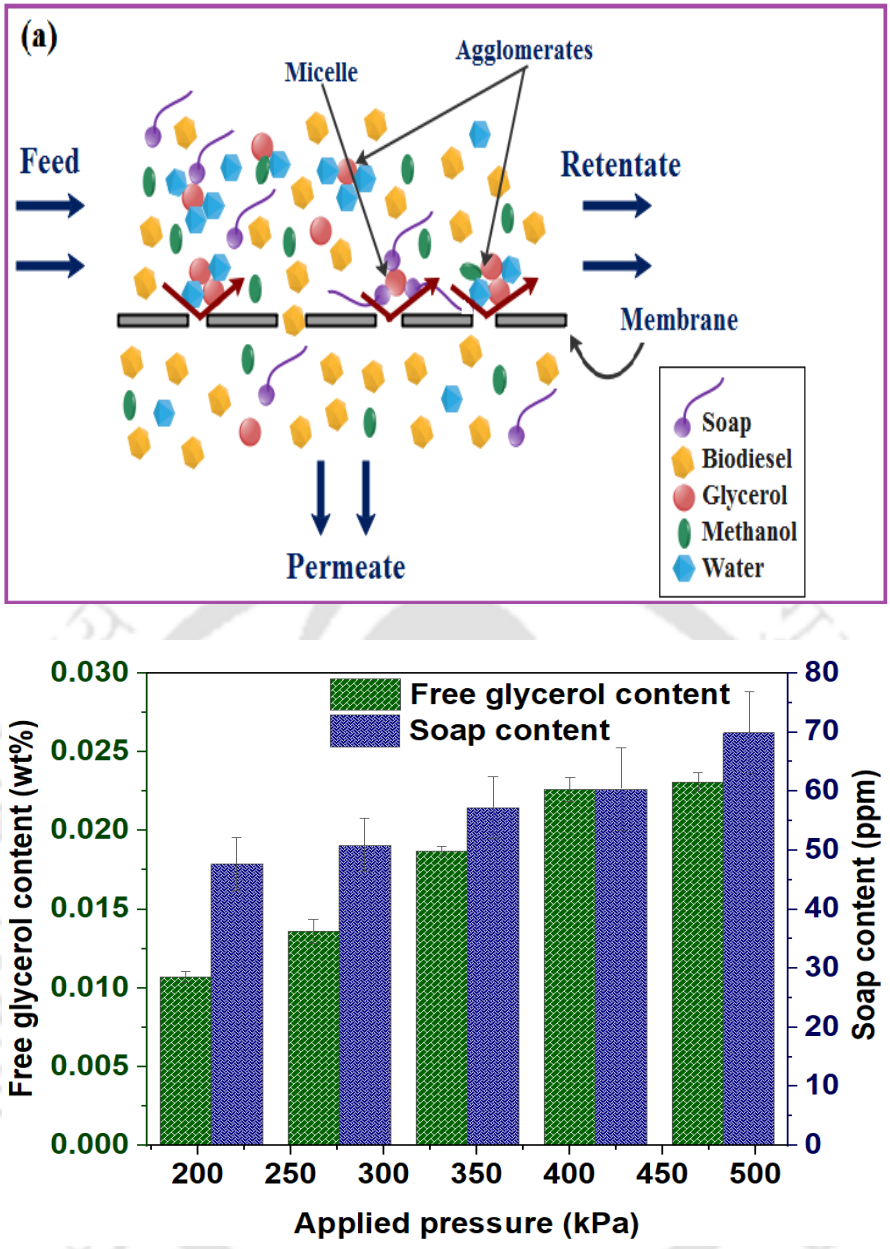

Fig. 4.19 (a) Glycerol separation mechanism across the membrane (b) Contents of soap and free glycerol in the permeates obtained under different applied pressures

While looking at the membranes' performance regarding glycerol retention from biodiesel, it can be said that the membrane successfully reduced the glycerol content of biodiesel from 8.33 wt.% (feed) to 0.0107-0.0231 wt.% (permeate) at various pressures (207 – 483 kPa) through the mechanism of size exclusion (Fig. 4.19). This can be attributed to the fact that in the emulsion of biodiesel, glycerol and acidified water is agglomerated due to their high affinity towards each other and constitutes the dispersed phase. These agglomerated compounds remain

suspended in the continuous phase of the emulsion, primarily consisting of biodiesel. Besides this, some residual soap molecules are retained even after the addition of acidified water combines with glycerol to form micelles. These micelles also contribute to the dispersed phase of emulsion and help in the retention of glycerol by the membrane. Methanol is found to be present in the continuous as well as the dispersed phase, owing to its affinity towards both the phases (Gomes et al., 2010; Gomes et al., 2011). It has been found that the droplets of dispersed phases have an average diameter of 31.11 µm at the experiment temperature, as observed under microscope (Fig. 4.20 (a)). Fig. 4.20 (b) represents the droplet size distribution of the emulsion, where it can be seen that most of the droplets formed are in size range of 11-20 µm and 31-40 µm. The mentioned average size of the dispersed droplets is far bigger than the pore size of the membrane, thus aiding in very high rejection of glycerol across the membrane. The permeate obtained primarily consists of biodiesel, with small quantity of methanol and traces of soaps, glycerol and water in it. The rejected agglomerates of water and glycerol are found in the retentate, along with the micelles formed by soap and glycerol. The schematic of the rejection of glycerol from biodiesel is depicted in Fig. 4.19 (a). These findings are in line with the works reported by Gomes et al. (Gomes et al., 2011). However, the increased pressure across the membrane slightly declined the retention performance of the membrane, leading to little higher free glycerol content in the permeate. At higher pressure, the augmented shear on membrane surface may lead to tearing of emulsion droplets, thus allowing a fraction of it to pass through the separation barrier (Sutrishna et al., 2012).

Similar observation was also noticed in the case of soap content in the permeate (Fig. 4.19). The soap content of the permeate was reduced to below 70 ppm, which is achieved by the combined action of acidified water as well as membrane filtration. Acid present in water reacts with the soap molecules, converting them to soluble salts (Gomes et al., 2011). A portion of the residual soap present even after addition of acidified water was further retained by

membranes. It has already been mentioned that the residual soap molecules combine with the available glycerol to form micelles, remaining dispersed in the emulsion along with glycerol and water (Wang et al., 2009). As these dispersed molecules have higher diameters as compared to the membrane pores, they are retained on the membrane surface in the process of filtration. However, the breakage of micelles takes place at higher pressures like the tearing of agglomerated droplets of water and glycerol, leading to slightly lesser retention of soap molecules on the membrane surface.

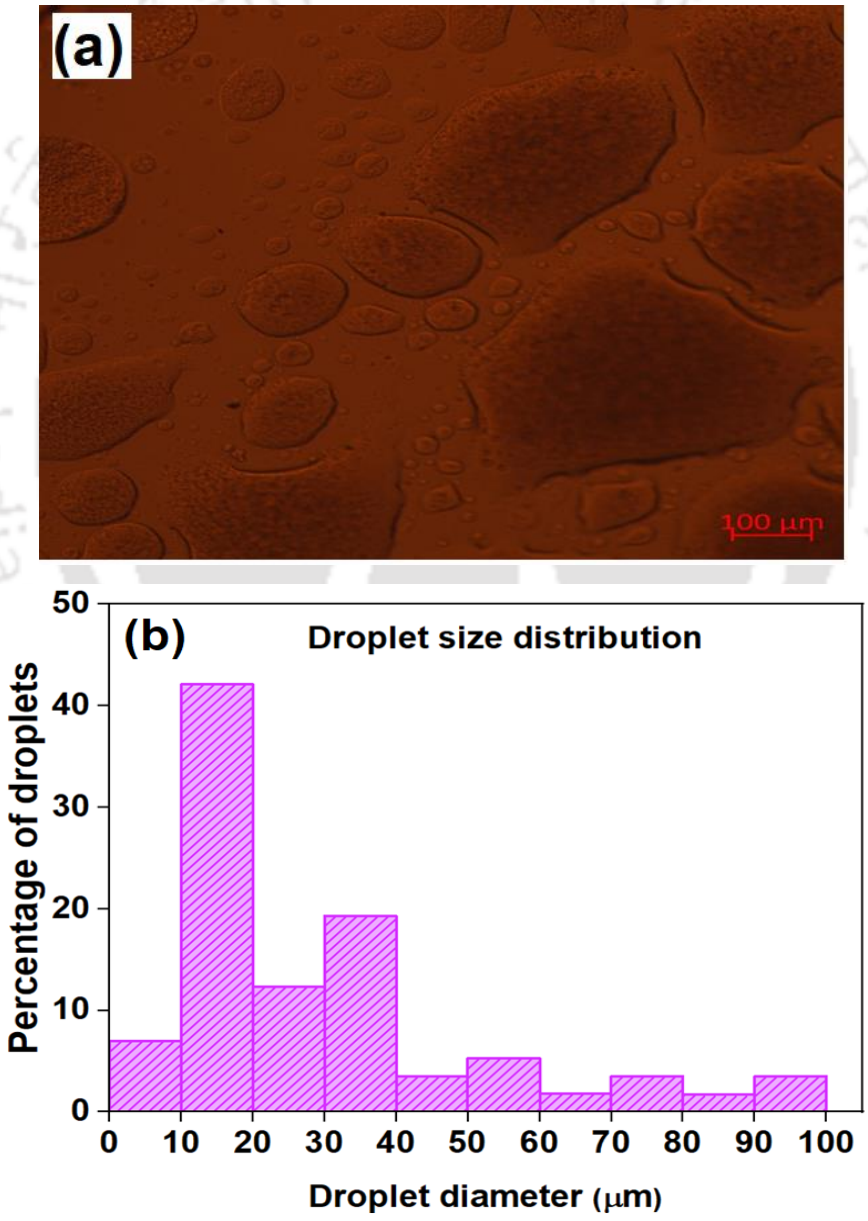

Fig. 4.20 (a) Microscopic image of biodiesel emulsion (b) Droplet size distribution of biodiesel emulsion

In this context, it is noteworthy to mention that Fig. 4.21 corresponds to the photo comparison of biodiesel emulsion before (feed) and after treatment, where a successful separation is clearly visible. However, the permeate obtained in the pressure ranges of 207-345 kPa contains less than 0.02 wt% free glycerol and thus satisfies the norms prescribed by ASTM D6751 and EN14214 (ASTM D6751-20; EN 14214). Though there are no specific norms provided regarding the soap content in biodiesel, a reduced content is always preferable as it minimizes the filter plugging of the engine. Moreover, burning of soap rich biodiesel in engine leads to the formation of sulphated ash, causing damage to the fuel injectors as well as to the combustion chamber (ASTM D6751-20). Considering the glycerol content in permeate sample, the applied pressures ranging from 207 - 276 kPa could be adequate to be used in separation of glycerol from biodiesel emulsion.

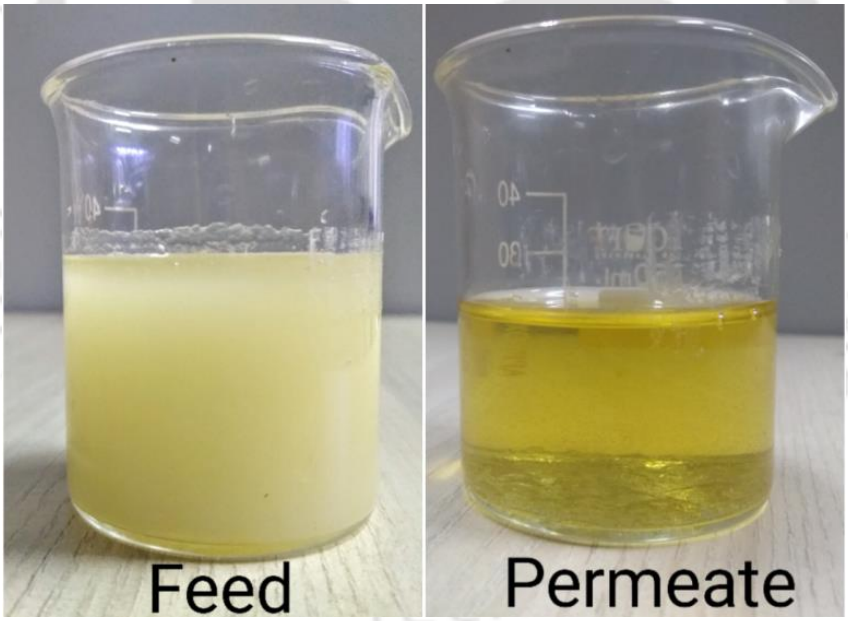

Fig. 4.21 Photo comparison of feed and permeate samples

Table 4.7 Performance evaluation of the membrane in the treatment of glycerol enriched biodiesel

Membrane composition	**Pore size**	**Experimental conditions**	**Free glycerol in permeate (wt%)**	**Permeate flux[#] (Steady state flux)**	**References**
Commercial α-AlO_3/TiO_2 membrane (Shumacher GmbH-Ti 01070)	0.2 µm	**T:** 60 ˚C **TMP:** 200 kPa **C_f:** 10 wt%	0.06±0.009	~50.00 kg/m^2h	(Gomes et al., 2010)
Commercial α-AlO_3/TiO_2 membrane (Jiangsu Jiuwu Hi-Tech Co., China)	0.02 µm	**T:** 40 ˚C **TMP:** 200 kPa **C_f:** 0.42 wt%	0.007	9.08 kg/m^2h	(Atadashi et al., 2012)
Commercial polyether sulfone membranes (GE Osmonics, USA)	10 kDa	**T:** 25 ˚C **TMP:** 400 kPa **C_f:** 0.049 wt%	0.020	55.00 kg/m^2h	(Alves et al., 2013)
Commercial α-AlO_3/TiO_2 membrane (Shumacher GmbH-Ti 01070)	20 kDa	**T:** 50 ˚C **TMP:** 300 kPa **C_f:** 6.80 wt%	0.014±0.002	70.00 kg/m^2h	(Gomes et al., 2013)
Polyacrylonitrile membrane	6 kDa	-	0.017	-	(Bansod and Rathod, 2018)
Fly ash, Quartz, Calcium Carbonate	**0.133 µm**	**T: 60 ˚C** **TMP: 345 kPa** **C_f: 8.33 wt%**	**0.0187**	**9.45 kg/m^2h**	**This work**

4.3.4 Distinction over prior arts

The encapsulation of literature regarding the separation of glycerol from biodiesel in Table 4.7 reveals the use of commercial membranes (both ceramic as well as polymeric), the disadvantages of which has already been mentioned in earlier sections (Gomes et al., 2010; Gomes et al., 2013; Atadashi et al., 2012). Moreover, the uses of ultrafiltration membranes cannot be justified in few cases where separation can also be achieved through microfiltration as the flux obtained in ultrafiltration processes is comparatively lower (Bansod and Rathod, 2018; Atadashi et al., 2012; Chamberland et al., 2019). However, the membrane used in this work efficiently reduces the cost of the separation process without compromising on glycerol rejection as well as permeate flux. The unavailability of literature regarding the use of low-cost membrane in glycerol separation from biodiesel further increases the applicability of this work in large scale processes. Few cases also reported the use of membrane separation in reduction of free glycerol content retained after decantation or water washing (Alves et al., 2013; Atadashi et al., 2012). However, the present system nullifies the use of a pre-treatment step and can remove the glycerol produced as a part of transesterification process. Acknowledging the benefits obtained through the use of this membrane (as evident from Table 4.7), the application of this membrane in industrial scale is highly recommended.

4.4 Summary

The performance of the membrane was evaluated by implementing it in three different separation processes, namely treatment of poultry slaughterhouse wastewater, treatment of starch processing wastewater and separation of glycerol from biodiesel. In case of poultry slaughterhouse wastewater treatment, the membrane showed complete rejection in terms of COD, TSS and turbidity at all applied pressures. Moreover, it was decided that 414 kPa is the optimum pressure at which microfiltration needs to be carried out. In case of starch processing

wastewater treatment, the membrane was successful in completely removing TSS and turbidity from wastewater, but there was a slight presence of COD, which was below the permissible limit as prescribed by Central Pollution Control Board, India. Experimental observations revealed that experiments carried out at 345 kPa applied pressure and 8.33×10^{-6} m^3/s cross flow velocity resulted in optimum membrane performance. While separating glycerol from biodiesel, there was very high rejection of glycerol with negligible free glycerol content in permeate. However, the permeate produced below 345 kPa applied pressure satisfied the norms as prescribed in D6751 and EN14214 regarding free glycerol content in biodiesel. Besides, the membrane also helped in reducing the soap content in biodiesel. Keeping note of the successful separations achieved in all the three aforementioned cases, it can be summarized that the membrane is quite versatile when comes to its performance in different separation operations and therefore, has the potential to be implemented in various other microfiltration operations

Chapter 5

Economic Feasibility Assessment of Membrane Fabrication Process and Separation Operations Incorporating the Fabricated Membrane

Economic Feasibility Assessment of Membrane Fabrication Process and Separation Operations Incorporating the Fabricated Membrane

The economic feasibility analysis is utmost important for ensuring successful scaleup of every project. With a view to develop a cost effective and sustainable technology, starting from membrane fabrication to separation process, detailed cost analysis has been discussed in this chapter. The cost analysis discussed here is primarily divided into two parts; the first part corresponds to the cost of membrane fabrication, while the second part represents the cost incurred during the separation processes. The cost estimation for all the three separation processes is carried out for both lab-scale as well as pilot-scale setups, the lab-scale setup consisting of one membrane (Filtration area: 0.00172788 m^2; Length: 100 mm; I.D.: 5.5 mm; O.D.: 11.5 mm) while the pilot-scale setup consisting of three parallel membrane housing, with seven membranes in each housing (Filtration area: 0.07257 m^2, Length: 200 mm; I.D.: 5.5 mm; O.D.: 11.5 mm).

5.1 Cost of membrane fabrication

Cost analysis of the membrane fabrication process involves calculation of expenses under various heads that incurred during the whole fabrication process. The total manufacturing expenses incurred during the fabrication process can be broadly categorized into two heads, namely Direct Manufacturing Cost and Indirect Manufacturing Cost. The Direct Manufacturing costs are the expenses that primarily occurs during the manufacturing of products and hence, can be sub-divided into the following categories:

1. Cost of raw materials
2. Labor cost
3. Cost of electricity consumed

4. Repair and maintenance cost
5. Laboratory cost
6. Packaging and shipping
7. Royalties and patents
8. Cost related to factory supplies, and so on.

On the contrary, Indirect Manufacturing Costs are the expenses that incurred indirectly as a result of productive operation. Indirect Manufacturing Costs can also be further categorized as:

1. Depreciation cost
2. Payroll Overhead
3. Factory overhead
4. Taxes and Insurances, and so on (Ghodrat et al., 2016; Winter, 1969).

However, in this cost analysis, the first five categories in the Direct Manufacturing Cost and Depreciation cost in case of Indirect Manufacturing Cost are considered for evaluating the total expenses incurred during the membrane fabrication process. Along with these expenses, the cost incurred while procuring the necessary equipment (Equipment cost) will also be considered for calculating the total cost associated with the membrane fabrication process.

The membranes are fabricated using three raw materials, namely Fly ash (75 wt.%), Quartz (20 wt.%) and Calcium carbonate ($CaCO_3$) (5 wt.%). 2 wt.% aqueous solution of sodium salt of carboxymethyl cellulose was used as a binder. Again, the capacity of the furnace to sinter membranes is limited to sixty numbers of membranes per batch. Hence, taking fabrication of sixty numbers of membranes as the basis, so that the full capacity of the furnace is utilized, the cost analysis will be carried out hereafter. It needs to mention that for fabrication of sixty numbers of such membranes, 950 grams of raw material mixture will be required.

Moreover, for kneading 950 grams of raw material mixture, 297 grams of such solution is required, where 5.94 (=297×0.02) grams will be Na-CMC and the rest amount will be water.

Taking the above-mentioned quantities as the basis, the detailed cost analysis is mentioned hereafter.

5.1.1 Direct manufacturing cost estimation

Cost of raw materials

The cost incurred in the procurement of raw materials is presented in Table 5.1. Though fly ash is collected from the industry free of cost, an expense amounting to 1000 INR incurred during transportation of 100 kg fly ash from Chandrapur Power Station, Guwahati to Indian Institute of Technology, Guwahati.

Table 5.1 Summary of cost of raw materials (1 USD = 73.38 INR as on 04 April, 2021)

Raw material	**Unit price (INR/kg)**	**Quantity used (g)**	**Cost incurred**	
			INR	**USD**
Fly ash	10.00	712.50	7.13	0.10
Quartz	20	190.00	3.80	0.05
Calcium Carbonate	640	47.50	30.40	0.41
Na-CMC	2400	5.94	14.26	0.19
	Total		**55.59**	**0.75**

Moreover, after cutting the membranes into desired length, abrasive paper (C-220) was used for smoothening the membranes. With an average of ten numbers of membranes being smoothened in a single abrasive paper, six numbers of such papers will be required for smoothening sixty numbers of membranes.

Now, cost of one number of abrasive paper = 20.00 INR

Hence, cost of such six numbers of abrasive papers = 120.00 INR = 1.64 USD

Therefore, total raw material cost incurred during

the process of membrane fabrication = (0.75+1.64) USD = 2.39 USD

Labor cost

Labor cost corresponds to the expense that needs to be paid to a skilled labor (with technical knowledge) for manufacturing the membranes. Assuming that in the process of fabricating one batch of membrane, the labor needs to work for a total duration of eight hours and a skilled labor working for eight hours in a day is paid 500.00 INR, the labor cost involved in the whole process is estimated as = 500.00 INR = 6.81 USD.

Cost of electricity consumed

Electricity is mainly consumed by four equipment, namely extruder, oven, furnace and bath sonicator.

The calculation of electricity consumption cost for all the above-mentioned equipment is shown separately hereafter. It needs to mention that for Educational Institutions of Assam, the tariff, as fixed by Assam Power Distribution Company Limited (APDCL) for Financial Year 2021-22 is 6.45 INR/kWh (Assam Power Distribution Company Limited, 2021). Hence, all the calculations regarding electricity consumption cost are carried out using this tariff.

Extruder

The power of the motor in the extruder that was

used for fabricating the membranes = 0.5 HP

= (0.5×0.7457) kW

= 0.3728 kW

For extruding sixty membranes, the extruder needs to be run for 2 hours.

Hence, the cost of power consumed = (0.3728×2×6.45) INR

= 4.81 INR = 0.07 USD

Hot air oven

The heating coil capacity of the oven = 1.5 kW

The oven is used to heat the membranes at 100 °C and 200 °C, the duration being 24 hours in each case. Moreover, it is also used for another six hours to dry the membranes after cleaning via sonication bath. Hence, total working hours of the oven will be 54 (=24+24+6) hours. As the temperature rises from ambient to 100 °C and then 100 °C to 200 °C is very fast in the oven, hence, time required for this is neglected.

Therefore, the cost of power consumed by the oven = (1.5×54×6.45) INR

= 522.45 INR = 7.12 USD

Furnace

The power of heating element of the furnace = 4 kW

The furnace is used to sinter the membranes at 1100 °C, for a duration of six hours. As in this case, heating rate needs to be maintained at 2 °C/min to avoid any bending/cracking of the membranes, the time required for temperature rise needs to be taken into consideration. At the mentioned heating rate, time required to reach 1100 °C from ambient is 537.5 $\left(= \frac{(1100-25)}{2}\right)$ minutes or 8.96 hours. Hence, total working hours of the oven will be 14.96 (=8.96+6) hours.

Therefore, the cost of power consumed by the furnace = (4×14.96×6.45) INR

= 385.97 INR = 5.26 USD

Ultrasonication Bath

The power requirement of the ultrasonication bath = 0.12 kW

This instrument is used for removing the loose particles that may get attached to the membranes during the process of smoothening. To clean all the sixty membranes, the instrument needs to

be run for 45 minutes (=0.75 hours) as the bath can accommodate twenty membranes in a batch and ultrasonication time for a batch of membrane is decided as 15 minutes.

Therefore, the cost of power consumed by the ultrasonication bath = (0.12×0.75×6.45) INR

= 0.58 INR = 0.008 USD

Therefore, total electricity consumption cost incurred during the process of membrane fabrication = (0.07+7.12+5.26+0.008) USD

= 12.458 USD ≈12.46 USD

Repair and maintenance cost

The repair and maintenance of the equipment need to be carried out from time to time during its service life. For that, the knowledge of fixed capital investment is utmost necessary, as the annual repair and maintenance cost is estimated to be the 2% of fixed capital investment per year, if no severe circumstances are faced (Winter, 1969).

The fixed capital investment of the equipment is dependent on the original delivered cost of the equipment. In this case, as the equipment has already completed certain fractions of its service life and has undergone depreciation, the book values will be taken as the basis for calculating its capital cost. It needs to mention that book value is "the difference between the original cost of a property, and all the depreciation charges made to date" (Peters and Timmerhaus, 1991).

Following the above-mentioned concept, the book values are calculated for all four equipment involved during the process. For calculating the book value, the straight-line depreciation method is followed as it is the most sought-after method for carrying out preliminary cost estimates (Peters and Timmerhaus, 1991; Winter, 1969).

In this method, book value of a property is calculated using Equation (5.1):

$$V_a = \frac{V_o - V_s}{n_s} \times a \quad (5.1)$$

Where, V_a is the book value of the equipment, V_0 is the original delivered cost of the equipment, n_s is the service life in years and a is the years of use of the equipment (Peters and Timmerhaus, 1991).

Assumption:

1. Service life of all the equipment is taken as 10 years (=79200 working hours considering 330 working days in a year) (Chakraborty et al., 2020).
2. Salvage value of all the equipment is taken as 10% of their original delivered cost (FAO, 1992).

Following the mentioned details, the calculated book values of all the equipment along with their original delivered cost, installation year and years of use are presented in Table 5.2.

It needs to be kept in mind that as the oven has already completed its service life, it will not be considered for calculating the fixed capital investment. Now, the above-mentioned book values will be the basis for evaluating the fixed capital investments of the equipment and subsequent repair and maintenance cost.

Table 5.2 Estimation of book value of all the equipment

Equipment	Original delivered cost (INR)	Year of installation	Years of use till 2021	Book value	
				INR	USD
Extruder	3,00,000.00	2014	7	1,11,000.00	1512.67
Hot air oven	40,000.00	2011	10	4,000.00	54.51
Furnace	1,50,000.00	2014	7	55,500.00	756.34
Ultrasonication bath	35,000.00	2015	6	16,100.00	219.41

Again, Fixed capital investment = Equipment cost or book value × Lang factor (Ghodrat et al., 2016; Lang, 1947).

Annual repair and maintenance cost = 2% of Fixed capital investment/year (Winter, 1969) (Here, only the remaining fraction of service life of each equipment will be considered for calculation purpose (Table 5.3)).

The Lang factor used for calculation of fixed capital investment is fixed as 3.1 for solid processing plant while it is fixed as 3.63 for solid-fluid processing plant (Ghodrat et al., 2016; Lang, 1947).

However, the repair and maintenance are completely dependent on equipment working hours. As the equipment is not run during the whole year, hence repair and maintenance cost calculated based on the duration in which equipment was used will be more appropriate. This concept of calculating repair and maintenance cost of equipment is followed by most of the industries and is based on "Machine Hourly Rate method" (FAO, 1992; Jain and Narang, 2015; Bhar, 2008). Detailed calculation of the repair and maintenance cost involved during membrane fabrication is presented in Table 5.4.

Though oven is not taken into consideration due to completion of service life, a lump sum of 0.01 USD is assumed as its repair and maintenance cost.

Hence, total cost for repair and maintenance = (0.04+0.01) USD

= 0.05 USD

Laboratory cost

Laboratory cost is estimated as the 20% of the labor cost (Winter, 1969).

Hence, Laboratory cost for this process = 20% of 6.81 USD

= 1.36 USD

The sum of all the mentioned heads will give the Direct manufacturing cost of the process.

Hence, Direct manufacturing cost = (2.39+6.81+12.46+0.05+1.36) USD

= 23.07 USD

Table 5.3 Estimation of annual repair and maintenance cost

Equipment	Book Value (USD)	Lang factor	Fixed capital investment (USD)	Years of service life remaining	Fixed capital investment/year (USD/year)	Annual repair and maintenance cost (USD/year)
Extruder	1512.67	3.1	4689.28	3	1563.09	31.26
Furnace	756.34	3.63	2745.51	3	915.17	18.30
Ultrasonication bath	219.41	3.63	796.46	4	199.11	3.98

Table 5.4 Estimation of repair and maintenance cost for the process

Equipment	Annual repair and maintenance cost (USD/year)	Hourly repair and maintenance cost (USD/hour)	Duration of use (hours)	Repair and maintenance cost for process duration (USD)
Extruder	31.26	0.0039	2	0.0078
Furnace	18.30	0.0023	14.96	0.0344
Ultrasonication bath	3.98	0.0005	0.75	0.0004
	Total			**0.0426 ≈ 0.04**

5.1.2 Indirect manufacturing cost estimation

The process of membrane fabrication involves only one head of indirect manufacturing cost, i.e., depreciation cost. As depreciation also depends completely on working hours of equipment, hence, depreciation is calculated based on the number of hours the equipment was used during the whole process of membrane fabrication (Table 5.5).

Depreciation is calculated using the same straight line depreciation method. The formula used for calculating depreciation is:

$$D = \frac{V_o - V_s}{n_s} \quad (5.2)$$

Where, D is the depreciation cost of the equipment, V_o is the original delivered cost of the equipment and n_s is the remaining service life of the equipment in hours (Peters and Timmerhaus, 1991). Here also, depreciation cost for oven will not be calculated as it has already completed its service life. Here, Salvage value of all the equipment is taken as 10% of their book value.

Hence, Indirect manufacturing cost of the membrane fabrication process = 0.55 USD

Table 5.5 Depreciation cost of all the equipment

Equipment	Book value (USD)	Years of service life remaining	Hourly depreciation cost (USD/hour)	Duration of use during fabrication (hours)	Depreciation cost for process duration (USD)
Extruder	1512.67	3	0.057	2	0.114
Furnace	756.34	3	0.029	14.96	0.434
Ultrasonication bath	219.41	4	0.006	0.75	0.005
		Total			**0.553 ≈0.55**

5.1.3 Equipment cost estimation

The cost involved while procuring the various equipment used in the manufacturing of membrane also needs to be considered along with the manufacturing costs. The equipment cost involved in the process of membrane fabrication is demonstrated in Table 5.6. As fixed capital cost corresponds to all the other expenses such as site preparation, handling and installation charges associated with the purchase of equipment, hence the fixed capital cost calculated earlier will be used for calculating the equipment cost (Peters and Timmerhaus, 1991). As the oven has already completed its full-service life, cost of procuring the oven is not considered while calculating the equipment cost.

Table 5.6 Equipment cost estimation

Equipment	Fixed capital cost (USD/year)	Hourly fixed capital cost (USD/hour)	Duration of use (hours)	Equipment cost for process duration (USD)
Extruder	1563.09	0.20	2	0.40
Furnace	915.17	0.12	14.96	1.80
Ultrasonication bath	199.11	0.025	0.75	0.02
	Total			**2.22**

5.1.4 Estimation of total cost involved in membrane fabrication

The total cost involved during the membrane fabrication process corresponds to the sum of direct and indirect manufacturing costs.

Hence, total cost = (23.07+0.55+2.22) USD

= 25.84 USD

This cost corresponds to sixty membranes.

Hence for fabricating one membrane, cost incurred = 0.43 USD

The fabricated membranes have inner diameter 5.5 mm, outer diameter 11.5 mm and length 100 mm. The surface area of membrane is 1.72788×10^{-3} m^2.

Hence, cost incurred per m^2 of the membrane = 248.86 USD ≈ 250.00 USD

The pie diagram depiction of cost analysis for the membrane fabrication process is shown in Fig. 5.1.

It is worth mentioning here that membranes used in various separation processes in earlier literatures are so expensive that their price are ranging from 460-4000 USD/m^2 and hence, using them in industrial separation processes, especially in small scale industries become a matter of concern (Chakraborty et al., 2020). It is well documented in literature that the price of membranes fabricated using α-alumina as one of its key precursors usually ranges from 989-1220 USD/m^2 (Krawczyk and Jönsson, 2014). The membrane fabricated as a part of this work costs USD 23.05 per m^2 in terms of raw material cost, which is in the price range of the low-cost membranes reported in the literature. The low-cost membranes reported in the available literature cost around USD 2.00-135.00 per m^2 in terms of raw material cost (Abdullayev et al., 2019). Besides, considering the other factors such as membrane repair and maintenance, depreciation and so on, the fabricated membrane costs USD 250.00 per m^2, which again falls under the purview of low-cost membranes reported in the literature with price ranging between USD 440.00-4000.00 per m^2 (Chakraborty et al., 2020; Suresh et al., 2016). Therefore, looking

at the aforementioned observations, it can certainly be concluded that the membrane fabricated in this work is a low-cost one and can be afforded by industries of all scale.

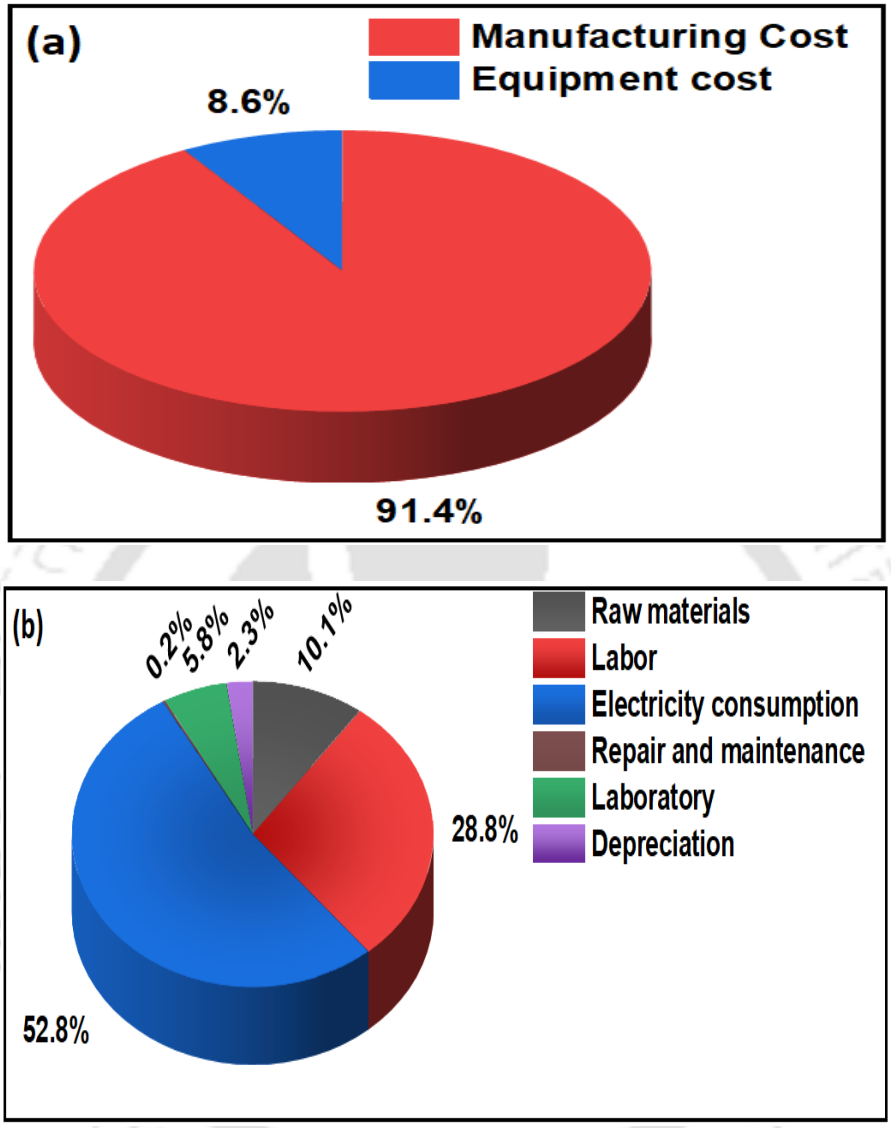

Fig. 5.1 (a) Total fabrication cost as percentages of manufacturing cost and equipment cost, (b) Splitting of manufacturing expenses incurred during membrane fabrication

5.2 Estimation of process cost on lab-scale

The lab-scale cost estimation is carried out based on the available permeation setup containing membrane housing that can accommodate a single membrane of inner diameter 5.5 mm, outer diameter of 11.5 mm and a length of 100 mm. The expenses incurred in the process can be categorized into two broad categories: capital cost and operating cost (Singh and Cheryan,

1998). Capital cost incurred in a process is regarded as the expenses associated with purchase and installation of equipment, obtaining necessary land and service facilities as well as erection of the plant with all the necessary piping, valves, controls and services (Peters and Timmerhaus, 1991). In evaluating the capital cost for the three separation processes carried out in the thesis (Treatment of poultry slaughterhouse wastewater, treatment of starch industry wastewater, separation of glycerol from biodiesel), the cost incurred in procuring the separation setup and necessary equipment along with the membrane cost will be considered. However, among the aforementioned expenses coming under capital cost, the expenses corresponding to procuring the permeation setup and necessary equipment will only constitute the fixed capital cost involved in the process (Monash, 2011).

The operating cost involved in a chemical process can be defined as the daily expenses incurred while running a plant and is the sum of various expenses such as electricity consumption cost, labor cost, cleaning and maintenance cost, depreciation cost and so on (Manzolini and Jansen, 2013). The sum of the capital cost as well as operating cost will correspond to the total cost incurred in the whole separation process.

Basis of calculation:

1. The fabricated membranes are having a shelf life of 3 years.
2. The permeation setup and all the necessary equipment used during the separation process will have a service life of 10 years (Chakraborty et al., 2020).
3. There will be 330 working days in a year (Chakraborty et al., 2020).

5.2.1 Cost analysis for poultry slaughterhouse wastewater treatment

The treatment process of poultry slaughterhouse wastewater in lab-scale is a five hours process, where 3 hours are used for filtration operation and the rest two hours are used for cleaning the setup as well as the membrane.

Hence, assuming 330 working days in a year, number

of working days used for filtration purpose $= \frac{3}{5} \times 330$ days = 198 days

Permeate flux reported (at P=345 kPa) $= 5.85\times10^{-6}$ m^3/m^2s

Hence, amount processed per year (using a lab-scale cross-flow setup having membrane area of 0.00172788 m^2) $= 5.85\times10^{-6}\times0.00172788\times24\times3600\times198$ m^3

$= 0.1729$ m^3 = 172.9 L

5.2.1.1 Estimation of capital cost

Cost of the permeation setup = 40, 000.00 INR

Filtration setup was installed in the year 2018. However, the poultry slaughterhouse wastewater treatment was carried out in the year 2019. Hence, the book value of the permeation setup in 2019 will be used for calculating the fixed capital cost corresponding to the permeation setup. The same equation (Equation (5.1)) mentioned previously is utilized here also for calculating the book value of the permeation setup (Peters and Timmerhaus, 1991; Winter, 1969).

Hence, book value at 2019 = 36400.00 INR

As the permeation setup can be regarded as a fluid processing plant, the Lang factor used for calculating the fixed capital will be 4.74 (Ghodrat et al., 2016; Lang, 1947).

Hence, the fixed capital = 36400.00×4.74 INR

= 172536.00 INR = 2351.26 USD

As the permeation setup completed one year of its service life, it has nine years of service life left. Hence, fixed capital cost incurred per year is 261.25 USD.

Fabrication cost of one membrane is 0.43 USD. As the membrane has a service life of 3 years, the capital cost involved in the process corresponding to membrane is 0.14 USD/year.

Hence, total capital cost incurred = (261.25+0.14) USD/year

= 261.39 USD/year

5.2.1.2 Estimation of operating cost

The various operating costs involved in the process of poultry slaughterhouse wastewater treatment are discussed below in detail.

Cost of electricity consumed

The power consuming equipment used during the separation process is a booster pump with a motor capacity of 36 W. The pump is used continuously for 330 days, as it is required for both the cases, namely filtration as well as membrane cleaning.

Considering the same electricity tariff rate mentioned previously (6.45 INR/kWh) (Assam Power Distribution Company Limited, 2021),

the cost of electricity consumed by the pump = (0.036×6.45×330×24) INR/year

= 1839.02 INR/year = 25.06 USD/year

Cleaning cost

In this separation process, the setup was initially flushed with millipore water for 30 minutes, which was followed by flushing the setup with 1 g/L surf excel solution for another 1 hour. Then, the setup was flushed once again with millipore water for another 30 minutes. Taking this process into consideration, cleaning cost is considered to be 4% of fixed capital cost incurred during poultry slaughterhouse wastewater treatment.

Hence, cleaning cost = 4% of fixed capital cost/year

= (0.04×261.25) USD/year = 10.45 USD/year

Maintenance cost

It is considered that maintenance cost is 3% of the fixed capital cost incurred during the separation process (Singh and Cheryan, 1998).

Hence, maintenance cost = 3% of fixed capital cost/year

= (0.03×261.25) USD/year = 7.83 USD/year

Labor cost

It is considered that labor cost is 2% of the fixed capital cost incurred during the separation process (Singh and Cheryan, 1998).

Hence, labor cost = 2% of fixed capital cost/year

= (0.02×261.25) USD/year = 5.23 USD/year

Laboratory cost

It is considered that laboratory cost is 20% of the labor cost incurred during the separation process (Winter, 1969)

Hence, laboratory cost = 20% of labor cost/year

= (0.2×5.23) USD/year = 1.05 USD/year

Depreciation cost

Assuming that the permeation setup possesses a salvage value which is equal to 10% of its book value in 2019, the depreciation cost per year for the rest 9 years of its service life, calculated using the same straight line depreciation method mentioned in the previous section, (Equation (5.2)) is 49.61 USD (Peters and Timmerhaus, 1991).

Therefore, total operating cost = (25.06+10.45+7.83+5.23+1.05+49.61) USD/year

= 99.23 USD/year

5.2.1.3 Estimation of total cost

The total cost incurred during the separation process is the sum of capital cost as well as operating cost.

Hence, total cost incurred during poultry slaughterhouse wastewater treatment = (261.39+99.23) USD/year

= 360.62 USD/year

As a total of 172.9 L of treated wastewater is obtained in the whole year, hence total cost incurred per liter of permeate obtained = 2.09 USD/L

The pie diagram representation of cost analysis for the treatment of poultry slaughterhouse wastewater is shown in Fig. 5.2.

5.2.2 Cost analysis for starch wastewater treatment

The treatment process of starch wastewater in lab-scale takes 250 minutes as a whole, where 180 minutes (3 hours) are used for filtration operation and the rest 70 minutes are used for cleaning the setup as well the membrane.

Hence, assuming 330 working days in a year, number of working days used for filtration purpose = $\frac{180}{250}$ ×330 days = 237.6 days = 238 days

Permeate flux reported (at P=345 kPa) = 9.56×10^{-6} m^3/m^2s

Hence, amount processed per year = $9.56\times10^{-6}\times0.00172788\times24\times3600\times238$ m^3

= 0.3398 m^3 = 339.8 L

5.2.2.1 Estimation of capital cost

Cost of the permeation setup = 40, 000.00 INR

Setup was installed in the year 2018. However, the treatment of starch wastewater was carried out in the year 2021. Hence, the book value of the permeation setup in 2021 will be used for calculating the fixed capital cost corresponding to the permeation setup.

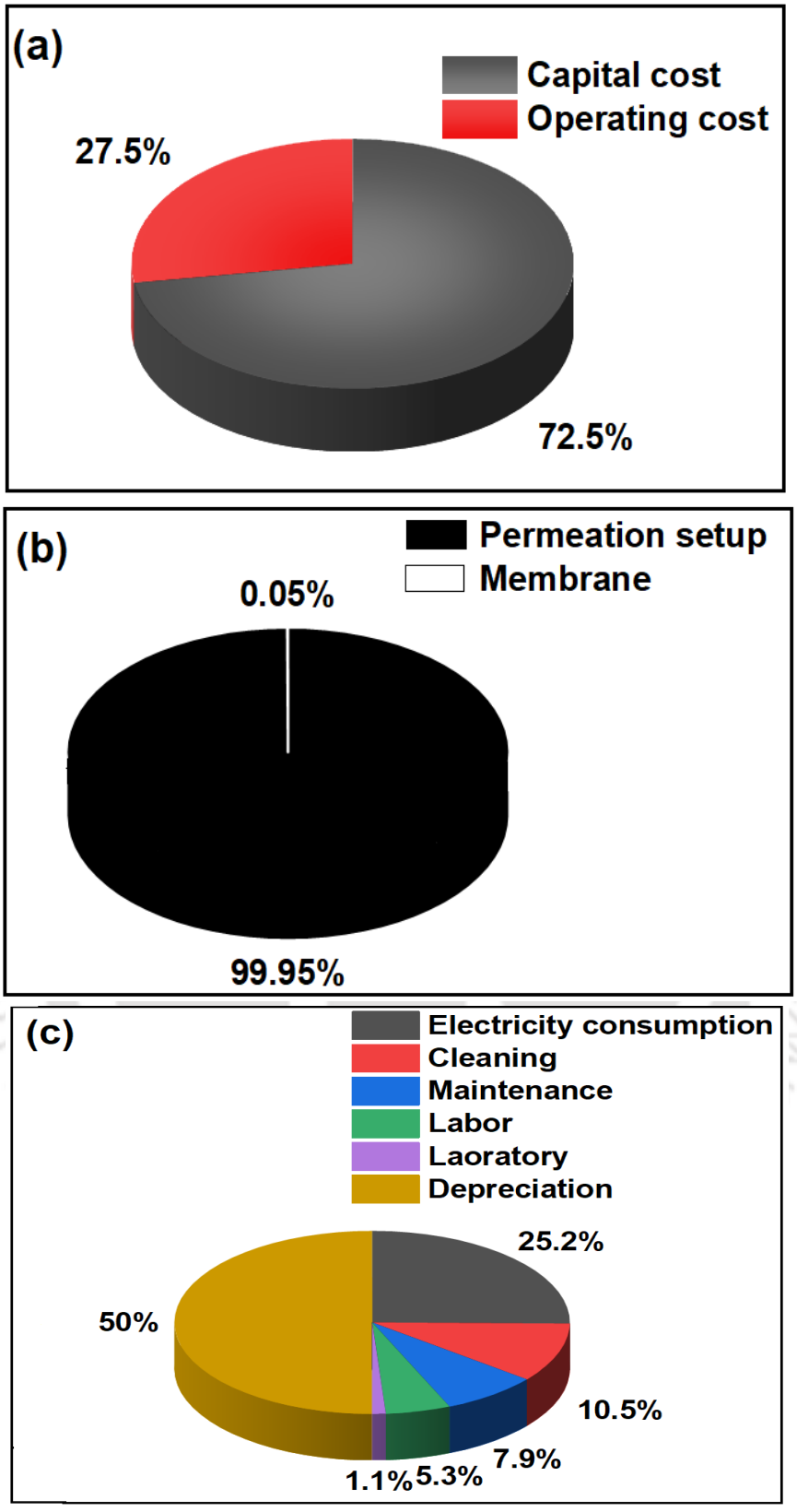

Fig. 5.2 (a) Total process cost as percentages of capital cost and operating cost (b) Splitting of total capital cost incurred during the process (c) Splitting of total operating cost incurred during poultry slaughterhouse wastewater treatment process (Lab-scale)

Book value at 2021 = 29200.00 INR

And, the fixed capital = 29200.00×4.74 INR

= 138408.00 INR = 1886.18 USD

As the permeation setup completed three years of its service life, it has seven years of service life left. Hence, fixed capital cost incurred per year is 269.45 USD.

Again, the capital cost involved in the process corresponding to membrane is 0.14 USD/year.

Hence, total capital cost incurred = (269.45+0.14) USD/year

= 269.59 USD/year

5.2.2.2 Estimation of operating cost

The various operating costs involved in the process of starch wastewater treatment are discussed below:

Cleaning cost

In this process, the setup was initially cleaned with millipore water for 30 minutes, which was followed by cleaning the setup with 1 g/L surf excel solution for 30 minutes. Then, the setup was flushed once again with millipore water for 20 minutes. Taking this steps into consideration, cleaning cost is considered to be 5% of fixed capital cost incurred during starch wastewater treatment.

Hence, cleaning cost = 5% of fixed capital cost/year

= (0.05×269.45) USD/year = 13.47 USD/year

Depreciation cost

The depreciation cost per year for the experimental setup with 7 years of its service life remaining, calculated using the same straight line depreciation method mentioned in the

previous section (Equation (5.2)) is 51.16 USD (Peters and Timmerhaus, 1991).

The other four costs, namely electricity consumption cost, maintenance cost, labor cost as well as laboratory cost are calculated using the same mathematical procedure that was used in the previous section.

Hence, Electricity consumption cost = 25.06 USD/year

Maintenance cost = 8.08 USD/year

Labor cost = 5.39 USD/year

Laboratory cost = 1.08 USD/year

Therefore, total operating cost = (25.06+13.47+8.08+5.39+1.08+51.16) USD/year

= 104.24 USD/year

5.2.2.3 Estimation of total cost

The total cost incurred during the process = (269.59+104.24) USD/year

= 373.83 USD/year

As a total of 339.8 L of permeate is obtained in the whole year by treating corn starch wastewater, hence total cost incurred per liter of permeate obtained = 1.10 USD/L

As a total of 223.23 L of permeate is obtained in the whole year by treating wheat starch wastewater, hence total cost incurred per liter of permeate obtained = 1.67 USD/L

As a total of 105.21 L of permeate is obtained in the whole year by treating rice starch wastewater, hence total cost incurred per liter of permeate obtained = 3.55 USD/L

The pie diagram representation of cost analysis for starch wastewater treatment is shown in Fig. 5.3.

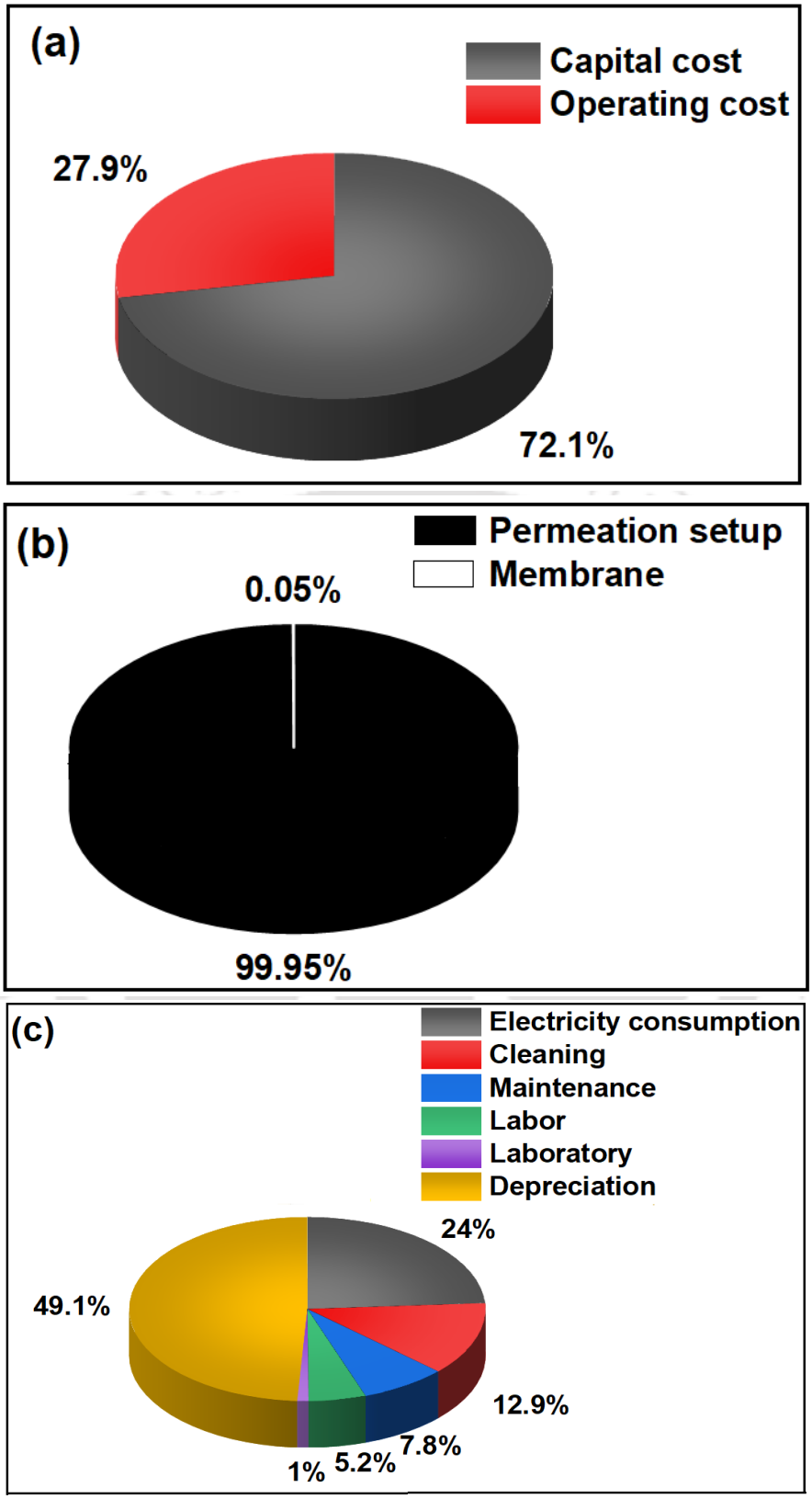

Fig. 5.3 (a) Total process cost as percentages of capital cost and operating cost (b) Splitting of total capital cost incurred during the process (c) Splitting of total operating cost incurred during starch wastewater treatment process (Lab-scale)

5.2.3 Cost analysis for separation of glycerol from biodiesel

The separation of glycerol from biodiesel emulsion in lab-scale is a five hours process, where 3 hours are used for filtration operation and the rest two hours are used for cleaning the setup as well the membrane.

Hence, assuming 330 working days in a year, number

of working days used for filtration purpose $= \frac{3}{5} \times 330$ days = 198 days

Permeate collected after 3 hours (at P=345 kPa) = 87.5 g

However, this permeate contains traces of water and methanol, which need to be removed in the Rotary evaporator.

Hence, after evaporating the methanol and water in the rotary evaporator for 30 minutes, the amount of permeate collected = 84.96 g

Assuming the density of biodiesel to be 877.2 kg/m^3 (Som et al., 2010), the permeate collected after 3 hours of run $= 9.68 \times 10^{-5}$ m^3

Hence, amount processed per year $= \frac{9.68 \times 10^{-5} \times 24 \times 198}{3}$ m^3

$= 0.1533$ m^3 = 153.3 L

5.2.3.1 Estimation of capital cost

Cost of the permeation setup = 40, 000.00 INR

Setup was installed in the year 2018. However, the separation of glycerol from biodiesel was carried out in the year 2020. Hence, the book value of the permeation setup in 2020 will be used for calculating the fixed capital cost corresponding to the permeation setup.

Book value at 2020 = 32800.00 INR

Hence, the fixed capital corresponding to permeation setup = 32800.00×4.74 INR

= 155472.00 INR = 2118.72 USD

As the permeation setup completed two years of its service life, it has eight years of service life left. Hence, fixed capital cost incurred per year is 264.84 USD.

Along with the permeation setup, a Rotary evaporator is also used for evaporating the traces of methanol and water present in the permeate. The Rotary evaporator used in this case had a purchase cost of 350000.00 INR in the year 2016.

Hence, book value at 2020 = 224000.00 INR

As Rotary evaporator is also considered to be a fluid processing plant, the Lang factor to be used for calculating fixed capital corresponding to Rotary evaporator will be 4.74 (Ghodrat et al., 2016; Lang, 1947).

Hence, fixed capital invested for procuring the Rotary evaporator = 22400.00×4.74 INR

= 1061760.00 INR

= 14469.34 USD

However, unlike the permeation setup, the rotary evaporator is not run continuously for 330 days. Rather, when the one run for the whole process of microfiltration and membrane cleaning takes five hours, the Rotary evaporator runs for only 30 minutes (= 0.5 hour) for evaporating traces of methanol and water present in the permeate. Hence, fixed capital investment per year for the Rotary evaporator will be calculated based on its effective working days in a year.

Hence, no. of effective working days $= \frac{0.5}{5} \times 330 \text{ days} = 33 \text{ days}$

Hence, fixed capital investment incurred per year $= \frac{33}{330 \times 6} \times 14469.34 \text{ USD}$

= 241.16 USD

Again, as mentioned earlier, the capital cost involved in the process corresponding to membrane is 0.14 USD/year.

Hence, total capital cost incurred = (264.84+0.14+241.16) USD/year

= 506.14 USD/year

5.2.3.2 Estimation of operating cost

The various operating costs involved in the process of separation of glycerol from biodiesel are discussed below in detail.

Cost of electricity consumed

The power consuming equipment used during the separation process is a booster pump, with a motor capacity of 36 W and the Rotary evaporator, with a wattage of 1.35 kW. The rotary evaporator is run only for 33 number of effective working days in a year.

The cost of electricity consumed by the pump = 1839.02 INR/year = 25.06 USD/year

The cost of electricity consumed by Rotary evaporator = (1.35×6.45×33×24) INR

= 6896.34 INR/year = 93.98 USD/year

Hence, total cost of electricity consumed = (25.06+93.98) USD/year

= 119.04 USD/year

Cleaning cost

During separation of glycerol from biodiesel, the setup, after microfiltration, was initially flushed with methanol for 30 minutes, which was followed by flushing the setup with 1 g/L surf excel solution for another 30 minutes. Then, the setup was flushed once again first with 1 wt% NaOH solution and then with millipore water, each for 30 minutes. Taking this process into consideration and also after use cleaning of the rotary evaporator, cleaning cost is considered to be 8% of fixed capital cost incurred during the process of glycerol separation from biodiesel.

Hence, cleaning cost = 8% of fixed capital cost/year

= (0.08×506.00) USD/year = 40.48 USD/year

Depreciation cost

The depreciation cost per year for the rest 8 years of service life of the experimental setup, calculated using same straight line depreciation method discussed in earlier section (Equation (5.2)) is 50.28 USD (Peters and Timmerhaus, 1991).

Again, for the rotary evaporator, considering its salvage value to be 10% of its book value at 2020, the depreciation cost incurred per year with only 33 number of effective working days is 45.79 USD.

Hence, total depreciation cost incurred = (50.28+45.79) USD/year

= 96.07 USD/year

The other three costs, namely maintenance cost, labor cost as well as laboratory cost are calculated using the same mathematical procedure that was used in the previous section.

Hence, Maintenance cost = 15.18 USD/year

Labor cost = 10.12 USD/year

Laboratory cost = 2.02 USD/year

Therefore, total operating cost = (119.04+40.48+15.18+10.12+2.02+96.07) USD/year

= 282.91 USD/year

5.2.3.3 Estimation of total cost

The total cost incurred during the process = (506.14+282.91) USD/year

= 789.05 USD/year

As a total of 153.3 L of permeate is obtained in the whole year, hence total cost incurred per liter of permeate obtained = 5.15 USD/L

The pie diagram representation of cost analysis for the separation of glycerol from biodiesel is shown in Fig. 5.4.

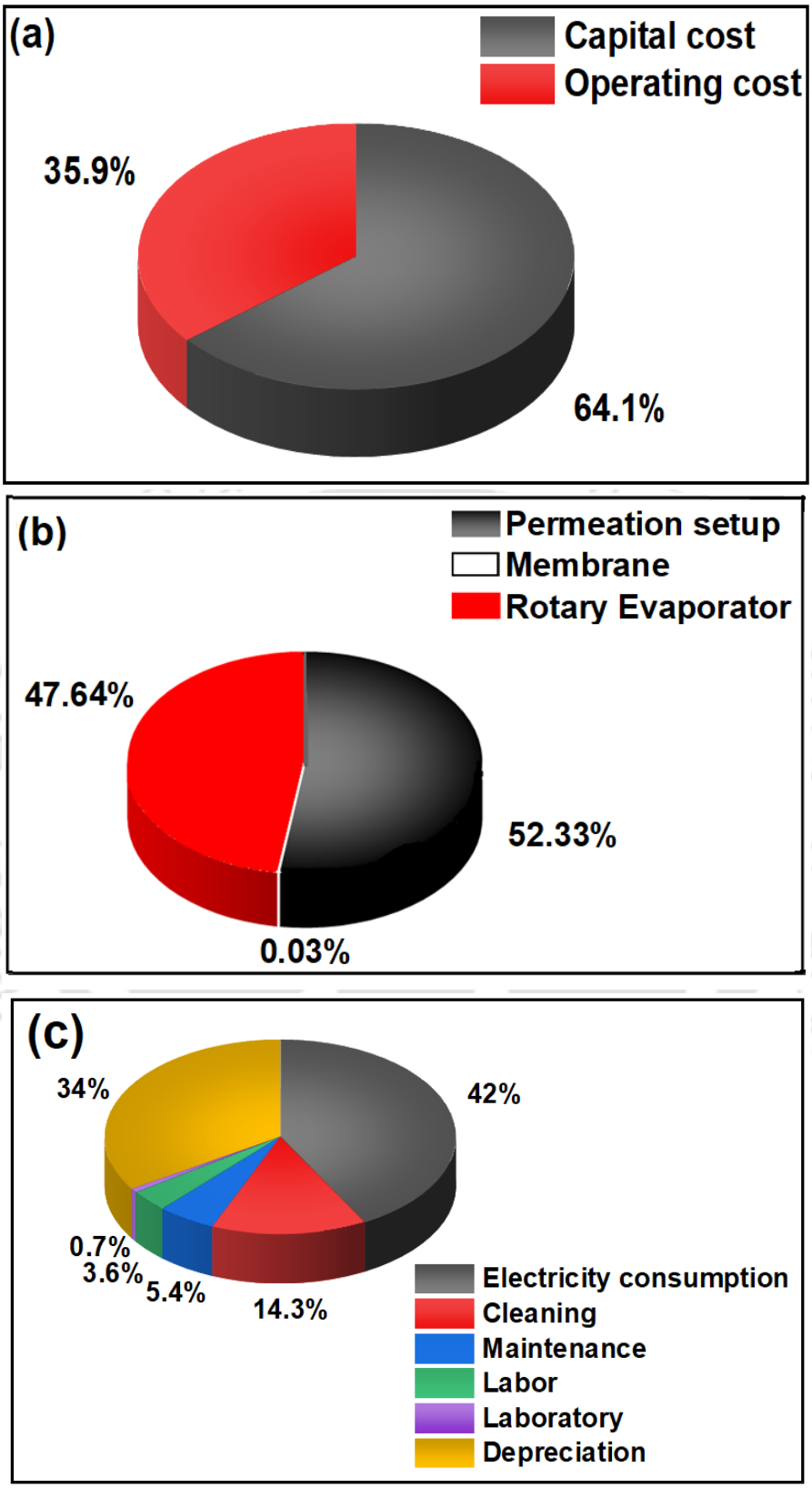

Fig. 5.4 (a) Total process cost as percentages of capital cost and operating cost (b) Splitting of total capital cost incurred during the process (c) Splitting of total operating cost incurred during glycerol separation from biodiesel (Lab-scale)

5.3 Estimation of cost for pilot-scale setup

Looking at the efficiency of the lab-scale setup and the capacity of the existing equipment to be scaled up into a pilot-scale setup with certain modifications, the following design of permeation setup is proposed. In this setup, the single housing of membrane module is replaced by three parallel membrane housings, each with 200 mm length. Each of such housings can accommodate 7 membranes inside it, thus utilizing a total of 21 membranes with 200 mm length, the inner as well as outer diameter of the membranes remaining the same. The reason behind chosing 200 mm length membranes is that the existing extruder can satisfactorily produce membranes up to 200 mm length. Moreover, the available furnace also can be used to sinter membranes upto 200 mm length.

Hence, for the above-mentioned setup, the effective filtration area becomes 0.07257 m^2. This setup will be used for estimating the cost for a pilot-scale setup in the following subsections. The schematic of the pilot-scale setup is shown in Fig. 5.5.

Basis of calculation:

1. The fabricated membranes will have a shelf life of 3 years.
2. The permeation setup and all the necessary equipment used during the separation process will have a service life of 10 years (Chakraborty et al., 2020).
3. There will be 330 working days in a year (Chakraborty et al., 2020).
4. As it is a proposed cost analysis, the current price for all the equipment is considered for estimating the cost incurred during the process. Hence, no depreciated value of equipment is calculated here as in previous cases.

5.3.1 Cost analysis for poultry slaughterhouse wastewater treatment

As mentioned earlier, permeate flux obtained (at P = 345 kPa) = 5.85×10^{-6} m^3/m^2s

Hence, amount processed per year (using a pilot-scale cross-flow setup having membrane area of 0.07257 m^2) = $5.85\times10^{-6}\times0.07257\times24\times3600\times198$ m^3

= 7.2625 m^3 = 7262.5 L

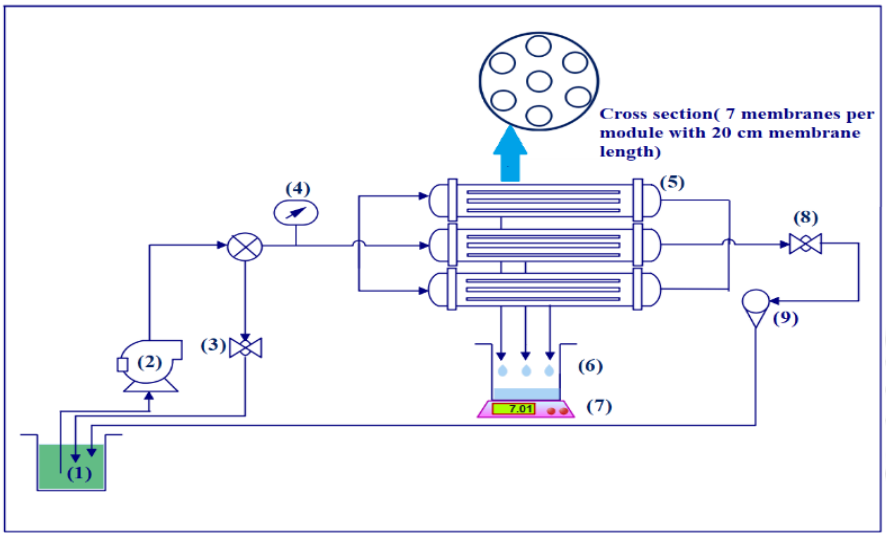

Fig. 5.5 Pilot plant setup [1: Feed tank; 2: Booster pump; 3,8: Valves; 4: Pressure gauge; 5: Membrane housings; 6: Permeate tank; 7: Weighing balance; 9: Rotameter]

5.3.1.1 Estimation of capital cost

Cost of the permeation setup = 1,00, 000.00 INR

Hence, the corresponding fixed capital = 100000.00×4.74 INR

= 474000.00 INR = 6459.53 USD

As the permeation setup has ten years of service life, hence, fixed capital cost incurred per year is 645.95 USD.

Fabrication cost per m^2 area of membrane is 250.00 USD. For obtaining the desired filtration area, the cost incurred will be 18.14 USD. As the membranes have a service life of 3 years, the capital cost involved in the process corresponding to the membrane is 6.05 USD/year.

Hence, total capital cost incurred = (645.95+6.05) USD/year

= 652.00 USD/year

5.3.1.2 Estimation of operating cost

Following the same operating procedure opted for calculating various sub-heads under operating cost for lab-scale set-up, the operating cost for the scaled-up setup was also estimated. However, in this case, owing to scale-up, a slightly larger capacity booster pump was considered having motor capacity of 60 W. Moreover, the depreciation cost of the permeation setup was calculated using its current purchase price and ten years of service life. The estimated cost under various sub-heads of operating cost is mentioned in Table 5.7.

Table 5.7 Operating cost estimation for treating poultry slaughterhouse wastewater (Pilot-scale)

Sub-heads	**Cost (USD/year)**
Electricity consumption	41.77
Cleaning cost	25.84
Maintenance cost	19.38
Labor cost	12.92
Laboratory cost	2.58
Depreciation cost	122.65
Total	**225.14**

5.3.1.3 Estimation of total cost

The total cost incurred in the process = (652.00+225.14) USD/year

= 877.14 USD/year

As a total of 7262.5 L of treated wastewater is obtained in the whole year, hence total cost incurred per liter of permeate obtained = 0.12 USD/L

The pie diagram representation of cost analysis for the treatment of poultry slaughterhouse wastewater is shown in Fig. 5.6.

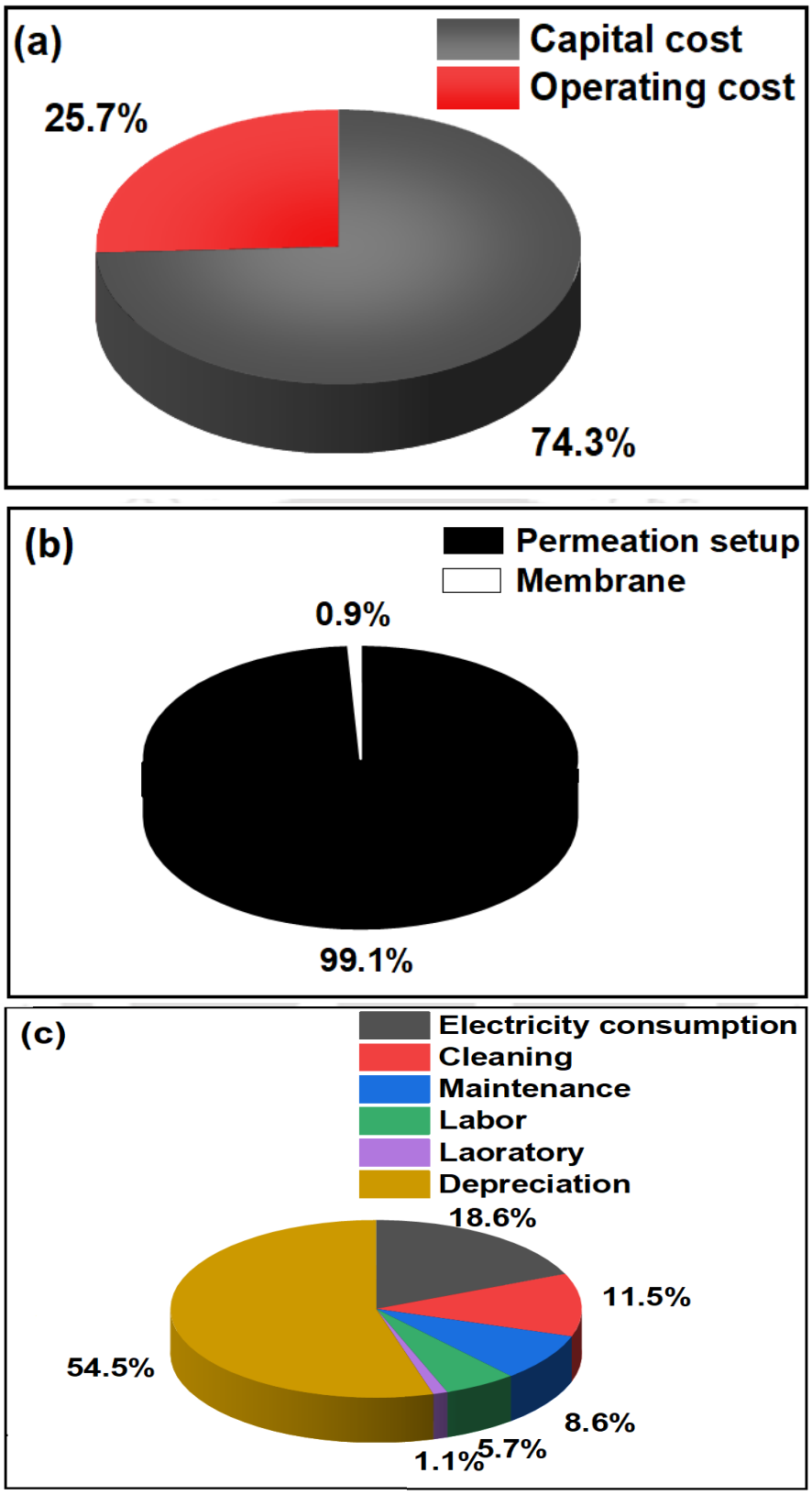

Fig. 5.6 (a) Total process cost as percentages of capital cost and operating cost (b) Splitting of total capital cost incurred during the process (c) Splitting of total operating cost incurred during poultry slaughterhouse wastewater treatment (Pilot-scale)

5.3.2 Cost analysis for starch wastewater treatment

Permeate flux reported (at P = 345 kPa) for corn starch wastewater = 9.56×10^{-6} m^3/m^2s

Hence, amount processed per year using a pilot-scale membrane of

area 0.07257 m^2 = $9.56\times10^{-6}\times0.07257\times24\times3600\times238$ m^3

= 14.2661 m^3 = 14266.1 L

Permeate flux reported (at P=345 kPa) for wheat starch wastewater = 6.28×10^{-6} m^3/m^2s

Hence, amount processed per year using a pilot-scale membrane

of area 0.07257 m^2 = $6.28\times10^{-6}\times0.07257\times24\times3600\times238$ m^3

= 9.3715 m^3 = 9371.5 L

Similarly,Permeate flux reported (at P = 345 kPa) for rice starch wastewater = 2.96×10^{-6} m^3/m^2s

Hence, amount processed per year using a lab-scale membrane

of area 0.07257 m^2 = $2.96\times10^{-6}\times0.07257\times24\times3600\times238$ m^3

= 4.4171 m^3 = 4417.1 L

5.3.2.1 Estimation of capital cost

Cost of the permeation setup = 1,00, 000.00 INR

Hence, the corresponding fixed capital = 100000.00×4.74 INR

= 474000.00 INR = 6459.53 USD

Hence, fixed capital cost incurred per year is 645.95 USD.

The capital cost involved in the process corresponding to membrane is 6.05 USD/year.

Hence, total capital cost incurred = (645.95+6.05) USD/year

= 652.00 USD/year

5.3.2.2 Estimation of operating cost

The operating expenses incurred during the starch industry wastewater treatment are presented

in Table 5.8. The cost estimation was carried out following the same procedure as done in the previous sections of this chapter.

Table 5.8 Operating cost estimation for starch industry wastewater treatment (Pilot-scale)

Sub-heads	**Cost (USD/year)**
Electricity consumption	41.77
Cleaning cost	32.30
Maintenance cost	19.38
Labor cost	12.92
Laboratory cost	2.58
Depreciation cost	122.65
Total	**231.60**

5.3.2.3 Estimation of total cost

The total cost incurred during the process = (652.00+231.60) USD/year

= 883.60 USD/year

The pie diagram representation of cost analysis for starch wastewater treatment is shown in Fig. 5.7.

As a total of 14266.1 L of permeate is obtained in the whole year, hence total cost incurred per liter of permeate obtained for corn starch wastewater = 0.06 USD/L

Similarly, as a total of 9371.5 L of permeate is obtained in the whole year, hence total cost incurred per liter of permeate obtained for wheat starch wastewater = 0.09 USD/L

And, as total of 4417.1 L of permeate is obtained in the whole year, hence total cost incurred per liter of permeate obtained from rice starch wastewater = 0.20 USD/L

5.3.3 Cost analysis for separation of glycerol from biodiesel

The quantity of permeate collected after 3 hours of run using a lab-scale cross-flow setup having membrane area of 0.00172788 m^2 = 9.68×10^{-5} m^3

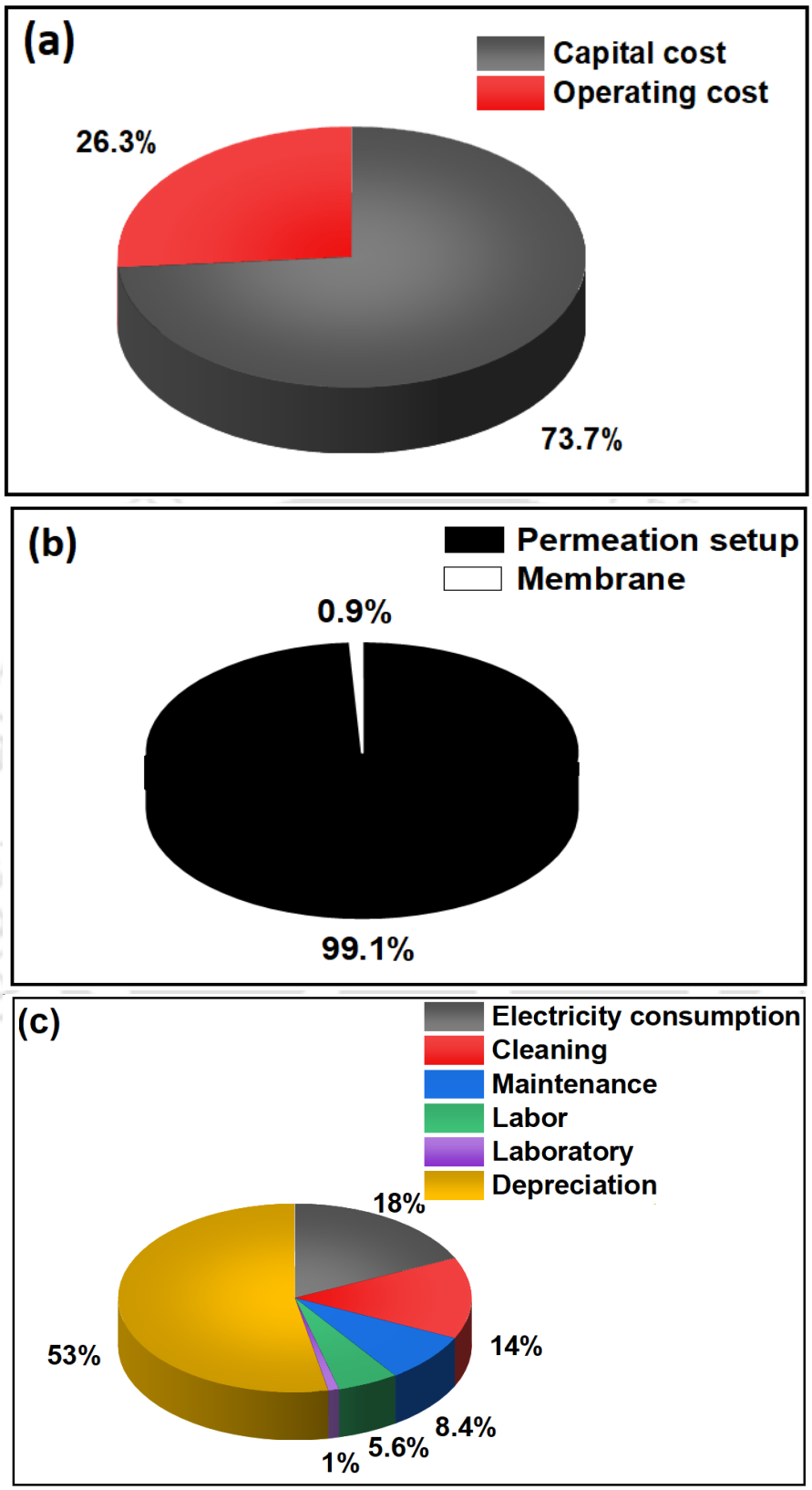

Fig. 5.7 (a) Total process cost as percentages of capital cost and operating cost, (b) Splitting of total capital cost incurred during the process, (c) Splitting of total operating cost incurred during starch wastewater treatment process (Pilot-scale)

Amount of permeate collected after 3 hours of run using a pilot-scale cross-flow setup having membrane area of 0.07257 m^2 $= 4.07\times10^{-3}$ m^3

Hence, amount processed per year using a pilot-scale cross-flow setup having membrane area of 0.07257 m^2) $= \frac{4.07\times10^{-3}\times24\times198}{3}$ m^3

$= 6.4469$ m^3 $= 6446.9$ L

5.3.3.1 Estimation of capital cost

Cost of the permeation setup = 1,00, 000.00 INR

Hence, the fixed capital corresponding to permeation setup = 474000.00 INR = 6459.53 USD

And therefore, the fixed capital cost incurred per year for the permeation setup is 645.95 USD.

Along with the permeation setup, a Rotary evaporator is also used for evaporating the traces of methanol and water present in the permeate. The present cost of the Rotary evaporator to be used in this case is 500000.00 INR.

Hence, fixed capital invested for procuring the Rotary evaporator = 500000.00×4.74 INR

= 2370000.00 INR

= 32297.63 USD

However, unlike the permeation setup, the rotary evaporator is not run continuously for 330 days. Rather, when the one run for the whole process of microfiltration and membrane cleaning takes five hours, the Rotary evaporator runs for 2.03 hours for evaporating traces of methanol and water present in the permeate produced using pilot-scale setup. Hence, fixed capital investment per year for the Rotary evaporator will be calculated based on its effective working days in a year.

Hence, no. of effective working days $= \frac{2.03}{5}\times330$ days = 134 days

Hence, fixed capital investment incurred per year $= \frac{134}{330\times10}\times 32297.63$ USD

= 1311.48 USD/year

As previously mentioned, the capital cost involved in the process corresponding to membrane is 6.05 USD/year.

Hence, total capital cost incurred = (645.95+6.05+1311.48) USD/year

= 1963.48 USD/year

5.3.3.2 Estimation of operating cost

Following the same operating procedure opted for calculating various sub-heads under operating cost, the operating cost for the scaled-up setup was also estimated. However, in this case, along with the booster pump, electricity consumption cost incurred due to the use of Rotary evaporator was also taken into account. Other considerations regarding estimation of cost for this scaled-up setup are similar to those used in previous sections. The estimated cost under various sub-heads of operating cost is mentioned in Table 5.9.

Table 5.9 Operating cost estimation for separating glycerol from biodiesel (Pilot-scale)

Sub-heads	**Cost (USD/year)**
Electricity consumption	423.39
Cleaning cost	156.59
Maintenance cost	58.72
Labor cost	39.15
Laboratory cost	7.83
Depreciation cost	371.66
Total	**1057.34**

5.3.3.3 Estimation of total cost

Total cost incurred during the process = (1963.48+1057.34) USD/year

= 3020.82 USD/year

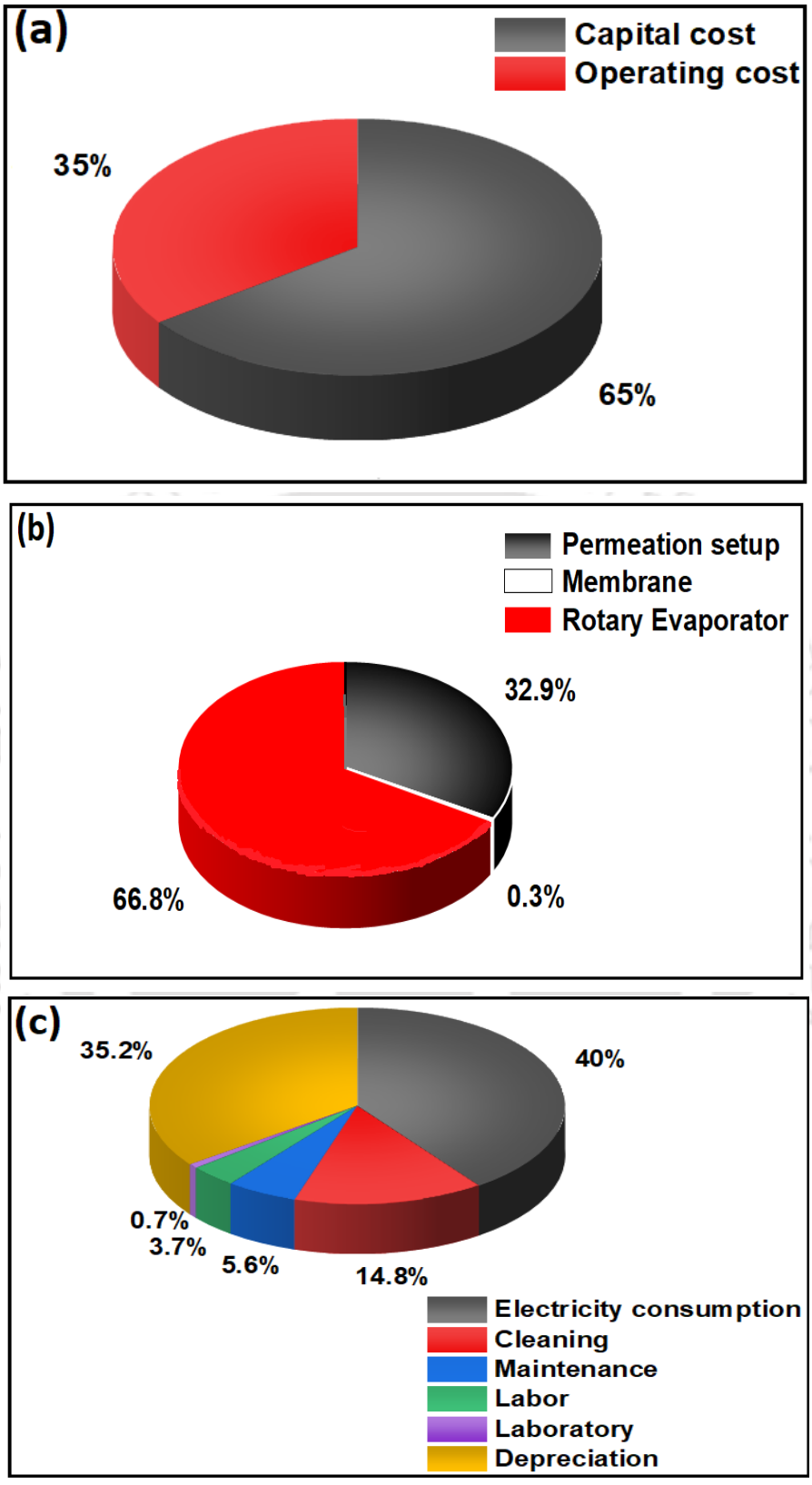

Fig. 5.8 (a) Total process cost as percentages of capital cost and operating cost (b) Splitting of total capital cost incurred during the process (c) Splitting of total operating cost incurred during separation of glycerol from biodiesel (Pilot-scale)

As a total of 6446.9 L of permeate is obtained in the whole year, hence total cost incurred per liter of permeate obtained = 0.47 USD/L

The pie diagram representation of cost analysis for the separation of glycerol from biodiesel is shown in Fig. 5.8.

5.4 Summary

The economic feasibility assessment of all three separation processes taken into consideration, namely poultry slaughterhouse wastewater treatment, treatment of starch processing wastewater and separation of glycerol from biodiesel, is successfully carried out. The process of cost estimation starts with estimating membrane fabrication cost, which is a sum of equipment cost and manufacturing expenses. The estimated cost per m^2 area of the membrane comes out to be 250.00 USD, which lies in the price range of low-cost membranes.

The next step of cost estimation process is to evaluate the cost associated with all the treatment processes. This is carried out for both lab-scale as well as pilot-scale setups, the lab-scale setup consisting of one membrane with an effective filtration area of 0.00172788 m^2; while the pilot-scale setup consisting of three parallel membrane housing, with seven membranes in each housing, the effective filtration area being 0.07257 m^2. The cost associated with each process is the sum of capital cost and operating cost incurred during the process. The total expenses associated with all the three separation operations taken into consideration lie between 1.10-5.15 USD per litre of permeate produced for lab-scale setup, which further reduced to 0.06-0.47 USD/L, when estimated for pilot-scale setup.

Chapter 6

Conclusions and Future Perspectives

Conclusions and Future Perspectives

This chapter summarizes the inferences drawn from the works carried out in this thesis and also provides some suggestions for future works that can be conducted, taking the work mentioned in this thesis as the basis. The main aim of this research was to fabricate a low-cost tubular ceramic membrane using fly ash as the key precursor. Further, the membrane with optimized raw material composition was used for three different liquid phase separation applications, namely poultry slaughterhouse wastewater treatment, starch processing wastewater treatment and separation of glycerol from biodiesel. All the interesting facts noted during the membrane fabrication and its subsequent application in liquid phase separation processes are outlined in this chapter.

6.1 Conclusions

- The raw material composition for fabrication of fly ash-based tubular ceramic membrane was optimized by conducting rigorous characterizations of membranes fabricated with different raw material compositions. Finally, membranes fabricated using 75 wt.% fly ash, 20 wt.% quartz and 5 wt.% calcium carbonate were found to display optimum properties suitable for different separation operations.
- Series of experiments conducted to study the effect of binder concentration on membrane properties revealed that the use of 2 wt% aqueous solution of Na-CMC as binder produced membranes with optimized properties.
- The optimized raw material composition as well as binder concentration resulted in membranes with an average porosity of 40.17% and pore size of 0.133 µm. Besides, the fabricated membrane also showed outstanding mechanical stability with a

compressive strength equal to 12.28 MPa along with very good corrosion resistance.

- It has been observed during the experiment that a very high binder concentration is detrimental to membrane properties as the increased viscosity of solution associated with increased binder concentration may lead to agglomeration of particles, causing the formation of big and uneven pores. Similarly, a very low binder concentration does not provide sufficient viscosity to hold ceramic particles together, ultimately leading to the formation of membranes with deformed shapes.
- The permeate produced from membrane filtration of poultry slaughterhouse wastewater is free from COD, TSS and turbidity, thus satisfying the Reuse and Discharge norms as prescribed by Central Pollution Control Board, India.
- Microfiltration of starch processing wastewater at different applied pressures and at different cross flow velocities yielded permeate with zero TSS, turbidity and slight COD content. The obtained permeate is safe to discharge into surface water as per the norms of Central Pollution Control Board, India. The membrane performed in a similar manner when incorporated in microfiltration of starch suspensions prepared using three different starch sources, namely corn, wheat and rice.
- During the separation of glycerol from biodiesel, though at all the applied pressures, a significant reduction in glycerol content was found in the permeate, but the purified biodiesel obtained after separation of glycerol at applied pressures below 345 kPa was found to satisfy ASTM D6751 and EN14214 regulations regarding the free glycerol content in biodiesel.
- A detailed cost analysis of membrane fabrication revealed that the fabricated membrane is a low-cost one, with the price being 250.00 USD/m^2 membrane area.

The use of cheaper and abundantly available raw materials in membrane fabrication was found to drastically reduce the cost of the membrane.

- Economic feasibility analysis was also carried out for all three separation processes in two ways: one for the lab-scale setup and the other is for the pilot-scale setup. In both the cases, the processes were found to be economically feasible for opting in industrial separation operations.
- The membrane developed using fly ash contributes greatly to the process of sustainable development. Sustainable Development Goals, 1987 has clearly defined sustainable development as the "*Development, which meets the needs of the people without compromising the ability of future generations to meet their own needs*". Utilization of fly ash in membrane fabrication has helped in conservation of mineral resources of earth, such as quartz, kaolin, dolomite and so on, as these materials were used for manufacturing low-cost ceramic membranes earlier. Recycling fly ash also helped in abating environmental pollution, thus putting an effort towards the protection of ecology and environment along with minimizing the various health hazards associated with its improper disposal. These facts are enough to realize that recycling fly ash will provide us low-cost ceramic membranes without compromising the safety of our planet. Rather, it will contribute positively towards obtaining a healthier and safer environment.
- Utilization of the fabricated membrane in three different separation operations can also be considered as another example for assuring sustainable development. The adoption of membrane technology in separation operations signifies the process intensification strategy, which is considered as one of the best realizations for sustainable growth. Process intensification focuses at development through substantially smaller, cleaner, safer and more energy efficient technology.

Implementation of low-cost ceramic membranes in the filtration processes not only reduces the cost associated with the process, but also makes efficient utilization of energy. Moreover, being regarded as clean technology, membrane-based separation is considered environmentally friendly. Hence, it can definitely be said that starting from membrane fabrication using fly ash to its implementation in separation processes, the entire process is a righteous example of sustainable development.

Therefore, it can be summarised that the fabricated membrane not only serves the purpose of filtration, but also helps in maintaining environmental sustainability through mitigation of pollution via fly ash recycling and is also quite affordable by all sections of the society.

6.2 Future perspectives

- Observing the membrane's outstanding separation efficiency in all the three separation processes carried out as a part of this research work, the versatility of fabricated membrane can further be explored by implementing in some other liquid phase separation processes such as separation of bacteria from milk, separation of casein proteins from serum protein of milk and so on. Increasing the number of separation processes that can be performed by a single membrane definitely enhances the membrane's utility.
- As the fabricated membrane is capable of performing microfiltration operations only, its usefulness can further be enhanced by making it worthy for implementing in ultrafiltration and nanofiltration operations. The membranes can be coated by several methods such as thermal spray coating, hydrothermal coating, dip coating and so on, so as to fabricate a composite membrane with one or multiple numbers of active layer having reduced pore size spread over the support membrane. The membrane surface can also be charged by coating it with different oxide compounds such as Magnesium

oxide, Yttria etc., as these compounds are known to aid in electrostatic membrane separation. After carrying out any of these steps, the composite membranes can be used further for various other separation operations such as separation of virus from contaminated water, treatment of silk floss processing wastewater, treatment of pulp and paper mill wastewater, just to name a few.

- As pilot plant setups are considered to be quite useful in practically testing and validating a process technology before commercialization, therefore, the scale-up of this lab-scale setup to a pilot-scale one can be carried out before recommending it for use in industrial applications.
- With very few literatures available regarding physical, chemical as well as physico-chemical cleaning of membranes, most of the researchers carry out the membrane cleaning process in a trial-and-error manner. Therefore, there is a need for the development of a systematic approach of membrane cleaning and regeneration for each separation operation, considering the various aspects of membrane fouling. An optimized cleaning process is known to reduce the operational cost significantly. Therefore, as a part of further research work, optimization of cleaning processes for all the three aforementioned separation operations can be carried out.

References

Abdulhameed, M.A., Othman, M.H.D., Al Joda, H.N.A., Ismail, A.F., Matsuura, T., Harun, Z., Rahman, M.A., Puteh, M.J., Jaafar, J., 2017. Fabrication and characterization of affordable hydrophobic ceramic hollow fibre membrane for contacting processes, *Journal of Advanced Ceramics*. 6, 330-340.

Abdullayev, A., Bekheet, M.F., Hanaor, D.A., Gurlo, A., 2019. Materials and applications for low-cost ceramic membranes, *Membranes. 9*, 105.

Adam, M.R., Othman, M.H.D., Sheikh Abdul Kadir, S.H., Mohd Sokri, M.N., Tai, Z.S., Iwamoto, Y., Tanemura, M., Honda, S., Puteh, M.H., Rahman, M.A., Jaafar, J., 2020. Influence of the natural zeolite particle size toward the ammonia adsorption activity in ceramic hollow fiber membrane, *Membranes*. 10, 63.

Adams, E.F., 1971. Slip cast ceramics, in: Alper, A.M. (Ed.), *Refractory Glasses, Glass—Ceramics, and Ceramics.* Elsevier, Netherlands, 145-184.

Agarwal, A., Samanta, A., Nandi, B.K., Mandal, A., 2020. Synthesis, characterization and performance studies of kaolin-fly ash-based membranes for microfiltration of oily waste water, *Journal of Petroleum Science and Engineering.* 194, 107475.

Ahmaruzzaman, M., 2010. A review on the utilization of fly ash, *Progress in Energy and Combustion Science*. 36, 327-363.

Almandoz, M.C., Marchese, J., Prádanos, P., Palacio, L., Hernández, A., 2004. Preparation and characterization of non-supported microfiltration membranes from aluminosilicates, *Journal of membrane science*. *241*, 95-103.

Alves, M.J., Nascimento, S.M., Pereira, I.G., Martins, M.I., Cardoso, V.L., Reis, M., 2013. Biodiesel purification using micro and ultrafiltration membranes, *Renewable Energy*. 58, 15-20.

Alzahrani, S., Mohammad, A.W., 2014. Challenges and trends in membrane technology implementation for produced water treatment: A review, *Journal of Water Process*

Engineering, 4, 107-133.

American Coal Ash Association, 2003. Fly Ash Facts for Highway Engineers. https://www.fhwa.dot.gov/pavement/recycling/fach00.cfm. (Accessed May 25 2020).

APHA, 1998. Standard methods for the examination of water and wastewater, American Public Health Association, Washington DC.

Assam Power Distribution Company Limited, 2021. Know Your Tariff. https://www.apdcl.org/website/docs/acts_and_rules/know_your_tariff_2021_22.pdf (Accessed 04 April 2021).

ASTM D6751-20, 2020. Standard specification for biodiesel fuel blend stock (B100) for middle distillate fuels, ASTM International, West Conshohocken, PA.

Atadashi, I.M., Aroua, M.K., Aziz, A.A., 2011. Biodiesel separation and purification: A review, *Renewable Energy.* 36, 437-443.

Atadashi, I.M., Aroua, M.K., Aziz, A.A., Sulaiman, N.M.N., 2012. High quality biodiesel obtained through membrane technology, *Journal of Membrane Science*. 421, 154-164.

Atadashi, I.M., Aroua, M.K., Aziz, A.A., Sulaiman, N.M.N., 2015. Crude biodiesel refining using membrane ultra-filtration process: An environmentally benign process. *Egyptian Journal of Petroleum*. 24, 383-396.

Avci, A.K., Önsan, Z.I., 2018. Energy Materials, in: Dincer, I., *Comprehensive Energy Systems*, Elsevier, Netherlands.

Avula, R.Y., Nelson, H.M., Singh, R.K., 2009. Recycling of poultry process wastewater by ultrafiltration, *Innovative Food Science and Emerging Technologies*. 10, 1–8.

Baker, R., 2012. Membrane Technology and Applications, John Wiley & Sons Ltd., California.

Balaganesh, A.S., Sengodan, R., Ranjithkumar, R., Chandarshekar, B., 2018. Synthesis and characterization of porous calcium oxide nanoparticles (CaO NPS), *International Journal of Innovative Technology and Exploring Engineering.* 2, 2278–3075.

Bansod, P., Rathod, D., 2018. Polyacronitrile ultra filtration membranes used for separation of glycerol from transesterification process of biodiesel production, *Asian Journal of Nanosciences and Materials*. 1, 157-165.

Basitere, M., Rinquest, Z., Njoya, M., Sheldon, M.S., Ntwampe, S.K., 2017. Treatment of poultry slaughterhouse wastewater using a static granular bed reactor (SGBR) coupled with ultrafiltration (UF) membrane system, *Water Science and Technology*. 76, 106-114.

Behera, A., Mallick, P., Mohapatra, S.S., 2020. Nanocoatings for anticorrosion: An introduction, in: Rajendran, N., Nguyen, T.A., Kakooei, Saeid, Yeganeh, M., Li, X. (Eds.), *Corrosion Protection at the Nanoscale*, Elsevier, Netherlands, 227-243.

Bell, R.W., 1925. The effect of heat on the solubility of the calcium and phosphorus compounds in milk. *Journal of Biological Chemistry*. 64, 391-400.

Benito, J., Conesa, A., Rubio, F., Rodríguez, M.A., 2015. Preparation and characterization of tubular ceramic membranes for treatment of oil emulsions, *Journal of European Ceramic Society*. 25, 1895-1903.

Beolchini, F., Vegho, F., Barba, D., 2004. Microfiltration of bovine and ovine milk for the reduction of microbial content in a tubular membrane: a preliminary investigation, *Desalination.* 161, 251-258.

Berk, Z., 2009. Membrane processes, Academic Press, United States.

Bhar, B.K., 2008. Cost Accounting: Methods and Problems, Academic Publishers, Kolkata.

Białas, W., Stangierski, J., Konieczny, P., 2015. Protein and water recovery from poultry processing wastewater integrating microfiltration, ultrafiltration and vacuum membrane distillation, *International Journal of Environmental Science and Technology*. 12, 1875–1888.

Bondioli, P., Della Bella, L., 2005. An alternative spectrophotometric method for the determination of free glycerol in biodiesel. *European Journal of Lipid Science and Technology*. 107, 153-157.

Bose, S., Das, C., 2014. Role of binder and preparation pressure in tubular ceramic membrane processing: design and optimization study using response surface methodology (RSM), *Industrial and Engineering Chemistry Research*. 53, 12319-12329.

Bouazizi, A., Saja, S., Achiou, B., Ouammou, M., Calvo, J.I., Aaddane, A., Younssi, S.A., 2016. Elaboration and characterization of a new flat ceramic MF membrane made from natural Moroccan bentonite. Application to treatment of industrial wastewater, *Applied Clay Science*. 132, 33-40.

Boudreau, B.P., 1996. The diffusive tortuosity of fine-grained unlithified sediments, *Geochimica et Cosmochimica Acta*. 60, 3139-3142

Boussemghoune, M., Chikhi, M., Ozay, Y., Guler, P., Ozbey Unal, B.,Dizge, N., 2020. The investigation of organic binder effect on morphological structure of ceramic membrane support, *Symmetry*. 12, 770.

British Plastics and Rubber, 2020. Viscometer or Rheometer – which is best for me? https://www.britishplastics.co.uk/blogs/guest-blog/viscometer-or-rheometer-%E2%80%93-which-is-best-for-me/#:~:text=This%20means%20a%20viscometer%20can,even%20the%20tackiness%20of%20a (Accessed 02 April, 2021).

Brown, J., Sobsey, M.D., 2010. Microbiological effectiveness of locally produced ceramic filters for drinking water treatment in Cambodia, *Journal of Water and Health.* 8, 1–10.

Brown, P.J., 2001. Hollow fibre membranes for gas separation, in: Tao, X. (Ed.), *Smart Fibres, Fabrics and Clothing*, Woodhead Publishing, United Kingdom, 200-215.

Buetehorn, S., Carstensen, F., Wintgens, T., Melin, T., Volmering, D., Vossenkaul, K., 2010. Permeate flux decline in cross-flow microfiltration at constant pressure. *Desalination.* 250, 985-990.

Bunshah, R.F., 1994. Handbook of deposition technologies for films and coatings: science, technology, and applications, William Andrew, New York.

Cancino, B., Rossier, F., Orellana, C., 2006. Corn starch wastewater treatment with membrane technologies: pilot test, *Desalination.* 200, 750-751.

Cancino-Madariaga, B., Aguirre, J., 2011. Combination treatment of corn starch wastewater by sedimentation, microfiltration and reverse osmosis, *Desalination.* 279, 285-290.

Cao, J., Dong, X., Li, L., Dong, Y., Hampshire, S., 2014. Recycling of waste fly ash for production of porous mullite ceramic membrane supports with increased porosity, *Journal of European Ceramic Society*. 13, 3181-3194.

Capar, G., Aygun, S.S., Gecit, M.R., 2008. Treatment of silk production wastewaters by membrane processes for sericin recovery, *Journal of Membrane Science*. *325*, 920–931.

Černý, V., Tůmová, E., 2016. Effect of firing temperature on the structure of the aggregate from sintered ashes, *Procedia Engineering*. 151, 345–351.

Chakraborty, S., Das, C., Uppaluri, R., 2020. Feasibility of low-cost kaolin–based ceramic membranes for organic Lagernaria siceraria juice production. *Food and Bioprocess Technology*. 13, 1009-1023.

Chamberland, J., Mercier-Bouchard, D., Dussault-Chouinard, I., Benoit, S., Doyen, A., Britten, M., Pouliot, Y., 2019. On the use of Ultrafiltration or microfiltration polymeric spiral wound membranes for cheesemilk standardization: Impact of process efficiency. *Foods.* 8, 198.

Chang, E.E., Liang, C.H., Huang, C.P., Chiang, P.C., 2017. A simplified method for elucidating the effect of size exclusion on nanofiltration membranes. *Separation and*

Purification Technology. 85, 1-7.

Chen, M., Zhu, L., Dong, Y., Li, L., Liu, J., 2016. Waste-to-resource strategy to fabricate highly porous whisker-structured mullite ceramic membrane for simulated oil-in-water emulsion wastewater treatment, *ACS Sustainable Chemistry & Engineering*. 4, 2098-2106.

Cheryan, M., 1998. Ultrafiltration and microfiltration handbook, CRC press, Florida, United States.

Cho, K., Cho, Y.J., Shrivastava, D.K., Kapre, S.S., 1994. Acute lung disease after exposure to fly ash, *Chest*, 106, 309-311.

Choi, H., Zhang, K., Dionysiou, D.D., Oerther, D.B., Sorial, G.A., 2005. Influence of cross-flow velocity on membrane performance during filtration of biological suspension. *Journal of Membrane Science.* 248, 189-199.

Ciston, S., Lueptow, R.M., Gray, K.A., 2008. Bacterial attachment on reactive ceramic ultrafiltration membranes, *Journal of Membrane Science.* 320, 101–107.

Clasen, T.F., Brown, J., Collin, S., Suntura, O., Cairncross, S., 2004. Reducing diarrhea through the use of household-based ceramic water filters: a randomized, controlled trial in rural Bolivia, *The American Society of Tropical Medicine and Hygiene*. 70, 651–657.

Clasen, T.F., Garcia Parra, G., Boisson, S., Collin, S., 2005. Household-based ceramic water filters for the prevention of diarrhea: a randomized, controlled trial of a pilot program in Colombia, *The American Society of Tropical Medicine and Hygiene*. 73, 790-795.

Corgneau, M., Gaiani, C., Petit, J., Nikolova, Y., Banon, S., Ritié-Pertusa, L., Le, D.T.L., Scher, J., 2019. Digestibility of common native starches with reference to starch granule size, shape and surface features towards guidelines for starch-containing food products. *International Journal of Food Science & Technology.* 54, 2132-2140.

Coskun, T., Debik, E., Kabuk, H.A., Demir, N.M., Basturk, I., Yildirim, B., Temizel, D., Kucuk, S., 2016. Treatment of poultry slaughterhouse wastewater using a membrane process, water reuse, and economic analysis, *Desalination and Water Treatment*. 57, 4944-4951.

Creighton, J.R., Ho, P., 2001. Introduction to chemical vapor deposition (CVD), Chemical vapor deposition, ASM International, Ohio, 1-22.

Cui, Z., 2016. Co-sintering Method for Ceramic Membrane Preparation, in: Drioli, E., Giorno, L., (Eds.), *Encyclopedia of Membranes*, Springer-Verlag Berlin Heidelberg, Berlin, 473-474.

Cui, Z.F., Jiang, Y., Field, R.W., 2010. Fundamentals of pressure-driven membrane separation processes, in: Cui, Z.F., Muralidhara, H.S. (Eds.), *Membrane technology*. Butterworth-Heinemann, United Kingdom, 1-18.

Das, N., 1999. Ceramic membrane for microfiltration application by tape casting technique, University of Calcutta, PhD dissertation.

Daufin, G., Escudier, J.P., Carrère, H., Bérot, S., Fillaudeau, L., Decloux, M., 2001. Recent and emerging applications of membrane processes in the food and dairy industry, *Food and Bioproducts Processing*, 79, 89-102.

Derlet, P.M., 2017. Sintering theory. Paul Scherrer Institut. 11.

Dhadse, S., Kumari, P., Bhagia, L.J., 2008. Fly ash characterization, utilization and Government initiatives in India: A review. *Journal of Scientific and Industrial Research*, 11-18.

Diana, S., Fauzan, R., Arahman, N., Razi, F., Bilad, M.R., 2020. Synthesis and characterization of ceramic membrane from fly ash and clay prepared by sintering method at low temperature, *RASĀYAN Journal of Chemistry*. 13, 1335-1341.

Diana, S., Fauzan, R., Elfiana, E., 2019. Removing *Escherichia Coli* bacteria in river water using ceramic membrane from mixed clay and fly ash material, *IOP Conference Series: Materials Science and Engineering.* 536, 012089.

Dickey, D.S., 2015. Tackling difficult mixing problems, *American Institute of Chemical Engineers.* 35-42.

Díez, B., Rosal, R., 2020. A critical review of membrane modification techniques for fouling and biofouling control in pressure-driven membrane processes, *Nanotechnology for Environmental Engineering*. 5, 1-21.

Dong, Y., Hampshire, S., Zhou, J. E., Lin, B., Ji, Z., Zhang, X., Meng, G., 2010. Recycling of fly ash for preparing porous mullite membrane supports with titania addition, *Journal of Hazardous Materials*. 180, 173-180.

Elhadidy, A.M., Peldszus, S., Van Dyke, M.I., 2013. An evaluation of virus removal mechanisms by ultrafiltration membranes using MS2 and φx174 bacteriophage, *Separation and Purification Technology*. 120, 215–223.

Emani, S., Uppaluri, R., Purkait, M.K., 2014. Cross flow microfiltration of oil–water emulsions using kaolin based low cost ceramic membranes, *Desalination, 341*, 61-71.

EN 14214, 2012. The pure biodiesel standard, European Committee of Standardization, Europe.

Fabiani, C., Pizzichini, M., Spadoni, M., Zeddita, G., 1996. Treatment of waste water from silk degumming processes for protein recovery and water reuse. *Desalination.* 105, 1–9.

Falamaki, C., Naimi, M., Aghaie, A., 2004. Dual behavior of $CaCO_3$ as a porosifier and sintering aid in the manufacture of alumina membrane/catalyst supports, *Journal of European Ceramic Society*. 24, 3195.

Falamaki, C., Naimi, M., Aghaie, A., 2006. Dip-coating technique for the manufacture of alumina microfilters using PVA and Na-CMC as binders: a comparative study, *Journal*

of European Ceramic Society. 26, 949–956.

Fan, P., Zhen, K., Zan, Z., Chao, Z., Jian, Z., Yun, Y., 2016. Preparation and development of porous ceramic membrane supports fabricated by extrusion technique, *Chemical Engineering Transactions*. 55, 277-282.

Fane, A.T., Wang, R., Jia, Y., 2011. Membrane technology: past, present and future, in: Wang, L.K., Chen, J.P., Hung, Y., Shammas, N.K. (Eds.), *Membrane and Desalination Technologies*. Humana Press, Totowa, 1-45.

Fang, J., Qin, G., Wei, W., Zhao, X., 2011. Preparation and characterization of tubular supported ceramic microfiltration membranes from fly ash, *Separation and Purification Technology*. 80, 585-591.

Fang, J., Qin, G., Wei, W., Zhao, X., Jiang, L., 2013. Elaboration of new ceramic membrane from spherical fly ash for microfiltration of rigid particle suspension and oil-in-water emulsion, *Desalination*. 311, 113-126.

Farrah, S.R., 1982. Chemical factors influencing adsorption of bacteriophage MS2, *Applied and Environmental Microbiology*. 43, 659–663.

Fatimah, I., Sahroni, I., Putra, H.P., Nugraha, M.R., Hasanah, U.A., 2015. Ceramic membrane based on TiO_2-modified kaolinite as a low cost material for water filtration, *Applied Clay Science, 118*, 207-211.

Ferna´ndez, L., Blanco, S.A´., Rodríguez, F.A.R., 2013. Review: Microfiltration applied to dairy streams: removal of bacteria, *Journal of the Science of Food and Agriculture*. 93, 187–196.

Fernández García, L., Rodríguez, F.A.R., 2015. Microfiltration of milk with third generation ceramic membranes, *Chemical Engineering Communications*. 202, 1455–1462.

Food and Agriculture Organization of the United Nations, 1992. Cost control in forest harvesting and road construction.

http://www.fao.org/3/T0579E/t0579e00.htm#Contents (Accessed 04 April, 2021).

Food and Agriculture Organization of the United Nations, 2020. Gateway to dairy production and products. http://www.fao.org/dairy-production-products/production/en/#:~:text=In%20the%20last%20three%20decades,%2C%20China%2C%20Pakistan%20and%20Brazil. (Accessed 30 November, 2020).

France, T.C., Bot, F., Kelly, A.L., Crowley, S.V., O'Mahony, J.A., 2010. The influence of temperature on filtration performance and fouling during cold microfiltration of skim milk, *Separation and Purification Technology*. 262, 118256.

Francis, L.F., 2016. Materials Processing: A Unified Approach to Processing of Metals, Ceramics and Polymers, Academic Press, United States.

Freedman, B.E.H.P., Pryde, E.H., Mounts, T.L., 1985. Variables affecting the yields of fatty esters from transesterified vegetable oils. *Journal of the American Oil Chemists' Society*. 61, 1638-1643.

Fritsch, J., Beliciu, C., Moraru, C.I., 2005. Microbial retention and membrane fouling during low temperature microfiltration of skim milk using ceramic membranes, *Ninth Topical Conference on Food Engineering*. 182-190.

Gadow, R., Kern, F., 2014. Ceramics, in: Mari, D., Miguel, L., Nebel, C.E. (Eds.), *Comprehensive hard materials*, Newnes, United Kingdom, 207-230.

Gall, M., Mariñas, B.J., Lu, Y., Shisler, J.L., 2015. Waterborne viruses: a barrier to safe drinking water, *PLoS Pathogens*. 11, e1004867.

Gamage, N., Liyanage, K., Fragomeni, S., Setunge, S., 2011. Overview of different types of fly ash and their use as a building and construction material. http://dl.lib.mrt.ac.lk/bitstream/handle/123/9367/SEC-11-35.pdf;sequence=1.

Gander, M.A., Jefferson, B., Judd, S.J., 2000. Membrane bioreactors for use in small wastewater treatment plants: Membrane materials and effluent quality, *Water Science*

and Technology. 41, 205–211.

GeÂsan-Guiziou, G., 2010. Removal of bacteria, spores and somatic cells from milk by centrifugation and microfiltration techniques, in: M. Griffiths (Ed.), *Improving the safety and quality of milk.* Woodhead Publishing, United Kingdom, 349-372.

Gerpen, V.G., Shanks, B., Pruszko, R., Clements, D., Knothe, G., 2004. Biodiesel production technology. *National Renewable Energy Laboratory*. 1-110.

Ghodrat, M., Rhamdhani, M.A., Brooks, G., Masood, S., Corder, G., 2016. Techno economic analysis of electronic waste processing through black copper smelting route, *Journal of Cleaner Production*. 126, 178-190.

Giwa, A., Ogunribido, A. (2012). The applications of membrane operations in the textile industry: a review. *Current Journal of Applied Science and Technology*, 296-310.

Gomes, M.C.S., Arroyo, P.A., Pereira, N.C., 2011. Biodiesel production from degummed soybean oil and glycerol removal using ceramic membrane, *Journal of Membrane Science*. 378, 453-461.

Gomes, M.C.S., Arroyo, P.A., Pereira, N.C., 2013. Influence of acidified water addition on the biodiesel and glycerol separation through membrane technology, *Journal of Membrane Science*. 431, 28-36.

Gomes, M.C.S., Arroyo, P.A., Pereira, N.C., 2015. Influence of oil quality on biodiesel purification by ultrafiltration, *Journal of membrane science*. *496*, 242-249.

Gomes, M.C.S., Pereira, N.C., de Barros, S.T.D., 2010. Separation of biodiesel and glycerol using ceramic membranes, *Journal of Membrane Science. 352*, 271-276.

Gray, J.R., Gylsson, G.D., Turcios, L.M., Schwarz, G.E., 2000. Comparability of Suspended-Sediment Concentration and Total Suspended Solids Data, US Geological Survey, Reston.

Gray, M.L., Killinger, A.H., 1996. Listeria monocytogenes and listeric infections, *Bacteriological Reviews*. 30, 309–382.

Griep, E.R., Cheng, Y., Moraru, C.I., 2018. Efficient removal of spores from skim milk using cold microfiltration: Spore size and surface property considerations, *Journal of Dairy Science*. 101, 9703-9713.

Gupta, V., Anandkumar, J., 2018. Protein Separation Using Fly-ash Microfiltration Ceramic Membrane, *CSVTU International Journal of Biotechnology, Bioinformatics and Biomedical*. 3, 17-25.

Gupta, V., Anandkumar, J., 2019. Synthesis of crosslinked PVA-ceramic composite membrane for phenol removal from aqueous solution, *Journal of the Serbian Chemical Society*. 84, 211-224.

Gupta, V., Raja, C., Anandkumar, J., 2020. Phenol Removal by Novel Choline Chloride Blended Cellulose Acetate-Fly Ash Composite Membrane, *Periodica Polytechnica Chemical Engineering*. 64, 116-123.

Gwak, G., Hong, S., 2018. Draw solute selection, in: Sarp, S., Hilal, N. (Eds.), *Membrane-Based Salinity Gradient Processes for Water Treatment and Power Generation*. Elsevier, Amsterdam, 87-122.

Harlacher, T., Wessling, M., 2015. Gas–gas separation by membranes, in: Tarleton, S. (Ed.), *Progress in Filtration and Separation.* Academic Press, United States, 557-584.

Hegel, C., Jones, C.A., Cabrera, F.A., Yañez, M.J., Bucala, V., 2014. Particle size characterization: Comparison of laser difraction (LD) and scanning electron microscopy (SEM). *Acta Microscopica*. 23, 11–7.

Hinková, A., Bubník, Z., Pour, V., Henke, S., Kadlec, P., 2005. Application of cross-flow ultrafiltration on inorganic membranes in purification of food materials, *Czech Journal of Food Sciences*. 23, 103-110.

Hoffmann, W., Kiesner, C., Clawinrädecker, I., Martin, D., Einhoff, K., Lorenzen, P.C., Meisel, H., Hammer, P., Suhren GTeufel, P., 2006. Processing of extended shelf life milk using microfiltration, *International Journal of Dairy Technology*. 59, 229-235.

Hofs, B., Ogier, J., Vries, D., Beerendonk, E.F., Cornelissen, E.R., 2011. Comparison of ceramic and polymeric membrane permeability and fouling using surface water, *Separation and Purification Technology*. 79, 365-374.

Holm, S., Malmberg, R., Svensson, K., 1989. *Method for producing milk with a lowered bacterial content*, Patent 4,876,100, Washington, DC: U.S. Patent and Trademark Office

Hong, S., Faibish, R.S., Elimelech, M., 1997. Kinetics of permeate flux decline in crossflow membrane filtration of colloidal suspensions. *Journal of Colloid and Interface Science*. 196, 267-277.

Huang, H., Young, T.A., Schwab, K.J., Jacangelo, J.G., 2012. Mechanisms of virus removal from secondary wastewater effluent by low pressure membrane filtration, *Journal of Membrane Science*. 409–410, 1–8.

Huang, S.C., Huang, C.T., Lu, S.Y., Chou, K.S., 1999. Ceramic/polyaniline composite porous membranes, *Journal of Porous Materials*. 6, 153-159.

Huisman, I.H., 2000. MEMBRANE SEPARATIONS | Microfiltration, in: Wilson, I.D. (Ed.), *Encyclopedia of Separation Science*. Academic Press, United States, 1764-1777.

Hwang, K.J., Liao, C.Y., Tung, K.L., 2008. Effect of membrane pore size on the particle fouling in membrane filtration, *Desalination*. 234, 16-23.

Hwang, S.J., Chang, D.J., Chen, C.H., 1996. Steady State permeate flux for particle cross-flow filtration. *The Chemical Engineering Journal and the Biochemical Engineering Journal*. 61, 171-178.

Ibrahim, S.S., Shahien, M.G., Seliem, A.Q., Abukhadra, M.R., Zayed, A.M., 2015. Marwit Rod El Leqah quartz deposits as a strategic source of high purity quartz, *Journal of Geoscience and Environment Protection*, 3, 41.

Ikonić, B.B., Zavargo, Z.Z., Jokić, A.I., Šereš, Z.I., Vatai, G.N., Peruničić, M.B., 2011. Microfiltration of wheat starch suspensions using multichannel ceramic membrane, *Hemijska industrija*, 65,131-138.

Jain, S.P., Narang, K.L., 2015. Cost Accounting, Kalyani Publications.

Jana, S., Purkait, M.K., Mohanty, K., 2010. Preparation and characterization of low-cost ceramic microfiltration membranes for the removal of chromate from aqueous solutions, *Applied Clay Science.* 47, 317-324.

Jedidi, I., Khemakhem, S., Saïdi, S., Larbot, A., Amar, R.B., 2009. Elaboration and characterisation of fly ash based mineral supports for microfiltration and ultrafiltration membranes, *Ceramics International*. 35, 2747-2753.

Jedidi, I., Khemakhem, S., Saïdi, S., Larbot, A., Elloumi-Ammar, N., Fourati, A., Charfi, A., Salah, A., Amar, R.B., 2011. Preparation of a new ceramic microfiltration membrane from mineral coal fly ash: Application to the treatment of the textile dying effluents, *Powder Technology*. 208, 427-432.

Jonsson, G., Guerra, A., Edelsten, D., Rasmussen, A., Waagner Nielsen, E., 1997. Low cross-flow velocity microfiltration of skim milk for removal of bacterial spores, *International Dairy Journal*. 7, 849–861.

Jung, S.Y., Ahn, K.H., 2019. Transport and deposition of colloidal particles on a patterned membrane surface: Effect of cross-flow velocity and the size ratio of particle to surface pattern. *Journal of Membrane Science.* 572, 309-319.

Kamara, S., Wang, W., Ai, C., 2020. Fabrication of Refractory Materials from Coal Fly Ash, Commercially Purified Kaolin, and Alumina Powders, *Materials*. *13*, 3406.

Kamoun, N., Hajjeji, W., Abid, R., Rodríguez, M.A., Jamoussi, F., 2020. Elaboration and properties of low-cost ceramic microfiltration membrane from local Tunisian clay for wastewater treatment, *Cerâmica*, *66*, 386-393.

Kaniganti, C.M., Emani, S., Thorat, P., Uppaluri, R., 2014. Microfiltration of synthetic bacteria solution using low cost ceramic membranes, *Separation Science and Technology*. 50, 121–135.

Kao, T., Cheng, C., Huang, C., Chen, J., 2015. Using coaxial electrospinning to fabricate core/shell-structured polyacrylonitrile-polybenzoxazine fibers as nonfouling membranes, RSC Advances. 5, 58760-58771.

Kaur, H., Bulasara, V.K., Gupta, R.K., 2016. Preparation of kaolin-based low-cost porous ceramic supports using different amounts of carbonates, *Desalination and Water Treatment.* 57, 15154-15163.

Kaur, H., Bulasara, V.K., Gupta, R.K., 2016. Preparation of kaolin-based low-cost porous ceramic supports using different amounts of carbonates. *Desalination and Water Treatment.* 57, 15154-15163.

Khemakhem, S., Larbot, A., Amar, R.B., 2009. New ceramic microfiltration membranes from Tunisian natural materials: application for the cuttlefish effluents treatment, *Ceramics International*, *35*, 55-61.

Kiss, A.A., Dimian, A.C., Rothenberg, G., 2006. Solid acid catalysts for biodiesel production-Towards sustainable energy, *Advanced Synthesis & Catalysis*. 348, 75-81.

Koltuniewicz, A.B., Field, R.W., Arnot, T.C., 1995. Cross-flow and dead-end microfiltration of oily-water emulsion. Part I: Experimental study and analysis of flux decline. *Journal of Membrane Science.* 102, 193-207.

Koros, W.J., Ma, Y.H., Shimidzu, T., 1996. Terminology for membranes and membrane processes (IUPAC Recommendations 1996), *Pure and Applied Chemistry*, *68*, 1479-1489.

Kouras, N., Harabi, A., Bouzerara, F., Foughali, L., Policicchio, A., Stelitano, S., Galiano F., Figoli, A., 2017. Macro-porous ceramic supports for membranes prepared from quartz sand and calcite mixtures, *Journal of European Ceramic Society*. 37, 3159–3165.

Krawczyk, H., Jönsson, A.S., 2014. The influence of feed flow channel diameter on frictional pressure drop, membrane performance and process cost in full-scale tubular ceramic membranes, *Chemical Engineering Research and Design*. 92, 174-180.

Kroll, S., de Moura, M.O.C., Meder, F., Grathwohl, G., Rezwan, K., 2012a. High virus retention mediated by zirconia microtubes with tailored porosity, *Journal of European Ceramic Society*. 32, 4111–4120.

Kroll, S., Brandes, C., Wehling, J., Treccani, L., Grathwohl, G., Rezwan, K., 2012b. Highly efficient enzyme-functionalized porous zirconia microtubes for bacteria filtration, *Environmental Science & Technology*. 46, 8739–8747.

Kroll, S., Treccani, L., Rezwan, K., Grathwohl, G., 2012c. Development and characterisation of functionalised ceramic microtubes for bacteria filtration, *Journal of Membrane Science*. 365, 447–455.

Kumar, P., Sharma, N., Ranjan, R., Kumar, S., Bhat, Z.F., Jeong, D.K., 2013. Perspective of membrane technology in dairy industry: A review, *Asian-Australasian Journal of Animal Sciences*. 26, 1347-1358.

Kumar, R., Bhakta, P., Chakraborty, S., Pal, P., 2011. Separating cyanide from coke wastewater by cross flow nanofiltration. *Separation Science and Technology*. 46, 2119-2127.

Kumar, R., Ghosh, A.K., Pal, P., 2020. Sustainable production of biofuels through membrane-integrated systems, *Separation and Purification Reviews*, 49, 207-228.

Kumar, R.V., Basumatary, A.K., Ghoshal, A.K., Pugazhenthi, G., 2015a. Performance assessment of an analcime-C zeolite–ceramic composite membrane by removal of Cr (VI) from aqueous solution, *RSC Advances*. 5, 6246–6254.

Kumar, R.V., Ghoshal, A.K., Pugazhenthi, G., 2015b. Elaboration of novel tubular ceramic membrane from inexpensive raw materials by extrusion method and its performance in microfiltration of synthetic oily wastewater treatment, *Journal of Membrane Science.* 490, 92-102.

Kumar, R.V., Ghoshal, A.K., Pugazhenthi, G., 2015c. Fabrication of zirconia composite membrane by in-situ hydrothermal technique and its application in separation of methyl orange, *Ecotoxicology and Environmental Safety*. 121, 73-79.

Kumar, R.V., Goswami, L., Pakshirajan, K., Pugazhenthi, G., 2016. Dairy wastewater treatment using a novel low cost tubular ceramic membrane and membrane fouling mechanism using pore blocking models, *Journal of Water Process Engineering.* 13, 168-175.

Kurtz, J.R., Goggins, J.A., McLachlan, J.B., 2017. Salmonella infection: Interplay between the bacteria and host immune system, *Immunology Letters.* 190, 42-50.

Lang, H.J., 1947. Cost relationships in preliminary cost estimation, *Chemical Engineering.* 54, 27.

Längauer, D., Čablík, V., Hredzák, S., Zubrik, A., Matik, M., Danková, Z., 2021. Preparation of Synthetic Zeolites from Coal Fly Ash by Hydrothermal Synthesis, *Materials*. 14, 1267.

Lemoisson, F., Froyen, L., 2005. Understanding and improving powder metallurgical processes, in: Seetharaman, S. (Ed.), *Fundamentals of Metallurgy*, Woodhead Publishing, United Kingdom, 471-502.

Li, H., Shi, W., Wang, W., Zhu, H., 2015. The extraction of sericin protein from silk reeling wastewater by hollow fiber nanofiltration membrane integrated process, *Separation and Purification Technology*. *146*, 342–350.

Liang, S., Lin, H., Habteselassie, M., Huang, Q., 2018. Electrochemical inactivation of bacteria with a titanium sub-oxide reactive membrane, *Water Research.* 145, 172–180.

Ling-Chee, S.S., Carvajal-Zarrabal, O., Nolasco-Hipólito, C., Abdullah, M.O., Shoji, E., Aguilar-Uscanga, M.G., Gregory, Z.A., Samawi, S., 2019. Separation of sago starch from model suspensions by tangential flow filtration, *Chemical Engineering Communications.* 206, 1058-1071.

Liu, D.M., 1997. Influence of porosity and pore size on the compressive strength of porous hydroxyapatite ceramic, *Ceramics International*. 23, 135-139.

Liu, Y., Duan, D., Li, Y., 2019. Binders and the bonding mechanism of fly ash and coke pelletization, *International Journal of Coal Preparation and Utilization*. 39, 159-168.

Lo, Y.M., Cao, D., Argin-Soysal, S., Wang, J., Hahm, T.S., 2015. Recovery of protein from poultry processing wastewater using membrane ultrafiltration, *Bioresource Technology*. 96, 687-698.

Lončarević, D., Čupić, Ž., 2019. The perspective of using nanocatalysts in the environmental requirements and energy needs of industry, in: Thomas, S., Grohen, Y., Pottathara, Y.B. (Eds.), *Industrial Applications of Nanomaterials*, Elsevier, Netherlands, 91-122.

Madaeni, S.S., Fane, A.G., Grohmann, G.S., 1995. Virus removal from water and wastewater using membranes, *Journal of Membrane Science.* 102, 65–75.

Madaeni, S.S., Yasemi, M., 2009. Milk sterilization using membranes, *Journal of Food Process Engineering*. 34, 1071-1085.

Madec, M.N., Mejean, S., Maubois, J.L., 1992. Retention of Listeria and Salmonella cells contaminating skim milk by tangential membrane microfiltration ("Bactocatch"

process), *Dairy Science Technology*. 72, 327-332.

Majouli, A., Tahiri, S., Younssi, S.A., Loukili, H., Albizane, A., 2012. Elaboration of new tubular ceramic membrane from local Moroccan Perlite for microfiltration process. Application to treatment of industrial wastewaters, *Ceramics International*, *38*, 4295-4303.

Malik, N., Bulasara, V.K., Basu, S., 2020. Preparation of novel porous ceramic microfiltration membranes from fly ash, kaolin and dolomite mixtures, *Ceramics International*. 46, 6889-6898.

Malmali, M., Askegaard, J., Sardari, K., Eswaranandam, S., 2018. Evaluation of ultrafiltration membranes for treating poultry processing wastewater, *Journal of Water Process Engineering*. 22, 218–226.

Manzolini, G., Jansen, D., 2013. Economic analysis of systems for electrical energy and hydrogen production: fundamentals and application to two membrane reactor processes, in: Basile, A. (Ed.), *Handbook of Membrane Reactors: Reactor Types and Industrial Applications*. Woodhead Publishing, United Kingdom, 528-550.

Martens, B.M., Gerrits, W.J., Bruininx, E.M., Schols, H.A., 2018. Amylopectin structure and crystallinity explains variation in digestion kinetics of starches across botanic sources in an in vitro pig model. *Journal of Animal Science and Biotechnology*. 9, 1-13.

Martín, M.M., 2016. Industrial Chemical Process Analysis and Design, Elsevier, Amsterdam.

McCutcheon, J. R., McGinnis, R. L., Elimelech, M., 2005. A novel ammonia—carbon dioxide forward (direct) osmosis desalination process, *Desalination*. 174, 1-11.

Michen, B., Fritsch, J., Aneziris, C., Graule, T., 2013. Improved virus removal in ceramic depth filters modified with MgO, *Environmental Science & Technology*. 47, 1526–1533.

Mishra, V.K., Goswami, R., 2018. A review of production, properties and advantages of biodiesel, *Biofuels.* 9, 273-289.

Mohammadzadeh, A., Zadeh, S.K.N., Saidi, M.H., Sharifzadeh, M., 2020. Mechanical engineering of solid oxide fuel cell systems: geometric design, mechanical configuration, and thermal analysis, in: Sharifzadeh, M. (Ed.), *Design and Operation of Solid Oxide Fuel Cells*, Academic Press, United States, 85-130.

Monash, P., 2011. Development and characterization of low cost ceramic membrane for liquid phase separation applications. Indian Institute of Technology, PhD Dissertation.

Monash, P., Pugazhenthi, G., Saravanan, P., 2013. Various fabrication methods of porous ceramic supports for membrane applications, *Reviews in Chemical Engineering.* 29, 357-383.

Mouiya, M., Abourriche, A., Bouazizi, A., Benhammou, A., El Hafiane, Y., Abouliatim, Y., Nibou, L., Oumam, M., Ouammou, M., Smith, A., Hannache, H., 2018. Flat ceramic microfiltration membrane based on natural clay and Moroccan phosphate for desalination and industrial wastewater treatment, *Desalination*, *427*, 42-50.

Mulder, M., 1996. Basic principles of membrane technology, Kluwer Academic Publishers, London.

Muntha, S.T., Kausar, A., Siddiq, M., 2016. Progress in applications of polymer-based membranes in gas separation technology, *Polymer-Plastics Technology and Engineering.* 55, 1282-1298.

Nandi, B.K., Uppaluri, R., Purkait, M.K., 2008. Preparation and characterization of low-cost ceramic membranes for micro-filtration applications, *Applied Clay Science.* 42, 102–110.

Nogueira, A.B., Wyllerson, E.G., Sartori, D.S., Mendes, R.K., Etchegaray, A., 2019. Determination of free glycerol in biodiesel using uv-visible spectroscopy: A validation study. *Revista Virtual de Química*. 11.

Norliza, I., Murthy, V., Teng, W.D., 2009. Ceramic membrane fabrication from industrial waste: Effect of particle size distribution on the porosity. *Journal of Applied Sciences, 9*, 3136-3140.

Olesen, N., Jensen, F., 1989. Microfiltration. The influence of operation parameters on the process, *Milchwissenschaft.* 44, 476–479.

Owa, F.W., 2014. Water pollution: sources, effects, control and management, *International Letters of Natural Sciences*. 3, 1–6.

Oyanedel-Craver, V.A., Smith, J.A., 2008. Sustainable colloidal-silver-impregnated ceramic filter for point-of-use water treatment, *Environmental Science & Technology*. 42, 927–933.

Padaki, M., Murali, R.S., Abdullah, M.S., Misdan, N., Moslehyani, A., Kassim, M. A., Hilal, N., Ismail, A.F., 2015. Membrane technology enhancement in oil–water separation. A review, *Desalination*, 357, 197-207.

Pafylias, I., Cheryan, M., Mehaia, M.A., Saglam, N., 1996. Microfiltration of milk with ceramic membranes, *Food Research International*. 29, 141–146.

Park, S.H., Park, Y.G., Lim, J.L., Kim, S., 2015. Evaluation of ceramic membrane applications for water treatment plants with a life cycle cost analysis, *Desalination and Water Treatment*. 54, 973-979.

Peters, M.S., Timmerhaus, K.D., 1991. Plant design and economics for Chemical Engineers, McGraw-Hill, New York.

Pfaffinger, M., Mitteramskogler, G., Gmeiner, R., Stampfl, J., 2015. Thermal debinding of ceramic-filled photopolymers, *Materials Science Forum.* 825, 75-81.

Pirooz, M., Akbari, N., Kamali, M., Biria, D., 2018. Investigation of the control of the fat, oil and grease in sewer lines and their removal by surfactant treatment. *Advances in Environmental Technology*. 4, 155-161.

Purnima, M., Manikandan, N.A., Pakshirajan, K., Pugazhenthi, G., 2020. Recovery of microalgae from its broth solution using kaolin based tubular ceramic membranes prepared with different binders. *Separation and Purification Technology.* 250, 117212.

Qin, G., He, J., Wei, W., 2016. Ultrafiltration carbon membranes from organic sol-gel process, *Chemical Engineering Communications*. 203, 381-388.

Qin, G., Lü, X., Wei, W., Li, J., Cui, R., Hu, S., 2015. Microfiltration of kiwifruit juice and fouling mechanism using fly-ash-based ceramic membranes, *Food and Bioproducts Processing*. 96, 278-284.

Rahayu, S.S., Mindaryani, A., 2007. Optimization of biodiesel washing by water extraction, *Proceedings of the World Congress on Engineering and Computer Science.* 24-26.

Rahman, M.A., Halfar, J., Shinjo, R., 2013. X-Ray Diffraction Is a Promising Tool to Characterize Coral Skeletons, *Advances in Materials Physics and Chemistry,* 03, 120–125. https://doi.org/10.4236/ampc.2013.31a015

Raman, A.A.A., Tan, H.W., Buthiyappan, A., 2019. Two-step purification of glycerol as a value added by product from the biodiesel production process, *Frontiers in Chemistry.* 7, 774.

Rawat, M., Bulasara, V.K., 2018. Synthesis and characterization of low-cost ceramic membranes from fly ash and kaolin for humic acid separation, *Korean Journal of Chemical Engineering*. 35, 725-733.

Reddy, K.A., 2015. Methods and materials characterization of sodium carboxymethyl cellulose, *International Journal of Advanced Research Foundation*. 2, 23-26.

Ren, L., Yu, S., Li, J., Li, L., 2019. Pilot study on the effects of operating parameters on membrane fouling during ultrafiltration of alkali/surfactant/polymer flooding wastewater: optimization and modelling. *RSC advances.* 9, 11111-11122.

Richardson, D.B., Blanzymski, T.Z., Gregory, E.N., Hutchinson, A.R., Wyatt, L.M., 1994. Manufacturing methods, in: Smith, E.H. (Ed.), *Mechanical Engineer's Reference Book*, Butterworth Heinemann, United Kingdom, 16-1-16-112.

Richardson, J.F., 1990. Separation processes, *Gas Separation & Purification*, *4*, 2-7.

Rocha, M.R., Virginie, M., Khodakov, A., Pollo, L.D., Marcílio, N.R., Tessaro, I.C., 2020. Preparation of alumina based tubular asymmetric membranes incorporated with coal fly ash by centrifugal casting, *Ceramics International*. 47, 4187-4196.

Rodrigues, S., Fernandes, F.A.N., 2012. Advances in fruit processing technologies, CRC Press, United States.

RRUFF Database: Raman, X-ray, Infrared, and Chemistry, Cristobalite R060648. http://rruff.info/cristobalite/R060648 (Accessed June 10 2019).

Saboya, L.V., Maubois, J., 2000. Current developments of microfiltration technology in the dairy industry, *Lait.* 80, 541-553.

Saleh, J., Tremblay, A.Y., Dube, M.A., 2010. Glycerol removal from biodiesel using membrane separation technology, *Fuel.* 89, 2260-2266.

Salsali, H., McBean, E., Brunsting, J., 2011. Virus removal efficiency of Cambodian ceramic pot water purifiers, *Journal of Water and Health*. 9, 306–311.

Samaei, S.M., Gato-Trinidad, S., Altaee, A., 2018. The application of pressure-driven ceramic membrane technology for the treatment of industrial wastewaters–A review, *Separation and Purification Technology*, 200, 198-220.

Sardari, K., Askegaard, J., Chiao, Y.H., Darvishmanesh, S., Kamaz, M., Wickramasinghe, S.R., 2018. Electrocoagulation followed by ultrafiltration for treating poultry processing wastewater, *Journal of Environmental Chemical Engineering*. 6, 4937–4944.

Sargolzaei, J., Moghaddam, A.H., Shayegan, J., 2011. Statistical assessment of starch removal from starchy wastewater using membrane technology, *Korean Journal of Chemical Engineering*. 28, 1889-1896.

Saxena, S., Choudhary, M.P., 2017. Performance Evaluation of Dairy Wastewater Treatment Plant. I*nternational Research Journal of Engineering and Technology*. 4, 1287-1291.

Saxena, S.K., Boersma, L., Lindstrom, F.T., Young, J., 1974. Effect of pore size on diffusion coefficients in porous media, *Soil Science*. 117, 80-86.

Scott, K., Hughes, R., 1996. Introduction to industrial membrane processes, in: Scott, K., Hughes, R. (Eds.), *Industrial membrane separation technology*. Springer Science & Business Media, Germany, 1-7.

Seidel, A., Elimelech, M., 2002. Coupling between chemical and physical interactions in natural organic matter (NOM) fouling of nanofiltration membranes: implications for fouling control. *Journal of Membrane Science.* 203, 245-255.

Shih, J. C. H., Kozink, M.B., 1980. Ultrafiltration treatment of poultry processing wastewater and recovery of a nutritional by-product, *Poultry Science Journal*. 59, 247-252.

Shubhaneel, N., Apurba, D., Kumar, C.P., 2018. Corn starch industry wastewater pollution and treatment processes-A review, *Journal of Biodiversity and Environmental Sciences.* 12, 283-293.

Shukla, R., Tandon, R., Nguyen, M., Cheryan, M., 2000. Microfiltration of starch suspensions using a tubular stainless steel membrane, *Membrane Technology*. 120, 5-8.

Sikora, M., Izak, P., 2006. Starch and its derivatives in ceramic processing. *Ceramika*. 93, 1-16.

Simão, L., Caldato, R.F., Innocentini, M.D.M., Montedo, O.R.K., 2015. Permeability of porous ceramic based on calcium carbonate as pore generating agent, *Ceramics International*. 41, 4782-4788.

Sinaki, N.Y., Scanlon, M.G., 2016. Flow Behavior of Native Corn and Potato Starch Granules in Aqueous Suspensions. *Food Biophysics.* 11, 345-353.

Singh, G., Bulasara, V.K., 2013. Preparation of low-cost microfiltration membranes from fly ash, *Desalination and Water Treatment*. 53, 1204-1212.

Singh, G.B., Subramaniam, K.V., 2018. Characterization of Indian fly ashes using different experimental techniques. *The Indian Concrete Journal*. *92*, 10-23.

Singh, N., Cheryan, M., 1998. Process Design and Economic Analysis of a Ceramic Membrane System for Microfiltration of Corn Starch Hydrolysate, *Journal of Food Engineering*. 38, 57-67.

Sinha, M.K., Purkait, M.K., 2013. Increase in hydrophilicity of polysulfone membrane using polyethylene glycol methyl ether, *Journal of Membrane Science*. 437, 7-16.

Som, S., Longman, D.E., Ramírez, A.I., Aggarwal, S.K., 2010. A comparison of injector flow and spray characteristics of biodiesel with petrodiesel, *Fuel*. 89, 4014-4024.

Suchecka, T., Biernacka, E., Piatkiewicz, W., 2003. Microorganism retention on microfiltration membranes, *Filtration & Separation.* 40, 50–55.

Suresh, K., Pugazhenthi, G., 2016. Development of ceramic membranes from low-cost clays for the separation of oil–water emulsion, *Desalination and Water Treatment*. 57, 1927-1939.

Suresh, K., Pugazhenthi, G., 2017. Cross flow microfiltration of oil-water emulsions using clay based ceramic membrane support and TiO_2 composite membrane, *Egyptian Journal of Petroleum*. 26, 679-694.

Suresh, K., Pugazhenthi, G., Uppaluri, R., 2016. Fly ash based ceramic microfiltration membranes for oil-water emulsion treatment: Parametric optimization using response surface methodology, *Journal of Water Process Engineering*. 13, 27-43.

Suresh, K., Pugazhenthi, G., Uppaluri, R., 2017. Preparation and characterization of hydrothermally engineered TiO_2-fly ash composite membrane, *Frontiers of Chemical Science and Engineering*. 11, 266-279.

Sutrishna, P.D., Lingganingrum, F.S., Wenten, I.G., 2012. Separation of oil-in-water emulsion using slotted pore membrane. *Jurnal Teknik Kimia Indonesia*. 11, 57-65.

Suwaileh, W., Johnson, D., Hilal, N., 2020. Membrane desalination and water re-use for agriculture: State of the art and future outlook, *Desalination, 491*, 114559.

Swami, S.K., 2011. Health benefits of drinking cow's milk, *Indian Cow (The): The Scientific and Economic Journal*. 8, 2-5.

Tan, L., Shi, R., Ji, Q., Wang, B., Quan, F., Xia, Y., 2017. Effect of Na^+ and Ca^{2+} on the thermal degradation of carboxymethylcellulose in air, *Polymers and Polymer Composites.* 25, 309–314.

Tatwawadi, B., 2017. Potable and non-potable wastewater reuse, AWWA India Conference & Exhibition (AICE).

Thriveni, T., Nam, S., Ahn, J., Um, N., 2014. Enhancement of arsenic removal efficiency from mining waste water by accelerated carbonation, *IMPC 2014 – Gecamin Digital Publications.* 1–9.

Tomasula, P.M., Mukhopadhyay, S., Datta, N., Porto-Fett, A., Call, J.E., Luchansky, J.B., Renye, J., Tunick, M., 2011. Pilot-scale crossflow-microfiltration and pasteurization to remove spores of Bacillus anthracis (Sterne) from milk, *Journal of Dairy Science*. 94, 4277–4291.

Trouvé, E., Maubois, J.A., Piot, M., Madec, M.N., Fauquant, J., Rouault, A., Tabard, J., Brinkman, G., 1991. Rétention de différentes espèces microbiennes lors de l'épuration du lait par microfiltration en flux tangential, *Le Lait*. 71, 1-13.

Trunec, M., Chilář, J., 1996. Removal of thermoplastic binders from ceramic green bodies. *Ceramics*. 41, 67-80.

Trunec, M., Maca, K., 2014. Advanced Ceramic Processes, in: Shen, J.Z., Kosmač, T.(Eds.), *Advanced Ceramics for Dentistry*, Butterworth Heinemann, United Kingdom, 123-150.

Urase, T., Yamamoto, K., Ohgaki, S., 1993. Evaluation of virus removal in membrane separation processes using coliphage Qβ, *Water Science and Technology*. 28, 9–15.

Urase, T., Yamamoto, K., Ohgaki, S., 1994. Effect of pore size distribution of ultrafiltration membranes on virus rejection in crossflow conditions, *Water Science and Technology*. 30, 199–208.

Urase, T., Yamamoto, K., Ohgaki, S., 1996. Effect of pore structure of membranes and module configuration on virus retention, *Journal of Membrane Science*. 115, 21–29.

Vaithanomsat, P., Kitpreechavanich, V., 2008. Sericin separation from silk degumming wastewater, *Separation and Purification Technology*. *59*, 129–133.

Van der Bruggen, B., 2018. Microfiltration, ultrafiltration, nanofiltration, reverse osmosis, and forward osmosis, in: Luis, P. (Ed.), *Fundamental Modelling of Membrane Systems*. Elsevier, Amsterdam, 25-70.

Van Halem, D., Heijman, S.G.J., Soppe, A.I.A., Van Dijk, J.C., Amy, G.L., 2016. Ceramic silver-impregnated pot filters for household drinking water treatment in developing countries: Material characterization and performance study, *Water Science & Technology. Water Supply*. 7, 9–17.

Van Voorthuizen, E.M., Ashbolt, N.J., Schäfer, A.I., 2001. Role of hydrophobic and electrostatic interactions for initial enteric virus retention by MF membranes, *Journal of Membrane Science*. 194, 69–79.

Vasanth, D., Pugazhenthi, G., Uppaluri, R., 2011. Fabrication and properties of low cost ceramic microfiltartion membranes for separation of oil and bacteria from its

solution, *Journal of Membrane Science*. 379, 154-163.

Vasanth, D., Pugazhenthi, G., Uppaluri, R., 2013. Cross-flow microfiltration of oil-in-water emulsions using low cost ceramic membranes, *Desalination*. 320, 86-95.

Villanueva, C.M., Cantor, K.P., Grimalt, J.O., Malats, N., Silverman, D., Tardon, A., Garcia-Closas, R., Serra, C., Carrato, A., Castaño-Vinyals, G., Marcos, R., Rothman, N., Real, F.X., Dosemeci, M., Kogevinas, M., 2007. Bladder cancer and exposure to water disinfection by-products through ingestion, bathing, showering, and swimming in pools, *American Journal of Epidemiology*. 165, 148-56.

Waller, K., Swan, S.H., DeLorenze, G., Hopkins, B., 1998. Trihalomethanes in drinking water and spontaneous abortion, *Epidemiology*. 9, 134–140.

Wallis, C., Henderson, M., Joseph, L., Melnick, J.L., 1972. Enterovirus concentration on cellulose membranes, *Applied Microbiology*. 23, 476–480.

Wang, D., Fritsch, J., Moraru, C.I., 2019. Shelf life and quality of skim milk processed by cold microfiltration with a 1.4-µm pore size membrane, with or without heat treatment, *Journal of Dairy Science*. 102, 8798-8806.

Wang, Y., Wang, X., Liu, Y., Ou, S., Tan, Y., Tang, S., 2009. Refining of biodiesel by ceramic membrane separation, *Fuel Processing Technology*. 90, 422-427.

Wang, Y.H., Zhang, Y., Liu, X.Q., Meng, G.Y., 2007. Sol-coated preparation and characterization of microporous α-Al_2O_3 membrane support, *Journal of Sol-Gel Science and Technology*. 41, 267-275.

Wani, A.A., Singh, P., Shah, M.A., Schweiggert-Weisz, U., Gul, K., Wani, I.A., 2012. Rice starch diversity: Effects on structural, morphological, thermal, and physicochemical properties - A review. *Comprehensive Reviews in Food Science and Food Safety*. 11, 417-436.

Wegmann, M., Michen, B., Graule, T., 2008. Nanostructured surface modification of

microporous ceramics for efficient virus filtration, *Journal of European Ceramic Society*. 28, 1603–1612.

Wei, Z., Hou, J., Zhu, Z., 2016. High-aluminium fly ash recycling for fabrication of cost-effective ceramic membrane supports, *Journal of Alloys and Compounds.* 683, 474-480.

Welker, R., 2010. Continuous contamination monitoring systems, Developments in Surface Contamination and Cleaning, William Andrew Publishing, United States.

Werner, J., Besser, B., Brandes, C., Kroll, S., Rezwan, K., 2014. Production of ceramic membranes with different pore sizes for virus retention, *Journal of Water Process Engineering*. 4, 201–211.

Whitehead, W.K., 1976. Monitoring poultry processing wastewater with total organic carbon. *Poultry Science*. 55, 679-684.

Winter, O., 1969. Preliminary economic evaluation of chemical processes at the research level, *Industrial & Engineering Chemistry Research*. 61, 45-52.

World Health Organisation, 2017. Water quality and health - review of turbidity: information for regulators and water suppliers. https://www.who.int/water_sanitation_health/publications/turbidity-information-200217.pdf (Accessed 20 October 2019).

Wu, M.H., Yue, J.X., Zhang, Y.Q., 2014. Ultrafiltration recovery of sericin from the alkaline waste of silk floss processing and controlled enzymatic hydrolysis, *Journal of Cleaner Production*. *76*, 154–160.

Wüstenberg, T., 2014. Cellulose and cellulose derivatives in the food industry: Fundamentals and applications, John Wiley and Sons, United States.

Xu, C., Dong, Y., Liu, Y., Li, H., Deng, X., 2019. Preparation and Properties of SiC Porous Ceramics with Double-Particle Size, *IOP Conference Series: Mater. Sci*. 585, 012001.

Yao, Z.T., Ji, X.S., Sarker, P.K., Tang, J.H., Ge, L.Q., Xia, M.S., Xi, Y.Q., 2015. A comprehensive review on the applications of coal fly ash, *Earth-Science Reviews*, 141, 105-121.

Yordanov, D., 2010. Preliminary study of the efficiency of ultrafiltration treatment of poultry slaughterhouse wastewater, *Bulgarian Journal of Agricultural Science*. 16, 700-704.

Youcai, Z., 2018. Pollution control Technology for Leachate from municipal solid waste: landfills, incineration plants, and transfer stations, Butterworth-Heinemann, United Kingdom.

Yousuf, A., Manzoor, S.O., Youssouf, M., Malik, Z.A., Khawaja, K.S., 2020. Fly ash: production and utilization in India-an overview, *Journal of Materials and Environmental Science*, 11, 911-921.

Zare, S., Kargari, A., 2018. Membrane properties in membrane distillation, in: Gude, V.G. (Ed.), *Emerging Technologies for Sustainable Desalination Handbook*. Butterworth-Heinemann, United Kingdom, 107-156.

Zhang, S.Q., Kutowy, O., Kumar, A., Malcolm, I., 1997. A laboratory study of poultry abattoir wastewater treatment by membrane technology. *Canadian Agricultural Engineering*. 39, 99-106.

Zhi, T., Shuai, Z., Ying, L., Wen-shuai, H., Lu, F., 2016. Study on the effect of carboxyl methyl cellulose on the property of alumina ceramic support, *Powder Metallurgy Technology*. 3, 9.

Zhu, L., Chen, M., Dong, Y., Tang, C. Y., Huang, A., Li, L., 2016. A low-cost mullite-titania composite ceramic hollow fiber microfiltration membrane for highly efficient separation of oil-in-water emulsion, *Water Research*. 90, 277-285.

Zhu, L., Dong, X., Xu, M., Yang, F., Guiver, M.D., Dong, Y., 2019. Fabrication of mullite ceramic-supported carbon nanotube composite membranes with enhanced performance

in direct separation of high-temperature emulsified oil droplets, *Journal of Membrane Science*. 582, 140-150.

Zhu, L., Dong, Y., Hampshire, S., Cerneaux, S., Winnubst, L., 2015a. Waste-to-resource preparation of a porous ceramic membrane support featuring elongated mullite whiskers with enhanced porosity and permeance, *Journal of the European Ceramic Society*. 35, 711-721.

Zhu, L., Dong, Y., Li, L., Liu, J., You, S.J., 2015b. Coal fly ash industrial waste recycling for fabrication of mullite-whisker-structured porous ceramic membrane supports, *RSC advances*. 5, 11163-11174.

Zou, D., Chen, X., Drioli, E., Qiu, M., Fan, Y., 2019c. Facile mixing process to fabricate fly-ash-enhanced alumina-based membrane supports for industrial microfiltration applications, *Industrial and Engineering Chemistry Research*. 58, 8712-8723.

Zou, D., Qiu, M., Chen, X., Drioli, E., Fan, Y., 2019a. One step co-sintering process for low-cost fly ash based ceramic microfiltration membrane in oil-in-water emulsion treatment, *Separation and Purification Technology*. 210, 511-520.

Zou, D., Xu, J., Chen, X., Drioli, E., Qiu, M., Fan, Y., 2019b. A novel thermal spraying technique to fabricate fly ash/alumina composite membranes for oily emulsion and spent tin wastewater treatment, *Separation and Purification Technology*. 219, 127-136.

Zulkifli, S.N.A., Mustafa, A., Othman, M.H.D., Hubadillah, S.K., 2019. Characteristic properties of ceramic membrane derived from fly ash with different loadings and sintering temperature, *Malaysian Journal of Fundamental and Applied Sciences. 15*, 414-420.

List of Publications

Publications in international journal:

1. **Kakali Priyam Goswami** and G. Pugazhenthi, Credibility of polymeric and ceramic membrane filtration in the removal of bacteria and virus from water: A review, *Journal of Environmental Management*, 268 (2020) 110583. https://doi.org/10.1016/j.jenvman.2020.110583.

2. **Kakali Priyam Goswami** and G. Pugazhenthi, Treatment of poultry slaughterhouse wastewater using tubular microfiltration membrane with fly ash as key precursor, *Journal of Water Process Engineering*, 30 (2020) 101361. https://doi.org/10.1016/j.jwpe.2020.101361.

3. **Kakali Priyam Goswami** and G. Pugazhenthi, Effect of binder concentration on properties of low-cost fly ash-based tubular ceramic membrane and its application in separation of glycerol from biodiesel, *Journal of Cleaner Production*, 319 (2021) 128679. https://doi.org/10.1016/j.jclepro.2021.128679.

4. **Kakali Priyam Goswami,** K. Pakshirajan and G. Pugazhenthi, Process intensification through waste fly ash conversion and application as ceramic membranes: A review, *Science of the Total Environment*, 808 (2022) 151968. https://doi.org/10.1016/j.scitotenv.2021.151968.

5. **Kakali Priyam Goswami** and G. Pugazhenthi, Elimination of pathogenic bacteria from milk using membrane technology: A review, *International Food Research Journal*. (Submitted).

6. **Kakali Priyam Goswami** and G. Pugazhenthi, Treatment of starch-rich wastewater using fly-ash based tubular ceramic membrane: An approach towards mitigating water pollution, *Environmental Progress & Sustainable Energy*. (Revision submitted).

Presentation in international/national conferences:

1. **Kakali Priyam Goswami** and G. Pugazhenthi, An investigation on effect of binder concentration on the alternation of properties of fly ash based tubular membrane, *International Conference on Multifunctional and Hybrid Materials for Chemical Process, Energy, Environment and Medical Applications (ICMHCEE 2019)*, 9-11 September 2019, National Institute of Technology (NIT), Tiruchirappalli, India.

2. **Kakali Priyam Goswami** and G. Pugazhenthi, Fabrication and characterization of tubular membrane using fly ash as precursor: A solution to fly ash disposal concern, The 2nd *Green Technologies for Sustainable Water 2019 (GTSW 2019)*, 1-5 December 2019, Ho Chi Minh City, Vietnam.

3. **Kakali Priyam Goswami** and G. Pugazhenthi, Membrane filtration as an efficient alternative for separation of bacteria from milk: A review, *Sustainable Technologies for Water Treatment and Desalination (STWTD - 2020)*, 18-19 December 2020, National Institute of Technology, Calicut, India.

4. **Kakali Priyam Goswami** and G. Pugazhenthi, Fly Ash Tubular Membrane: An Efficient Alternative for the Treatment of Poultry Slaughterhouse Wastewater, *9th DAE-BRNS Biennial Symposium on Emerging Trends in Separation Science and Technology (SESTEC-2020)*, 22-26, March 2021, Bhabha Atomic Research Centre, Mumbai, India.